University of California
Santa Barbara

Three Essays on Climate Risk

A dissertation submitted in partial satisfaction
of the requirements for the degree

Doctor of Philosophy
in
Geography

by

Maximilian Salavador Stiefel

Committee in charge:

Professor Stuart Sweeney, Chair
Professor Susan Cassels
Professor Simone Pulver

March 2022

The Dissertation of Maximilian Salavador Stiefel is approved.

Professor Susan Cassels

Professor Simone Pulver

Professor Stuart Sweeney, Committee Chair

March 2022

Three Essays on Climate Risk

by

Maximilian Salavador Stiefel

Acknowledgements

To the UCSB Department of Geography for all the assistance and training, particularly my committee members for their suggestions and insight; my colleagues at ClimateCheck; my scientific collaborators; and my friends and family–especially Juan, Jessica, Genie, Alev, and Warren–for your feedback and my parents for support.

Curriculum Vitæ

Maximilian Salavador Stiefel

Education

2022	Ph.D. in Geography, University of California, Santa Barbara.
2016	M.A. in Geography, University of California, Santa Barbara.
2014	B.S. in Environmental and Sustainability Studies, University of Utah
2014	B.A. in Economics, University of Utah

Abstract

Three Essays on Climate Risk

by

Maximilian Salavador Stiefel

Climate change is forcing a shift in the characteristics of many natural hazards. Alongside other trends–such as increasing global interdependence, the rate of population and economic growth, and widening social inequalities–the risk from climate-sensitive natural hazards presents an expanding source of danger across the world. Research and practice on climate risk began by establishing standards for assessing hazards and implementing structural solutions to mitigate consequences. The field has evolved since then to include behavioral decision making and the multidimensionality in differences among people and places as determinants of exposure and vulnerability, respectively. These paradigm shifts in selecting factors for climate risk assessment happened alongside developments in modeling divergences between statistical and perceived risk as well as policy and scientific attention towards the distribution of hazards along socioeconomic and demographic lines. This dissertation, Three Essays on Climate Risk, contributes to answering pressing questions in climate risk research. The first essay, 'Validating Social Vulnerability in Disaster Loss Models' suggests that climate risk assessments should account for social vulnerability but practice caution since the relative contribution of social indicators varies across climate hazards. In the second essay, 'Social and Spatial Inequalities in Climate Hazard Distributions,' we compared multiple inequality metrics to find that exposure heterogeneously varies across metrics by choice of demographic and geographic partitioning. Researchers should therefore carefully design studies based

upon theories of inequality formation and policy relevance. Preliminary results from the third essay, 'Measuring Climate Risk Perception with Twitter Data,' indicate that user-generated big data may soon serve as an appropriate supplement to survey data for measuring complex socio-cognitive phenomena. These essays advance climate risk measurement & modeling, unpack geographies of climate risk, and illustrate implications of improving climate risk information.

Contents

List of Tables

List of Figures

Chapter 1

A Climate Risk Literature Review

Introduction

Natural hazards present a substantial source of danger across the world. Climate change is forcing a shift in the characteristics of many of these hazards. Shifting characteristics have refocused attention towards current hazard estimates as well as incentivized the incorporation of projected hazard in risk assessments. Other factors–such as increasing global interdependence, the rate of population and economic growth, and widening social inequalities–present an added impetus for better understanding our shared risk from climate-sensitive natural hazards, which we refer to as climate risk. Research and practice on climate risk formally began at the beginning of the twentieth century through the establishment of standards for assessing hazard and implementation of structural solutions to mitigate consequences. These efforts developed alongside trends in the physical and social sciences to integrate uncertainty as a fundamental feature of hazard estimates, decision making as a determinant of exposure, and vulnerability as a multidimensional moderator of negative consequences from hazard events. Growing interest in the roles of

risk perception and inequality happened tangentially to these paradigm shifts in climate risk research.

As a contribution to the expanding literature and importance of climate risk research, this dissertation addresses pressing questions regarding concepts and methods in the study of climate hazard modeling, exposure to hazards, vulnerability as a moderator of hazard event outcomes, and the implications of perception and inequality on the aforementioned phenomena. This first chapter provides a climate risk literature review on the history of related fields and explanation of parameters used in climate risk models. Each following chapter studies aspects of climate risk with an empirical approach across five different hazards: extreme precipitation, extreme heat, drought, wildfire, and flooding. The second chapter, 'Modeling Social Vulnerability Determinants of Disaster Loss,' estimates the relative contribution of social indicators to variability in disaster loss. The third chapter, 'Mapping Climate Risk Inequalities,' assesses the social and spatial distribution of climate hazards by comparing multiple types of inequality metrics. The fourth chapter, 'Measuring Climate Risk Perception with Twitter Data,' builds a dataset of socio-cognitive characteristics from user-generated social media data. Our goal in these studies is to advance measurement and modeling of climate risk, both the contributing factors and the societal implications of changing physical hazard and risk information. We proceed in this chapter with an overview of climate risk including major research questions facing relevant fields, explaining parameters in climate risk modeling, and a case study that demonstrates the dynamic application of concepts presented in this review.

Climate Risk: An Overview

Risk analysis and associated fields have applications across numerous academic disciplines and applied contexts. Although the modern fields of risk research developed in the post-war era as a response to needs across different sectors–notably in aerospace, nuclear, and chemical process (Bedford & Cooke, 2001)–the study and management of risk by groups and societies has occurred since prehistory (Bernstein, 1996; Covello & Mumpower, 1985). At the micro scale, individuals have always informally managed risk as part of cognitive decision making processes (Boholm, 2015). Risk in this context is generally understood as the representation of consequences associated with a given hazard frequency and intensity.

Hazards are a source of sub-optimal outcomes, such as losses, shortcomings, or reversals. Furthermore, since the probability of any hazard realizing a given frequency and intensity constitutes the uncertainty inherent to all risks, every risk estimate is associated with some degree of uncertainty (Kaplan & Garrick, 1981).

Natural hazards, i.e., those that historically were exogenous to human forcing, such as earthquakes, pandemics, and heatwaves, therefore lend themselves to being studied with the risk analysis approach. Traditional risk-hazard research regarded the presence, effectiveness, and integrity of structural engineering solutions as the primary driver for risk reduction (White, 1945). This structural paradigm centered around engineered solutions to reduce risk despite society still experiencing increased exposure from people moving into hazardous areas, either structurally protected or not. Because of this, disaster losses were greater than before a structural fix in case of technological failure, people were taken by surprise when extremes were more intense than predicted, and risk was unmanageable when people behaved in unexpected ways. Questions concerning the hazard research community include: at what point does a phenomenon become a hazard, how

do we characterize and model hazards, how and when will climate change force shifts in natural hazard characteristics, and which outcomes are associated with hazard event occurrence?

By mid-century, led by the research of Gilbert White, we acknowledged that structural solutions were not sufficient and began explaining risk reduction through both structural solutions and behavioral interventions (White, 1974). Different ways of explaining why and how individuals made risk management decisions were proposed, notably through bounded rationality and preference models. From this vantage point it was understood that individuals would make decisions based on factors such as risk tolerance and past experience rather than maximum risk aversion. The National Flood Insurance Program (NFIP) in the United States is a direct result of this paradigm shift. NFIP allowed better management of the myriad ways people expose themselves to risk yet still left out considerations of factors at the individual and community levels producing unexplained variability in disaster outcomes. This approach was eventually deemed too simplistic, rational, and reliant on modernization (Watts, 2008). It became clear that risk could not be sufficiently managed by only addressing hazard and exposure.

Vulnerability became a focus of risk-hazard research following critiques of the structural and behavioral approaches to reducing disaster loss (Turner et al., 2003). These newer lines of inquiry focused on applying a diverse mixture of factors attributed to structural, social, economic, institutional, and environmental elements and processes to risk assessment (Wisner, Blaikie, Blaikie, Cannon, & Davis, 2004). The variation in loss outcomes therefore came to be understood as the result of differences across people and places in characteristics such as opportunity structures, quality of the built environment, emergency management systems, and social networks. Most assessments recognize that accounting for any one dimension of vulnerability in a localized or national-level assess-

ment only partially represents the full risk profile (Wisner, 2016). Research questions stemming from the incorporation of vulnerability in the risk modeling framework include: when a hazard event occurs, which factors moderate variation in outcomes while holding hazard constant?; how do we model statistical risk–the formal relationship among hazards, outcomes, and moderators?; and do moderators differ across hazard types?

With an understanding that climate risk parameters broadly relate to either physical hazard, exposure, and vulnerability, it became clear that worsening climate hazards do not necessarily lead to greater loss (Mitchell, Devine, & Jagger, 1989). From a risk reduction vantage point, recognizing this variability as attributable to the spatial distribution of population and factors of production meant that agents can reconfigure towards places with relatively lower hazard, leaving less potential for loss from a hazard event. Similarly, capacity building and adaptation could fortify agents against the worst potential outcomes. Beyond the explicitly modeled parameters, individual and governmental perceptions of the need to modify risk through these types of measures is featured as a determinant of whether risk reduction occurs before disaster strikes. However, the opportunity and necessity of making these adjustments is not equally distributed along socioeconomic, demographic, and geographic lines.

In the simplest sense, to understand climate risk we need to measure each explanatory term from equation 1, which can also be seen in Figure **??** provided by the Intergovernmental Panel on Climate Change (IPCC):

$$ClimateRisk_{itj} = H_{itj} \cdot E_{itj} \cdot V_{itj}$$

Climate risk is a function of hazard H, exposure E, and vulnerability V, all per geographic unit i at time t for outcome j (Kron, 2002). The subscripts are important for several

reasons. First, estimating climate risk depends on the geographic unit of interest. This is to say that the dimensions of vulnerability (and the other terms) differ according to i. For an individual property owner, dimensions might include social context and the built environment whereas vulnerability for a forest relates to water scarcity and plant species distribution. These vulnerabilities also depend on which outcome j we are estimating–the risk for what. An individual's vulnerability to property loss depends on hazard proofing and structural solutions while for loss of life it likely concerns a person's age and type of housing. Lastly, hazard, exposure, and vulnerability all depend on time t, particularly in the context of climate change where we will experience a substantial shift in the hazard term over the next century.

There are several important features of this equation. Each term is not independent and rather interactive and dependent on every other term across time, space, and outcome. Thus vulnerability depends on hazard intensity since below a certain threshold a dimension may not be relevant to the outcome. We can estimate statistical climate risk for single or multiple hazards, the choice of which then influences how we measure the hazard term and which factors we take into consideration for measuring exposure and vulnerability. Climate risk is like a great river: it sinuously builds from many sources, the magnitude is managed yet unmanageable, and we only truly know the danger when it overwhelms its common course.

Explicitly modeled parameters are not the only sources of variability in assessing statistical climate risk–perception and inequality also play critical moderating roles. Since anthropogenic climate change occurs on the scale of decades to centuries and there is such a high degree of uncertainty about mitigation intentions and actions, perception has limited pertinence in this modeling framework to the physically determined hazard term. However, perception does influence decisions to reduce risk through exposure and vul-

nerability. Reduction becomes actionable at a certain level of hazard (risk) perception. Units (individuals, households, organizations, etc) may choose to shift physical location or build disaster response capabilities beyond this point. Similarly, risk perception influences extra-unit decisions to reduce risk, leading to knock-on effects across society, such as building levees or requiring household protection for insurance eligibility.

Widening inequalities, particularly an expansion at the lower end of socioeconomic distributions and hazard distributions along socioeconomic lines, would limit the capacity for units in aggregate to reduce exposure and vulnerability, thus increasing climate risk. Public focus on the inequality of climate risk has spurred key research areas including whether marginalized communities bear disproportionate climate risk, how and why climate risk varies across populations and places, and the differential capacity of units to mitigate climate risk. Inequality is a concern for risk assessment, since models at levels higher than the individual miss disaggregated variability, as well as for risk reduction because relative advantage, as compared to absolute, plays a similar role for capacity building. Inequality therefore moderates climate risk through vulnerability and exposure while simultaneously interacting with these factors across every stage of the disaster cycle. Research questions addressing the roles of parameters in climate risk modeling that extend beyond hazard, exposure, and vulnerability–such as perception and inequality–include: Which other factors indirectly determine risk across the disaster cycle? What is the distribution of risk across people and places? How do moderators shape risk distributions? Does perceived and statistical climate risk align? Which factors determine differences between perceived and statistical climate risk?

Evidence of present climate risk comes from increasingly destructive weather and climate related disasters over the past decade (Smith, 2020). Recent disasters have caused huge losses–costing hundreds of billions of dollars (NOAA, 2020), claiming many lives (Center

for Public Integrity, 2020), and destabilizing the livelihoods of thousands to millions of people. To name just a few, many of which have broken historical records:

2011-2017 California Drought, the longest and driest in state history (Seager et al., 2015) 2012 Midwest Drought, resulted in excessive crop loss (Mallya, Zhao, Song, Niyogi, & Govindaraju, 2013) 2012 Heat Wave, one of the most severe in the historical record and led to dozens of directly attributable deaths (NASA, 2012) 2017-2020 California wildfire seasons, successively shattered most records from previous wildfire seasons (Williams et al., 2019) 2017 Hurricane Harvey, brought historic flooding to Houston (Trenberth, Cheng, Jacobs, Zhang, & Fasullo, 2018) 2017 Hurricane Maria, a few weeks after Harvey and which devastated Puerto Rico, killing thousands (Keellings & Ayala, 2019) 2018 Hurricane Michael, the first category five hurricane to hit the conterminous US in over 25 years (NOAA, 2019) 2019 Midwest Flooding, three billion dollars in loss, affected 14 million people, and set high water marks throughout the region (Center for Disaster Philanthropy, 2019)

The chapters in this dissertation address aspects of many of the research questions outlined previously. In the first chapter, 'Modeling Social Vulnerability Determinants of Disaster Loss,' we test the role of social vulnerability in moderating disaster loss across climate hazards. The research questions we ask include: How do social vulnerability values and the relative contributions of social indicators vary by input data selection? Which social vulnerability indicators are most important in moderating disaster loss? Is there a statistically significant relationship between disaster loss and social vulnerability?

The second chapter, 'Mapping Climate Risk Inequalities,' explores the distribution of climate hazards across populations and places. We ask the following questions: How unequally distributed are climate hazards: vertically, horizontally, and spatially? Which population groups and places experience unequal climate hazard burdens? Do differ-

ent representations of climate hazard inequalities lead to varying environmental justice interpretations?

For the last empirical chapter, 'Measuring Climate Risk Perception with Twitter Data,' our research questions include: Does Twitter data provide a robust and reliable basis for measuring individual-level predictors of complex phenomena, such as climate risk perception? How closely do climate risk perception measurements from Twitter data match those from survey data? What is the relationship between statistical climate risk and climate risk perception?

Our goal in this review is to orient the reader with concepts and methods applied in the following empirical chapters. We will briefly cover the history and use of hazard, exposure, and vulnerability in climate risk assessment as well as address the moderating roles of perception and inequity. The focus will be on how individuals, households, and communities navigate the disaster cycle, disaster loss, and the social construction of risk. Understanding the complicated factors and complexity of climate risk requires a large diversity of scholarship to produce insights that, although uncertain, offer actionable recommendations for navigating our shared future.

Climate Hazards

Conceptual

Many natural hazards exist in the earth system. Some are independent of the climate, such as earthquakes, whereas others, such as flooding, are not. The climate influence on the latter group comes through meteorological phenomena: precipitation, temperature, wind, and so on. People have dealt with climate hazards–wildfires, floods, heatwaves,

storms, and droughts–since prehistory. Since the danger posed by climate hazards has existed alongside human evolution, the geography of settlement and activity has developed around it, and for good reason. The nature of a climate hazard is that it is, in effect, the tail end of a resource availability distribution (Burton, 1993; Kates, 1971). Among other reasons, humans settled in hazard exposed areas while acknowledging the necessary tradeoffs: inland and coastal flooding for access to fresh water and trading, heatwaves and droughts for longer growing seasons, and wildfires for environmental management. By doing so we were able to consistently access those resources.

Extreme events would eventually occur and cause a range of disruptions (Leroy, 2006) , the frequency and duration of which varied by hazard and place. In coastal California, wildfires occurred every twenty years in Redwood forests but only every half century in the chaparral (Steel, Safford, & Viers, 2015). Hurricanes hit areas of the southeastern US nearly every year whereas devastating riverine floods might strike just once in a generation. Whether a slow onset drought or a fleeting forest fire, many settlements were able to manage these hazards. Yet, other hazardous events extended to near or total systems collapse (Dunning, Beach, & Luzzadder-Beach, 2012; Kuil, Carr, Viglione, Prskawetz, & Blöschl, 2016). Despite such outcomes, not having access to crucial resources associated with hazard proximity was not a viable solution (Di Baldassarre et al., 2013).

The net-benefit of this tradeoff, at least in most places, allowed for continuous settlement. As civilization advanced, we reduced vulnerability by depending less on local environments and managing our environment through engineering solutions. The latter solution coupled massive infrastructure projects, such as dams for water storage and levees to prevent storm surges, with codes and standards for sites and structures. Climate hazards became dangerous phenomena that were manageable and even negligible in certain cases (Kates & Burton, 2008). Therein lies the current problem.

Our expectations of distributed dependence and environmental management are based on historical observations. We established farmland in abundant regions, assigned water rights according to average river flow, and built stormwater systems to withstand certain flood return periods. This made sense given that climate variability was consistent over time. At the very least, the rate of climate change was neither noticeable nor actionable. There were of course exceptions to this. Longer and shorter deviations occur, such as the well documented Medieval Climatic Anomaly and El Nino Southern Oscillation respectively, but the climate remained relatively stable and therefore dependable throughout most of human history.

Historically unprecedented global warming and the associated changes to our climate and environment render historical precedent no longer valid. The resource systems and hazard management solutions we developed must now be reassessed, redesigned, and reconstructed. In some cases we will change where and when we cultivate food and materials, how we organize production networks, and the places we deem safe enough for housing. In others we will implement technological fixes to avoid such disruption. Some of those fixes will only be temporary, buying us just a few more years until we finally concede to our changing climate hazard landscape.

Empirical

Climate change is altering the geography and characteristics of physical hazards. The primary characteristics when measuring climate hazards fall under the categories of spatiotemporality, intensity, and severity. Hazards vary by areal extent (size of affected area), spatial patterning (dispersion and contiguity), frequency (rate of return), duration (length of event), intensity (deviation from average conditions), and severity (degree and type of impacts), all of which human activity moderates through climate, environmen-

tal, and land use change (K. Smith, 2013). Despite efforts to mitigate climate change, the momentum of social, technological, and physical systems has locked in a minimum guaranteed amount of greenhouse gas emissions and therefore global warming (Samset, Fuglestvedt, & Lund, 2020). According to the geologic record, many recent climate hazard events are abnormal for the period of time in which humans have inhabited these areas (Griffin & Anchukaitis, 2014; T. T. Smith et al., 2013). Many studies have contributed to understanding the attributable portion of these disasters to anthropogenic climate change (Peterson, Stott, & Herring, 2012), ranging from floods (van der Wiel et al., 2017), heatwaves (Vogel, Zscheischler, Wartenburger, Dee, & Seneviratne, 2019), and drought (Funk, Hoell, & Stone, 2014).

From a risk reduction perspective, hazards with smaller areal extents allow for engineering solutions or nearby relocation of a settlement. Less frequent events provide enough time for recovery and reconstruction. Lower intensity hazards avoid the most severe impacts. The severity of some hazard impacts simply leads to reduced well being whereas others end in loss of property and life. The particular combination of these parameters is crucial. Low intensity but frequent events, such as high tide (sunny day) flooding, render places uninhabitable. High intensity or severity hazards are clearly undesirable but may be unavoidable if the areal extent is large enough, as is the case of tropical cyclones in the southeastern US.

Modeling these hazards therefore relies on data with sufficient spatial, temporal, and measurement resolution. The most common approach to quantifying climate hazards is to estimate frequency and intensity, which depends on the hazard and event under study. In practice this requires making decisions about how we choose to define extremes. Taking a step back from specific instances, such as the 100-year flood, the frequency and intensity that we are interested in estimating is that of extreme exceedances. The value

beyond which we consider an event extreme typically relies on one or more of three things: historical observations, design standards, and probable loss. The second item is an issue of risk management, which is not the focus of this review and merely discussed as a rhetorical tool for contextualizing relevant information about risk assessment. The third item relates to exposure and will therefore be covered later.

How we compare historical observations, typically the underpinning of what is extreme, to climate change projections is not necessarily straightforward. For example, say a historical 100-year flood will likely result in a 30 centimeter flood depth x at location i. A 1 in 100 year flood is based on historical observations of the precipitation event that has a daily occurrence probability of 0.000028, happening just once every one hundred years. When looking across time periods T in the context of climate change, if 21st century projected data from Global Climate Models (GCMS) show an increase in precipitation, the 100-year precipitation event intensity might instead occur once every eighty years. So, for the 100-year flood at location i we would expect some increase from historical to projected time in depth x. In projected time, the depth exceedance of the historical 100-year flood is now more frequent and the projected 100-year flood is more intense.

As we are applying appropriate estimation protocols to represent change in hazardous events over the next several decades, the accuracy, precision, and spatiotemporal resolution of climate hazard models are also improving. An example of these developments can be found in modeling the costliest natural hazard in the US, flooding (Wing, Pinter, Bates, & Kousky, 2020). Local studies to assess flood hazard are expensive and slow, resulting in poor spatial coverage. Two-dimensional flood models (2DFM) simulated over a large area (continental scale) and at high resolution have filled these coverage gaps, improved existing estimates, and allowed for efficient hazard assessment as we model a range and uncertainty of impacts from projected changes in precipitation.

Recent advances have substantially lowered the complexity, computational cost, and data requirements for large area 2DFM implementation, usually by either simplifying solutions to the shallow water equations or proposing an altogether different modeling framework. Fathom Flood Risk Intelligence, a research organization affiliated with the University of Bristol, has produced reliable high resolution 2DFM estimates globally and for the US (Bates, Horritt, & Fewtrell, 2010). Compared to Federal Emergency Management Agency (FEMA) National Flood Hazard Layer data–a highly labor and resource intensive hazard product that is the gold standard for building codes, siting decisions, and insurance determinations–Fathom found replicability within error. This demonstrated continental scale viability of this modeling approach for decision-making purposes (Wing et al., 2017) and found around three times as many people (from 13 to 41 million) live in the 100 year floodplain (Wing et al., 2018).

Climate change projections suggest that climate hazards, on average, will increase in areal extent, frequency, duration, intensity, and severity over the 21st century (Aalst, 2006; Abatzoglou & Williams, 2016; Hirabayashi et al., 2013a; Luber & McGeehin, 2008; Papalexiou & Montanari, 2019; Wilby & Keenan, 2012). Hazards under study by academics with potential impacts include heatwaves (Lau & Nath, 2012; Tuholske et al., 2021), droughts (Overpeck, 2013), extreme storms (Knutson et al., 2010), wildfires (Moritz et al., 2012), inland flooding (Quinn et al., 2019), and sea level rise-related permanent inundation and coastal flooding (Neumann, Vafeidis, Zimmermann, & Nicholls, 2015).

An increase in global temperatures is expected to lead to a mixture of changes in characteristics for each climate hazard. The US Global Change Research Program provides an overview of projected climate hazards, on average, across the conterminous US. Historical trends and future projections for the next century point to increases in heatwave

frequency and intensity; drought intensity and duration in the Southwest; hurricane frequency, intensity and duration; winter storm frequency and intensity; precipitation amounts, especially at higher latitudes and during winter; extreme precipitation frequency and intensity; and frequency and intensity of all types flooding (high tide, storm surge, fluvial, and pluvial) (USGCRP, 2017).

Published literature projects the Western US as a climate change hotspot under intermediate and higher levels of emissions forcing (Diffenbaugh & Giorgi, 2012). Relative to the rest of the globe, North America has avoided prolonged droughts in recent history even when considering crises in California and the Midwest. Increasing aridity on the continent may turn that trend on its head over the next few decades (Dai, 2011). The Southwest will likely see drier springs and summers, the latter of which will also plague the Midwest (Swain & Hayhoe, 2015; Woodhouse, Meko, MacDonald, Stahle, & Cook, 2010). Flooding looks to increase in the Pacific Northwest (Tohver, Hamlet, & Lee, 2014). Acreage burned per year by wildfires has gone up for nearly every state in the 21st century (Hoover & Hanson, 2020). The intensity and severity of wildfire hazard is expected to continue to increase, especially in summer and fall, in the West, Northern Midwest, and Southeast, and prospects point to greater areal extents and longer wildfire seasons (Liu, L. Goodrick, & A. Stanturf, 2013).

The aforementioned hazard characteristics are not the only factors increasing dangerous potential. Event timing leads to different outcomes, such as higher mortality from earlier season heatwaves (Anderson G. Brooke & Bell Michelle L., 2011). More wintertime precipitation as rain and earlier snowmelt runoff will increase springtime flooding (Trenberth, 2011). Land use change also influences hazard variability. Western US forests have a 'fire deficit' due to misguided wildfire management practices. These forests have only begun to overcome the deficit in the past couple of decades (Marlon et al., 2012). A

deficit coupled with drought, record high temperatures, insect blight, and construction in the Wildland-Urban Interface has led to a wildfire crisis in the west (Westerling, Hidalgo, Cayan, & Swetnam, 2006). Mitigation and management is particularly challenging for wildfires compared to other natural hazards because of idiosyncrasies in fire regimes across ecosystems and large uncertainty surrounding ignition and weather conditions.

Exposure

Conceptual

The least complex but perhaps most important term in the climate risk equation is exposure. Specifically, it refers to who and what is exposed to climate hazards (Peduzzi, Dao, Herold, & Mouton, 2009). From the population side, it's about how many people are exposed and what function those people have in a society and in the disaster cycle. Population distribution (location, density, and size) determines the amount of lives exposed to disruption, harm, or loss from a climate hazard. Population exposure includes the amount of commuters impacted from a hurricane, person-days of wildfire smoke, or farm workers under a 'heat dome'. Beyond population distribution, there is also the social function of exposed peoples. 'Essential', 'front line', and 'key' are terms used to describe workers making society function smoothly, the incidental backbone of society. Risk is not only a function of how many people are exposed to hazards but on the role that an exposed person plays in society.

The property side of exposure relates to the utility and cost of things that have instrumental value. There are other categories of exposed things, but these are not typically considered in a climate risk or loss assessment context. Using the philosophical approach

of understanding value, there are also exposed things of intrinsic or aesthetic value, such as a unique habitat for a species with limited range or an outdoor recreation destination. Clearly these things are valuable to many people, but neither do they receive a fraction of the attention afforded to people and property nor are they easily operationalized for the climate risk equation. Thus, people and property are the two main categories of exposure.

Climate hazard events generate myriad loss-related consequences. Conditions ripe for disaster outcomes are not necessary for these losses to occur, but typically increase loss probability and severity. Loss categories implicated by climate hazards include commodities (e.g. crops), fixed assets (e.g. buildings), wellbeing (e.g. air quality), and survival, among others. Each type of hazard produces different types of consequences, however there is broad overlap. Tangible hazards (wildfire and flooding) can feasibly result in almost any type of loss while intangible hazards (temperature, precipitation, and drought) tend to not impact fixed assets.

All climate hazards can reduce water supply and quality, damage crops, and increase injuries and fatalities, although there is mostly an indirect relationship between drought and the latter. Wildfire and flooding, and to a lesser extent extreme precipitation and heat, disrupt transportation, communication, and utilities infrastructure. Some explainable interactions in hazard dynamics exist; droughts increase wildfire risk which increases flood risk. Wildfires and flooding are the main culprits of property damage. Furthermore, increasing climate hazards coupled with population growth means greater risk for disaster loss. Economic growth also increases the absolute amount of damage, particularly from hurricanes (Mendelsohn, Emanuel, Chonabayashi, & Bakkensen, 2012). This list is not exhaustive and simply provides a succinct overview of climate hazard-related types of loss. Beyond direct losses there are innumerable wellbeing impacts on mental

and physical health, economic output and opportunity, and quality of life.

Empirical

A growing population means greater exposure to climate hazards. Bureau (2020) projects the US population to increase by about 25 percent over the next few decades (from around 320 to 400 million in 2060), the spatial distribution of which will play an important role in the amount of people exposed to climate hazards. Over the past few decades there has been a trend of relatively higher net migration to southern, western states compared to other regions (Bureau, 2019). If this trend holds over the next few decades, a higher proportion of people will be exposed to intense droughts, wildfires, hurricanes, and heatwaves. The relative geographic distribution of population aside, more intense climate hazards will barrel through already populated areas–four to six times as many people will be exposed to extreme heat by the latter half of this century (Jones et al., 2015).

As an example, California has long been recognized as an epicenter for wildfire risk due to population growth in the Wildland-Urban Interface (WUI) (Hammer, Radeloff, Fried, & Stewart, 2007; Radeloff et al., 2018)). While neither the largest nor most deadly, the 1991 fire in the Oakland-Berkeley hills was a foreshadowing of an increasingly common fire pattern: human ignition starts a minor fire and it escalates uncontrollably, spurred on by arid conditions and strong winds (FEMA, 1991). Simulations consistently show that this pattern is likely to grow as a result of climate change, population growth, and land use change (Bryant & Westerling, 2014; Kloster, Mahowald, Randerson, & Lawrence, 2012; Westerling & Bryant, 2008).

Government and industry are committing increasingly numerous resources to assessing property exposed to natural hazards as climate change becomes an immediate reality.

Similar to the population side of assessment, property exposure depends on the amount and functionality (Schumacher & Strobl, 2011). Supply chain disruptions ensue if a hurricane renders a port unusable and lives are lost if riverine flooding cuts off access to essential services. Yet a wildfire burning through a recreational forest may go unnoticed except by firefighters and those downwind of the smoke. Dissimilar to the people part of the exposure term is that property has differential value.

The differential value of property is therefore the feature that primarily compels stakeholders to make accurate and precise exposure estimates. There are many valuation approaches for property and types of value therein, the discussion of which would be beyond the scope of this review (Damodaran, 2012). Essential to note is that in the disaster cycle, ex ante valuations often differ in both quantity and quality than ex post (Kamin & Rachlinski, 1995; Shogren & Crocker, 1991). Much of this is because there are insufficient data and modeling capabilities for direct disaster loss and knock-on effects across all levels, from organizational to the global economy. Another part may be due to accounting tricks for reducing risk portfolios and mitigation costs while attributing loss to hazard events as expansively as possible for reaping greater insurance and government payouts (Bulut, 2017). Lastly, exposure is endogenous to hazard events due to shifts in risk perception and asset prices (Daniel, Florax, & Rietveld, 2009). It is thus easier to estimate generalized effects of historical hazard events on property loss than it is to model risk (Kellenberg & Mobarak, 2011).

One way to reduce exposure is by simply divesting in places exceeding a certain climate hazard threshold. There are likely two paths occurring in tandem for incorporating better climate hazard estimates into a variety of financial decisions including lending and investment. The mapping path asserts that institutions will adopt better hazard estimates as standard practice. The lender path suggests lenders will cooperate among

each other to share local information (Keenan & Bradt, 2020). Taking either path, we can see how this might proceed in the housing market. Units rely on a variety of in-house, contracting, and governmental agencies to determine climate risk. An example of this occurs under FEMA's National Flood Insurance Program (NFIP), which assesses flood hazard at a property level to produce the National Flood Hazard Layer (NFHL). The NFHL contains flood zone and zone subtype, which determine the quantitative and qualitative flood risk, mitigation infrastructure, planned administrative works, and the localized socio-environmental situation stemming from hydrologic and built context. Units reference Flood Insurance Rate Maps (FIRMs) from the NFHL to make decisions on where to build houses, lend mortgages, and write insurance (Frazier, Boyden, & Wood, 2020). Relative home values in climate risky areas will likely decrease over the next few decades (Union of Concerned Scientists, 2018).

However, predicting where property values will depreciate over the temporal scale that climate change operates–decades to centuries– is not a straightforward process. House prices are a function of risk avoidance but also demand, amenities, profit seeking, and more. Assigning value to, and determining the function of, property in the distant future holds massive uncertainty (Anda, Golub, & Strukova, 2009; Nordhaus, 2007, 2013; Pizer, 1999). Valuation methods aside–depreciation, net present value, etc–the key issues stem from not knowing the relative value of property over future time as well as the interaction between hazard and exposure (Dietz, Bowen, Dixon, & Gradwell, 2016). The former assumes that some property will become relatively less functionally important as society changes, which decreases value.

Obvious targets of this are industries facing inevitable change as we increasingly address problems of climate change, conservation, and ethics. Fossil fuels, plastics, and animal farming are all encountering swift regulatory and demand-side changes that will result

in varying degrees of reduced market share. Some of the property associated with this industrial decline will be transitioned and the remainder will inevitably lose value and function (Bansal, Ochoa, & Kiku, 2016). The latter issue, hazard-exposure interactions, presents an equally challenging task of assessing future value in places that will experience unmanageable or very costly changes in hazard (Giglio, Maggiori, Rao, Stroebel, & Weber, 2021). Persistent inundation, relentless wildfires, and unquenchable droughts will transform where and how we live and operate our economy.

Ultimately, exposure is a numbers game. The more people and property exposed to climate hazards the greater the probability and degree of loss. One of the most salient examples of reducing exposure is a policy called managed retreat. Communities, governments, and organizations will reduce climate risk by relocating exposed units if there is enough exposure and a hazard becomes too frequent, too intense, or if the economics indicate relatively favorable conditions elsewhere (Hino, Field, & Mach, 2017; Siders, 2019). There is essentially no risk once people and property are out of harm's way. In line with the 'spatial fix' of globalization (Harvey, 2001), we will expand and restructure our society to fit a changing hazard landscape. ## Vulnerability {-}

Conceptual

Not all people and property exposed to climate hazards will exhibit the same outcomes throughout the disaster cycle. The basis of these differential outcomes is in vulnerability, which Tellman, Schank, Schwarz, Howe, & de Sherbinin (2020) define as the… 'propensity for loss of lives, livelihood or property when exposed to a hazard'. Our understanding of vulnerability has burgeoned from decades of risk-hazard research, e.g. White (1974), Hewitt (1983); Birkmann & Wisner (2006); Turner et al. (2003); Wisner et al. (2004); Adger (2006); Eakin & Luers (2006); Watts (2008), to name just a few. Social behav-

ior and situation moderate hazard event severity, i.e. negative consequences associated with a hazard event. Socioeconomic marginalization, faulty infrastructure, environmental degradation, and limited institutional support render communities at higher risk. The inverse of resilience and coping capacity, vulnerability has been conceptualized and operationalized with myriad sets of characteristics that comprise the susceptibility of a community to suffer harm from exposure to stresses and shocks.

Exposure and vulnerability have many overlapping aspects. For example, if exposure disparities are along socioeconomic and demographic lines, a disproportionate number of essential workers are from marginalized (i.e. vulnerable) groups, and if those two populations overlap, then societal dysfunction during hazard events becomes even more likely. This means that higher flood hazard in more vulnerable neighborhoods with a relatively higher proportion of essential workers could lead to critical staffing shortages in health, transport, and utilities during a major hurricane event.

Adjacent communities hit by the same climate hazard event may experience vastly different consequences due to variation in vulnerability among populations and places. The vulnerability paradigm was therefore a reaction to the realization that engineering accomplishments failed to protect people from loss and behavioral theories never fully captured the complexity and complications of human-environment interactions (Eakin & Luers, 2006). Risk models that account for vulnerability include Hazards-of-Place (HPM) (Cutter, 1996), Pressure and Release (PRM), Access (AM) (Wisner et al., 2004), shown in Figure **??**. A key similarity of these models is the recognition that there are factors predisposing us to greater risk beyond hazard, exposure, and mitigation thereof. HPM specifically accounts for biophysical and social vulnerability, although the biophysical aspect in this context is not so much vulnerability as it is exposure. Social vulnerability resembles a recipe within HPM, whereby each ingredient can be specified, measured, and

the result is greater than the sum of its parts. PRM considers vulnerability as a deterministic progression of contexts that produce unsafe conditions: disaster occurs when the root causes (e.g. racism), dynamic pressures (e.g. redlining), and unsafe conditions (e.g. poor stormwater infrastructure) coincide with intense hazard events. AM explicates disaster as a process and the societal factors comprising vulnerability serve as mediators and moderators of severity as well as dynamic elements at every stage along the disaster cycle.

AM best explains the reality of hazard events and consequences, yet it falls short of providing a succinct model for empirical testing. PRM is also theoretically compelling and serves as a considerate framework for qualitatively explaining the multi-level forces interacting to increase climate risk. HPM and it's related models, methods, and measurements have become the quantitative and governmental standard for social vulnerability research and policy. In all three of these models, social vulnerability determines how effectively communities are able to cope with and respond to hazards.

Empirical

Theoretically, greater social vulnerability increases loss from climate hazard events (Cutter, Boruff, & Shirley, 2003). This means that in a region impacted by the same hazard event, such as a hurricane, areas with higher social vulnerability likely experience more property and crop damage, injuries, and fatalities. Although this relationship generally holds across places and time, there are some specific dynamics which deserve mention. Vulnerability is a latent concept requiring the construction of an index or similar metric. Not all variables included in such metrics, such as the HPM-based Social Vulnerability Index (SoVI), are significantly correlated with dangerous outcomes (Tellman et al., 2020). Similarly, although SoVI (or another index) may positively correlate with disaster loss,

some variables comprising it may be negatively correlated. Other relationships may not be linear nor monotonic and could vary depending on the particular set of circumstances. Lastly, some relationships may vary over the disaster cycle, whereby a social vulnerability factor initially correlates positively and over time negatively, or vice versa.

Studies recommend looking at both an aggregate social vulnerability measure and at individual variables used to construct it when conducting vulnerability assessments (Spielman et al., 2020). To this end there are only a few large area, quantitative validations, but some studies have found certain associations with disaster loss for specific hazards (Bakkensen, Fox-Lent, Read, & Linkov, 2017; Rufat, Tate, Emrich, & Antolini, 2019; Tellman et al., 2020; Yoon, 2012; Zahran, Brody, Peacock, Vedlitz, & Grover, 2008). These studies typically build statistical models, e.g. OLS regressions, to infer significance, direction, and magnitude of relationships (Yoon, 2012), however other studies have begun introducing machine learning models for additional predictive power (Tellman et al., 2020).

There are two common ways to operationalize social vulnerability (Yoon, 2012). The deductive approach selects variables based on theory and empirical evidence of their relevance, e.g., Flanagan, Gregory, Hallisey, Heitgerd, & Lewis (2011). The inductive approach selects variables based on statistical relationships, e.g., SoVI from Cutter et al. (2003). Deductive approaches tend to standardize selected variables whereas inductive approaches utilize data reduction techniques such as Principal Component Analysis (PCA).

Organizations and government agencies across the US have utilized the concept and construction of social vulnerability in adaptation planning for at least a decade. In recommending social vulnerability indices (SVI) as a disaster preparedness and management tool for communities, the CDC has developed a construction method and resulting index

(Flanagan, Hallisey, Adams, & Lavery, 2018), which is based on a deductive approach. It consists of 15 census variables across four categories: a) socioeconomic status, b) household composition, c) race/ethnicity/language, and d) housing/transportation. Census tracts receive a nationally relative ranking for each category and for all categories combined.

SoVI, based on an inductive approach, was first introduced by Cutter et al. (2003) as a concise and measurable representation for the latent concept of social vulnerability to natural hazards. The hazards-of-place model forms the theoretical basis for SoVI, whereby physical hazard (e.g. 100-yr flood probability and depth) interacts with mitigation efforts (e.g. levees) to produce hazard potential, which varies by site (geographic location) & situation (natural and built environmental context) and is moderated by social fabric (Cutter, 1996; Cutter, Mitchell, & Scott, 2000). Social vulnerability is the product of these dynamics.

Constructing SoVI requires more than two dozen Census derived variables, including race/ethnicity, age, education, employment, income, poverty, home value, and renter tenancy. The methods developed and employed to estimate SoVI utilize PCA, which is a process for grouping weighted subsets of variables from a dataset into orthogonal components. These composite components are then subjectively assigned labels, such as socioeconomic status or housing, that characterize the variables grouped into that set. The SoVI value for any place is based on the summed components from a PCA, each of which is based on weighted sums of all variables included in constructing SoVI (Spielman et al., 2020; Tate, 2012).

As noted earlier, there are types of vulnerability beyond social. The IPCC breaks out dimensions of vulnerability for climate risk assessment into three broad categories: environmental, social, and economic (Cardona et al., 2012). Environmental factors in-

clude: physical site and situation, human-environment interactions, the built environment, level of development, spatial clustering, and urbanicity. Social factors incorporate: demographics, migration, displacement, marginalization, education, health, well-being, culture, institutions, and governance. Economic factors comprise income, tax revenue, savings, financial markets, debt-finance interactions, jobs, and livelihoods.

These factors range from individual to national and in some cases even global. When measuring vulnerability it is therefore vital to select the relevant set of factors for the outcome and geographic unit of interest. In the case of our focus, an individual to community level of analysis for the conterminous USA, many of the stated factors are not worth measuring. This could be due to sufficient similarity between geographic units or low correlation with the outcome at our level of analysis, such as financial markets and institutions. There are also factors that are either hard to operationalize or difficult to measure, such as culture.

In light of these limitations, it is sometimes sufficient to only measure aspects of vulnerability for which a researcher has data or considers more important in assessing a specific aspect of the risk profile. Data about physical context and economic situation, such as building hazard proofing and emergency management systems, hold great informative potential (Douglas, 2007). However, obtaining these data for large area analyses may not be feasible. In such cases, researchers might substitute these data for higher-level mediating variables and leverage statistical modeling techniques that control for spatiotemporally invariant variables.

The problems mentioned above are relevant to specifying and estimating vulnerability in climate risk models across any vulnerability factor and dimension. Despite these hurdles, the suggested modeling approaches provide an outline for achieving minimally biased model specifications that include one dimension of vulnerability. Our discussion has

been focused on social vulnerability to climate hazards since this is the only dimension of vulnerability considered throughout the dissertation. To that end, we focus on the modeling and interpretation of how social factors produce variation in loss outcomes across similar hazard and exposure levels. The data and methods required to include vulnerability factors from additional dimensions is beyond the scope of this research.

Climate Risk Perception

Everyone experiences some degree of risk. This is often represented as statistical risk, such as being twice as likely to die in the event of a traffic accident without a seat-belt. We typically derive statistical risk from observed, historical data related to risk event frequency and magnitude, among other metrics. However, people perceive this risk differently, even when provided with statistical risk estimates, according to subjective valuations (Slovic, 2000; Slovic, Fischhoff, & Lichtenstein, 1980). Therefore, statistical risk and perceived risk typically differ. The study of risk perception and the role it plays in risk assessment, specifically climate risk, sprouted from researchers noticing disparities in statistical and perceived risk for both common and rare hazards.

Concern over climate risk varies greatly across individuals and places. This variability, despite overwhelming scientific consensus on the causes and broad consequences of anthropogenic climate change, generates a great deal of interest in understanding the determinants and spatiotemporal patterning of climate change risk perception (CCRP). Explaining CCRP is of special interest to practitioners since it influences individual policy support for and behavioral intentions towards climate change mitigation and adaptation(Brody, Grover, & Vedlitz, 2012; Krosnick, Holbrook, Lowe, & Visser, 2006; O'Connor, Bord, & Fisher, 1999; Smith & Leiserowitz, 2014). Scholars have developed

several theoretical and methodological approaches to explain these differences, i.e., what determines risk perception. These largely fall into three categories.

1. anthropological: cultural theory of risk (CTR)
2. sociological: social amplification of risk (SARF) and social representations theory (SRT)
3. psychological: psychometric paradigm

The cultural theory of risk (Douglas, 2004) posits that the way an individual relates to society influences their cultural worldviews, which in turn determines risk perception. Sociological theories (SARF and SRT) emphasize the role of social networks and influential social institutions, such as the media, in disseminating and shaping risk perceptions at the individual and societal levels (Kasperson et al., 1988; Moscovici, 1984). Amplification and representation of risk often influences governmental policies, individual behaviors, and resource distributions, which we have seen in excellent display during the COVID-19 pandemic. The psychometric paradigm, a brainchild of the quantitative revolution, asserts that risk perception, and the variability explaining factors therein, can be measured, statistically modeled, and predicted, preferably at the individual level (Slovic, 1987). Psychometric models typically operationalize risk perception as a cognitive process that is guided by a set of heuristics (mental shortcuts). This model of risk perception lends to methodological coherence for studying perception of quantifiable risks–climate hazards are a good example.

Several theories have bolstered the psychometric paradigm, such as bounded rationality (Kahneman, 2003). Complete risk information is rarely available, risk tolerance differs, past experience matters, and other factors constrain perceptions (e.g. emotions). These additional parameters help guide individual choice beyond convenient decision tools and optimal outcomes. Extensions of this framework include models of satisficing, whereby

individuals seek at least some satisfactory minimum outcome (Brown & Sim, 2008), and preference, such that risks are tolerated if associated benefits are preferable (Lusk & Coble, 2005). However, individuals may accept a risk despite the level of risk being unacceptable, as determined by some standard, e.g., accepting low housing costs in a 100-year floodplain.

Understanding what determines risk perception is important for several reasons. The first is to better understand which statistically high risk issues people tend to perceive sparingly, which informs risk communication programs (McCarthy, Brennan, Boer, & Ritson, 2008). A clearer idea of risk perception determinants also helps to crystallize the mechanisms operating within behavior change models (Brewer, Weinstein, Cuite, & Herrington, 2004). Information on which types of risk people discount and the probability of changing either perception or behavior can then be used for policy and planning purposes (Slovic, Fischhoff, & Lichtenstein, 1982).

One of the highest profile topics with the starkest differences between perceived and statistical risk is climate change. It poses multiple, massive risks to humans across many aspects of society, including food and water shortages (Gosling & Arnell, 2016; Wheeler & Braun, 2013), property destruction from extreme weather events (Hsiang et al., 2017), and mass population displacement (Sherbinin et al., 2011). Despite such high projected statistical risk at both the individual and global levels, climate change risk perception varies vastly among individuals (Maibach, Leiserowitz, Roser-Renouf, & Mertz, 2011). In the US, it has historically been much less of a priority when compared to other risks, terrorism for instance (Motel, 2014). Yet, perceptions of climate change as a high risk issue that should be addressed have increased over the past decade (Funk & Kennedy, 2020).

Figure **??** presents several theoretical models to explain CCRP variation and the factors

that influence it over time and across places. These models vary both in structure and content. Models (a) (Xie, Brewer, Hayes, McDonald, & Newell, 2019) and (b) (Bradley, Babutsidze, Chai, & Reser, 2020) posit that risk perception serves as a mediator among relationships for a set of factors (knowledge, affect, etc.) and outcomes, such as behavioral willingness and psychological capacity to adapt to climate change. Model (c) (Echavarren, Balžekienė, & Telešienė, 2019) does not consider factors such as knowledge or emotions. Model (d) (van der Linden, 2017) proposes a general schema for how external perceptions and societal pressures influence individual risk perception. As with any model, there are issues. Some models omit potentially important variables, e.g., demographics (a). Most do not consider selection effects, such as risk perception influencing residential exposure if individuals select out of places with high climate change risk (b). However, they do provide a general understanding of the way risk perception researchers think about relevant factors and the relational structure for model building.

Climate Hazard Inequalities

Inequality is generally understood as the unequal distribution of some element, climate hazards in this case, across place and population (Allison, 1978). Research on inequality tends to focus on methods for measuring it and theories on how it forms. Some applied and empirical studies address questions of justice, equity, or a related topic, while others inform how inequality affects a phenomenon under examination. Measuring inequality depends on how a researcher chooses to define it. Once defined, several measurement considerations include spatiotemporal scale, population weights, distribution sensitivity, and relational orientation. These technical problems are most relevant when comparing measures of inequality across units, but could even be considered when assessing inequal-

ity within a unit. Spatiotemporal scale concerns the ecological fallacy, which describes the problem of incorrect inferences due to aggregation (Ash & Fetter, 2004; Piantadosi, Byar, & Green, 1988), and stationarity bias by assuming that relationships are stable over space and time.

Population weights influence the intensity of inequality and the robustness of the inequality measure (Boyce, Zwickl, & Ash, 2016). Say we estimate an inequality statistic, such as the Gini coefficient, for units A and B, with populations 10k and 100k respectively and each with 10 sub-units. If we do not account for population but instead estimate inequality by spatial hazard distribution across sub-units, we may find that unit B has more hazard inequality. However, if we weight for population, it could instead be true that unit A, with a more spatially dispersed population, has greater hazard inequality. Regarding robustness, if we estimate the distribution of individual-level hazard between unit A and B for two groups, white and non-white, we may find greater inequality in A. Yet this finding could be due to a smaller sample size and make the inference statistically insignificant.

The relational orientation of an inequality metric can be either vertical (across the variable being measured) or horizontal (across the population) (Boyce et al., 2016). Vertical metrics include the Gini coefficient and the Theil index. Horizontal modes of comparison typically look at the distribution for a variable of interest for different groups of a population characteristic such as poverty, race/ethnicity, and other demographic variables of public concern. Distributional sensitivity refers to how an inequality metric responds to changes at different segments of the distribution. Some metrics are more sensitive to changes in the middle of a distribution whereas others may respond more strongly to changes at the tail ends (Atkinson, 1970; Duro, 2012). Choosing the appropriate metric thus requires considering what kind of relationship inequality has with climate risk. If

reducing extreme hazard creates greater equality then we would choose a metric sensitive to changes in the tails.

From the theoretical side, the definition of inequality has evolved over time from an outcome-oriented (e.g. income) to opportunity-oriented (e.g. early life circumstance) perspective. This is similar to the distinction between inequality and inequity. There are elaborations of this, such as Sen (2000) capabilities and functionings distinction, whereby individuals may have the opportunity to achieve some outcome but society is not structured in a way that allows for this realization. Theories on inequality tend to focus on the formation and navigation of opportunity structures that produce unequal outcomes.

Walker (2011) proposed an environmental justice theory that distinguishes inequalities in three interacting categories: distribution, procedure, and recognition. Distribution relates to the variable being measured, e.g. climate hazards, clean air and water, green space, and nutritious food, etc. Procedure concerns the social pathways for addressing inequalities in distribution, e.g. free and fair access to legal and political systems. Recognition refers to social acceptance and attention towards the distributional inequality, e.g. respectful media coverage and official designations of injustices. These distinctions highlight that inequalities form and exist across social dimensions beyond just the distribution of a climate hazard. Each community facing distributional inequalities does not have equal capacity for remediation. Without procedural capabilities, communities have less power in decision making processes to reduce inequalities. This affords them less respect and perceived credibility, thus crippling their capacity to gain recognition of the impacts. This chain of inequalities produces a positive-feedback loop, thereby generating greater inequality often disproportionately and cumulatively against marginalized groups, in line with theories of cumulative advantage (DiPrete & Eirich, 2006).

Another theoretical approach proposed by PELLOW (2000), environmental inequality

formation (EIF), emphasizes, "(a) the importance of process and history, (b) the role of multiple stakeholder relationships, and (c) a life-cycle approach to the study of hazards". The EIF model suggests that environmental inequalities form when stakeholders bargain for access to and control of scarce resources. In the case of climate hazard distributions across households, the scarce resource is housing. The more advantaged in a society will have greater opportunity to live in less hazardous homes. Inequalities may also result from seemingly pro-justice decisions and policies with consensus from multiple stakeholders but without recognition of inequalities arising from unintended consequences, collateral damage, or among the most marginalized. Those with abundant social and economic resources have the highest likelihood to reduce exposure to climate hazards. For the less advantaged, inequalities might produce a parallel system of social opportunity through status segmentation and physical displacement. Status segmentation occurs when resource accumulation is not equitable, social and environmental 'bads' are disproportionately experienced, the modes of procedural participation are asymmetric, and recognition of challenges are avoided. These exclusions expand into housing and labor markets, which results in physical displacement. Marginalized groups, often low-income and racial/ethnic minority communities, are thus relegated to 'ecological sacrifice zones' (Bullard, 2011).

Inequalities could therefore manifest unintentionally as a result of complex processes comprising antagonistic stakeholders seeking power and scarce resources. Another way inequalities develop is through discrimination, which pervades every aspect of US society. It is practiced on the basis of race, ethnicity, gender, sexual orientation, age, disability, and class. Oftentimes, discrimination is overt and the consequences profound. Black women are three to four times more likely to die during pregnancy than white women (Chaves et al., 2018). Black individuals are twice as likely to be unemployed

and earn 25% less when employed (Bertrand & Mullainathan, 2003). These disparities exist across countless metrics and for many other marginalized communities. Systemic discrimination leads to greater inequalities, further marginalization, and, partial or total disenfranchisement from opportunity structures.

Historically in the United States, socially vulnerable populations had been systematically disenfranchised in housing markets, notably through a practice known as redlining, whereby socially 'risky' neighborhoods were deemed bad investments (Aaronson, Hartley, & Mazumder, 2017). The practice began in the 1930s when the Home Owners' Loan Corporation (HOLC) drew maps socio-spatially demarcating the investment risk profile of neighborhoods. Redlining has traditionally been understood as the unjustifiable discriminatory practice of refusing to provide or limiting credit in predominantly racial/ethnic minority neighborhoods. This has limited the ability that communities of color have for wealth generation through home ownership and segregated many into neighborhoods lacking social, health, and infrastructural services has had devastating, long-term repercussions. Redlining is a model example of discrimination-based inequalities resulting in disenfranchisement. A more detailed definition from the Interagency Fair Lending Examination Procedures:

"Redlining is a form of illegal disparate treatment in which a lender provides unequal access to credit, or unequal terms of credit, because of the race, color, national origin or other prohibited characteristic(s) of the residents of the area in which the credit seeker resides or will reside or in which the residential property to be mortgaged is located. Redlining may violate both the Fair Housing Act and the Equal Credit Opportunity Act." (*Interagency Fair Lending Examination Procedures*, n.d.)

The Fair Housing Act and related redlining prevention and restitution policies have been established because applicants were routinely denied loans on the basis of racial/ethnic

background. Lenders selected out of investing in 'risky' neighborhoods, those lined in red ink on the map (Woods, 2012). It should be noted that some dispute exists about whether HOLC maps were a root cause of discriminatory lending (Hillier, 2003). Redlining has traditionally been acknowledged in a mortgage lending context, however many other types of discriminatory practices resembling redlining exist in housing markets and beyond. The term could generally refer to any systematic discriminatory practice towards racial/ethnic minorities in the provision of resources on the basis of neighborhood of residence. Other examples of redlining include homeowners insurance (Squires, 2003; Squires, Velez, & Taeuber, 1991), labor markets (L'Horty, Bunel, & Petit, 2019), and credit cards (Cole, 2011). Long-term impacts include increased segregation that peaked around 1970, and decreases in home ownership, house values, and credit scores (Aaronson et al., 2017).

Despite regulations signed into law against redlining and related discriminatory mortgage lending practices more than fifty years ago, housing market inequalities persist. Quillian, Lee, & Honoré (2020) recently found that in the mortgage market… "black and Hispanic borrowers are more likely to be rejected when they apply for a loan and are more likely to receive a high-cost mortgage, conditional on loan approval. [Their] meta-analysis of studies of racial disparities in the mortgage market suggests that discrimination in loan denial and cost has not declined much over the previous 30–40 years, a disturbing finding." This disheartening description of the persistence of discriminatory lending practices does not bode well for impacts to come from changing climate hazard. Rising seas, stronger hurricane winds, more frequent floods, and uncontrollable wildfires will exacerbate the disproportionate redistribution of resources and risk in an already inequitable system.

Socially vulnerable communities already bear a bigger share of previously unknown hazard exposure as we improve our climate risk estimates. Data from Fathom, the research

organization advancing flood hazard modes, has helped to reveal hazard disparities on race, ethnicity, income, and other demographic characteristics. The share of hidden flood exposure for minority residents in over two-thirds of states is higher than the state average. Neighborhoods with predominantly African American residents in Chicago and Fort Lauderdale have flood exposure that is 30 and 36 percentage points higher than previous estimates (Flavelle, Lu, Penney, Popovich, & Schwartz, 2020). Around 87 percent of paid flood claims between 2007 and 2017 in Chicago occurred in predominantly minority communities (Briscoe, 2020).

Tying Climate Risk Concepts Together: A Guide for this Dissertation

There is a sprouting phenomenon synthesized from a couple of trends that connect the concepts discussed in this review. First, the acknowledgment of climate change as necessitating adaptive risk management has become ubiquitous in most sectors of the economy. Second, access to, and quality of, property-level climate risk information has improved substantially in recent years. With these improvements, both households and organizations are gaining access to tools and recognizing the importance of managing their climate risk. Residential housing markets are among those sectors that have begun to exhibit adaptive risk management behaviors, particularly in where people choose to live. The most alarmed, dissatisfied, and risk averse to climate change will select out of places with high climate risk, as long as they have sufficient social opportunity. Developers, mortgage lenders, and insurance writers–housing services firms–will also choose to disinvest in those places as a risk management strategy. This process may create greater climate hazard disparities in housing markets along socioeconomic lines. Historic disen-

franchisement from housing markets and the newer trend of climate lining–a potential term for systemic disinvestment in and depopulation of places with high and increasing climate hazard–will likely compound to increase social and environmental inequalities to the disadvantage of already marginalized groups.

Researchers have only just begun documenting how these trends, such as out-migration of the socially advantaged and disinvestment from housing services firms, might serve as adaptive risk management solutions for climatically risky places. There is broad recognition that these processes will occur in some form and in some places (Hino, Field, & Mach, 2017; Siders, 2019). However, many questions remain unanswered and even unaddressed, specifically how multiple climate risks interact with these trends over large areas, the relationship between historical housing market disenfranchisement and current climate risk exposure, whether historical trends in housing data suggest neighborhood sorting on climate risk, and what happens to housing markets as information on climate risk improves. The most socially vulnerable may find themselves literally and financially underwater.

This already occurs with flood risk and the NFIP. Bakkensen & Ma (2020) "find clear evidence that low income and minority residents are more likely to move into high risk flood zones." This means the reciprocal is also true, at least for flood risk; individuals with socioeconomic advantage have moved and will continue to move out of harm's way. Systemic disinvestment will follow suit as housing services firms apply better climate risk estimates in their algorithmic, data-driven decision-making processes. Many communities will inevitably be left lacking the necessary infrastructure, investment, and insurance to mitigate consequences from climate hazard events (O'Neill & O'Neill, 2012). Although this dissertation does not explicitly study climate lining, we hope that the chapters lay some groundwork for understanding the current state of climate risk dimensions

determining the trajectory of this phenomenon. We believe it may be one of the greatest impacts from climate change at a household level across the world. It will be particularly problematic in higher income countries where the relative human suffering may evoke less visceral reactions than places with absolute devastation resulting in innumerable 'climate refugees'.

Each chapter utilizes climate hazard estimates for addressing distinct aspects of the literature reviewed in this introduction. Hazards are generally estimated as multi-year averages of extreme event frequency and intensity. The second chapter, 'Modeling Social Vulnerability Determinants of Disaster Loss,' estimates the relative contribution of social indicators to variability in disaster loss. In this chapter we draw from the vulnerability literature to model the relationship among consequence, hazards, and vulnerability. The consequence we focus on is disaster loss, which includes property and agricultural damage from a hazard event. Vulnerability comprises social indicators such as poverty, racial/ethnic status, and primary mode of transport. Our goal in modeling this relationship is to validate specifications of the vulnerability parameter by hazard type for the climate risk equation. This chapter aims to primarily address the following gap in the literature: Which non-hazard factors moderate variation in outcomes when a hazard event occurs?

The third chapter, 'Mapping Climate Hazard Inequalities,' assesses the social and spatial distribution of climate hazards by comparing multiple types of inequality metrics. In this chapter we use measures and methods from the inequality literature to describe different manifestations and aspects of climate hazard inequalities. By doing so we can tease apart whether, for which groups, and where inequalities exist for each climate hazard. This chapter aims to primarily address the following gap in the literature: How do climate hazards distribute over people and places?

The fourth chapter, 'Measuring Climate Risk Perception with Twitter Data,' builds a dataset of socio-cognitive characteristics from user-generated social media data. Our aim is to test whether a novel data source and set of methods can be used to construct measures that would traditionally be gathered through a survey instrument. The implication of this type of validation is that additional data sources can supplement surveys to better represent a target population, offer higher spatiotemporal resolutions, and provide access to harder to measure characteristics such as social networks. This chapter contributes to answering a central research question in climate risk perception research: Which factors determine differences between perceived and statistical climate risk? However, it primarily focuses on the measurement of those factors and borrows theoretical specifications from previously published articles.

Climate risk is an increasingly important area of study due to climate change, the rate of population and economic growth, and widening social inequalities. The fields of risk research on climate hazards have evolved over time from only estimating physical hazard and structural solutions, then accounting for individual and organizational decision making as a determinant of exposure, and eventually considering the multidimensionality of vulnerability to negative consequences resulting from hazard events. These paradigm shifts in selecting factors for climate risk assessment happened alongside developments in modeling the determinants of risk perception as well as the implications for deviations between statistical and perceived risk. The unequal distribution of climate risk among marginalized groups and places has garnered scientific and policy attention to mitigate inequitable outcomes over the next several decades.

Appendix

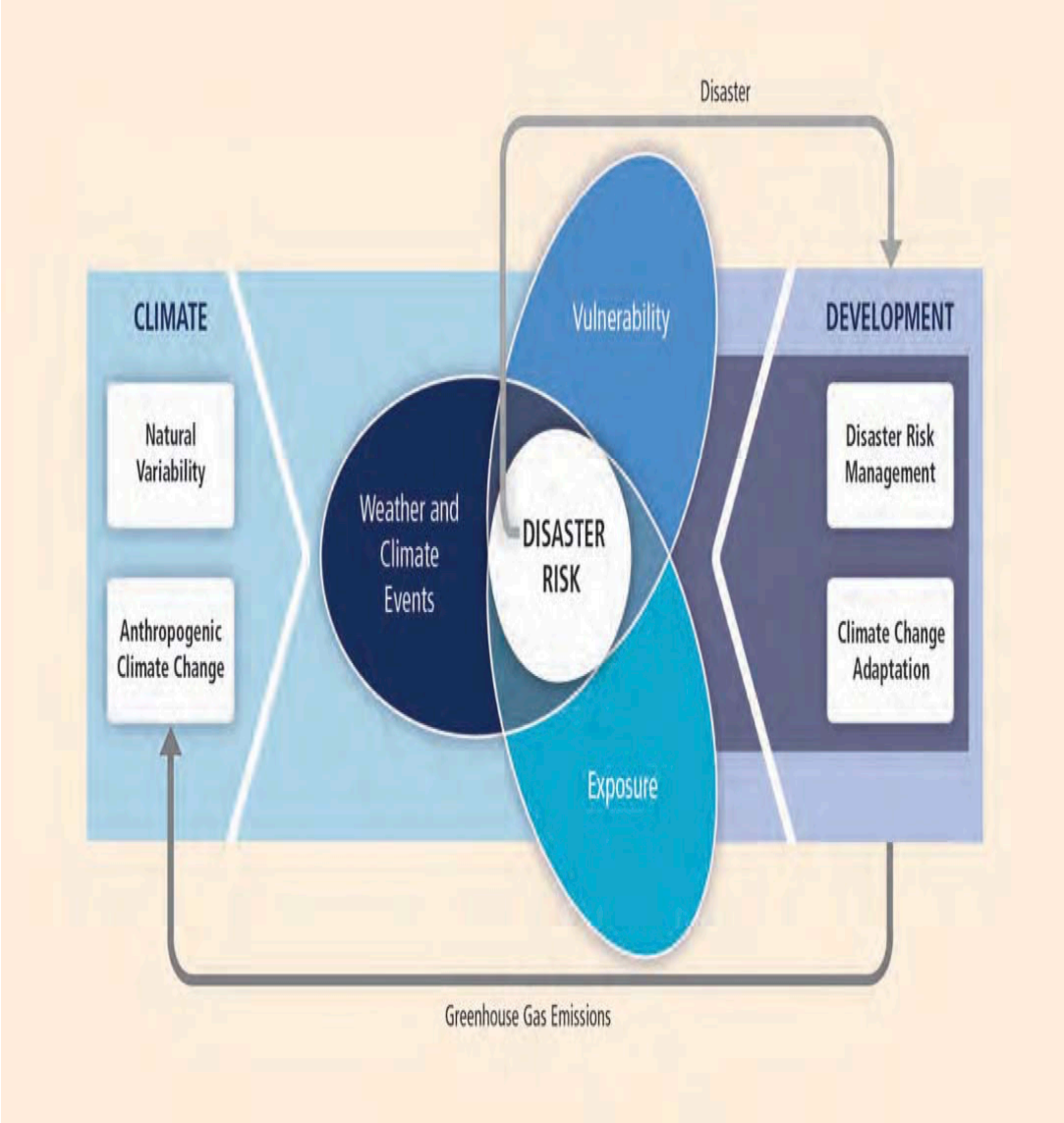

Figure 1.1: IPCC disaster and climate risk model where risk is a function of hazard, exposure, and vulnerability Kron (2002).

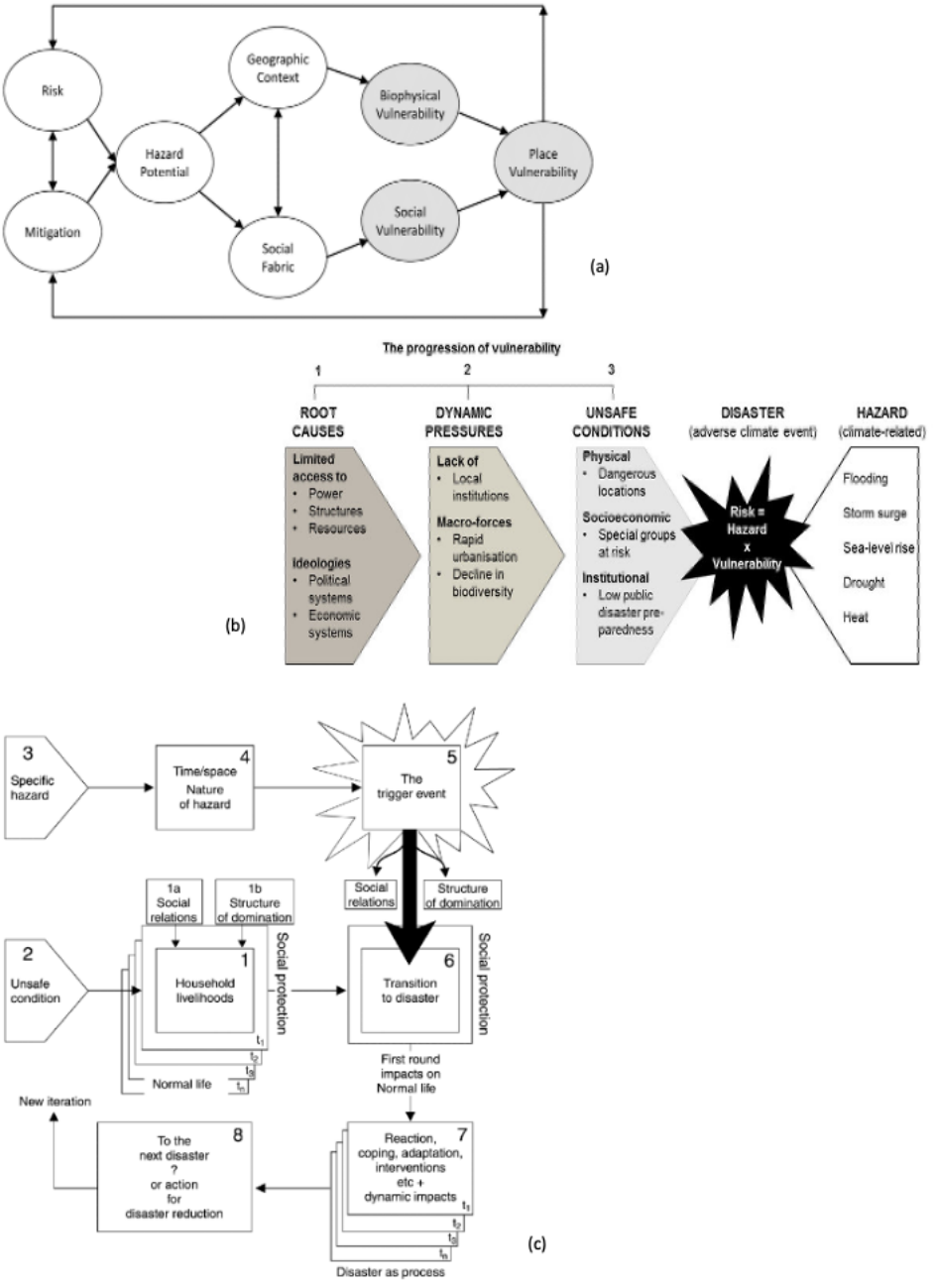

Figure 1.2: Risk models that account for vulnerability include Hazards-of-Place (HPM) Cutter (1996), Pressure and Release (PRM), Access (AM) Wisner et al. (2004). A key similarity of these models is the recognition that there are factors predisposing us to greater risk beyond hazard, exposure, and mitigation thereof.

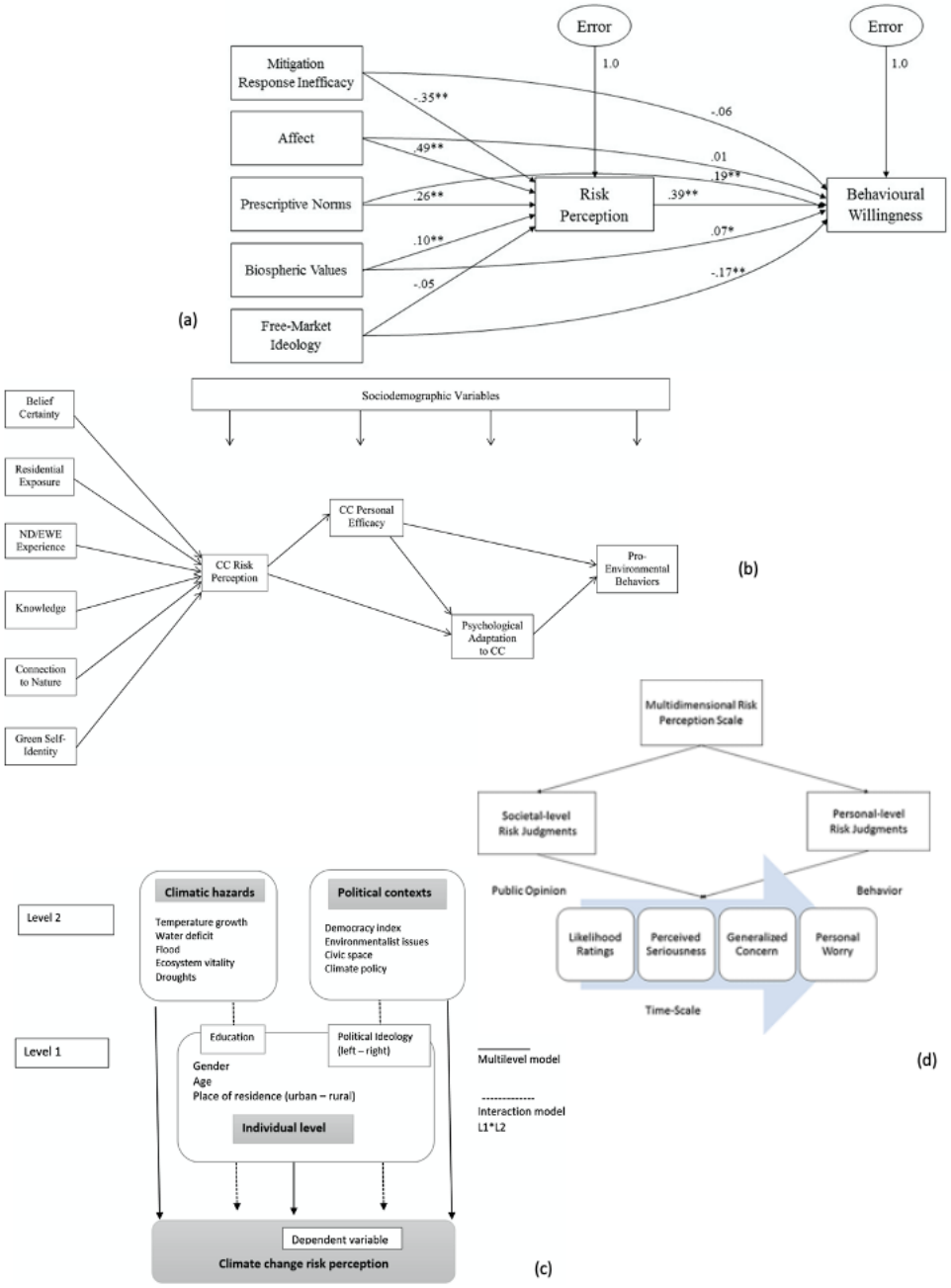

Figure 1.3: Climate Change Risk Perception Models. Models (a) Xie et al. (2019) and (b) posit that risk perception serves as a mediator among relationships for a set of factors (knowledge, affect, etc.) and outcomes, such as behavioral willingness and psychological capacity to adapt to climate change. Model (c) Echavarren et al. (2019) does not consider factors such as knowledge or emotions. Model (d) van der Linden (2017) proposes a general schema for how external perceptions and societal pressures influence individual risk perception.

Chapter 2

Modeling social vulnerability determinants of disaster loss

A common outcome of climate hazard events is disaster loss, which is moderated by social vulnerability. To understand which social vulnerability factors have the largest moderating effect, many studies model the relationship among social vulnerability, climate hazard, and disaster lossa. This study validates social indicators that have been identified in the literature and in practice as influential for moderating adverse outcomes from environmental hazards. We first demonstrate that social vulnerability indices, measures for aggregating multiple social indicators into one variable, are not internally consistent as values range drastically when including different input data nor are they theoretically consistent since the relative contribution of each indicator to index values also changes. We then build several statistical models of the relationship between climate hazard, social vulnerability, and disaster loss in order to examine which social indicators are the strongest predictors of loss. Our results suggest that climate risk modeling should account for social vulnerability and that the relative contribution of social indicators varies

across hazards. Context also appears to be important, whereby certain indicators may represent a larger explanatory share of outcome variation, in this case loss, depending on the levels of other indicators and model parameters.

Introduction

A common outcome of climate hazard events is disaster loss, which is moderated by social vulnerability. To understand which social vulnerability factors have the largest moderating effect, many studies model the relationship among social vulnerability, climate hazard, and disaster loss. These studies aid in understanding the disaster process and mitigating disaster loss. However, vulnerability-hazard-loss studies typically exhibit at least one of several issues, including climate hazard-agnostic construction of social vulnerability indices (SoVI); samples with few hazard events; omission of climate hazard measurement; and looking at climate hazards and/or social vulnerability in aggregate. Respectively, the presence of these weaknesses in the study designs result in lack of: transferability, since SoVI construction is sensitive to input data selection; generalizability, considering that hazard events and the affected areas may be significantly idiosyncratic; interpretability, because there is no observable relationship between disaster loss and hazard exposure; and applicability, as discrete climate hazards and social vulnerability factors require different adaptive actions.

We address these issues in the conterminous United States by validating the the role of social vulnerability in climate risk modeling. Data comes from the US Decennial Census and American Community Survey on social indicators, government and academic extreme sources related to climate hazards (precipitation, extreme heat, drought, wildfire, and flooding), and the Spatial Hazard Events and Losses Database for the United States

(SHELDUS). Our solutions to the aforementioned problems include: a climate hazard-specific SoVI construction; a large sample of hazard events; explicit measurement and modeling of climate hazards; and a hazard-specific disaggregation of explained variance from social vulnerability indicators on disaster loss. Climate hazards we study include extreme precipitation, extreme heat, drought, wildfire, and flooding. We first test the internal and external validity of the SoVI in a climate hazard-specific context. Then we run a series of statistical models on the relationship between disaster loss and social vulnerability while controlling for climate hazard. Our primary research goal is to explain the climate hazard-specific relative importance of individual social vulnerability factors in constructing a SoVI and moderating disaster loss. To achieve this we ask the following research question per climate hazard:

Research questions

How does the social vulnerability index vary by input data selection? Is there a statistically significant relationship between disaster loss and social vulnerability for each climate hazard? Which social indicators contribute most to the social vulnerability index and disaster loss outcomes?

1. How do SoVI values and factor-level relative contributions vary by input data selection?
2. Which social vulnerability indicators are most important in moderating disaster loss?
3. Is there a statistically significant relationship between disaster loss and social vulnerability?

Disaster mitigation helps reduce loss by tailoring plans to specific climate hazards. Wild-

fire mitigation strategies rely on ecosystem science-based fuels reduction and prescribed burn strategies alongside residential developments built to withstand extreme temperatures (Schoennagel et al., 2017). Flood mitigation requires extensive depth pattern mapping and implementing defense infrastructure (Wilby & Keenan, 2012). Social vulnerability reduction targeting is likely also hazard-specific. Many studies either disregard the individual variables used to construct social vulnerability indices or address them only in a descriptive manner. Instead, we examine the importance of each SoVI variable to better understand how vulnerability manifests for different hazards both as a latent measurement through index construction as well as in the applied context of disaster loss. Since disaster loss depends not only on climate hazard and social vulnerability but also on other characteristics, such as the built environment and institutions, we control for these to reduce specification error (specifically omitted variable bias) in modeling the relationship between social vulnerability and disaster loss while controlling for climate hazards.

We hypothesize that social vulnerability increases the probability of disaster and the associated loss at any level of climate hazard and that the social factors most impacting disaster outcomes can be addressed with in-place adaptation planning, e.g., by improving transportation infrastructure as opposed to moving the elderly away from a hazard. This would mean that reducing social vulnerability could always be a priority in an adaptive risk management context and that there are discrete ways in which this can be done.

Literature Review

Disasters often occur when the root causes (e.g. racism), dynamic pressures (e.g. redlining), and unsafe conditions (e.g. poor stormwater infrastructure) of social vulnerability

coincide with intense hazard events (K. Smith, 2013; Wisner et al., 2004). There are myriad disaster losses generated by climate hazards. Conditions ripe for disaster outcomes are not necessary for these losses to occur, but typically increase loss probability and severity. Loss categories implicated by climate hazards include commodities (e.g. crops), fixed assets (e.g. buildings), wellbeing (e.g. air quality), and human life, among others. Each type of hazard produces different types of loss, however there is broad overlap. Tangible hazards (wildfire and flooding) can feasibly result in almost any type of loss while intangible hazards (temperature, precipitation, and drought) tend to not impact fixed assets. In our context, and since the disaster loss database we utilize only measures 'direct losses' (property and crop damage, injuries, and fatalities), we focus on these for the remainder of this study.

Social vulnerability, the propensity of social systems to suffer harm from exposure to external stresses and shocks, determines how effectively communities are able to cope with and respond to climate hazards. Human activity therefore moderates hazard severity, i.e. losses accrued. Living in exposed areas, building faulty infrastructure, and limiting the quality and availability of institutional support often renders communities at higher climate risk, disaster probability and loss from the interaction of hazard, exposure, and vulnerability.

Theoretically, greater social vulnerability increases disaster loss from climate hazards (Cutter et al., 2003). This means that in a region impacted by the same hazard event, such as a hurricane, areas with higher social vulnerability likely experience more direct losses. Although this relationship generally holds across places and time, there are some specific dynamics which deserve mention. The first is that not all variables included in constructing indices such as SoVI are significantly correlated with disaster loss (Tellman et al., 2020). Similarly, although SoVI may positively correlate with disaster loss,

some variables comprising it may negatively correlate. Other relationships may not be monotonic and vary depending on the particular set of circumstances. Lastly, some relationships may vary over the disaster cycle, whereby a social vulnerability factor initially correlates positively and over time negatively, or vice versa.

Constructing SoVI requires more than two dozen Census derived variables, including race/ethnicity, age, education, employment, income, poverty, home value, and renter tenancy. The methods developed and employed to estimate SoVI utilize Principal Component Analysis (PCA), which is a process for grouping weighted subsets of variables from a dataset into orthogonal components. These composite components are then subjectively assigned labels, such as socioeconomic status or housing, that characterize the variables grouped into that set. The SoVI value for any place is based on the summed principal components, each of which is based on weighted sums of all variables included in constructing SoVI (Spielman et al., 2020; Tate, 2012).

Studies recommend looking at both an aggregate social vulnerability measure and at individual variables used to construct it when conducting vulnerability assessments (Spielman et al., 2020). To this end there are only a few large area, quantitative validations, but some studies have found certain associations with disaster loss for specific hazards (Bakkensen et al., 2017; Rufat et al., 2019; Tellman et al., 2020; Yoon, 2012; Zahran et al., 2008). These studies typically build statistical models, e.g. OLS regressions, to infer significance, direction, and magnitude of relationships (Yoon, 2012), however other studies have begun introducing machine learning models for additional predictive power (Tellman et al., 2020).

As mentioned, there are one or more methodological issues facing existing studies that attempt to validate social vulnerability variables in disaster loss outcomes. Climate hazard-specific SoVI construction is almost never conducted as most research uses the

classic SoVI variable set and includes all possible geographies (Cutter et al., 2003; Gaither et al., 2011; Lehnert, Wilt, Flanagan, & Hallisey, 2020; Spielman et al., 2020; Tellman et al., 2020). Studies that use hazard event occurrence and magnitude do sometimes gather a large sample of hazard events, but others will look at only one or a few events (Fekete, 2009; Finch, Emrich, & Cutter, 2010; Rufat et al., 2019). Others do not measure hazard magnitude (Bakkensen et al., 2017).

In terms of explicit measurement and modeling of independent and interactive climate hazard, there are studies that account only for average climate hazard (Emrich & Cutter, 2011; Gaither et al., 2011), hazard events (Tellman et al., 2020), or neither (Bergstrand, Mayer, Brumback, & Zhang, 2015; Cutter et al., 2003; Lehnert et al., 2020; Nelson, Abkowitz, & Camp, 2015). The latter group fails to measure or incorporate climate hazard exposure while either modeling the relationship to disaster loss or investigating some aspect of social vulnerability in a climate hazard context, although there are usually no explanatory claims. We found no studies modeling interactive climate hazard.

Hazard-specific disaggregation of explained variance from SoVI (and the variables used to construct it) on disaster loss is rarely done. Those that have done so usually refer to the approach as validation (Bakkensen et al., 2017) and conduct it for a singular hazard (Rufat et al., 2019; Tellman et al., 2020). These are the most similar studies to our efforts, however there is still room for improvement, as outlined earlier. For example, Tellman et al. (2020) only investigates flooding at the county level and without an average climate hazard measure. Robust estimates of causal effects are limited in the literature since generalization is difficult due to unique selection processes operating across diverse combinations of social context and climate hazards. These limitations apply even to the most clever natural experiments (Frankenberg, Laurito, & Thomas, 2014).

Beyond studies that attempt to explain the vulnerability-hazard-loss relationship, there

are many providing other types of information, such as spatially descriptive analysis (Bergstrand et al., 2015; Emrich & Cutter, 2011; Lehnert et al., 2020; Spielman et al., 2020; Tate, 2012); SoVI sensitivity analysis across a variety of construction methods (Spielman et al., 2020; Tate, 2012); and non-loss outcomes such as population redistribution from wildfires (Hammer, Stewart, & Radeloff, 2009), Hurricanes Andrew (Smith & McCarty, 1996) and Katrina (Donner & Rodríguez, 2008), and sea level rise in Louisiana (Hauer, Hardy, Mishra, & Pippin, 2019).

Data and Methods

Our approach involves matching disaster loss, climate hazard, and social vulnerability indicators at the census tract level. We focus on direct economic loss (property damage, crop loss, etc.), five climate hazards (extreme precipitation, extreme heat, drought, wildfire, and flooding), and a set of over twenty social vulnerability indicators. The first analytical task compares how SoVI rankings and the relative contributions of social vulnerability indicators vary when including different geographic subsets– hazard-specific places of higher exposure. Then we build several statistical models testing the association between social vulnerability and disaster loss.

Climate hazards

To estimate climate hazard we first determine the relevant spatial unit of analysis and integrate many datasets to comparable spatial and temporal scales. Climate model output (precipitation and temperature) come from tens of internationally accepted global climate models which have been validated as part of the Coupled Model Intercomparison Project Phase 5 (Taylor, Stouffer, & Meehl, 2012). Researchers have downscaled

these data to higher resolution across the US by utilizing local information (e.g. weather patterns, hydrodynamics, etc.) and leveraging the empirical linkages between coarse resolution and fine resolution climate. We use the downscaled data products to produce high spatiotemporal resolution estimates of general climate risk for a given raster cell. Other hazards (drought, wildfire, and flooding) use these climate averages as input data alongside myriad other data sources (terrain, vegetation, soil type, etc.) in more complex modeling frameworks to estimate water scarcity through supply and demand relationships, fire weather and burn probabilities, and flood depths and return intervals, respectively. Figure **??** displays the climate hazards we estimate and the average climate hazard aggregated at the tract level. Table 2.1 provides summary statistics. @ref(#climate-hazard-estimation) offers a detailed explanation of how we estimate each climate hazard.

Social vulnerability

We measure social vulnerability with data from the US Decennial Census and American Community Survey (ACS). These data are available at the Census Tract level, which is typically around 8,000 people (there are approximately 73,057 Census Tracts in the US). We rely on the Cutter et al. (2003) implementation to construct SoVI and make comparisons to the CDC index when appropriate. Table 2.2 contains summary statistics and Figure **??** maps SoVI and a subset of social factors across the US.

Disaster loss

We derive disaster loss from the Spatial Hazard Events and Losses Database for the United States (SHELDUS) (CEMHS, 2020), which provides annual county-level disaster

loss estimates for multiple natural hazards from 1960 to 2020. These estimates comprise the response variables for our statistical models. Years 2001-2020 were chosen for two reasons. The first is that we matched disaster loss at each observation year with corresponding social vulnerability indicator estimates from the Census and five year ACS. Sub-five year ACS releases do not typically target Census Tracts. For years and variables without inter-decadal ACS estimates, we did a linear interpolation between the two closest dates. The second reason is that we use disaster loss relative to GDP and Census Tract, which we calculate by dividing county-level disaster loss by GDP and weighting by tract-level area and population size. These county-level GDP data are available for years 2001-2020 and come from the Bureau of Economic Analysis (BEA) (BEA, 2021). This process is shown for the state of Oregon in 2.7. We look exclusively at property damage and crop loss across the following hazards specified by SHELDUS, which we aggregate to match the broader hazard categories we study:

1. **Storm**: lightning, severe storm/thunder storm, tornado, winter weather, wind, fog, hail
2. **Heat**: heat
3. **Wildfire**: wildfire
4. **Drought**: drought
5. **Flooding**: coastal, flooding, hurricane/tropical storm, landslide

Rank correlation

We estimate Spearman's rank correlation coefficient for each social factor and climate hazard (see Figure 2.5). Darker blue (towards 1) represents a stronger positive correlation and darker red (towards -1) represents a stronger negative correlation. An X in the cell represents a non-significant relationship at the 0.01 level.

The strongest positive correlation is between renter and minority and the strongest negative correlation is between income and SoVI. Among social factors and climate hazards, the strongest positive correlation is between minority and drought while the strongest negative correlation is between minority and flood. This means that tracts with a higher proportion of minorities tend to have higher drought risk and lower flood risk.

Internal and theoretical consistency

We adapt methods from Spielman et al. (2020) to assess the internal and theoretical consistency of SoVI in a climate hazard context. SoVI construction follows methods used in Spielman et al. (2020), which extends upon methods established by Cutter et al. (2003), Schmidtlein, Deutsch, Piegorsch, & Cutter (2008), and Tate (2012). This uses Principle Components Analysis with a varimax rotation to construct thematic *components* of input variables (e.g. race/ethnicity, housing, etc.). Components with eigenvalues greater than or equal to 1 contribute to the final index.

For each hazard, we bin census tracts by 2050 hazard risk (terciles) to experiment with how including different input data impacts the sensitivity of relative SoVI ranks for census tracts, known as *internal consistency*. For example, how does the state-wide rank of a census tract in North Carolina change when including data for: (a) all US census tracts, (b) census tracts in the same hazard tercile across the the US, (c) census tracts for the FEMA region containing North Carolina, and (d) only census tracts in North Carolina.

To test *theoretical consistency*, we again look at different scopes for constructing SoVI. For each of these census tract-level input datasets, we first calculate the variable-wise contribution to SoVI. Using the expected contribution for each variable from the literature, we test how the variable contribution direction changes with each SoVI calculation. Variables are ranked by contributions after each SoVI estimation run.

Hazard-specific determinants of vulnerability

Our analysis on theoretical consistency ranks variables by relative contribution to SoVI for each climate hazard. However, estimates from the PCA used to construct SoVI do not present a rigorous enough way to infer the relative importance of social factors across climate hazard contexts. To build upon this, we assess the relative influence of SoVI and social vulnerability indicators on disaster loss outcomes by fitting separate models for each type of climate hazard. Our goal is to further identify the most important social factors determining vulnerability for each climate hazard. Per hazard, each final dataset for every statistical model is an annual, Census Tract-level panel with the average climate hazard, total disaster loss, and social vulnerability indicators (typically proportions or averages). We convert all continuous variables to Z-scores with mean 0 and standard deviation 1.

Our level of analysis remains at the census tract across all models and the primary outcome variable is relative disaster loss, derived from the SHELDUS data described earlier. We find the relative disaster loss per county by dividing the estimated disaster loss by the county Gross Domestic Product, both of which are deflated to 2012 dollars. We then refine the spatial resolution to the census tract by weighting relative disaster loss estimates by population size and area. The first model looks at the annual probability of experiencing disaster loss for census tract i in year t:

$$logit(P_{it}) = H_{it}\beta_H + X'_{it}\beta_X$$

Where P is the probability of disaster loss, H is hazard exposure, and X' is a vector of social vulnerability factors, such as income, race/ethnicity, and unemployment. Figure 2.8 displays the average annual probability of disaster loss across levels of hazard exposure, bound by 95% confidence intervals. We chose a logistic model since the outcome is

binary; that is, whether a census tract experienced disaster loss in any given year. Tables 2.7 provides regression results for our logistic models across each hazard and compared to the null model (excluding social vulnerability indicators).

The second modeling experiment explores the way vulnerability manifests across different climate hazards. We first match census tracts on demographic similarity using Coarsened Exact Matching (CEM) (Iacus, King, & Porro, 2012). A similar purpose to the commonly used method of Propensity Score Matching (PSM), CEM divides our sample into treatment and control groups. PSM relies on a score to assign observations to either group whereas CEM coarsens variables and matches observations according to the coarsening. The treatment group in this case contains census tracts with high hazard exposure and the control group are census tracts with low hazard exposure.

With the census tracts matched, we derive demographic profiles for communities with highest climate risk, as measured by the most vulnerable to high hazard exposure and the least resilient to low hazard exposure. To do this we separately estimate impacts of climate hazard exposure on disaster loss for the treatment and control groups in each matched strata, which is the CEM term for a group of similarly matched units (census tracts). We apply third-order polynomial transformations to the hazard exposure estimates to account for non-linearity in the response, which we model as the natural logarithm of disaster loss so that fractional changes are equivalent.

We find the census tracts with highest climate risk by iteratively selecting units with both the largest climate hazard effect and the smallest difference in climate hazard coefficients for the independently estimated treatment and control models. Explained analytically, we select the first n matched units across each of two ranked value sets, the treatment group effect (descending) and the effect difference between groups (ascending).

We then run two multivariable fractional polynomial (MFP) models–a semi-automatic

approach to estimating non-linearity in multivariate models (Zhang, 2016)–one each for the treatment and control groups, per hazard. Each MFP model allows up to four degrees of freedom per term to flexibly estimate the relationship between social vulnerability on disaster loss for census tract i and year t:

$$ln(L_{it}) = FP_{SoVI}(SoVI_{it}) + H_{it}\beta_h + \epsilon_{it}$$

Where the dependent variable $ln(L)$ represents the natural logarithmic transformation of disaster loss, H is hazard exposure, and social vulnerability is modeled as FP_{SoVI}. MFP models iteratively evaluate for non-linear and non-significant relationships between the dependent and independent variables and each non-linear term found is represented as:

$$FP_H(H_{it}) = \beta_1 H_{it}^{p1} + \beta_2 H_{it}^{p2} + \beta_3 H_{it}^{p3} + \beta_4 H_{it}^{p4}$$

MFPs are effective at modeling odd tail-end behavior and capturing non-linear effects of weather variables on economic outcomes such as crop yields (Blanc & Sultan, 2015), which are included in our disaster loss estimates. It restricts the polynomial power terms to a small predetermined set of values, which can be both integers and non-integers, allowing models to produce a wide array of curve shapes without the necessity of estimating powers (Ambler & Benner, 2015). Figure 2.10 shows disaster loss on the y axis across levels of social vulnerability per hazard, bound by 95% confidence intervals. The x-axis shows absolute changes in the social vulnerability index. These curves demonstrate the influence of social vulnerability on disaster loss between exposure categories.

Our last set of models estimates the influence of social vulnerability factors on on disaster loss outcomes while controlling for climate hazard using a two-way fixed-effects model for census tract i and year t:

$$ln(L_{it}) = f_H(H_{it}) + X'_{it}\beta + \lambda_i + \phi_i t + \epsilon_{it}$$

Where the dependent variable $ln(L)$ represents the natural logarithmic transformation

of disaster loss, H is hazard exposure, X' is a vector of social vulnerability factors, λ are tract fixed effects which account for time invariant differences between tracts that we do not observe, such as soil type, topography, and disaster management. ϕ are time period fixed effects which control for unmeasured idiosyncrasies within tracts over time such as gradual changes in the built environment and disaster mitigation infrastructure. These fixed effects are added to control for past and present climate hazard management. Crucially, these fixed effects capture variability in disaster loss associated with tract-level differences in relevant local dynamics. Fixed effects demean the dependent variable, transforming our hazard exposure variables into estimates of exogenous shocks (Blanc, 2017). After comparing the AIC and BIC for several polynomial expressions (quadratic, cubic, and quartic), we chose to model the explanatory variable H as a third-order polynomial:

$$f_H(H_{it}) = \beta_1 H_{it} + \beta_2 H_{it}^2 + \beta_3 H_{it}^3$$

Figure 2.11 illustrates disaster loss across levels of climate hazard exposure, bound by 95% confidence intervals. Disaster loss values on the y axis above 1 represent loss that is relatively greater than tract level GDP. The x-axis shows absolute changes in hazard exposure.

The typical statistics used to compare non-linear models are the Akaike and Bayesian Information Criteria, AIC and BIC respectively. Neither statistic can be interpreted independently and a lower value is preferable when comparing values across models as this indicates lower out of sample prediction error. We also use the proportion of explained deviance, a pseudo R2 measure for non-linear models. We also made sure there was minimal multicollinearity among the covariates in all of our models, which led us to remove 11 variables from the statistical analysis. Variable inflation coefficients were used to assess multicollinearity by determining whether a false positive would be interpreted

due to high correlation with one or more covariates.

Spatial autocorrelation is a common problem to consider when modeling data with a spatial component. This is because it violates the assumption of independent and identically distributed observations (in space), which biases the statistical estimates. In our case, all of our variables are positively spatially correlated, which can be found with Moran's I, a global measure of spatial autocorrelation. The Moran's I statistic indicates the degree of linear spatial association between the variable of interest x and spatially weighted averages vector of neighboring values W_x, where W is the summed spatial weight matrix w_{ij} which formalizes the adjacency structure of the dataset (Moran, 1948). The Moran's I statistic is computed as:

$$I = \frac{N}{W} \frac{\sum_{i=1}^{N} \sum_{j=1}^{N} w_{ij}(x_i - \bar{x})(x_j - \bar{x})}{\sum_{i=1}(x_i - \bar{x})^2}$$

With N as the total number of spatial units, all for reference unit i and comparison units j. Values usually range from -1 to 1. The closer the statistic is to 1, the greater the degree of positive spatial autocorrelation while a value closer to -1 indicates stronger negative spatial autocorrelation. We found the highest degree of spatial correlation with the disaster loss data, since the loss estimates were equally distributed across affected counties, next are climate hazards (flood being the lowest and storm the highest), and lastly the social vulnerability indicators. Systematic subsampling can address spatial autocorrelation within our modeling framework, whereby we sub-sample Census Tracts at sufficient spatial separation (either in terms of distance or degree of neighbor) such that the resulting observations are mostly spatially uncorrelated. . The variogram, a tool to find an optimal distance for sample filtration, defines co-variation as a function of spatial distance. We used half the range of the variogram, which is the distance under which the sample is spatially autocorrelated. Sample sizes for each climate hazard can be found in Table 2.4.

Results

Our primary goal in this research is to validate the role of social vulnerability indicators in moderating disaster loss from climate hazards. To do so we modeled the annual relationship among disaster loss, climate hazard, and social vulnerability. Prior studies with similar goals have omitted climate hazard estimates, modeled social vulnerability indicators and climate hazards in aggregate, and used generalized indices for social vulnerability. Our approach has produced results to this end across several analytical tasks, both descriptive and inferential. We first used Principal Components Analysis (PCA), a dimensionality reduction technique, to estimate the Social Vulnerability Index (SoVI) across different geographic scales and samples. With these different samples we conducted tests on measurement validity for both internal and theoretical consistency. The next task employed a statistical matching method known as Coarsened Exact Matching (CEM) to identify community archetypes, with which we then modeled the relationship between climate hazard and disaster loss to select the highest climate risk strata as indicated by high climate hazard-driven disaster loss and low resilience provided by social factors. Lastly, we built several statistical regression models to test the added explainability on disaster loss that social vulnerability indicators provide.

Hazard-Specific SoVI Measurement Validity

By repeating SoVI estimation experiments for all US Census Tracts (a) and then for Census Tracts by risk terciles of each hazard (b), FEMA region (c), and state (d), we observe, as input data varies, shifts in the relative SoVI ranking for census tracts within a state. We demonstrate the large variation in relative ranking as we switch the scope, and amount, of input data by using the state of North Carolina. We estimated SoVI

eight times for each Census Tract, which are then ranked statewide. Out of 2192 census tracts in North Carolina, over 748 tracts vary in rank by over 500 places. The maps by hazard in Figure 2.6 display the relative ranking for census tracts in North Carolina. SoVI has questionable internal consistency as a latent construct of social vulnerability since the value and relative rank for an administrative unit depends on the geographic scope. We demonstrate similar results to Spielman et al. (2020) by looking at the range in SoVI rankings for hazard specific contexts.

Table 2.3 displays results on theoretical consistency. We sort social indicators by the average rank in contribution to SoVI across all the runs. When using all census tracts within the conterminous US, four variables exhibit different contribution directions than expected ('Per Capita Income', 'Group Quarters', 'Unemployed', and 'Multi-Unit Housing'). The variables with the most reversals in direction (how many times they differed from the expected direction) are Unemployed and Multi-Unit Housing. The variables with the highest and lowest average ranks are, respectively, 'Per Capita Income' and 'Renter'. 'Age Dependence' has the smallest range in relative ranks.

Climate Risky Communities

The CEM procedure results in about 80 strata, which means 160 models in total across high and low climate hazard exposure groups. Control variables include the full set of social vulnerability factors. Presented in Figure 2.9 are the top three community archetypes per hazard. These sets represent socio-demographic compositions with both the greatest association between climate hazard and disaster loss and least difference in outcomes between high and low social vulnerability. The most notable result here is for flood, which represents similarly composed communities that tend to be right around average across social vulnerability indicators.

Validating Social Vulnerability across Hazards

Across all models our regression analyses found better model fits, using AIC and BIC as the metric, when including social vulnerability indicators. Regression output is provided in Table 2.7, Table 2.13, and Table 2.16. Similarly, looking at the difference in proportion of explained deviance, we find better model explainability for those including social vulnerability indicators. The best performing type of model are the two way fixed effects models of disaster loss, with predicted curves and output in Figure 2.11 and Tables 2.16, which we find by summing the proportion of explained variance for the models including social vulnerability indicators. The logistic models of disaster loss probability are the next best performing (curves in Figure 2.8 and output in Tables 2.7) while the multivariable fractional polynomials of disaster loss between high and low climate hazard groups were the poorest performing (curves in Figure 2.10 and output in Table 2.13).

Climate hazards are a statistically significant predictor of disaster loss in almost all models except for the MFP analysis on heat and drought. The hazard-specific model with the best performance is the TFE model for heat. However, the relationship between heat and disaster loss is negative, which contradicts hypotheses about greater hazard producing higher loss. For positive hazard-loss relationships, the highest performing model is logistic for drought. The climate hazard that has the strongest relationship with disaster loss is the MFP model for flood in the high climate hazard group. Across all model types the strongest relationship is for drought, but this hazard is not significant in the MFP model sets. The hazard that is significant across all model sets with the strongest average relationship with disaster loss is flood. The hazard with the weakest relationship is wildfire. Hazards holding disaster loss relationships inconsistent with theory (i.e. negative) are storm, heat, and the aggregate climate hazard.

There are no social vulnerability indicators that always have a positive (meaning a unit increase in the SVI is associated with increased loss) or negative (meaning a unit increase in the SVI is associated with decreased loss) and statistically significant relationship with disaster loss. The indicators with the most consistent positive relationship are poverty, living in group quarters, uninsured, no high school diploma, and renters. Those with the most consistent negative relationships are crowded housing, age dependency, population density, mobile homes, and no vehicle. The social vulnerability indicator that has the strongest average positive relationship with disaster loss across all model types is percent uninsured while that with the strongest negative is the age dependency ratio. Relationships with the lowest effect size include minorities and disabled. Taking just the average effect from positive and negative coefficients, the strongest relationships are group quarters and the age dependency ratio, respectively. The effect direction for SoVI is inconsistent across models as well.

Discussion

These results offer evidence that social vulnerability plays an essential role in moderating disaster loss from the climate hazards of extreme precipitation, extreme heat, drought, wildfire, and flooding for the conterminous USA. The average increase in explained variation among all models was about double when including social vulnerability indicators as opposed to the null model that just accounted for climate hazard. The hazard holding the strongest positive associations with disaster loss are flooding and drought. For social vulnerability indicators it seems to be percent living in group quarters and uninsured. Flood risk does have a theoretical and empirical relationship with these variables, particularly group quarters (Khunwishit & McEntire, 2012; Lowe, Ebi, & Forsberg, 2013).

People living in group quarters do not own their property and therefore are unable to invest in risk insurance and mitigation. Furthermore, not having health insurance (percent uninsured) likely correlates with not having homeowners insurance to help recoup after a hazard event.

We did not focus on whether including individual social vulnerability indicators improved model specification over an aggregated metric such as SoVI, which has been shown in numerous studies (Rufat, Tate, Burton, & Maroof, 2015; Spielman et al., 2020; Tellman et al., 2020). Instead, we focused on validating which aspects of these social vulnerability profiles were most important across each climate hazard.

Despite evidence supporting the hazards of place model and social vulnerability as an essential term in the climate risk equation, it is also the case that indicators are not consistent predictors of disaster loss across different hazards. Effect directions and magnitude additionally vary by model type. It may further be true that indicators provide inconsistent prediction even within hazard type but for different hazard events. Although we haven't explicitly tested for this in the present study, the results suggest it is likely the case. The reason these dynamics exist is due to variability in aspects we weren't able to measure.

Aspects include differences in hazard mitigation among places, ranging from large infrastructure projects to household hardening, and across time, since we used over two decades of hazard events in our panel. Although we attempted to control for this in our two way fixed effects models, there is certainly some degree of variability still unexplained by these factors. Even so, the TFE models did achieve the best model performance. Other reasons may be specific to event characteristics (temporality, intensity, areal extent, etc.) that result in disparate relationships with social vulnerability indicators.

Culprits beyond the theoretical reasons why social vulnerability indicators are not con-

sistent predictors of disaster loss are the methodological issues with our approach. The hazard loss data that we use is at the county level, which has been equally assigned across all affected counties by the data provider. We then extrapolated to the census tract, both of which might present problems. There is also the possibility of omitted variable bias by not including hazard mitigation factors. Furthermore, we use an overall hazard risk instead of explicitly modeling the characteristics of each hazard event that produced loss. Other papers have included approximations of hazard event characteristics in their modeling with similar discrepancies across vulnerability indicator-loss relationships (Tellman et al., 2020).

Perhaps communities facing similar climate hazards exhibit greater convergence of SoVI values, relative rankings of SoVI, and variable contributions to both SoVI and explaining disaster loss, yet it appears that is not the case. Our results highlight the need for place, community, and hazard-specific vulnerability assessments. If relying on SoVI, adaptation planning for any climate-sensitive hazard will generate vastly different recommendations depending on which populations are included in the construction of the index. For example, if the goal is to conduct capacity building on five targeted social factors, we would likely consider a different set of factors for every unique set of census tracts included in the analysis. We can see this in Figure **??**, which highlights the average relative contributions to SoVI and disaster loss explained variance. Even the recommended direction and degree for influencing any social vulnerability indicator will vary by the scale, scope, and scenario of the mitigation plan.

Conclusion

Our study supports the inclusion of social vulnerability in climate risk modeling. Indicators comprising the latent concept of social vulnerability are evidently significant and robust in a statistical modeling framework. However, this conclusion does not give a good idea as to the relationship direction and magnitude under varying hazard and exogenous conditions. We recommend several ways to attain a better sense of how exactly these indicators relate to disaster loss and the climate risk model. First, include data on hazard mitigation. This could come from a range of sources, including government repositories such as the National Inventory of Dams, FEMA FIRM maps, state and local climate action plans, and private data from the insurance industry. Second, include an overall hazard risk alongside event specific measurements. It is not possible to correctly measure event characteristics for every event sampled, but an overall hazard risk can provide added explanatory support. Third, utilize higher spatial resolution disaster loss data that is accurately spatially attributed. We believe a more rigorous and reliable modeling framework will result from implementing these recommendations. Only when enough studies consistently validate social vulnerability indicators would it be reasonable to recommend that institutions focus resources towards them for disaster loss mitigation. Localized studies of specific hazards still likely provide the best evidence to support mitigation planning.

Appendix

Table 2.1: Climate hazard summary statistics. Values range from 0 to 100.

varNames	mean	sd	median	min	max
Extreme Precipitation	60.43	22.04	68.66	0.0	98.93
Extreme Heat	52.26	22.08	53.94	0.0	100.00
Drought	35.85	24.27	31.00	0.0	96.00
Wildfire	19.88	14.61	19.00	0.0	84.00
High tide flood	4.90	15.87	0.00	0.0	100.00
Inland flood	60.29	16.35	62.64	0.0	99.80
Storm surge flood	4.75	15.98	0.00	0.0	100.00
Composite flood	63.65	17.48	65.57	0.0	100.00
Climate	46.41	8.68	47.36	10.6	73.56

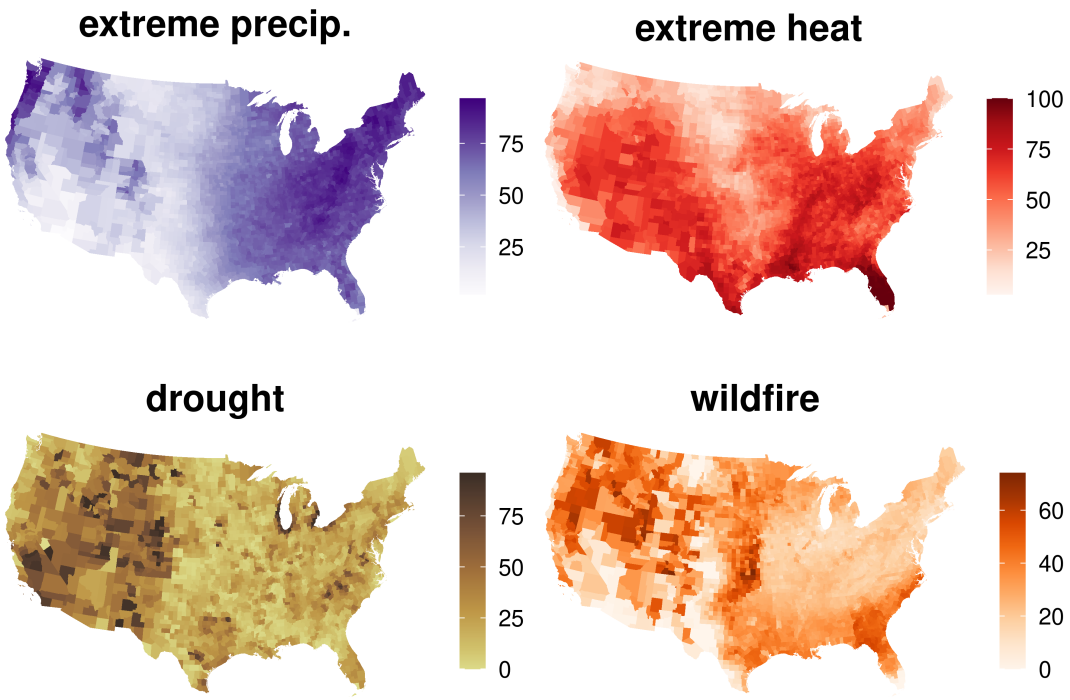

Figure 2.1: County-level climate hazards. Values range from 0 to 100.

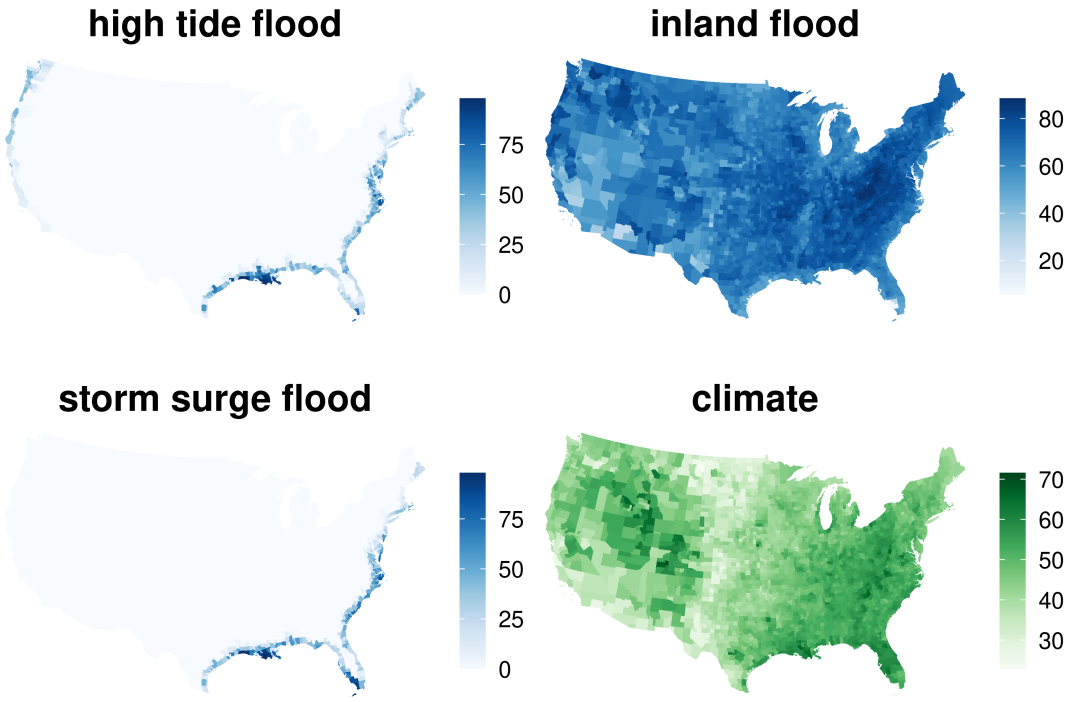

Figure 2.2: County-level climate hazards. Values range from 0 to 100.

Table 2.2: Social Vulnerability Indicator Summary Statistics

varNames	mean	sd	median	min	max
Age Dependency (pct)	0.44	0.14	0.44	0.0	1.75
Crowded Housing (pct)	3.52	5.18	1.80	0.0	100.00
Disability (pct)	13.28	5.96	12.50	0.0	100.00
Group Quarters (pct)	2.67	9.54	0.20	0.0	100.00
Limited English (pct)	4.14	6.81	1.30	0.0	100.00
Minority (pct)	38.22	29.88	29.80	0.1	100.00
Mobile Home (pct)	6.02	10.73	0.70	0.0	100.00
Multi-Unit Housing (pct)	12.26	18.46	4.50	0.0	100.00
No High School (pct)	13.10	10.49	10.30	0.1	100.00
No Vehicle (pct)	9.32	12.22	5.20	0.0	100.00
Per Capita Income	32082.59	16967.81	28438.00	0.0	227064.00
Population Density	5406.16	11960.15	2258.08	0.0	263992.73
Poverty (pct)	15.31	11.87	12.20	0.1	100.00
Renter (pct)	46.90	25.15	43.60	1.1	99.90
Singe Parent (pct)	9.19	6.43	7.80	0.0	100.00
Unemployed (pct)	6.42	4.63	5.30	0.1	100.00
Uninsured (pct)	9.32	7.10	7.60	0.0	100.00
Social Vulnerability Index	50.00	28.78	50.00	0.0	100.00

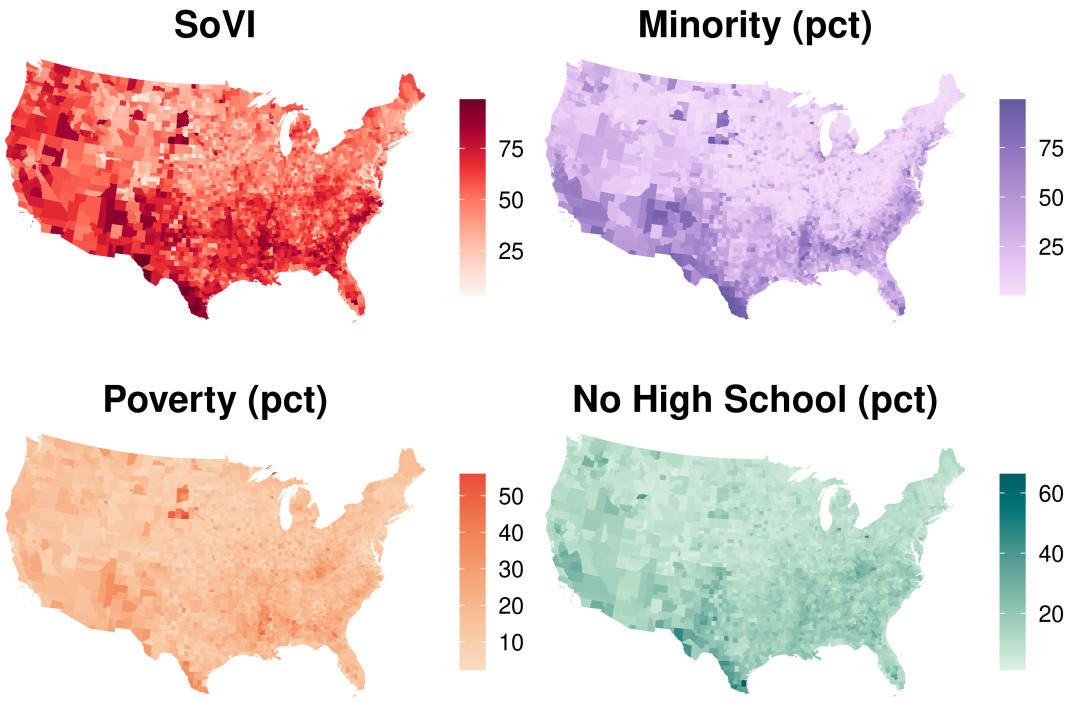

Figure 2.3: County-Level Social Vulnerability Index (SoVI) and indicators.

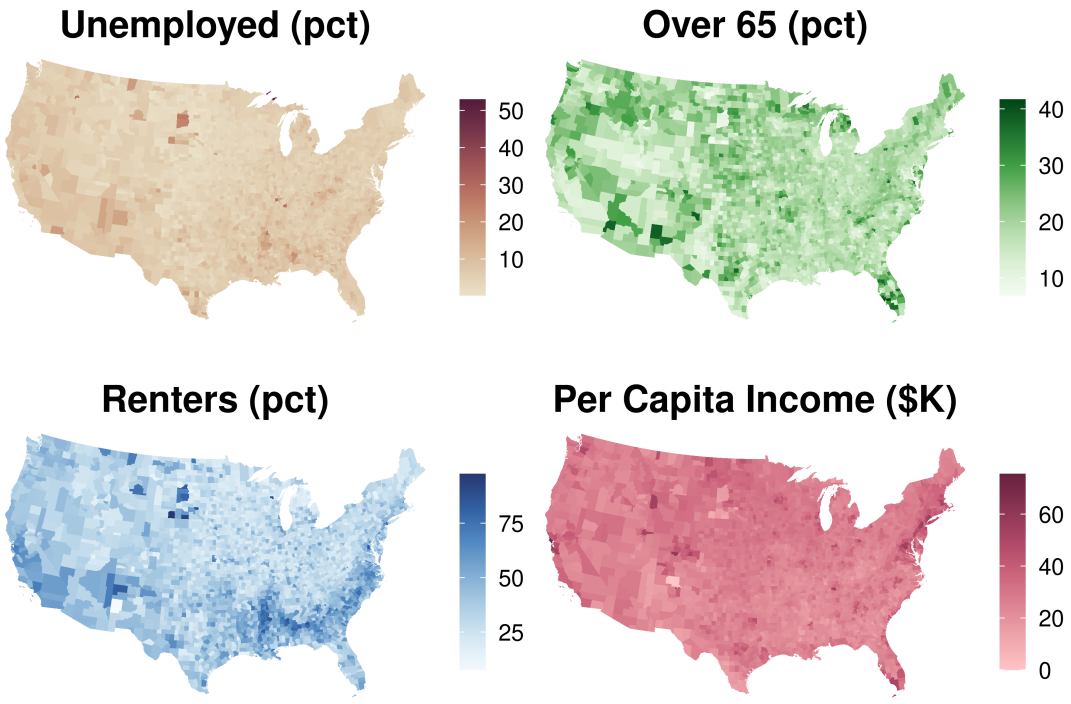

Figure 2.4: County-Level Social Vulnerability Index (SoVI) and indicators.

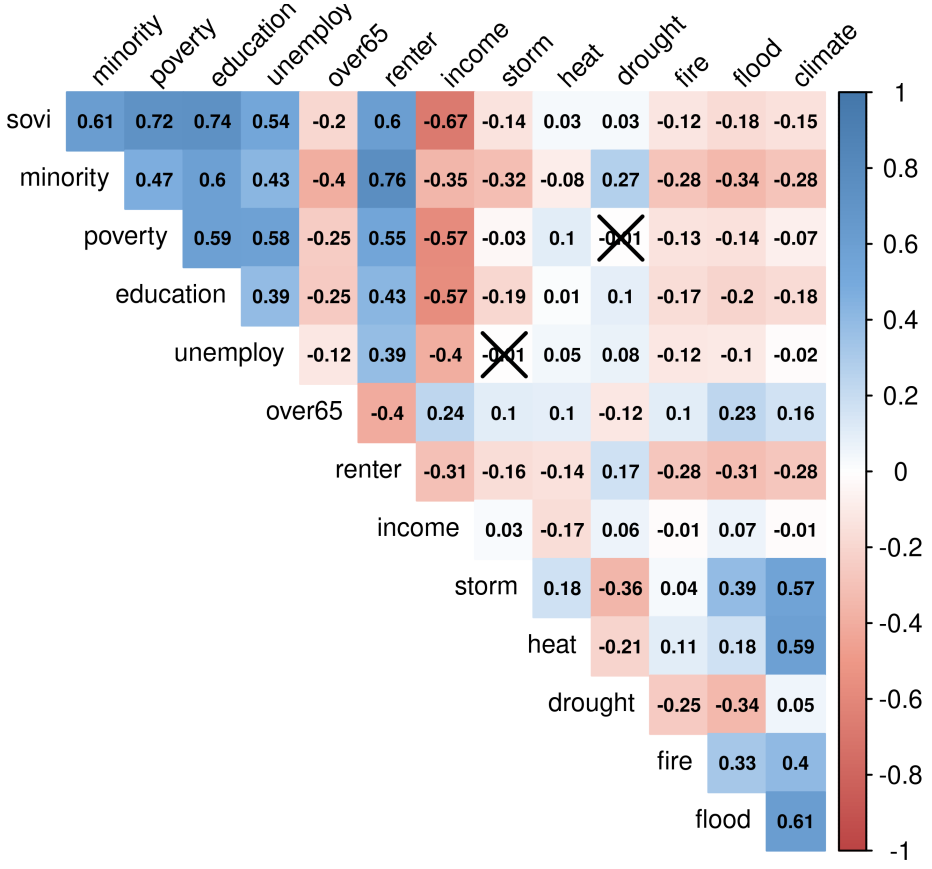

Figure 2.5: Spearman's Rank Correlation matrix among climate hazards and social vulnerability indicators.

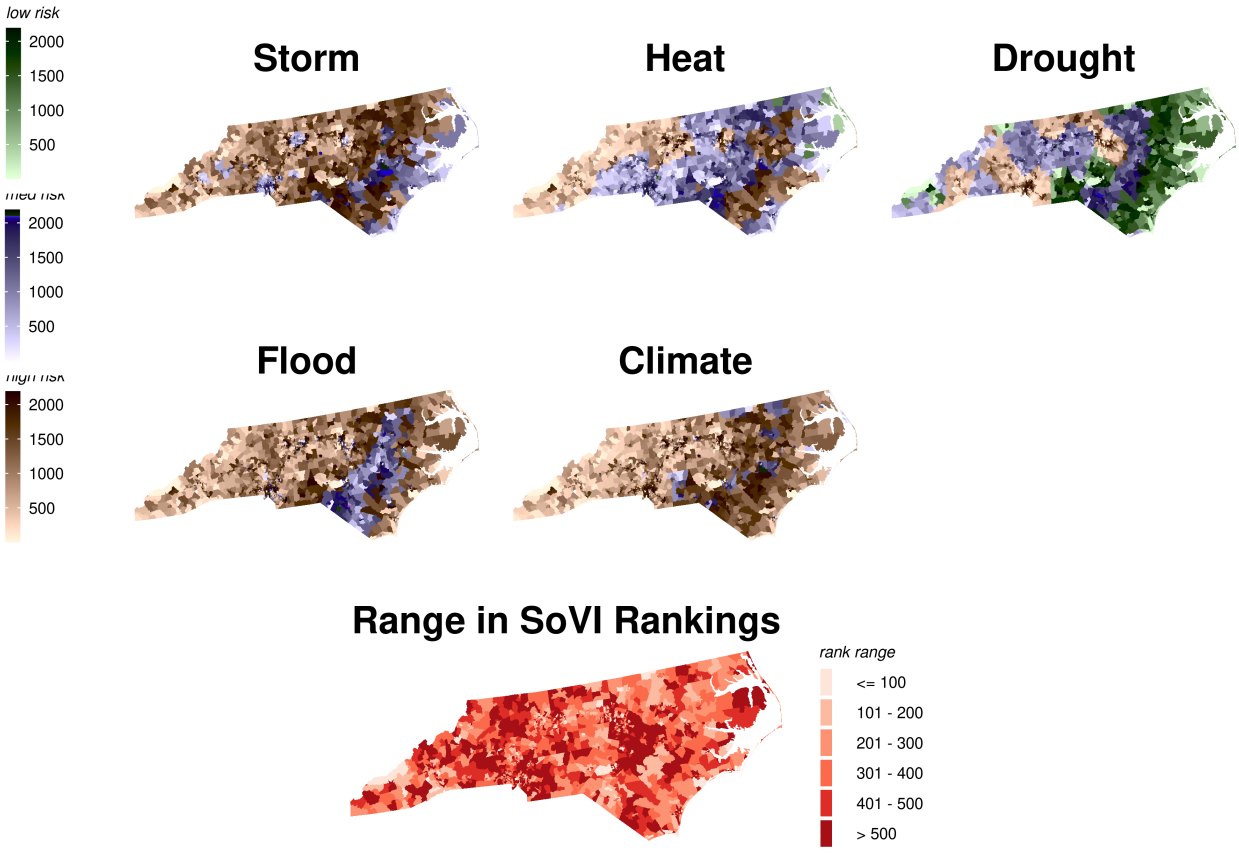

Figure 2.6: Census Tract Vulnerability Rankings per Hazard Grouping for North Carolina. By repeating SoVI estimation experiments eight times: for all US Census Tracts (a), for Census Tracts by risk terciles of each hazard (b), FEMA region (c), and state (d), we observe, as input data varies, shifts in the relative SoVI ranking for census tracts within a state. The relative ranking varies greatly as we switch the scope, and amount, of input data. Ranked statewide, out of 2192 census tracts in North Carolina, over 748 tracts vary in rank by over 500 places.

Table 2.3: Social indicator variable contributions to the Social Vulnerability Index. Sorted social by the average rank in contribution to SoVI across all the estimation runs. When using all census tracts within the conterminous US, four variables exhibit different contribution directions than expected

varNames	expected	original	reversals	maxRank	minRank	avgRank
Age Dependency (pct)	-	+	6	2	6	3
Crowded Housing (pct)	+	-	5	1	15	4
Disability (pct)	+	-	13	2	16	6
Group Quarters (pct)	+	+	0	4	14	8
Limited English (pct)	+	+	1	3	17	8
Minority (pct)	+	+	0	6	12	8
Mobile Home (pct)	+	+	0	7	11	8
Multi-Unit Housing (pct)	+	+	0	7	11	9
No High School (pct)	+	+	0	2	16	10
No Vehicle (pct)	+	-	13	2	17	10
Per Capita Income	+	+	0	3	16	10
Population Density	+	+	5	1	17	11
Poverty (pct)	+	+	0	2	17	11
Renter (pct)	+	+	0	9	13	11
Singe Parent (pct)	+	+	0	5	15	11
Unemployed (pct)	+	+	0	7	16	13
Uninsured (pct)	+	+	0	6	17	13

Heat

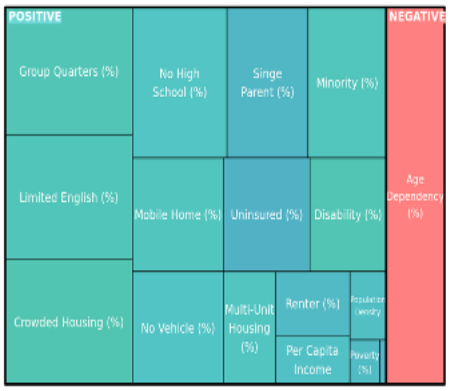

Storm

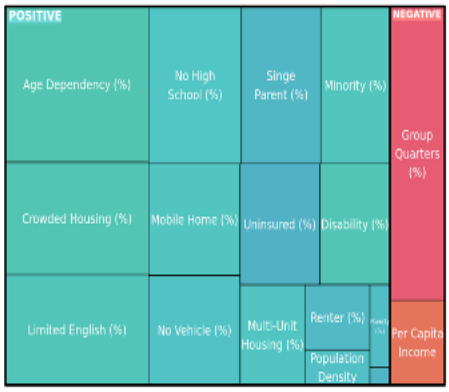

Climate

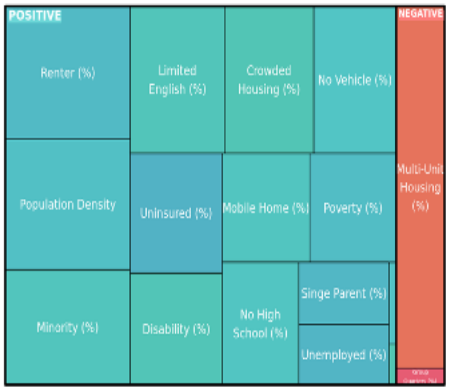

Drought

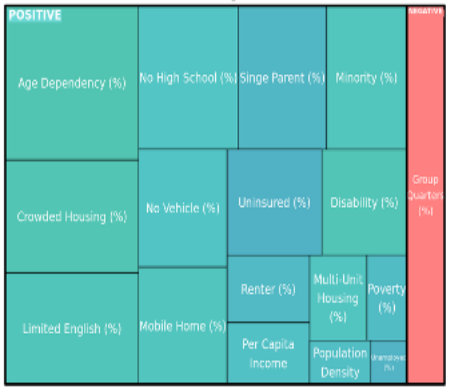

Flood

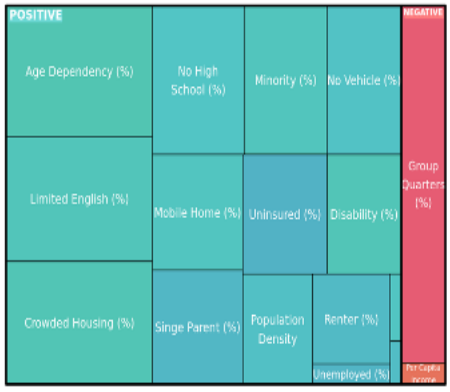

Table 2.4: Spatial subsample sizes by climate hazard.

hazard	n
climate	6898
drought	2916
fire	6958
flood	14557
heat	1816
storm	1241

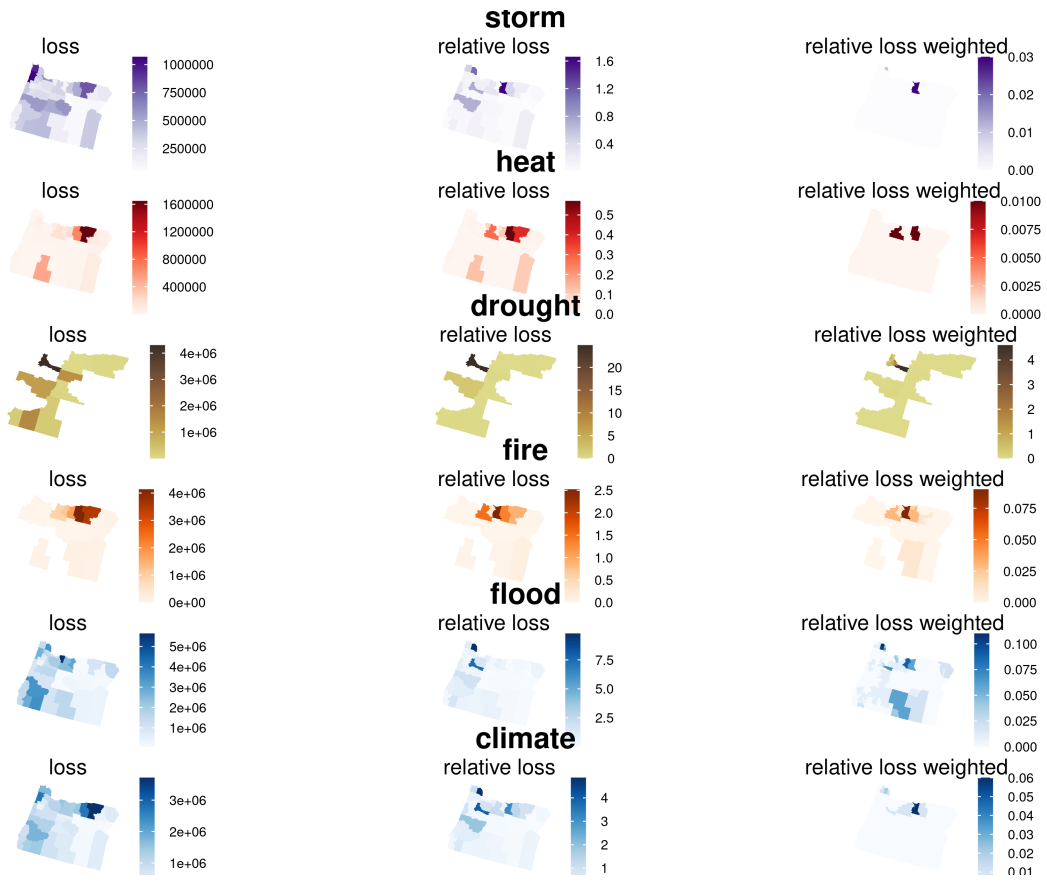

Figure 2.7: Relative disaster loss calculated by dividing county-level disaster loss by GDP and weighting by tract-level area and population size.

Table 2.5: Logistic model summaries across hazards.

	Null (Storm)	Storm + SVI	Null (Heat)	Heat + SVI	Null (Drought)	Drought + SVI
Constant	−0.604***	−0.614***	−1.304***	−1.342***	−0.510***	−0.546***
	(0.008)	(0.008)	(0.017)	(0.017)	(0.028)	(0.030)
Climate Hazard	−0.143***	−0.137***	−0.124***	−0.176***	0.500***	0.300***
	(0.008)	(0.010)	(0.017)	(0.019)	(0.028)	(0.032)
Age Dependency		−1.274		−5.461		0.862
		(1.869)		(3.630)		(8.031)
Crowded Housing		−0.124***		−0.091***		0.294***
		(0.012)		(0.025)		(0.047)
Disability		−0.069***		0.034		0.072+
		(0.012)		(0.023)		(0.041)
Group Quarters		0.011		0.056*		0.036
		(0.011)		(0.022)		(0.037)
Limited English		0.049***		0.254***		0.367***
		(0.014)		(0.030)		(0.064)
Minority		−0.028+		0.118**		0.448***
		(0.016)		(0.037)		(0.056)
Mobile Home		−0.183***		−0.018		0.108**
		(0.011)		(0.020)		(0.035)
Multi-Unit Housing		0.035**		−0.055*		−0.087*
		(0.011)		(0.024)		(0.041)
No High School		0.129***		0.107**		−0.623***
		(0.017)		(0.036)		(0.069)
No Vehicle		−0.011		−0.174***		−0.077+
		(0.013)		(0.028)		(0.041)
Per Capita Income		0.052***		0.062*		0.176***
		(0.013)		(0.026)		(0.042)
Population Density		0.014		−0.111**		0.101*
		(0.010)		(0.038)		(0.042)
Poverty		0.003		0.041		0.169***
		(0.016)		(0.030)		(0.049)
Renter		−0.003		0.172***		0.160**
		(0.016)		(0.036)		(0.052)
Singe Parent		0.011		−0.074**		−0.150***
		(0.012)		(0.024)		(0.043)
Unemployed		0.015		0.056*		0.202***
		(0.011)		(0.022)		(0.038)
Uninsured		−0.035**		−0.146***		−0.186***
		(0.011)		(0.023)		(0.039)
Num.Obs.	64 508	64 508	21 652	21 652	5702	5702
AIC	83 563.2	82 601.2	22 440.2	21 869.0	7249.3	6770.6
BIC	83 581.4	82 791.8	22 456.2	22 036.6	7262.6	6910.3
Log.Lik.	−41 779.616	−41 279.593	−11 218.106	−10 913.497	−3622.663	−3364.317

+ $p < 0.1$, * $p < 0.05$, ** $p < 0.01$, *** $p < 0.001$

Table 2.6: Logistic model summaries across hazards.

	Null (Wildfire)	Wildfire + SVI	Null (Flood)	Flood + SVI	Null (Climate)	Climate + SVI
Constant	−0.515***	−0.526***	−0.790***	−0.798***	−0.137***	−0.138***
	(0.006)	(0.006)	(0.004)	(0.004)	(0.003)	(0.003)
Climate Hazard	0.079***	0.059***	0.012**	0.061***	−0.138***	−0.099***
	(0.006)	(0.006)	(0.004)	(0.004)	(0.003)	(0.004)
Age Dependency		−4.885***		−0.725		−2.828***
		(1.166)		(0.736)		(0.674)
Crowded Housing		−0.101***		0.052***		−0.046***
		(0.009)		(0.005)		(0.005)
Disability		−0.032***		−0.010+		−0.052***
		(0.008)		(0.005)		(0.005)
Group Quarters		0.104***		−0.016***		0.021***
		(0.008)		(0.004)		(0.004)
Limited English		0.066***		0.039***		0.045***
		(0.010)		(0.006)		(0.005)
Minority		0.180***		0.201***		0.050***
		(0.013)		(0.007)		(0.006)
Mobile Home		−0.060***		0.025***		−0.056***
		(0.008)		(0.005)		(0.004)
Multi-Unit Housing		0.056***		0.044***		0.026***
		(0.008)		(0.005)		(0.004)
No High School		0.039**		−0.069***		0.070***
		(0.012)		(0.007)		(0.006)
No Vehicle		−0.061***		0.007		0.008
		(0.009)		(0.005)		(0.005)
Per Capita Income		−0.072***		0.078***		0.039***
		(0.010)		(0.005)		(0.005)
Population Density		−0.114***		0.036***		0.014***
		(0.010)		(0.005)		(0.004)
Poverty		0.002		0.002		−0.059***
		(0.011)		(0.006)		(0.006)
Renter		−0.021+		−0.099***		−0.007
		(0.012)		(0.007)		(0.007)
Singe Parent		−0.067***		0.022***		0.021***
		(0.009)		(0.005)		(0.005)
Unemployed		−0.113***		0.039***		−0.011*
		(0.008)		(0.004)		(0.004)
Uninsured		0.077***		0.007		−0.043***
		(0.008)		(0.005)		(0.004)
Num.Obs.	120 172	120 172	353 911	353 911	377 714	377 714
AIC	158 725.0	156 273.7	439 390.6	436 049.2	520 095.8	517 121.2
BIC	158 744.4	156 477.4	439 412.1	436 275.5	520 117.5	517 348.8
Log.Lik.	−79 360.489	−78 115.865	−219 693.279	−218 003.603	−260 045.892	−258 539.584

+ p < 0.1, * p < 0.05, ** p < 0.01, *** p < 0.001

Table 2.7: Logistic model proportions of explained deviance.

Null (Storm)	0.00359
Storm + SVI	0.01552
Null (Heat)	0.00252
Heat + SVI	0.0296
Null (Drought)	0.04379
Drought + SVI	0.11198
Null (Wildfire)	0.00111
Wildfire + SVI	0.01677
Null (Flood)	2e-05
Flood + SVI	0.00772
Null (Climate)	0.00341
Climate + SVI	0.00918

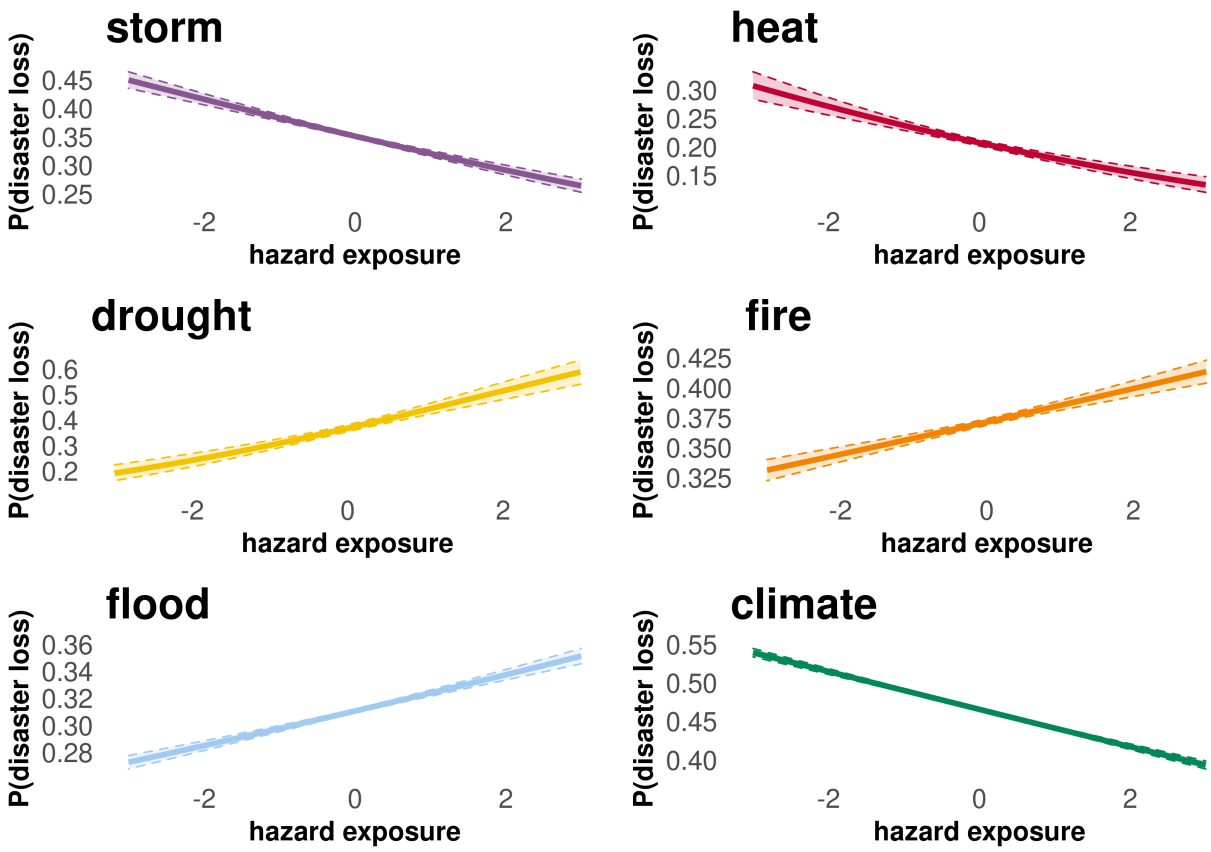

Figure 2.8: Logistic models of disaster loss probability. Z-scores for climate hazard are on the x-axis and the probability of experiencing disaster loss is on the y-axis.

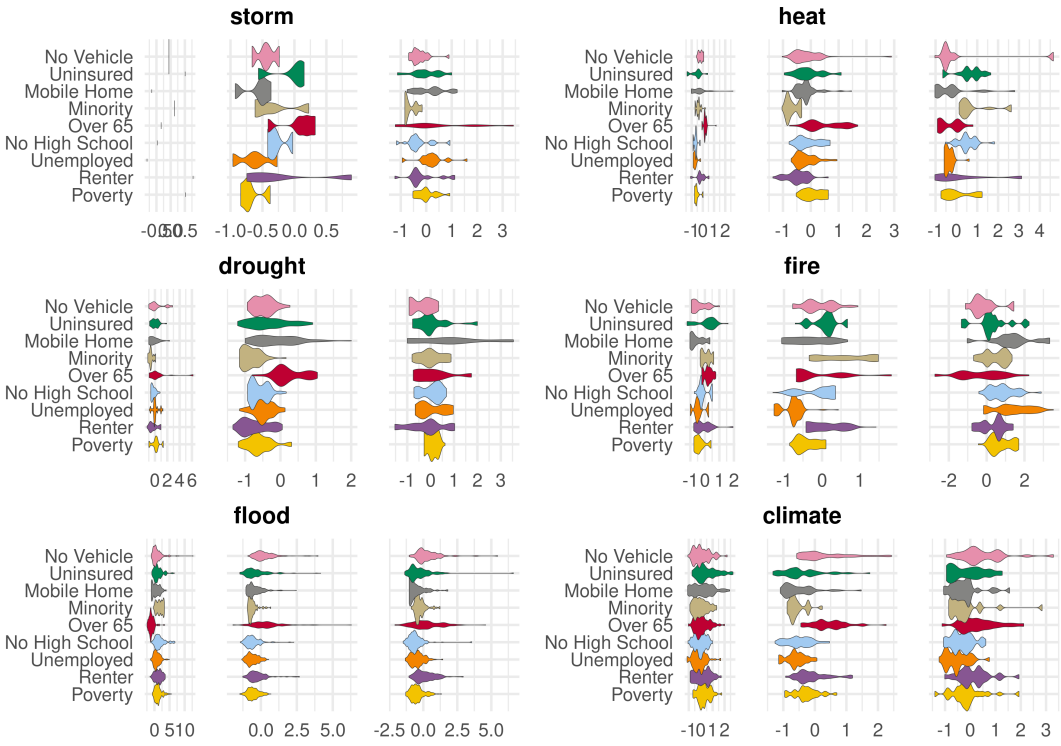

Figure 2.9: Demographic profiles for archetypal high climate risk communities.

Table 2.8: Multivariable Fractional Polynomial model summaries across hazards: exposed populations

	Null (Storm)	Storm + SVI	Null (Heat)	Heat + SVI	Null (Drought)	Drought + SVI
Constant	8.417***	8.525***	6.786***	6.919***	7.223***	7.234***
	(0.071)	(0.076)	(0.079)	(0.086)	(0.411)	(0.423)
Climate Hazard	−0.426***	−0.468***	−0.043	−0.197*	0.383	0.353
	(0.064)	(0.065)	(0.078)	(0.078)	(0.268)	(0.268)
SoVI		−0.226***		0.496***		−0.109
		(0.042)		(0.084)		(0.232)
Num.Obs.	21 094	21 094	10 062	10 062	1489	1489
AIC	102 222.0	102 074.9	54 701.9	54 515.9	8029.0	8027.0
BIC	102 245.8	102 122.6	54 723.6	54 559.2	8044.9	8058.8
Log.Lik.	−51 107.987	−51 031.452	−27 347.965	−27 251.952	−4011.498	−4007.500

+ p < 0.1, * p < 0.05, ** p < 0.01, *** p < 0.001

Table 2.9: Multivariable Fractional Polynomial model summaries across hazards: unexposed populations

	Null (Storm)	Storm + SVI	Null (Heat)	Heat + SVI	Null (Drought)	Drought + SVI
Constant	8.494***	8.636***	7.128***	7.383***	7.547***	7.557***
	(0.019)	(0.024)	(0.047)	(0.056)	(0.085)	(0.105)
Climate Hazard	−0.052**	−0.114***	−0.891***	−0.862***	0.263*	0.254*
	(0.020)	(0.021)	(0.047)	(0.047)	(0.118)	(0.118)
SoVI		−0.278***		−0.331***		0.162
		(0.035)		(0.067)		(0.127)
Num.Obs.	43 414	43 414	11 590	11 590	4213	4213
AIC	225 526.3	225 265.1	59 556.5	59 451.3	23 129.3	23 108.4
BIC	225 552.4	225 317.2	59 578.6	59 495.4	23 148.3	23 146.5
Log.Lik.	−112 760.169	−112 626.571	−29 775.271	−29 719.633	−11 561.650	−11 548.189

+ p < 0.1, * p < 0.05, ** p < 0.01, *** p < 0.001

Table 2.10: Multivariable Fractional Polynomial model summaries across hazards: exposed populations

	Null (Wildfire)	Wildfire + SVI	Null (Flood)	Flood + SVI	Null (Climate)	Climate + SVI
Constant	8.511***	8.586***	7.525***	7.665***	8.913***	8.980***
	(0.013)	(0.017)	(0.008)	(0.010)	(0.011)	(0.013)
Climate Hazard	0.399***	0.399***	0.148***	0.134***	−0.255***	−0.259***
	(0.013)	(0.013)	(0.010)	(0.010)	(0.012)	(0.012)
SoVI		−0.258***		0.266***		0.254***
		(0.025)		(0.015)		(0.015)
Num.Obs.	82 684	82 684	267 209	267 209	203 955	203 955
AIC	428 290.1	427 849.2	1 413 011.6	1 410 143.3	1 032 489.3	1 030 822.3
BIC	428 318.1	427 905.2	1 413 043.1	1 410 206.3	1 032 520.0	1 030 883.6
Log.Lik.	−214 142.062	−213 918.622	−706 502.812	−705 065.667	−516 241.645	−515 405.135

+ p < 0.1, * p < 0.05, ** p < 0.01, *** p < 0.001

Table 2.11: Multivariable Fractional Polynomial model summaries across hazards: unexposed populations

	Null (Wildfire)	Wildfire + SVI	Null (Flood)	Flood + SVI	Null (Climate)	Climate + SVI
Constant	8.052***	8.480***	7.523***	7.596***	9.027***	9.189***
	(0.046)	(0.048)	(0.022)	(0.025)	(0.013)	(0.014)
Climate Hazard	−0.325***	−0.236***	0.400***	0.443***	−0.327***	−0.372***
	(0.042)	(0.042)	(0.015)	(0.015)	(0.012)	(0.012)
SoVI		0.153***		0.089***		−0.117***
		(0.037)		(0.026)		(0.017)
Num.Obs.	37 488	37 488	86 702	86 702	173 759	173 759
AIC	196 581.4	195 688.2	461 370.3	460 915.7	903 260.7	902 343.5
BIC	196 607.0	195 739.4	461 398.4	460 971.9	903 290.8	902 403.9
Log.Lik.	−98 287.678	−97 838.101	−230 682.128	−230 451.860	−451 627.325	−451 165.743

+ p < 0.1, * p < 0.05, ** p < 0.01, *** p < 0.001

Table 2.12: MFP models proportion of explained deviance: exposed

Null (Storm)	0.00212
Storm + SVI	0.00934
Null (Heat)	3e-05
Heat + SVI	0.01893
Null (Drought)	0.00137
Drought + SVI	0.00672
Null (Wildfire)	0.01048
Wildfire + SVI	0.01581
Null (Flood)	8e-04
Flood + SVI	0.01149
Null (Climate)	0.0021
Climate + SVI	0.01025

Table 2.13: MFP models proportion of explained deviance: unexposed

Null (Storm)	0.00016
Storm + SVI	0.00629
Null (Heat)	0.03023
Heat + SVI	0.0395
Null (Drought)	0.00118
Drought + SVI	0.00754
Null (Wildfire)	0.0016
Wildfire + SVI	0.02527
Null (Flood)	0.00816
Flood + SVI	0.01341
Null (Climate)	0.0044
Climate + SVI	0.00967

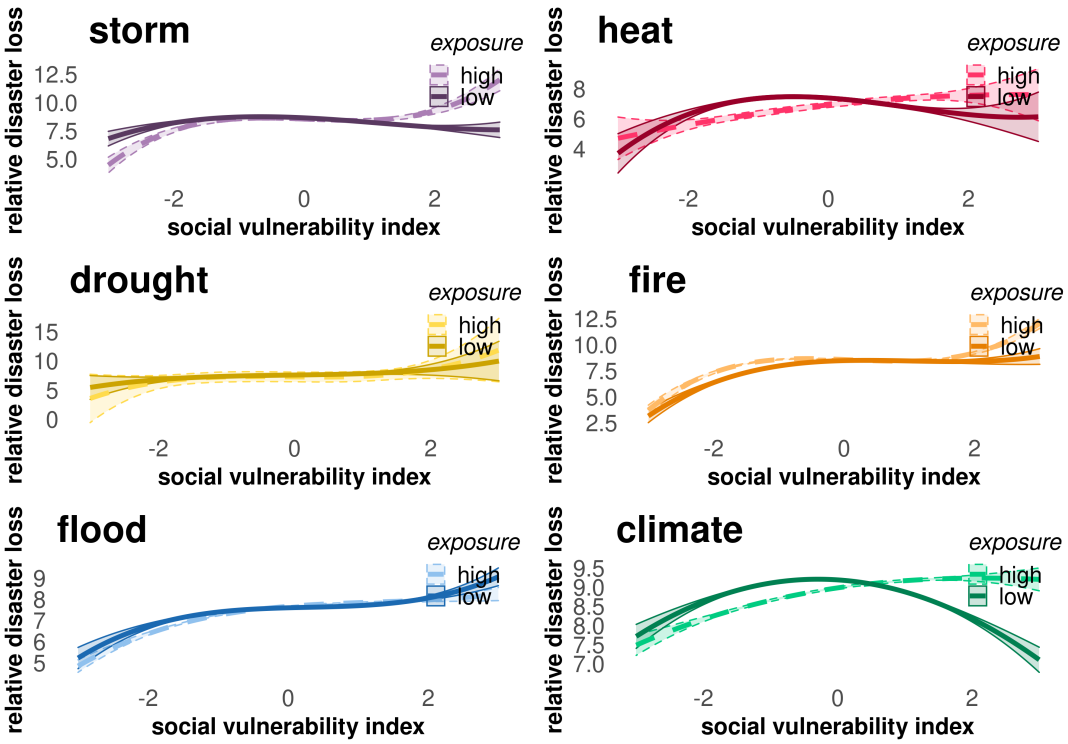

Figure 2.10: Multivariable Fractional Polynomial (MFP) models of disaster Loss and SoVI between high and low hazard Census Tracts. Z-scores for SoVI are on the x-axis and relative disaster loss is on the y-axis.

Table 2.14: Two Way Fixed Effects model summaries across hazards.

	Null (Storm)	Storm + SVI	Null (Heat)	Heat + SVI	Null (Drought)	Drought + SVI
Constant	8.660***	8.545***	7.255***	7.174***	7.454***	7.414***
	(0.018)	(0.018)	(0.031)	(0.031)	(0.077)	(0.077)
Climate Hazard	−0.932***	−0.867***	−1.072***	−1.000***	0.438**	0.403**
	(0.024)	(0.025)	(0.043)	(0.044)	(0.136)	(0.143)
Age Dependency		3.661		−2.195		−4.783
		(2.631)		(4.705)		(13.185)
Crowded Housing		−0.301***		−0.391***		0.382***
		(0.017)		(0.034)		(0.077)
Disability		−0.128***		−0.198***		0.143*
		(0.016)		(0.030)		(0.069)
Group Quarters		0.138***		0.289***		0.053
		(0.016)		(0.029)		(0.061)
Limited English		−0.117***		0.027		0.275**
		(0.021)		(0.041)		(0.101)
Minority		−0.592***		−0.501***		0.259**
		(0.023)		(0.049)		(0.092)
Mobile Home		−0.185***		−0.078**		0.016
		(0.014)		(0.026)		(0.058)
Multi-Unit Housing		−0.081***		−0.113***		−0.115+
		(0.016)		(0.029)		(0.069)
No High School		0.430***		0.477***		−0.630***
		(0.024)		(0.048)		(0.106)
No Vehicle		0.008		−0.196***		−0.101
		(0.018)		(0.034)		(0.068)
Per Capita Income		−0.260***		−0.410***		−0.275***
		(0.018)		(0.034)		(0.070)
Population Density		−0.235***		−0.178***		−0.235***
		(0.015)		(0.026)		(0.068)
Poverty		0.072**		0.125**		0.042
		(0.022)		(0.038)		(0.082)
Renter		0.126***		0.101*		0.139
		(0.023)		(0.047)		(0.088)
Singe Parent		−0.020		−0.269***		−0.290***
		(0.017)		(0.032)		(0.072)
Unemployed		−0.188***		−0.219***		−0.008
		(0.016)		(0.030)		(0.062)
Uninsured		0.144***		0.325***		0.170**
		(0.016)		(0.029)		(0.064)
Num.Obs.	64 508	64 508	21 652	21 652	5702	5702
AIC	327 063.9	323 585.2	114 421.1	112 178.4	31 157.4	31 003.5
BIC	327 109.3	323 803.0	114 461.0	112 370.0	31 190.6	31 163.1
Log.Lik.	−163 526.966	−161 768.606	−57 205.557	−56 065.202	−15 573.683	−15 477.769

+ p < 0.1, * p < 0.05, ** p < 0.01, *** p < 0.001

Table 2.15: Two Way Fixed Effects model summaries across hazards.

	Null (Wildfire)	Wildfire + SVI	Null (Flood)	Flood + SVI	Null (Climate)	Climate + SVI
Constant	8.510***	8.451***	7.508***	7.431***	8.983***	8.960***
	(0.012)	(0.011)	(0.007)	(0.007)	(0.006)	(0.006)
Climate Hazard	0.408***	0.259***	0.303***	0.173***	−0.462***	−0.492***
	(0.015)	(0.015)	(0.007)	(0.008)	(0.008)	(0.008)
Age Dependency		−10.563***		0.109		−1.747+
		(1.744)		(1.143)		(1.028)
Crowded Housing		−0.153***		−0.031***		−0.222***
		(0.013)		(0.008)		(0.007)
Disability		−0.048***		0.035***		−0.058***
		(0.012)		(0.008)		(0.007)
Group Quarters		0.368***		0.129***		0.122***
		(0.012)		(0.007)		(0.006)
Limited English		−0.131***		−0.113***		−0.149***
		(0.015)		(0.009)		(0.008)
Minority		−0.069***		−0.165***		−0.280***
		(0.019)		(0.011)		(0.010)
Mobile Home		−0.198***		0.062***		−0.090***
		(0.012)		(0.007)		(0.006)
Multi-Unit Housing		0.053***		−0.034***		−0.007
		(0.012)		(0.007)		(0.007)
No High School		0.145***		0.023*		0.327***
		(0.018)		(0.011)		(0.009)
No Vehicle		−0.137***		0.025**		−0.014*
		(0.013)		(0.008)		(0.007)
Per Capita Income		−0.491***		−0.270***		−0.233***
		(0.014)		(0.008)		(0.007)
Population Density		−0.461***		−0.197***		−0.318***
		(0.011)		(0.007)		(0.006)
Poverty		0.081***		0.126***		−0.008
		(0.016)		(0.010)		(0.009)
Renter		0.068***		−0.007		0.161***
		(0.018)		(0.011)		(0.010)
Singe Parent		−0.201***		0.011		0.000
		(0.013)		(0.008)		(0.007)
Unemployed		−0.336***		−0.120***		−0.198***
		(0.012)		(0.007)		(0.006)
Uninsured		0.261***		0.172***		0.083***
		(0.012)		(0.007)		(0.007)
Num.Obs.	120 172	120 172	353 911	353 911	377 714	377 714
AIC	624 896.5	614 945.2	1 874 428.9	1 864 497.0	1 936 243.0	1 920 788.0
BIC	624 945.0	615 178.0	1 874 482.8	1 864 755.6	1 936 297.2	1 921 048.2
Log.Lik.	−312 443.251	−307 448.621	−937 209.433	−932 224.489	−968 116.513	−960 370.016

+ p < 0.1, * p < 0.05, ** p < 0.01, *** p < 0.001

Table 2.16: Two Way Fixed Effect models proportion of explained deviance.

Null (Storm)	0.0309
Storm + SVI	0.08232
Null (Heat)	0.04078
Heat + SVI	0.13668
Null (Drought)	0.00408
Drought + SVI	0.03703
Null (Wildfire)	0.00975
Wildfire + SVI	0.08874
Null (Flood)	0.0078
Flood + SVI	0.03536
Null (Climate)	0.01273
Climate + SVI	0.0524

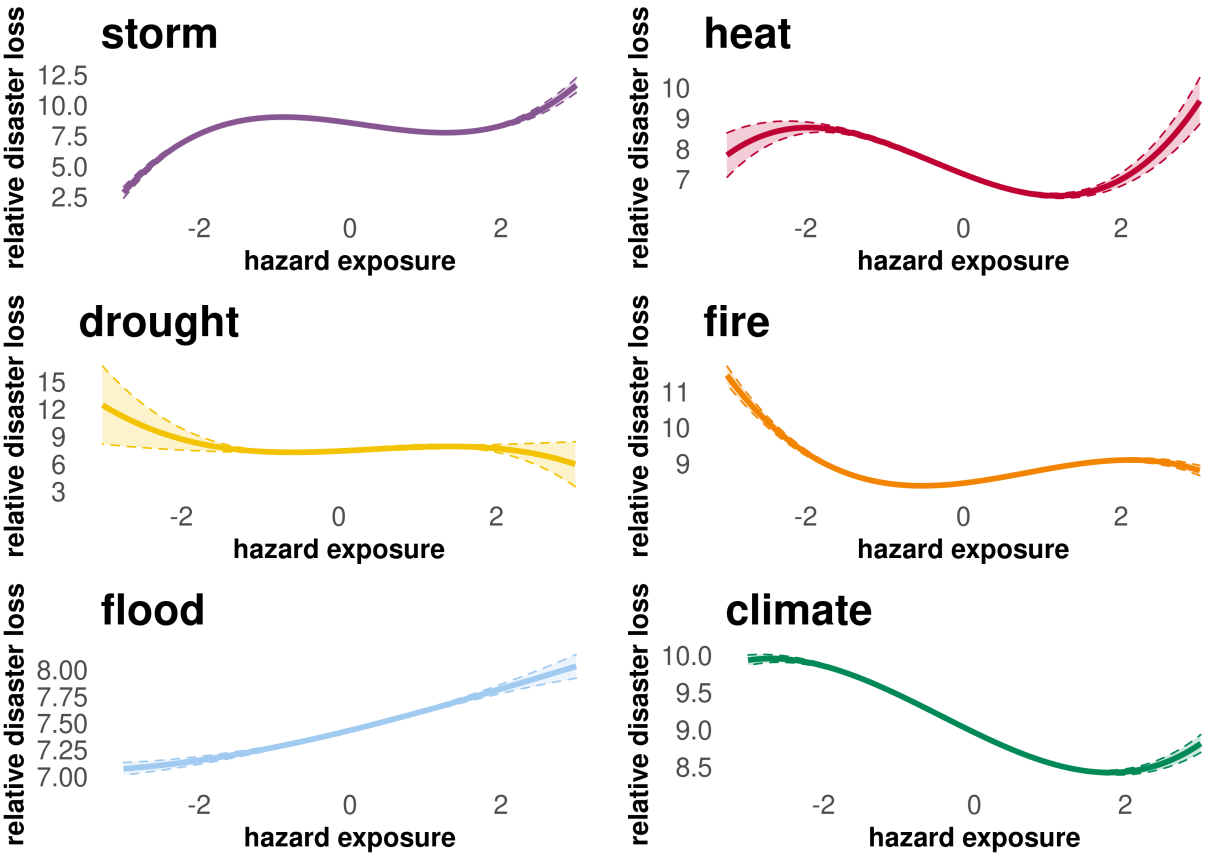

Figure 2.11: Two-Way Fixed Effect models of disaster loss and climate hazard. Z-scores for climate hazard are on the x-axis and the probability of experiencing disaster loss is on the y-axis.

Chapter 3

Mapping Climate Risk Inequalities

Environmental hazards are unequally distributed along geographic, demographic, and socioeconomic lines. This study leverages differences among distinct metric formulations and types to examine diverse representations of inequality for distinct climate hazards. We study the vertical, horizontal, and spatial dimensions of inequality. Vertical inequalities manifest across either space or population, horizontal inequalities are those between population groups, and spatial inequalities assess the similarity of nearby values. Each climate hazard has varying degrees of vertical inequality when looking among states and at the national level. Horizontal inequalities are present between high and low social vulnerability groups, but it is not necessarily the case that lower social vulnerability groups lived in more hazardous places. Hazards tend to be highly spatially unequal, which is in accordance with the underlying physical processes producing hazard geographies. This study suggests that–since inequality varies greatly across hazards, places, and metrics–researchers should carefully select inequality metrics specific not only to the research question but also based on the identification of theoretical processes for inequality formation and policy-relevant implications.

Introduction

Environmental hazards, such as pollution, are unequally distributed along geographic, demographic, and socioeconomic lines. Environmental hazards that are climate-sensitive pose danger to not only human well-being but also property. It is therefore crucial to understand how, and for whom, inequalities manifest across the distributions of climate hazards. There are typically two ways to measure inequalities, vertically and horizontally. Vertical metrics assess variation for the variable of interest, in this case a climate hazard (e.g. wildfire), and horizontal metrics measure variation among population groups (e.g. race/ethnicity). A spatial approach to representing the 'where' of inequality has also garnered attention as a way to understand spatial processes influencing a distribution. The vulnerability framework for hazard inequality analysis is often used to accurately represent factors contributing to climate risk. Although studies have emphasized the importance of measuring both aspects of climate risk (hazard and vulnerability) in different ways (vertical, horizontal, and spatial), there exist several issues with prior approaches, including a lack of attention toward organizational processes influencing hazard siting and mitigation (Weinberg, 1998); too narrow a set of environmental inequality outcomes (Downey, 2005); contradictory results depending on the choice of areal unit (Fielding & Burningham, 2005); conflating inequality with injustice as well as proximity with impacts (Walker, Mitchell, Fairburn, & Smith, 2005); biased statistical modeling (Hajat, Hsia, & O'Neill, 2015); and an aspatial conceptualization of inequality formation (Galster & Sharkey, 2017).

Studies often present inequalities from the hazard perspective, e.g., "high exposure areas are 50% more likely to have vulnerable residents," which doesn't necessarily represent the presence of inequalities across the whole population group or large-area geographies

since vulnerable individuals may also be less likely to live in high exposure areas. Similarly, inequalities are communicated through the geographic perspective, wherein studies make claims such as… '2/3 of states see 30% higher hazard exposure for vulnerable populations', which could significantly change with any modification to the areal units (Mitchell & Walker, 2007). We propose a multi-hazard and multi-dimensional analysis of climate hazard inequalities for extreme precipitation, extreme heat, drought, wildfire, and flooding. Our first task, risk mapping, describes the spatial distribution of risk as the bivariate association among hazards and social vulnerability. This exploratory step helps to better understand the spatial codistribution of risk terms. Next we estimate several vertical inequality metrics and then break risk up by population to measure horizontal inequalities between high and low vulnerability groups. Then we assess inequalities across space through a spatially dependent vertical inequality metric and by looking at patterns and intensity of high risk spatial clusters. We contribute to a growing literature on climate risk inequalities by asking the following research questions:

Research questions

1. How unequally distributed are climate hazards: vertically, horizontally, and spatially?
2. Which population groups and places experience unequal climate hazard burdens?
3. Do different representations of climate hazard inequalities lead to varying environmental justice interpretations?

Although many studies have addressed climate hazard inequalities, there has been no published research to date that provides a succinct yet representative analysis across different inequality metrics, climate hazards, and social vulnerability indicators for the conterminous United States. Our overarching question is whether the burden of climate

hazard falls on vulnerable communities, which we define using the social vulnerability framework. We expect hazards to be unequally distributed across all inequality metrics and disproportionately high in vulnerable communities. Knowing the distributions of these hazards is helpful in contexts where risk should be spread and resources are limited, such as insurance underwriting and public infrastructure planning. A better understanding of climate hazard inequalities will help target resources and attention towards groups and places requiring greater assistance towards climate adaptation and mitigating disaster loss.

Literature Review

The study of unequal resource distributions represents a long history in the social and environmental sciences. Inequality is generally understood as the unequal distribution of some element, climate hazards in this case, across place and population (Allison, 1978). Theories of inequality tend to focus on what inequality is, how we measure it, and how it forms. Some applied and empirical studies address questions of justice, equity, or a related topic, while others inform how inequality affects a phenomenon under examination. Income inequality has received perhaps the most attention in this regard (Kuznets, 1955; Piketty & Saez, 2003).

A primary reason so much interest has been directed towards income inequality is to understand the efficacy of the development process. As an economy develops, typically measured by national GDP, income inequality was hypothesized to initially increase to a peak and then decrease; this inverted U-shape is known as the Kuznets curve (Kuznets, 1955). This hypothesized pattern has not borne out in the US or several other high-income countries. In the US a historical pattern that had followed the Kuznets curve

gave way to increasing income inequality in the late twentieth and early twenty-first century (Morris, Bernhardt, & Handcock, 1994; Morris & Western, 1999; Rey & Janikas, 2005). If we agree on a just development process and therefore a minimum increase in wellbeing for all, inequality research into who and how many get marginalized and left out provides pivotal information.

There are two common types of inequality measurement, vertical and horizontal, referred to as the relational orientation (Handcock & Morris, 1999; Jayaraj & Subramanian, 2006). Vertical metrics include the Gini coefficient and the Theil index. Horizontal modes of comparison typically look at the distribution for a variable of interest across different groups of a population characteristic such as poverty, race/ethnicity, or other demographic variables of public concern. Some technical considerations with taking these measures include spatiotemporal scale, population weights, and distributional sensitivity. These problems are most relevant for comparing measures of inequality across units, but could even be considered when assessing inequality within a unit. Distributional sensitivity refers to how an inequality metric responds to changes at different segments of the distribution. Some metrics are more sensitive to changes in the middle of a distribution whereas others may respond more strongly to changes in the tails of a distribution.

Spatiotemporal scale concerns the ecological fallacy–incorrect inferences due to aggregation (Ash & Fetter, 2004; Piantadosi et al., 1988)–and stationarity bias–assuming that relationships are stable over space and time [Cazelles & Hales (2006); Kwan (2021). Population weights influence the intensity of inequality and the robustness of the inequality measure depending on the unit of analysis (Gluschenko, 2018). A simple example exists for equal area raster cells and equal population polygons, which have unequal population and area, respectively. An inequality analysis would use equal area units if the research addresses an absolute right to a certain level of some resource with any deviation too

far from that level considered unacceptable. However, equal population units would be used if the researcher were concerned with the total impact of inequality and whether places with unacceptable levels of the resource also contained a disproportionately large number of people [Reardon & O'Sullivan (2004).

Beyond income, environmental hazards are another variable of distributional concern that have received attention from researchers to better understand environmental inequalities. Air, soil, and water, pollution comprise the central hazards in this effort (Bell & Ebisu, 2012; Bullard, 2005; Mitchell & Dorling, 2003). Akin to income inequality research, the literature of environmental inequalities raises fundamental questions about development: for whom and at what cost? The modern environmental justice movement stems from this endeavor and has been both established as a central tenant of environmental hazards research and governmental responsibility for the people. Importantly, environmental inequalities are usually understood as both caused by and ameliorated by people, similar to income.

Natural hazard inequalities have not received as much attention as anthropogenic 'environmental hazards' in both research and practice. To some extent this history makes sense given that natural hazard landscapes are largely fixed and out of our control, disaster mitigation notwithstanding. Even when humans bear responsibility for a 'natural disaster', e.g., through the failure of critical infrastructure, it has not always been considered an issue of environmental justice. Events in recent decades contradict these assumptions, some notable examples including Hurricane Katrina and wildfires in Santa Rosa.

Insofar as there is a tendency to consider natural disasters separate from human culpability, climate change demands a rethinking of hazard inequalities. Not only will climate hazards change over the next century (more than they already have), but individuals,

organizations, and governments will adapt accordingly. Access to an adaptation process for a changing hazard landscape that is conditional on privilege will undoubtedly disenfranchise more vulnerable populations. As with environmental hazards, marginalized communities on the front lines of climate change will be relegated to 'ecological sacrifice zones', a term from the environmental justice literature describing communities with high hazard levels and limited resources, all but forgotten by policymakers and the public (Bullard, 2011).

Understanding physical contexts in which climate hazards occur, such as low elevation coastal towns inundated by rising sea levels, is crucial for hazard mitigation. However, losses related to climate hazards, typically resulting from a disaster, do not only vary as a function of the hazard distribution. Losses vary by place, whereby adjacent communities with nearly identical hazard exposure experience markedly different loss outcomes. This variation may be due to differences in built environment, institutions, and social vulnerability. Although the former two categories are tremendously important in mitigating disaster loss, it is the last category, social vulnerability, that we focus on for this study. Since social vulnerability increases the risk of a climate hazard creating disaster loss, physical context is not sufficient for building a localized or national-level risk profile as it only captures part of the climate risk equation. It is also the case that social vulnerability is more predictive of the support provided against hazard exposure from the built environment and institutions than the reciprocal (Anderson, 2007; Bloomberg, 2020; Bullard, 2001; Lichter, Parisi, Grice, & Taquino, 2007; O'Neill & O'Neill, 2012; Troesken, 2002). Therefore, identifying where and who is at greatest risk from a combination of high hazard and vulnerability can inform efforts towards strengthening aspects of these other categories.

We typically describe vulnerability as the propensity of social and ecological systems to

suffer harm from exposure to external stresses and shocks, thus denoting the antonym of resilience. Social vulnerability has been conceptualized and operationalized with myriad constructions of social, economic, political, and technological characteristics that comprise the susceptibility of a community to climate hazard-related disaster loss. Examples include general indices by Cutter et al. (2003) and the CDC (Flanagan et al., 2011), as well as hazard- and place-specific indices, such as flooding in Germany (Fekete, 2009). Higher social vulnerability typically increases the risk posed by climate hazards. Since the spatial distribution of climate hazard exposure is not uniform, higher social vulnerability does not always produce greater climate risk (disaster probability and loss from the interaction of social vulnerability and climate hazards). It is therefore necessary to measure both dimensions of climate risk.

Thus, we could consider social vulnerability as the degree to which communities are prepared for, cope with, and recover from climate hazards (Cutter et al., 2003), yet other researchers propose a simpler definition (Turner et al., 2003; White, 1974) as the… 'propensity for loss of lives, livelihood or property when exposed to a hazard' (Tellman et al., 2020). Conceptualizing the social vulnerability of a community in this way has a wide-ranging and well-established history as an accessible and representative measurement scheme despite relying on indirect and, sometimes, contested variables. Population characteristics, such as average income, racial/ethnic background, and housing quality, serve as proxy measurements for ways that individuals and communities mitigate disaster loss; the accessibility, efficacy, and robustness of institutional support; and perhaps even the quality and size of social networks. Climate risk mapping combines the geographies of social vulnerability and climate hazards to better understand where, who, and what is most at risk.

Disaster mitigation is a resource scarce endeavor that benefits from targeting projects

to specific places and groups of people, which we represent here through social vulnerability indicators. Places with the highest climate risk require the greatest attention, and well-designed, targeted projects are more effective in ensuring community adoption and efficacy. We find this in cases ranging from stormwater (Dudula & Randhir, 2016), small private forests (Mostegl, Pröbstl-Haider, Jandl, & Haider, 2019), and the urban heat island (Hertel & Schlink, 2019). The relationship between social vulnerability and disaster mitigation varies by climate hazard. Targeting projects towards places with high climate risk will rely on knowing the climate hazards facing communities, which in turn determines the social vulnerability factors requiring the most resources.

Improvements in data and methods for estimating climate hazards indicate that socially vulnerable communities already bear a bigger share of previously unknown risk. New estimates suggest the share of flood exposure for minority residents in over two-thirds of states is higher than the state average. Neighborhoods with predominantly African American residents in Chicago and Fort Lauderdale have flood exposure that is 30 and 36 percentage points higher than previous estimates (Flavelle et al., 2020). Around 87 percent of paid flood claims between 2007 and 2017 in Chicago occurred in predominantly minority communities (Briscoe, 2020). High flood risk is a product of not only hazard exposure but also floodplain infrastructure. Since more than 85 percent of levees are funded, owned, and maintained primarily by local authorities or entities ("Levees," 2017), higher risk typically falls in places with lower tax bases because they lack the capital to construct hazard management infrastructure (@bagstadTaxesSubsidiesInsurance2007; Bloomberg, 2020). Communities with a lower tax base oftentimes consequently have less political power to attract state, federal, and private investment in large infrastructure projects (Crain & Oakley, 1995; Dwarka & Feitelson, 2013; O'Neill, 2018). Even infrastructure in places with limited political power, a low tax base, and socioeconomic marginalization

may fall into disrepair or lag behind what is presently needed thus leading to disastrous consequences such as when the levees broke during Hurricane Katrina in New Orleans (Van Heerden, 2007).

Our climate hazard future is uncertain. This stems from how much mitigation we achieve, how (and where) society develops, and the limits to our climate models. Hurricane frequency may not increase (Walsh et al., 2016), and even if it does, we don't know exactly where in the Atlantic and Gulf of Mexico region will experience the greatest increases (Marsooli, Lin, Emanuel, & Feng, 2019). Droughts may persistently affect even more of North America (Jeong, Sushama, & Naveed Khaliq, 2014) yet not be as much of a concern for potable water resources due to increased precipitation, as long as proper catchment infrastructure is in place (Wanders & Wada, 2015). Increasing flood losses may merely be driven by asset expansion in exposed areas (Kundzewicz et al., 2014) as flood risk projections are highly variable from region to region and model to model (Hirabayashi et al., 2013a). The present rate of climate change will modify wildfire regimes. How they modify those regimes is highly uncertain since the current rate of climate change is without proxy in the geologic record (Marlon et al., 2009). Despite this uncertainty, we do know that high climate risk has the potential for severe losses and that understanding the distribution of this risk can help to inform loss mitigation.

Data and Methods

Our approach involves measuring the distributional inequalities of climate hazards nationally and at the state level. We match five climate hazards (extreme precipitation, extreme heat, drought, wildfire, and flooding) and a set of over twenty social vulnerability indicators, as well as the Social Vulnerability Index (SoVI), at the Census Tract

level. First we describe bivariate distributions of climate hazards and SoVI. Then we measure vertical inequality, that which is across the distribution of each climate hazard. The next measurement is of horizontal inequality, which we assess through a series of metrics, including the proportion of Census Tracts with both high climate hazard and social vulnerability index values, inequality at the median and 90th percentile of the group-wise hazard distributions, the disparity from average climate hazard between groups, and the probability of each group living in a high hazard place. Lastly, we look at spatial inequalities using the spatial Gini coefficient and Moran's I, a measure of spatial clustering.

Climate hazards

To estimate climate hazard we first determine the relevant spatial unit of analysis and integrate many datasets to comparable spatial and temporal scales. Climate model output (precipitation and temperature) come from tens of internationally accepted global climate models which have been validated as part of the Coupled Model Intercomparison Project Phase 5 (Taylor et al., 2012). Researchers have downscaled these data to higher resolution across the US by utilizing local information (e.g. weather patterns, hydrodynamics, etc.) and leveraging the empirical linkages between coarse resolution and fine resolution climate. We use the downscaled data products to produce high spatiotemporal resolution estimates of general climate risk for a given raster cell. Other hazards (drought, wildfire, and flooding) use these climate averages as input data alongside myriad other data sources (terrain, vegetation, soil type, etc.) in more complex modeling frameworks to estimate water scarcity through supply and demand relationships, fire weather and burn probabilities, and flood depths and return intervals, respectively. In Chapter 2, Figure **??** displays the climate hazards we estimate and the average climate

hazard aggregated at the tract level. Table 2.1 provides summary statistics. Appendix A @ref(#climate-hazard-estimation) offers a detailed explanation of how we estimate each climate hazard.

Social vulnerability

Social vulnerability is generally operationalized as an index made up of dozens of census variables across the categories of socioeconomic status, household composition, race/ethnicity/language, and housing/transportation. There are two common ways to operationalize social vulnerability (Yoon, 2012). The deductive approach selects variables based on prior knowledge of their relevance (e.g. Flanagan et al. (2011)). The inductive approach selects variables based on statistical relationships (e.g. SoVI from Cutter et al. (2003)). Although deductive approaches are commonly used and simpler, this study only utilizes an inductive method to construct SoVI.

We measure social vulnerability with data from the US Decennial Census and American Community Survey (ACS). These data are available at the Census Tract level, which is typically around 8,000 people (there are approximately 73,057 Census Tracts in the US). We rely on the Cutter et al. (2003) implementation to construct SoVI. In Chapter 2, Table 2.2 contains summary statistics and Figure **??** maps SoVI and a subset of social factors across the US.

Bivariate associations of climate risk

We observe the tract level bivariate association between the SoVI and five climate hazards as well as the aggregate climate hazard. In the legend in Figure 3.1, the climate hazard categories increase vertically upward whereas the social vulnerability factors increase

laterally rightward. Climate risk on this scale is divided into nine categories by each of three bins from social vulnerability and the climate hazards.

Vertical Inequalities

1. Gini Coefficient

The most commonly used metric for measuring vertical inequality is the Gini Coefficient. It has been applied primarily for income and related variables (Cowell, 2011; Dorfman, 1979), but can be leveraged to measure inequality in any variable of interest such as galaxy morphology (Abraham, Bergh, & Nair, 2003), species abundance (Scheffer, Bavel, Leemput, & Nes, 2017), and public facilities access (Cromley, 2019). The Gini Coefficient serves as an efficient and intuitive indicator for inequality, adheres to necessary characteristics for an inequality metric such as symmetry, mean and population size independence, and Pigou Dalton Transfer Sensitivity (Haughton & Khandker, 2009), but it is less sensitive to changes at the tails of the distribution (Atkinson, 1970; Duro, 2012; Sitthiyot & Holasut, 2020). We estimate the Gini Coefficient with the following formula:

$$Gini = 1 + \frac{1}{n} - [\frac{2}{MEANHAZ*n^2}] \sum_{i=1}^{n} [n - i + 1) * HAZARD_i]$$

Where i is the geographic unit (Census Tract), MEANHAZ is the average hazard across all units, HAZARD is the hazard estimate for unit i, and n is the number of Tracts. Gini values range from 0 to 1 with higher values representing more inequality.

2. Theil Index

Alternative metrics to estimate vertical inequality address the previously mentioned issue with the Gini Index, limited sensitivity to changes at the tails of the distribution. They

fall under the Generalized Entropy (GE) family of inequality metrics and allow for varying sensitivity at different segments of the distribution depending on the formulation. The Theil index is most sensitive to changes in the lower range of the distribution, which we calculate as:

$Theil = \sum_{i=1}^{n}(\frac{w_i}{N})(\frac{HAZARD_i}{MEANHAZ})log(\frac{HAZARD_i}{MEANHAZ})$

where w is the population weight for unit i. Theil values range from 0 to infinity with higher values representing more inequality.

3. Generalized Entropy

An alternative GE metric that is sensitive to changes in the upper range of the distribution is:

$GE = \frac{1}{2} * [(\sum_{i=1}^{n}(\frac{w_i}{N})(\frac{HAZARD_i}{MEANHAZ})^2) - 1)]$

GE values range from 0 to infinity with higher values representing more inequality.

Horizontal Inequalities

Another way to measure inequality is by summarizing key aspects of the distribution among different groups of a population. Often these groups are based on demographic characteristics, such as poverty, minority status, home ownership, etc. We use the previously described set of social vulnerability indicators to partition climate hazard distributions, thereby producing two groups for each indicator, e.g. above/below the poverty line, non-Hispanic white/non-white, renter/owner, etc. Many of these characteristics are outlined as explicit inequality concerns in US Federal and state government policy and law (Clinton, 1994).

The metric on which we base our horizontal inequality measurements is the hazard for each population group, which we calculate at the median as:

$$HAZARD_j = \frac{\sum_{i=1}^{n} HAZARD_i * POPULATION_i * X_{ij}}{\sum_{i=1}^{n} POPULATION_i * X_{ij}}$$

Where POPULATION is the population in Census Tract i and X is the proportion of population group j. With this equation we can derive alternative statistics such as hazard at the 90th percentile of the distribution for each population group, which we find by looking at the distribution of the numerator in equation (**??**). Other inequality metrics we calculate include inequality at the 90th percentile of the group-wise hazard distributions, the proportion of Census Tracts with high climate hazard and high social vulnerability, the disparity from average climate hazard between groups, and the probability of each group living in a high hazard place.

Hazard at the median. Median hazard experienced by each group. This provides a view of the average hazard experienced between groups. Values range from 0 to the maximum of the hazard statistic.

Hazard at the 90th percentile. Hazard at the 90th percentile for each group. Looking at inequalities across different segments of the group-wise hazard distribution informs whether there is variation in the hazard ratio between groups at lower and higher hazard levels. Values range from 0 to the maximum of the hazard statistic.

Proportions of high climate hazard and high social vulnerability. We order Census Tracts into terciles (high, medium, low) on SoVI and climate risk. Then we calculate the proportion of Census Tracts per administrative unit, either state or county, with high social vulnerability and high climate hazard. This statistic can be thought of as the spatial intensity of high climate risk for a geographic unit. Values range from 0 to 1.

Disparities in hazard. Average difference in climate hazard relative to the mean. We con-

sider this as a measure of the group-specific skewness for the climate hazard distribution. Values range from 0 to the maximum of the hazard statistic.

Probabilities of high hazard. The number of individuals experiencing high hazard divided by the total population to estimate the probability of each group experiencing high hazard. This statistic can be thought of as the spatial frequency of high climate risk for an aggregated unit. Values range from 0 to 1.

The values we report in our results represent ratios of the hazard metric between groups. A value greater than 1 indicates higher hazard burden for the socially vulnerable whereas below 1 is lower.

Spatial inequality

Disaster mitigation and climate adaptation targeting, at least from a federal or state perspective, becomes even more efficient when we identify clusters of high risk areas, i.e., hotspots. Spatial inequalities are also important for understanding spatial processes producing and patterns resulting from opportunity structures and inequality formation across space. One way to assess clustering of values for a continuous spatial field is with Moran's I statistic, a measure of spatial autocorrelation. The global Moran statistic is a single value that measures the degree of spatial autocorrelation across the whole dataset. It represents how similar or dissimilar values are as a function of space for one variable, typically ranging from -1 to 1, the closer the statistic is to 1, the greater the degree of positive spatial autocorrelation; while the closer it is to -1 indicates stronger negative spatial autocorrelation. -1 is perfect dispersion, +1 is perfect clustering, and 0 is complete spatial randomness. It indicates the degree of linear spatial association between the variable of interest x and spatially weighted averages vector of neighboring values W_x, where W is the summed spatial weight matrix w_{ij} if it is row-standardized

and which formalizes the adjacency structure of the dataset (Moran, 1948). Moran's I statistic is computed as:

$$I = \frac{N}{W} \frac{\sum_{i=1}^{N} \sum_{j=1}^{N} w_{ij}(x_i - \bar{x})(x_j - \bar{x})}{\sum_{i=1}(x_i - \bar{x})^2}$$

With N as the total number of spatial units, all for reference unit i and comparison units j. A bivariate Moran's I is akin to the univariate Moran's I statistic, except that rather than determining the level of spatial autocorrelation within one variable (spatial clustering for values of one variable), the bivariate statistic determines spatial autocorrelation between two variables (spatial clustering for values across two variables). We use this bivariate measure to estimate clustering of values for the SoVI and climate hazard. Like the univariate Moran's I, a bivariate Moran's I usually ranges between -1 and 1. An estimate of 0 implies no spatial autocorrelation. It provides an indication of the degree of linear association between an observation variable in one region x_i and a different variable in nearby regions y_j according to the spatial weight matrix w_{ij} which formalizes the neighborhood or contiguity structure of the dataset (Moran, 1948). The bivariate Moran's I statistic is computed as:

$$I^{bivariate} = \frac{N}{W} \frac{\sum_{i=1}^{N} \sum_{j=1}^{N} x_i x_j w_{ij}}{\sum_{i=1}^{N} x_i^2}$$

where x_i is the variable that we are testing and is measured as deviation from the mean, i.e. $x_i = X_i – \bar{X}$. The location variable for the area's proximity is given by w_{ij} which is the element from the corresponding spatial weight matrix. A bivariate global Moran's I statistic only provides information about the average degree of spatial autocorrelation between two variables across the full sample. To examine bivariate localized spatial autocorrelation, we estimate the local Moran's I, which provides similar information to the global statistic, except that it is specific to an area surrounding a spatial unit i:

$$I_i^{bivariateLocal} = \frac{\sum_j x_i x_j w_{ij}}{\sum_i x_i^2}$$

The local Moran's I represents climate hazard and social vulnerability clusters for each hazard. We identify high hazard and high social vulnerability (high-high) spatial clusters of US Census Tracts.

Results

We first describe the spatial distribution of climate risk as represented by the bivariate association between the social vulnerability index and each climate hazard across the conterminous USA. Then we present results for our vertical and horizontal inequality estimates at the national level. To get a better idea of how inequality varies throughout the US and the relationship among different inequality metrics, we also estimate metrics at the state level. We report these state level results and look at correlations among different metrics to explain similarities and differences across different ways of measuring inequality. Lastly, we present findings at the state and national level on spatial inequality and clustering. Table 3.1 maps the social indicator variable names to the characteristics they represent.

Inequality within hazard distributions

Table 3.9 displays inequality metrics for all hazards. Wildfire is the most unequal according to the Gini Coefficient while flooding is the least. Drought is also relatively less equal than other hazards across all metrics. The aggregate climate hazard is usually less unequal than flooding, suggesting that hazard burdens are more uniform across space and the population when considering any-type hazard. The first generalized entropy metric, the Theil index, inversely places wildfire as nearly the most equal alongside storm, whereas the second entropy metric reconfirms wildfire as the most unequally distributed

hazard. This likely suggests that a main driver of wildfire inequalities comes from changes in the middle and upper end of the wildfire distribution since the Theil index is most sensitive to changes at the bottom. Furthermore, we see that the Theil index is lower across all hazards than the other GE metric, similarly indicating greater influence from changes at the upper end of distributions.

Tables present correlations among vertical inequality metrics. The statistics are positive and high (above .9) except for between Theil and Gini for wildfire. This lower correlation also signals that there is a great deal of inequality among places with lower wildfire hazard but that as wildfire hazard increases so does the equality of hazard values.

Among group inequalities

Table **??** displays the most and least unequal groupings per hazard and inequality metric. We see that hazard differences at the median are highest for those living in mobile homes (heat, fire, flood, and climate), minorities (drought), and those without vehicles (storm). Differences at the 90th percentile are highest for the disabled across all hazards except drought, which is for renters. Average disparities are highest for those without vehicles aside from those in mobile homes for storm. Similarly, the probability of living in a high hazard area is also highest for those without vehicles in all but two hazards, drought and storm.

Inequalities among groups vary by hazard and metric. The least unequal groupings include those who live in crowded housing for hazard at the median; communities with limited English, multiunit housing, mobile homes for hazards at the 90th percentile; mobile homes, no vehicle, group quarters, poverty for average disparities; and those in poverty, disabled, mobile homes, unemployed for the probability of living in high hazard. Overall, social indicators comprising the least unequal groupings are more mixed than

the most unequal.

We also present the highest and lowest hazards and social indicators per state in Table 3.10. We see that drought and fire are the most unequally vertically distributed hazards at the state level while climate and storm tend to be the least. The most horizontally unequal hazards vary by state, but fire and flooding are notably unrepresented in the mixture. At the minimums, fire tends to be one of the least unequally distributed alongside drought. The grouping for which inequalities are at a greatest include those living with a disability, in a mobile home, without high school diplomas, minorities, and the uninsured. The least unequal groupings are for multi-unit housing, group quarters, and limited English.

Inequality metric correlations by hazard

Another way to understand the relationship among inequality metrics, variables of interest, and population groupings is by observing correlations between estimates. Tables 3.9 provides these correlations. To present a snapshot of these relationships, we found the social indicators with the highest inequality per hazard and then calculated Spearman's Rank Correlations among ratios for hazard at the median and 90th percentile. We find relatively low and inconsistent correlations among the various metrics aside from the vertical inequality correlations described earlier. Of particular interest are low correlations between hazard at the median and at the 90th percentile, suggesting that hazard inequalities are rather variable at different segments of the distributions. We also observe low and often negative correlations between vertical and horizontal inequalities. It is therefore not necessarily the case that a state with a highly unequal vertical hazard distribution portends greater inequality between population groups.

Spatial Inequalities

Spatial variation is clearly visible when looking across inequality metrics for different states. An additional way to view these spatial inequalities is through descriptive mapping, cluster detection, and spatially-explicit statistical measures. We observe high climate risk and high social vulnerability patterns across several measurements. The maps shown in Figures 3.1, 3.9, and 3.14 display distinct regions of high climate risk for each hazard: east of the Mississippi River and the Pacific Northwest for storm and flood; the Desert Southwest and Southeast for heat; rural areas west of the Rocky Mountains for fire and drought; and rural, inland areas west of the Rocky Mountains, coastal tracts in Gulf states, Appalachia, and central to southern Florida for the aggregated climate risk.

The spatial inequality statistics calculated per hazard across the whole dataset can be found in Table 3.11. The univariate Global Moran's I statistics for every hazard are high (above .7) and all positive. Flood is the least spatially clustered whereas heat and storm are the most clustered. The bivariate Moran is relatively low (under .01) and positive for heat and drought. Spatial Gini statistics represent the spatial decomposition of the Gini index. We see that all of the inequality in the Gini Index comes from non-neighboring Census Tracts.

Figure 3.14 displays bivariate local indicators of spatial autocorrelation at the 0.05 significance level. Tracts that are not significant do not exhibit any meaningful spatial clustering of similar or dissimilar values. We find distinct high social vulnerability index and high hazard clusters in the following areas: storm concentrates in the pacific northwest and from the mid-Atlantic to northeast, heat in the southeast and southwest, drought in the desert southwest and mountain west, fire in the forested west, flood is throughout the east and the pacific northwest, and the aggregate climate hazard is in the Great Basin, Appalachia, and the Gulf of Mexico.

The disparity measurements calculated for Figures **??** and **??** provide a slightly different picture of the spatial and social distribution of climate risk. Counties with the largest disparities exist in nearly every state across the conterminous USA, at least where there is hazard exposure (e.g. wildfire hazard is very low in the Great Lakes and Northeast, so many states west of the Mississippi have few risk disparities). Distinct patterns still exist and generally follow the geography outlined in the previous paragraph.

Discussion

This analysis has compared different ways of measuring inequalities across multiple climate hazards and social indicators. Our goal was to better understand different aspects of climate hazard inequalities and whether these hazards are distributed in an unjust way. We posed the following questions: How unequally distributed are climate hazards: vertically, horizontally, and spatially? Which population groups and places experience unequal climate hazard burdens? Do different representations of climate risk inequalities lead to varying environmental justice interpretations?

We find mixed results regarding the nature of hazard inequalities at a national and state level among different population groups. Importantly, the presence of one type of inequality (vertical, horizontal, or spatial) does not necessarily indicate the existence of other types of inequalities. Similarly, inequalities for one vulnerable group, as designated by a specific social indicator, provide limited insight into inequalities for the 'socially vulnerable'. Climate hazards tend to be less unequally distributed when compared to Gini index estimates for other variables, which is not part of the present analysis. Only drought and fire are more unequally distributed than income (0.25) and none are more unequally distributed than pollution (0.76) (Boyce et al., 2016). It makes sense that

drought and fire are the most vertically unequal since the spatial distribution of high hazard is disproportionately greater in the western half of the country whereas high storm, heat, and flooding hazard are present in nearly every state. Furthermore, wildfire and drought are functions of fuel and population, respectively, both of which are characterized by spatially unequal surface characteristics. It seems that vertical inequalities at the national level are not a particularly concerning feature of climate hazard distributions. Even so, state-specific analyses present varying insights on a hazard-by-hazard basis. Many states have hazard inequalities much greater than the national average, examples include Nevada for storm, California for heat, Oregon for drought, Arizona for fire, and New York for flooding. Although vertical inequality metrics offer a broad insight into the distribution of climate hazards, they do not provide any evidence towards issues of distributive justice.

Horizontal inequality metrics do compare hazard burdens for distinct population groups and therefore deal in issues of justice if any comparison group is socially vulnerable. Inequalities between groups are present but not in the same direction for all hazards, social indicators, and places. Ratios between lower and higher social vulnerability groups are usually less than 1 for hazard at the median, hazard at the 90th percentile, average hazard disparities, and high hazard probabilities, indicating that less vulnerable groups often experience greater hazard (Table 3.9. Even ratios that exceed 1 tend to not be very extreme. Exceptions include high ratios for minorities and drought as well as mobile homes and fire. Interestingly, nearly all ratios decrease at higher segments of the distribution, indicating that more vulnerable populations do not usually bear a greater or increasing share as hazard increases. We see this with decreasing and flat trends in Figure **??**, which shows ratios for a selected subset of social indicators across hazard distributions. Lower inequalities in certain indicators (multi-unit housing, limited en-

glish, and group quarters) seem to indicate that urban areas have lower hazard exposure. Keeping in mind that horizontal inequalities do vary by geographic aggregation, our results nonetheless suggest that there is not a sweeping environmental justice concern at the national-level for climate hazards. However, looking at smaller area (county, state, region, etc) horizontal distributions across different social indicators does appear to be necessary.

Even though looking at vertical and horizontal inequality metrics independently gives us a good sense of the inequality patterns, it does not inform how different facets of inequality relate to one another. Correlations among inequality metrics suggest that inequality is multi-dimensional for hazards, populations, and places, thereby highly sensitive to the metrics, input data, and data partitioning (demographic and spatial) selected by a researcher. Negative correlations between our inequality metrics and different segments across the hazard distribution further indicate that places with low hazard are not necessarily less unequal and in fact may often be more unequal by focusing hazard exposure in a few small areas with a higher proportion of vulnerable groups.

Hazard distributions across space are also a large source of inequality. We observe near perfect clustering for climate hazards according to the univariate Moran's I (although less clustered for wildfire and flooding) and spatially random patterning between social vulnerability and climate hazards when referring to the bivariate Moran's I. The bivariate statistic is an expected result considering the myriad stochastic processes underlying formation of climate risk landscapes, which include both social and physical determinants. A potential reason why flooding and wildfire are less spatially dependent than other hazards is that the models for these hazards contain more than just meteorological parameters, including terrain, land use, and vegetation. The spatial Gini decomposition adds to a picture of spatially concentrated hazard. Nearby Tracts tend to be more simi-

lar since all of the inequality stems from non-neighboring Tracts. Moreover, local Moran statistics show clear regions of clustering among high and low risk tracts. Yet, the vertical and horizontal inequality metrics taken as a whole offer up the perspective that inequalities are disperse and diverse. The spatial intensity of inequalities and ubiquity across states, alongside clearly defined regional differences, presents both challenges and opportunities for disaster mitigation and climate adaptation planning.

Climate hazard inequalities have not inspired the same level of interest as those of income and pollution, two variables which have garnered a great deal of attention by both inequality researchers and policymakers. A primary reason is that climate hazards are not fully manageable by humans (they are 'natural', to some extent), which implores the question as to whether people should be afforded safety below a certain level of hazard. Whereas this is the case for income and pollution–there is broad consensus that extending below or beyond a certain income or pollution level is unacceptable and means should be implemented to mitigate such circumstances. One reason the literature suggests there is this disparity in acceptable levels between climate hazards and variables, such as income and pollution, is that many people select into higher climate hazard areas to access other qualities that have recreational and aesthetic value (skiing, sea views, etc.) (Harries, 2008; Plattner, Plapp, & Hebel, 2006). However, people also make similar decisions to be exposed to more pollution or have lower relative incomes to access amenities of value (e.g. large, expensive cities) (Millimet & Slottje, 2002).

Despite lacking an objectively agreed upon or legally binding level of acceptable climate hazard, inequalities in these distributions still elicit concern. There is keen interest in both literature and policy on whether marginalized communities and the socially vulnerable bear a disproportionately high climate hazard burden. We see this in studies on how differences in degrees of warming produce varying levels of hazard inequalities (King &

Harrington, 2018), the planning implications of climate change on the most vulnerable in society (Frosch, Pastor, Sadd, & Shonkoff, 2018), the sociology of climate justice (Dunlap & Brulle, 2015); and hazard-dependent home value appreciation rates, termed climate gentrification (Keenan, Hill, & Gumber, 2018). Governments and organizations also set goals and invest in programs for reducing these inequalities and the negative externalities they produce (Yarmuth, 2021).

Observing inequalities can help inform decisions towards investing in hazard mitigation. First and foremost, using inequality metrics advises decision making towards reducing inequalities in places and populations with high hazard and high socially vulnerability–ecological sacrifice zones (Bullard, 2011). Yet, inequality metrics highlight that high hazard is not a sufficient premise for disaster mitigation support. If this was always given to geographies with the highest hazard, potential issues would arise when there are large differences among the contrasting types of inequalities facing people and places (Braun, Oßenbrügge, & Schulz, 2018). Not only does this approach potentially lead to moral hazards by encouraging people to move into higher hazard places, it also advantages those who would choose to accept higher hazard. To prevent this, investments can be more equally distributed along two tracks: reducing inequalities and reducing exposure in the highest hazard places. Inevitably, the former will sometimes occur in relatively lower hazard places.

Future research should address several items. Exploring hazard inequalities at larger scales using higher resolution hazard data to illuminate intra- county and city and inequalities. Examining how inequalities change over time along with population characteristics, both historically and by projecting out to the future, will provide evidence regarding differences among groups for selection into and out of hazardous areas. Investigating the processes underlying spatial inequality formation and opportunity structures

is an imminently important endeavor, but one that likely necessitates place-based, qualitative, legal, and other research approaches extending beyond the methodological scope of this type of study. A crucially important research topic will be to understand how society responds to shifting climate hazard from an inequality lens. Extending our analysis beyond social vulnerability indicators to features of disaster mitigation and climate adaptation would tease out processes underway that will either ameliorate or exacerbate existing inequalities.

Conclusion

Our research informs both the overall degree of climate hazard inequality as well as inequalities between people and places. We compared vertical inequality metrics with sensitivities to changes in different parts of the hazard distribution, the variation in horizontal inequalities by categorization of the socially vulnerable, how vertical and horizontal inequality metrics inform and contradict each other at the state and national levels, and the geographies of spatial inequalities. We find a great deal of variability among inequality metrics and rankings for states, hazards, and social indicators. Our findings suggest that choosing appropriate types of inequality metrics (vertical, horizontal, and spatial) for a particular use case should be emphasized. Identifying different formulations of a metric also has implications. For example, a vertical inequality metric most sensitive to changes in the middle of a distribution would miss inequalities manifesting at the tail ends, producing a false negative for identifying an issue of distributional concern. If the study were to instead use a metric sensitive to changes in the tails then the recommendation would likely be to mitigate and reduce exposure to extreme hazards for greater equality.

Another key takeaway is that horizontal inequalities vary substantially across different vulnerability categories. Researchers and practitioners should consider this in their project design. One way to do this is by looking at social vulnerability indicators of explicit concern, such as those outlined in environmental justice laws. An alternative approach would be to select the indicators most determinant of some negative hazard outcome, such as hazard loss, by looking at and conducting validation studies to this end. Lastly, it appears that climate hazards are not ubiquitously unequally distributed across population groups, suggesting less of a need for abatement investments to the same extent as those for pollution hazards. Instead, climate hazard inequality concerns may bear out through responses to changing hazard in the form of depopulation, disinvestment, and disenfranchisement of climate risky places. Attention should be directed towards communities at risk of marginalization from the climate adaptation process and how to provide support for them.

Appendix

Table 3.1: Social indicator variable abbreviations and descriptions.

abbreviation	social indicator
AGEDEP	Age Dependency (pct)
CROWD	Crowded Housing (pct)
DISABL	Disability (pct)
GROUPQ	Group Quarters (pct)
LIMENG	Limited English (pct)
MINRTY	Minority (pct)
MOBILE	Mobile Home (pct)
MUNIT	Multi-Unit Housing (pct)
NOHSDP	No High School (pct)
NOVEH	No Vehicle (pct)
PCI	Per Capita Income
POPDENS	Population Density
POV	Poverty (pct)
RENT	Renter (pct)
SNGPNT	Singe Parent (pct)
UNEMP	Unemployed (pct)
UNINSUR	Uninsured (pct)

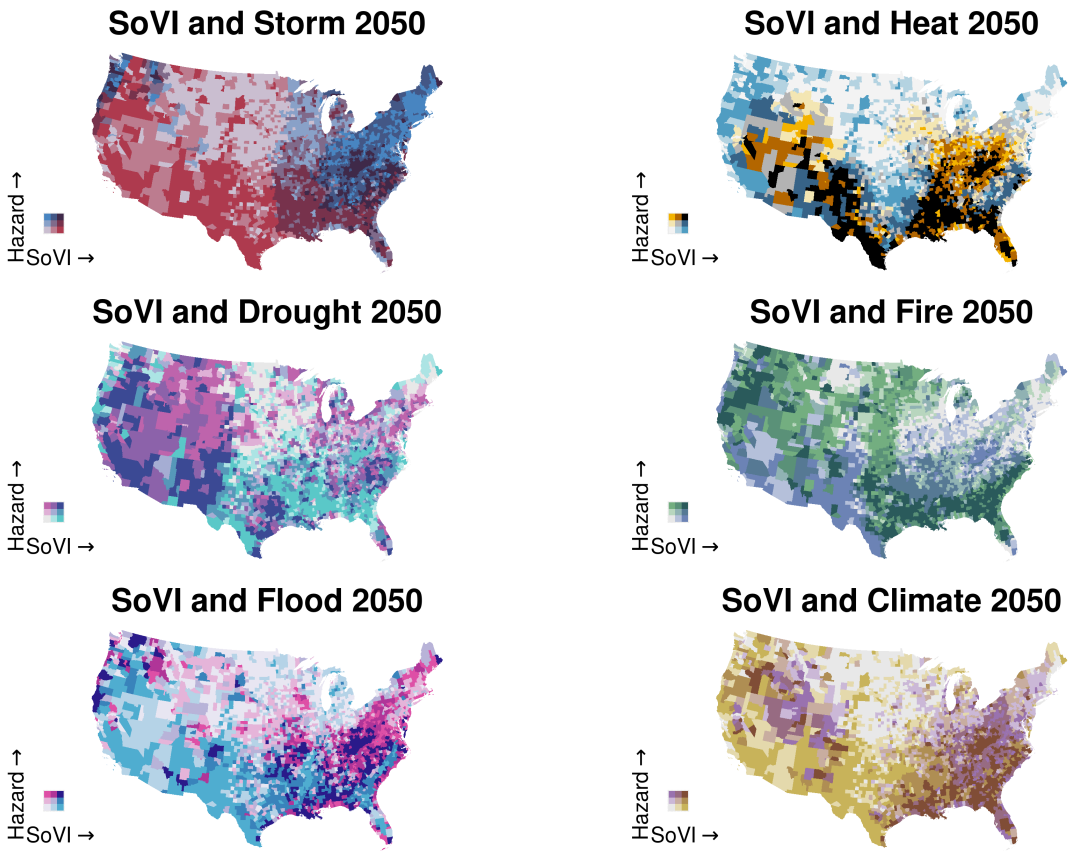

Figure 3.1: Bivariate association across climate hazards and the Social Vulnerability Index (SoVI).

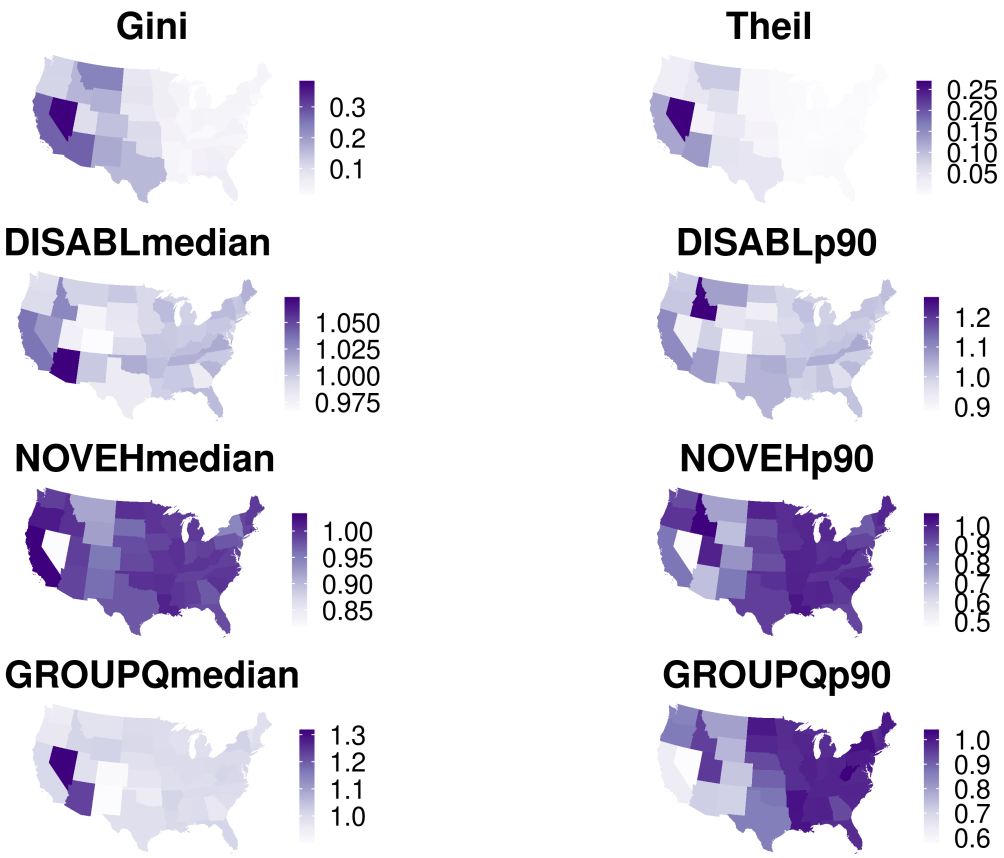

Figure 3.2: State-level Storm hazard inequalities for the vertical Gini and Theil Indices, median across the full hazard distribution, and p90 at the 90th percentile of hazard.

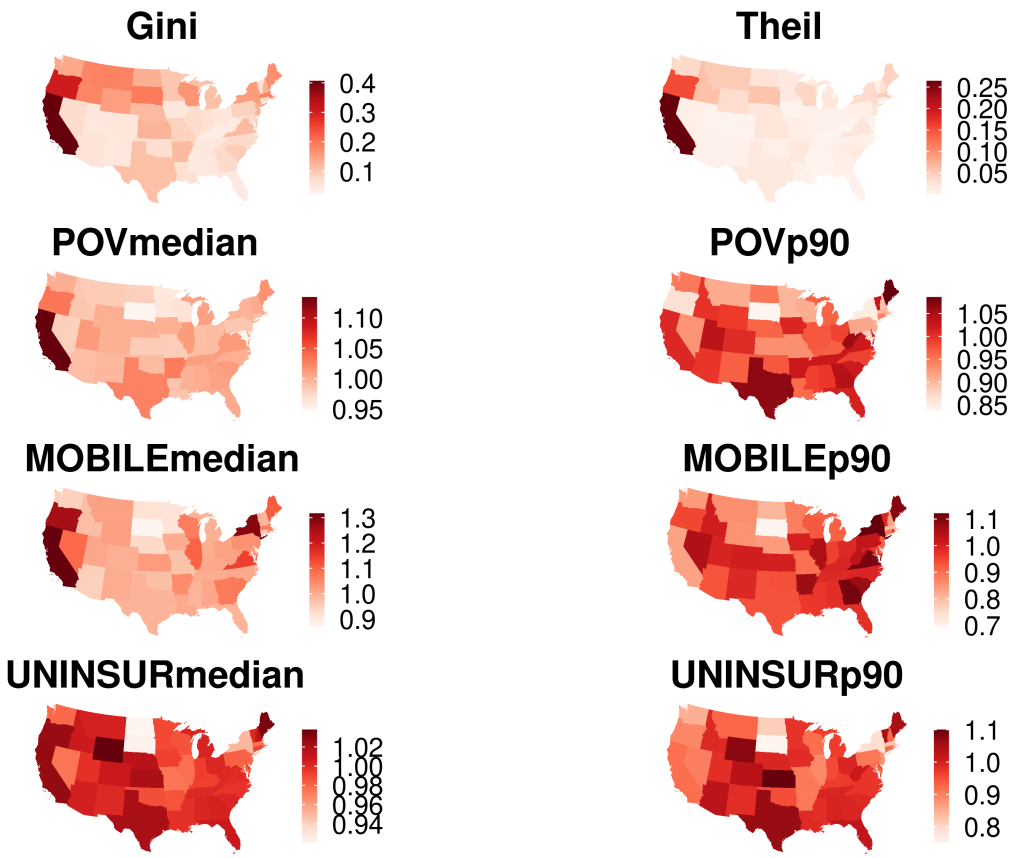

Figure 3.3: State-level Heat hazard inequalities for the vertical Gini and Theil Indices, median across the full hazard distribution, and p90 at the 90th percentile of hazard.

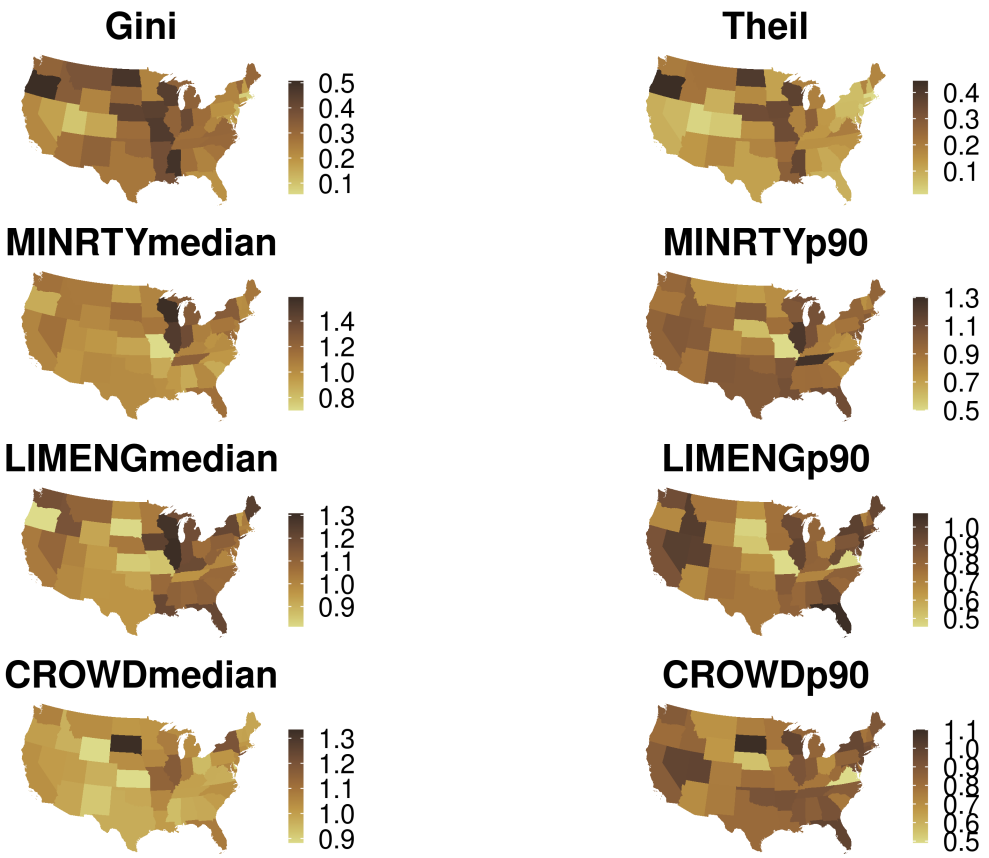

Figure 3.4: State-level Drought hazard inequalities for the vertical Gini and Theil Indices, median across the full hazard distribution, and p90 at the 90th percentile of hazard.

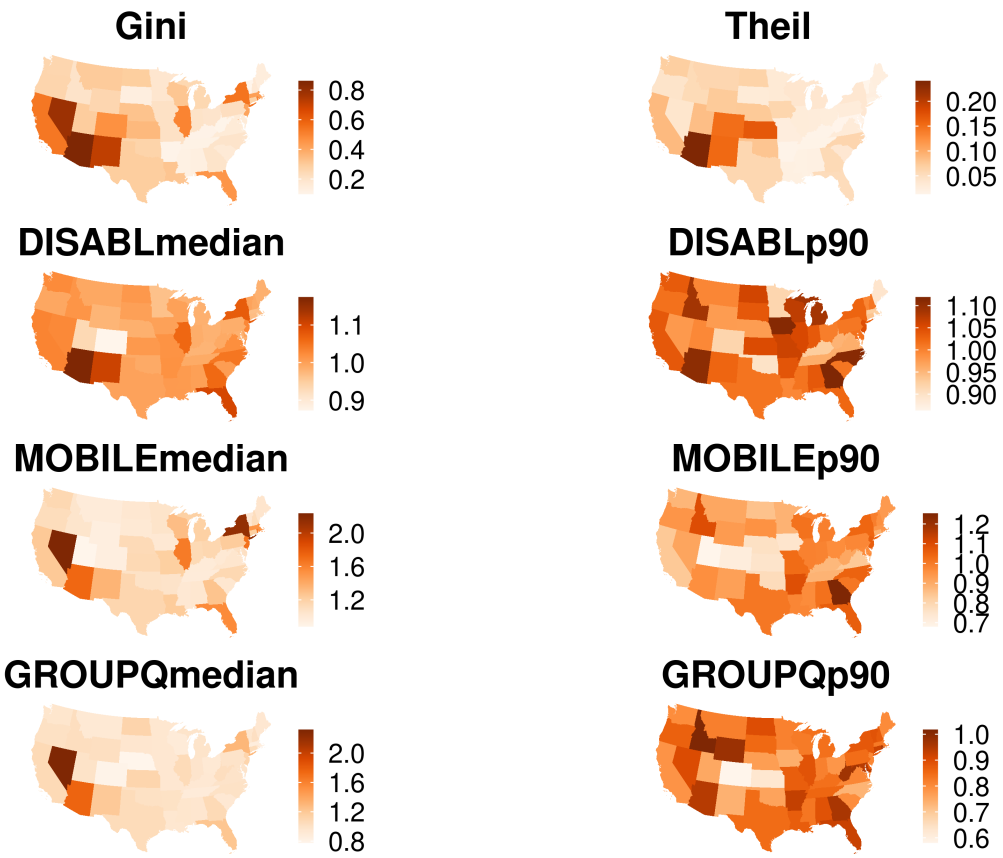

Figure 3.5: State-level Fire hazard inequalities for the vertical Gini and Theil Indices, median across the full hazard distribution, and p90 at the 90th percentile of hazard.

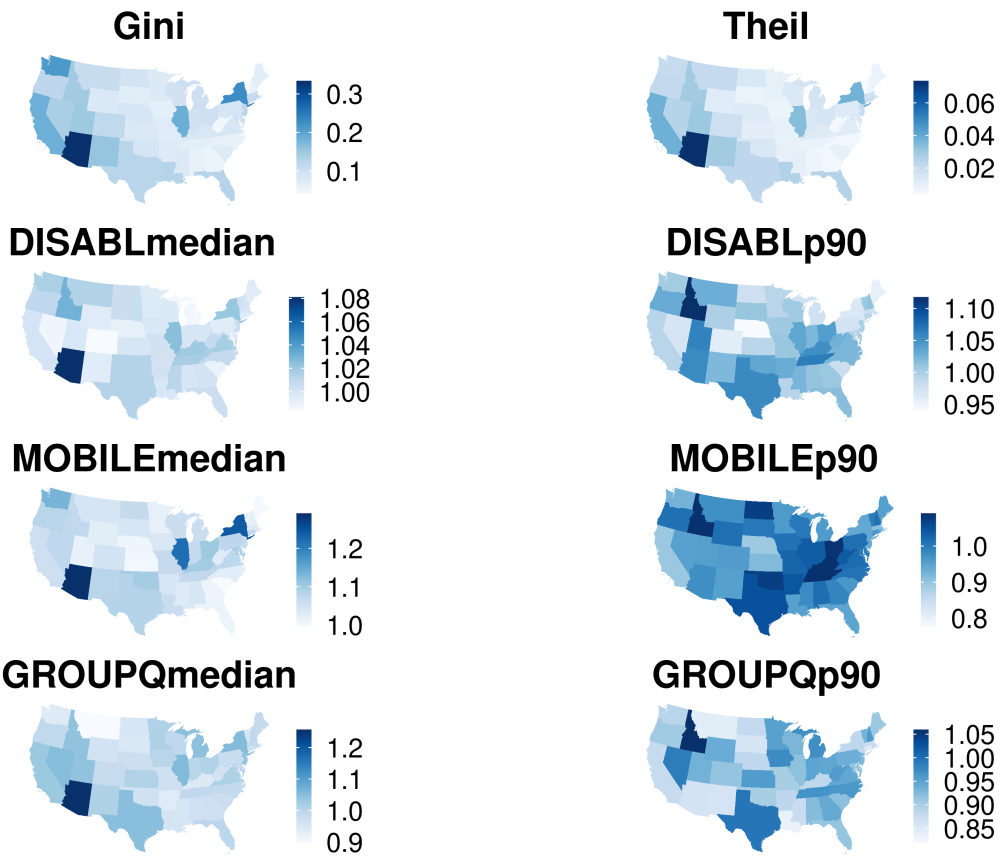

Figure 3.6: State-level Flood hazard inequalities for the vertical Gini and Theil Indices, median across the full hazard distribution, and p90 at the 90th percentile of hazard.

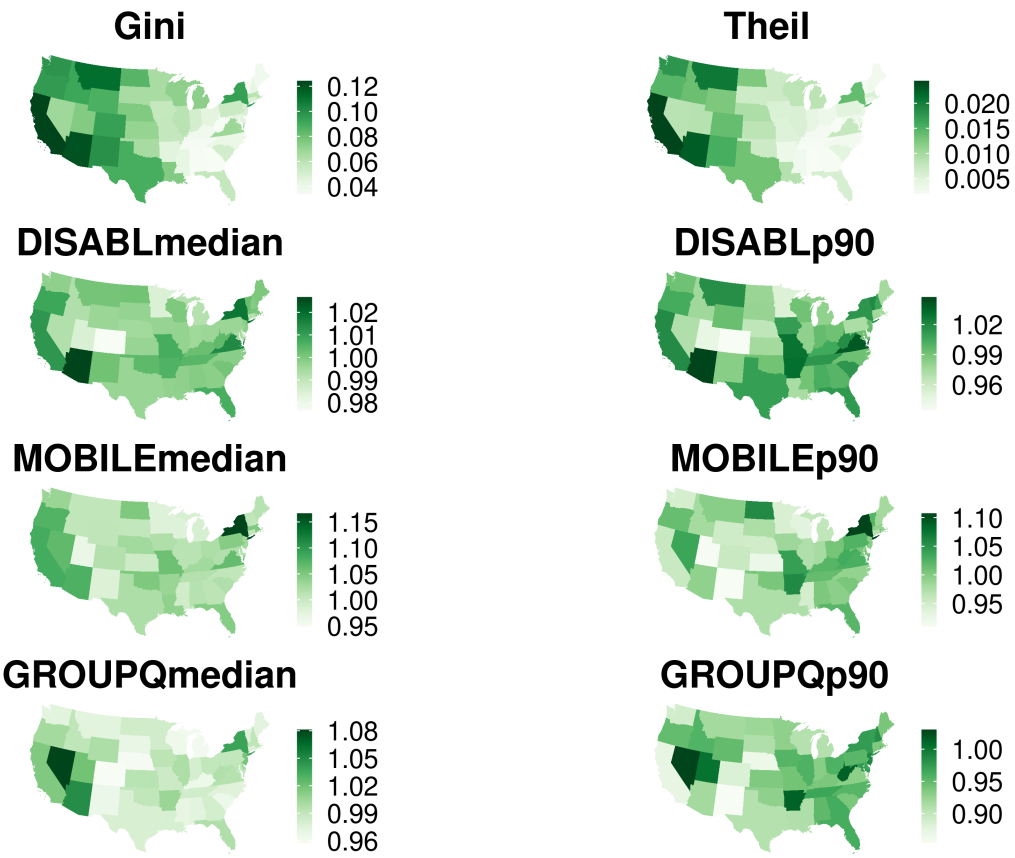

Figure 3.7: State-level Climate hazard inequalities for the vertical Gini and Theil Indices, median across the full hazard distribution, and p90 at the 90th percentile of hazard.

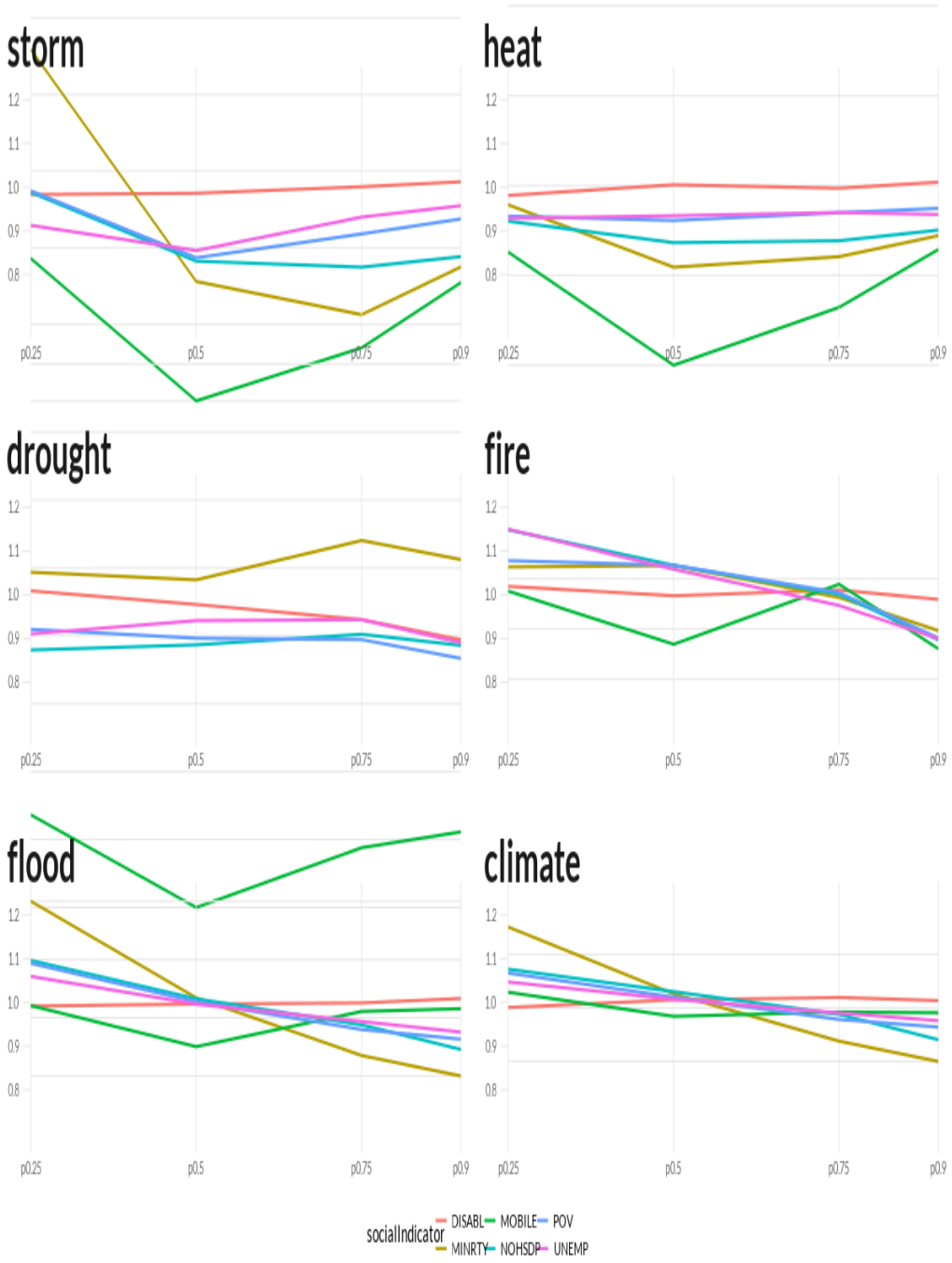

Figure 3.8: Horizontal inequality ratios by hazard percentile across climate hazards. A ratio above 1 indicates higher hazard burden for socially vulnerable groupings.

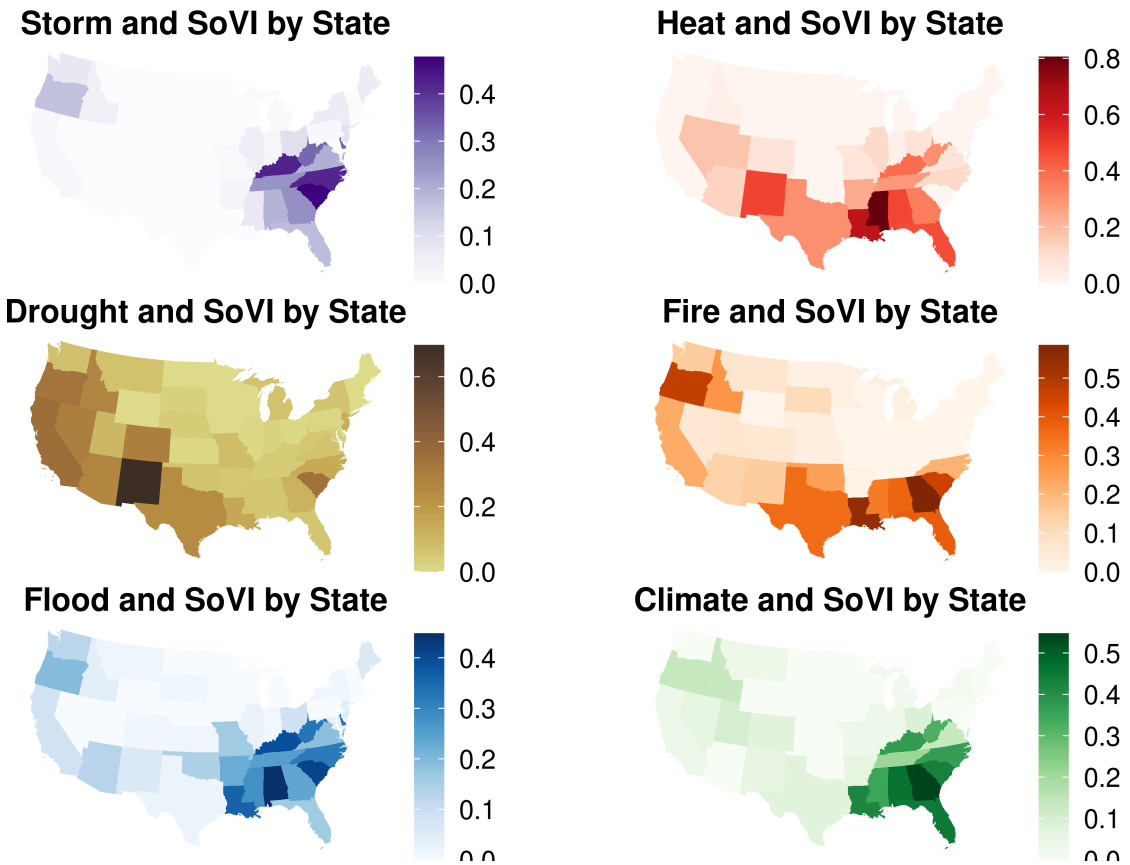

Figure 3.9: State-level proportions of high climate risk census tracts, defined as tracts in the top tercile of hazard and social vulnerability.

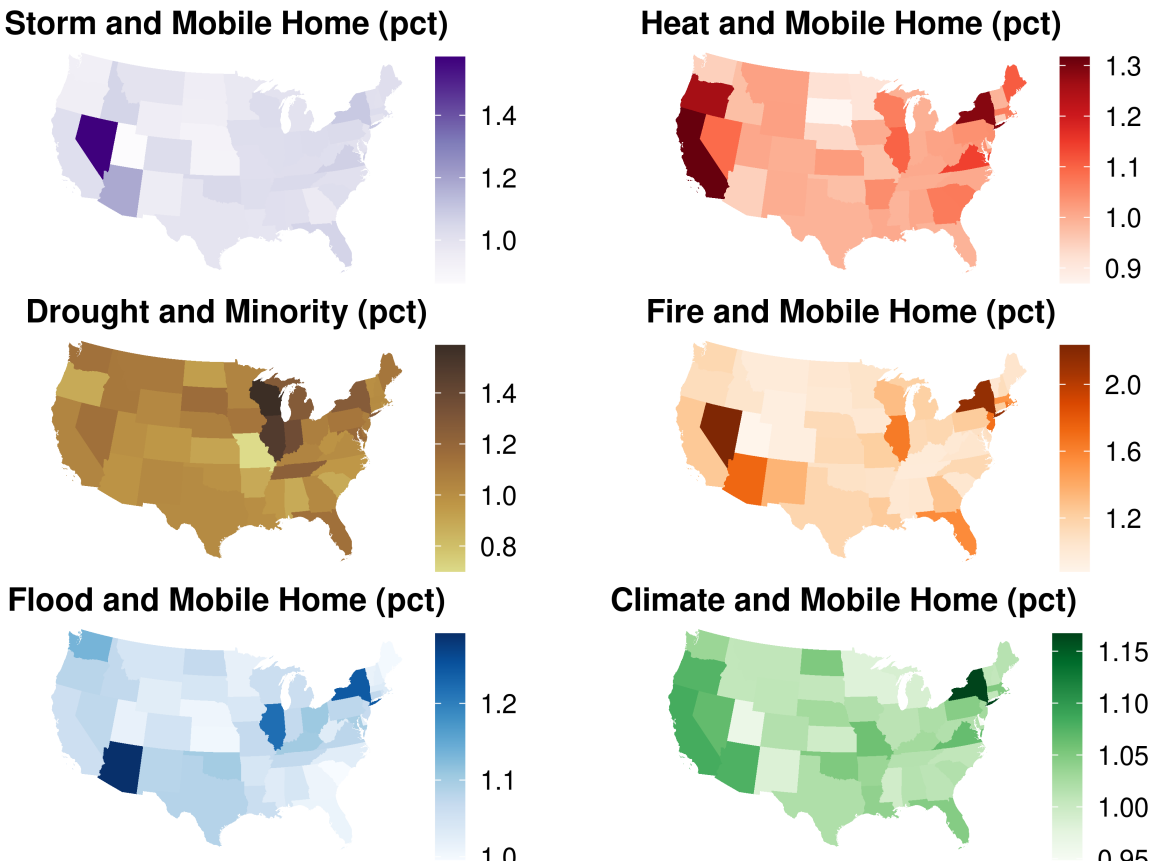

Figure 3.10: Hazard disparities by State calculated as the verage difference in climate hazard relative to the mean for each group We consider this as a measure of the group-specific skewness for the climate hazard distribution. A ratio above 1 indicates higher hazard burden for socially vulnerable groupings.

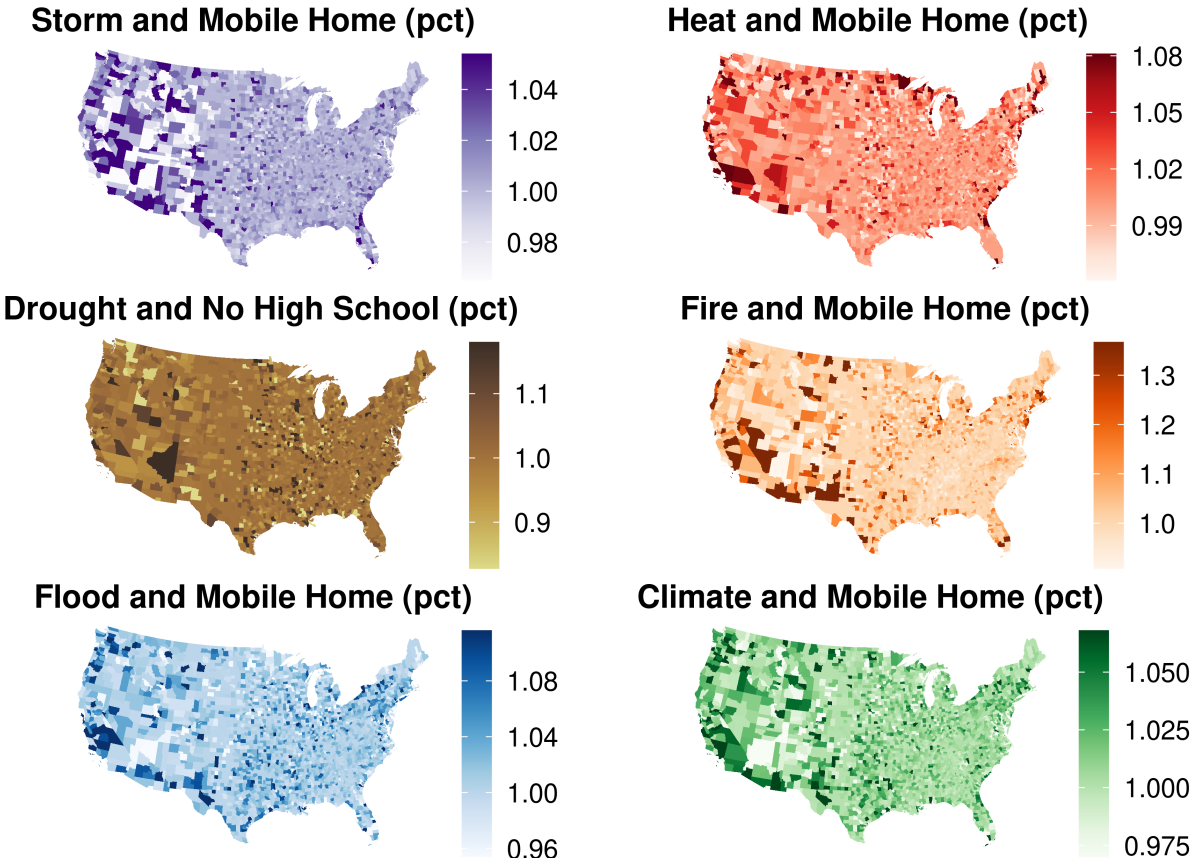

Figure 3.11: Hazard disparities by County calculated as the verage difference in climate hazard relative to the mean for each group We consider this as a measure of the group-specific skewness for the climate hazard distribution. A ratio above 1 indicates higher hazard burden for socially vulnerable groupings.

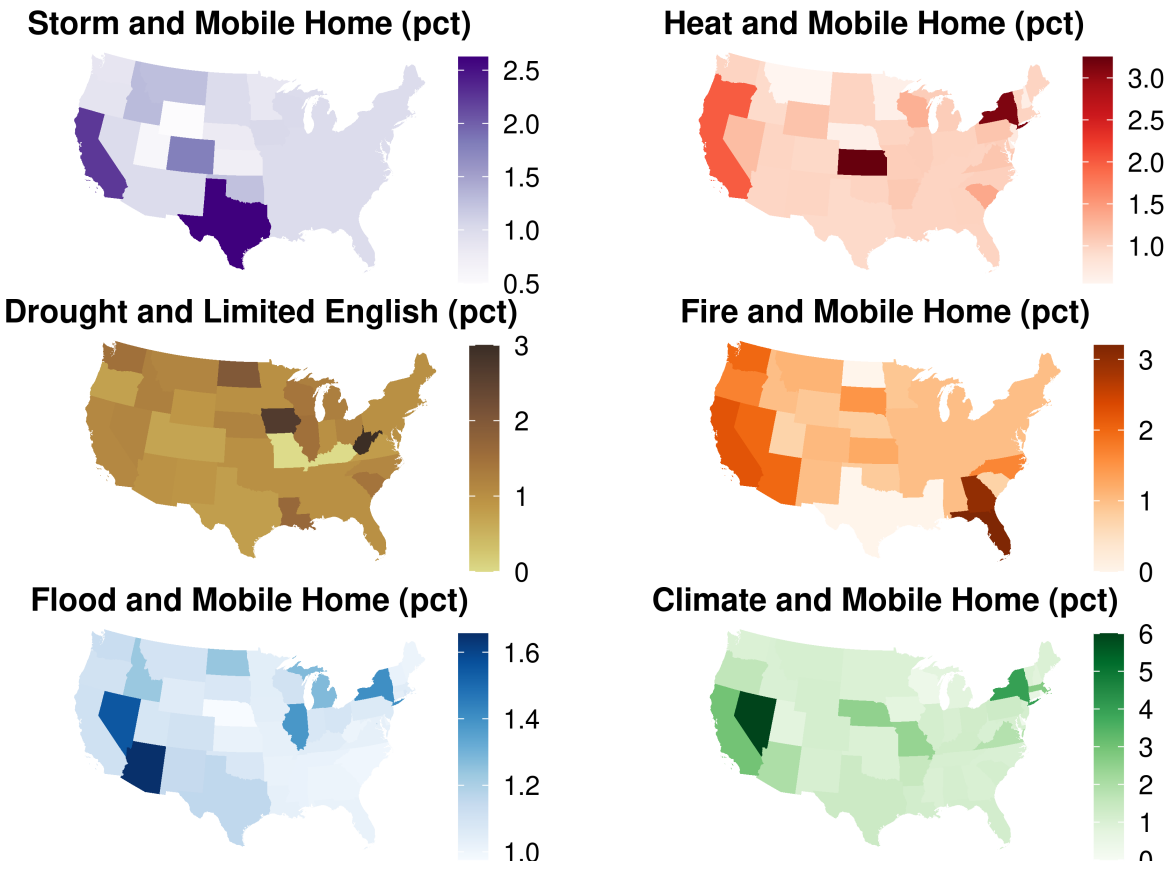

Figure 3.12: High hazard probabilities by State calculated as the number of individuals experiencing high hazard divided by the total population. This statistic can be thought of as the spatial frequency of high climate risk for an aggregated unit. A ratio above 1 indicates higher hazard burden for socially vulnerable groupings.

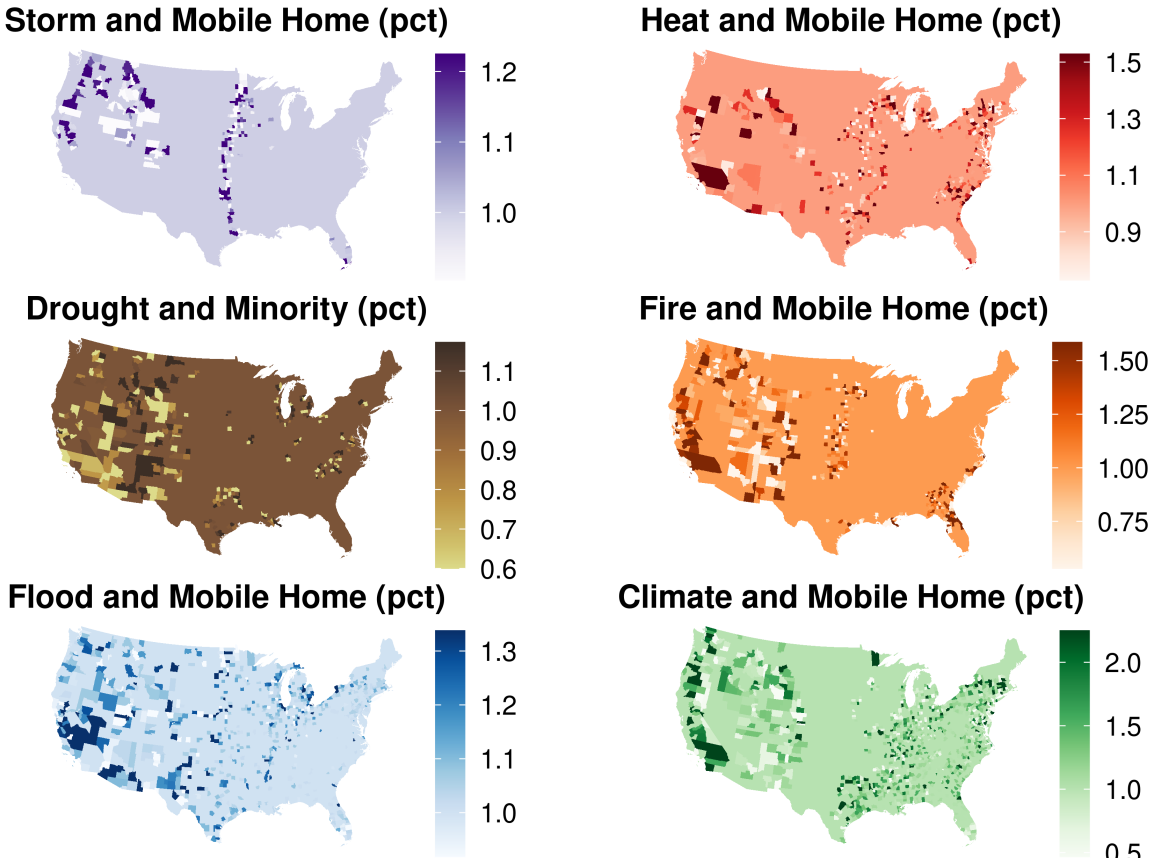

Figure 3.13: High hazard probabilities by County calculated as the number of individuals experiencing high hazard divided by the total population. This statistic can be thought of as the spatial frequency of high climate risk for an aggregated unit. A ratio above 1 indicates higher hazard burden for socially vulnerable groupings.

Table 3.2: National climate hazard inequality metrics

variable	storm	heat	drought	fire	flood	climate
Gini	0.20	0.24	0.37	0.41	0.15	0.10
Theil	0.08	0.10	0.22	0.10	0.03	0.02
entropy	0.10	0.11	0.25	0.53	0.07	0.02
RENTmedian	0.93	0.93	1.12	0.83	0.92	0.95
POVmedian	0.98	1.04	0.99	0.92	0.96	0.98
UNEMPmedian	0.99	1.01	1.03	0.94	0.98	0.99
NOHSDPmedian	0.92	1.00	1.07	0.88	0.94	0.96
DISABLmedian	1.03	1.03	0.94	1.03	1.02	1.01
SNGPNTmedian	0.98	1.02	1.02	0.94	0.97	0.99
MINRTYmedian	0.84	0.96	1.24	0.79	0.89	0.93
LIMENGmedian	0.81	0.91	1.23	0.67	0.86	0.90
MUNITmedian	0.96	0.91	1.12	0.70	0.91	0.94
MOBILEmedian	1.02	1.15	0.82	1.35	1.10	1.07
CROWDmedian	0.80	0.86	1.21	0.77	0.87	0.89
NOVEHmedian	1.06	0.90	1.06	0.65	0.90	0.94
GROUPQmedian	1.04	1.00	0.89	1.01	1.02	1.00
UNINSURmedian	0.94	1.08	1.00	0.98	0.97	0.99
RENTp90	0.93	0.94	1.08	0.97	0.89	0.90
POVp90	0.93	0.95	0.85	0.90	0.92	0.94
UNEMPp90	0.96	0.94	0.89	0.90	0.93	0.96
NOHSDPp90	0.84	0.90	0.88	0.90	0.89	0.91
DISABLp90	1.01	1.01	0.90	0.99	1.01	1.00
SNGPNTp90	0.92	0.92	0.86	0.88	0.91	0.94
MINRTYp90	0.82	0.89	1.08	0.92	0.83	0.86
LIMENGp90	0.59	0.63	0.82	0.78	0.79	0.83
MUNITp90	0.78	0.73	0.80	0.71	0.85	0.87
MOBILEp90	0.78	0.86	0.46	0.88	0.99	0.98
CROWDp90	0.65	0.68	0.84	0.85	0.85	0.87
NOVEHp90	0.96	0.86	0.86	0.80	0.88	0.92
GROUPQp90	0.83	0.75	0.54	0.75	0.91	0.93
UNINSURp90	0.87	0.97	0.85	0.95	0.92	0.95
proportion	0.08	0.12	0.10	0.11	0.11	0.10
dispNOVEH	0.98	1.02	1.07	1.21	1.06	1.03
dispGROUPQ	1.00	1.00	1.06	1.01	1.00	1.00
dispDISABL	1.00	1.00	1.02	1.04	1.01	0.99
dispMOBILE	1.02	1.00	1.02	0.92	0.99	0.99
dispUNEMP	0.99	1.00	1.03	0.95	0.98	0.99
dispPOV	0.99	1.00	1.01	0.93	0.98	0.99
probNOVEH	0.72	0.55	0.15	0.05	0.91	0.34
probGROUPQ	0.72	0.53	0.15	0.05	0.86	0.30
probDISABL	0.73	0.53	0.13	0.05	0.85	0.29
probMOBILE	0.72	0.53	0.14	0.04	0.83	0.28
probUNEMP	0.73	0.53	0.14	0.04	0.83	0.29
probPOV	0.72	0.53	0.14	0.04	0.83	0.28

median: across the full hazard distribution
p90: at the 90th percentile of hazard
proportion: proportion of high hazard and high social vulnerability tracts
disp: disparities from the average hazard
prob: probability of living in a high hazard tract

Table 3.3: Storm hazard rank rorrelations among state-level inequality metrics.

	Gini	Theil	entropy	DISABLmed	DISABLp90	NOVEHmed	NOVEHp90	GROUPQmed	GROUPQp90
Gini	1.000	0.943	0.952	0.339	0.130	-0.568	-0.826	0.532	-0.927
Theil	0.943	1.000	0.999	0.403	0.026	-0.664	-0.867	0.730	-0.870
entropy	0.952	0.999	1.000	0.406	0.040	-0.646	-0.862	0.717	-0.878
DISABLmed	0.339	0.403	0.406	1.000	0.592	0.101	-0.185	0.588	-0.209
DISABLp90	0.130	0.026	0.040	0.592	1.000	0.362	0.278	0.022	0.063
NOVEHmed	-0.568	-0.664	-0.646	0.101	0.362	1.000	0.820	-0.523	0.521
NOVEHp90	-0.826	-0.867	-0.862	-0.185	0.278	0.820	1.000	-0.618	0.839
GROUPQmed	0.532	0.730	0.717	0.588	0.022	-0.523	-0.618	1.000	-0.364
GROUPQp90	-0.927	-0.870	-0.878	-0.209	0.063	0.521	0.839	-0.364	1.000

Table 3.4: Heat hazard rank rorrelations among state-level inequality metrics.

	Gini	Theil	entropy	POVmed	POVp90	MOBILEmed	MOBILEp90	UNINSURmed	UNINSURp90
Gini	1.000	0.944	0.935	0.500	-0.271	0.557	-0.369	0.108	-0.351
Theil	0.944	1.000	0.998	0.660	-0.157	0.612	-0.313	0.198	-0.260
entropy	0.935	0.998	1.000	0.669	-0.140	0.601	-0.316	0.201	-0.250
POVmed	0.500	0.660	0.669	1.000	0.461	0.614	0.117	0.484	0.147
POVp90	-0.271	-0.157	-0.140	0.461	1.000	-0.063	0.421	0.498	0.689
MOBILEmed	0.557	0.612	0.601	0.614	-0.063	1.000	0.414	0.221	-0.160
MOBILEp90	-0.369	-0.313	-0.316	0.117	0.421	0.414	1.000	0.227	0.361
UNINSURmed	0.108	0.198	0.201	0.484	0.498	0.221	0.227	1.000	0.791
UNINSURp90	-0.351	-0.260	-0.250	0.147	0.689	-0.160	0.361	0.791	1.000

Table 3.5: Drought hazard rank rorrelations among state-level inequality metrics.

	Gini	Theil	entropy	MINRTYmed	MINRTYp90	LIMENGmed	LIMENGp90	CROWDmed	CROWDp90
Gini	1.000	0.967	0.951	-0.012	-0.250	0.076	-0.467	0.105	-0.307
Theil	0.967	1.000	0.970	-0.004	-0.249	0.053	-0.439	0.101	-0.285
entropy	0.951	0.970	1.000	0.039	-0.191	0.117	-0.344	0.150	-0.181
MINRTYmed	-0.012	-0.004	0.039	1.000	0.599	0.603	0.385	0.387	0.330
MINRTYp90	-0.250	-0.249	-0.191	0.599	1.000	0.322	0.561	0.150	0.614
LIMENGmed	0.076	0.053	0.117	0.603	0.322	1.000	0.632	0.175	0.172
LIMENGp90	-0.467	-0.439	-0.344	0.385	0.561	0.632	1.000	-0.013	0.591
CROWDmed	0.105	0.101	0.150	0.387	0.150	0.175	-0.013	1.000	0.470
CROWDp90	-0.307	-0.285	-0.181	0.330	0.614	0.172	0.591	0.470	1.000

Table 3.6: Fire hazard rank rorrelations among state-level inequality metrics.

	Gini	Theil	entropy	DISABLmed	DISABLp90	MOBILEmed	MOBILEp90	GROUPQmed	GROUPQp90
Gini	1.000	0.576	0.974	0.440	0.057	0.751	-0.106	0.631	-0.050
Theil	0.576	1.000	0.472	0.364	0.237	0.102	-0.340	0.323	-0.399
entropy	0.974	0.472	1.000	0.483	0.035	0.790	-0.022	0.701	0.086
DISABLmed	0.440	0.364	0.483	1.000	0.570	0.504	0.438	0.540	0.269
DISABLp90	0.057	0.237	0.035	0.570	1.000	0.091	0.426	0.173	0.093
MOBILEmed	0.751	0.102	0.790	0.504	0.091	1.000	0.294	0.703	0.221
MOBILEp90	-0.106	-0.340	-0.022	0.438	0.426	0.294	1.000	0.105	0.591
GROUPQmed	0.631	0.323	0.701	0.540	0.173	0.703	0.105	1.000	0.250
GROUPQp90	-0.050	-0.399	0.086	0.269	0.093	0.221	0.591	0.250	1.000

Table 3.7: Flood hazard rank rorrelations among state-level inequality metrics.

	Gini	Theil	entropy	DISABLmed	DISABLp90	MOBILEmed	MOBILEp90	GROUPQmed	GROUPQp90
Gini	1.000	0.958	0.927	0.617	0.107	0.744	-0.341	0.714	-0.298
Theil	0.958	1.000	0.825	0.628	0.173	0.682	-0.304	0.774	-0.281
entropy	0.927	0.825	1.000	0.692	0.089	0.777	-0.279	0.648	-0.277
DISABLmed	0.617	0.628	0.692	1.000	0.570	0.683	0.185	0.562	-0.090
DISABLp90	0.107	0.173	0.089	0.570	1.000	0.241	0.607	0.181	0.350
MOBILEmed	0.744	0.682	0.777	0.683	0.241	1.000	0.210	0.579	-0.127
MOBILEp90	-0.341	-0.304	-0.279	0.185	0.607	0.210	1.000	-0.164	0.464
GROUPQmed	0.714	0.774	0.648	0.562	0.181	0.579	-0.164	1.000	0.171
GROUPQp90	-0.298	-0.281	-0.277	-0.090	0.350	-0.127	0.464	0.171	1.000

Table 3.8: Climate hazard rank rorrelations among state-level inequality metrics.

	Gini	Theil	entropy	DISABLmed	DISABLp90	MOBILEmed	MOBILEp90	GROUPQmed	GROUPQp90
Gini	1.000	0.984	0.983	0.196	0.008	0.324	-0.196	0.211	-0.527
Theil	0.984	1.000	1.000	0.258	0.092	0.341	-0.166	0.222	-0.514
entropy	0.983	1.000	1.000	0.258	0.093	0.339	-0.167	0.216	-0.515
DISABLmed	0.196	0.258	0.258	1.000	0.837	0.672	0.519	0.321	-0.005
DISABLp90	0.008	0.092	0.093	0.837	1.000	0.435	0.519	0.164	0.127
MOBILEmed	0.324	0.341	0.339	0.672	0.435	1.000	0.718	0.487	0.054
MOBILEp90	-0.196	-0.166	-0.167	0.519	0.519	0.718	1.000	0.304	0.465
GROUPQmed	0.211	0.222	0.216	0.321	0.164	0.487	0.304	1.000	0.558
GROUPQp90	-0.527	-0.514	-0.515	-0.005	0.127	0.054	0.465	0.558	1.000

Table 3.9: Maximum and minimum inequality metrics by hazard and social indicator.

hazard	median	p90	disparity	probability
Maximum				
storm	NOVEH	DISABL	MOBILE	DISABL
heat	MOBILE	DISABL	NOVEH	NOVEH
drought	MINRTY	RENT	NOVEH	NOVEH
fire	MOBILE	DISABL	NOVEH	NOVEH
flood	MOBILE	DISABL	NOVEH	NOVEH
climate	MOBILE	DISABL	NOVEH	NOVEH
Minimum				
storm	CROWD	LIMENG	NOVEH	NOVEH
heat	CROWD	LIMENG	GROUPQ	GROUPQ
drought	MOBILE	MOBILE	POV	DISABL
fire	NOVEH	MUNIT	MOBILE	MOBILE
flood	LIMENG	LIMENG	UNEMP	MOBILE
climate	CROWD	LIMENG	DISABL	MOBILE

Table 3.10: Selection of maximum and mininimum state-level hazard inequality metrics.

states	MaxHV	MinHV	MaxHH	MinHH	MaxIH	MinIH
alabama	drought	climate	storm	drought	DISABL	GROUPQ
arizona	fire	heat	heat	drought	MOBILE	LIMENG
arkansas	drought	storm	heat	drought	MOBILE	LIMENG
california	fire	climate	drought	fire	DISABL	MUNIT
colorado	fire	heat	heat	fire	MOBILE	LIMENG
connecticut	fire	storm	storm	fire	DISABL	LIMENG
delaware	drought	storm	storm	fire	MUNIT	MOBILE
district of columbia	fire	storm	drought	flood	MINRTY	GROUPQ
florida	fire	climate	heat	fire	MOBILE	LIMENG
georgia	drought	climate	heat	drought	MOBILE	LIMENG
idaho	drought	climate	flood	drought	DISABL	MUNIT
illinois	fire	storm	drought	fire	DISABL	LIMENG
indiana	drought	storm	storm	fire	DISABL	GROUPQ
iowa	drought	heat	heat	fire	DISABL	MUNIT
kansas	fire	climate	heat	fire	DISABL	LIMENG
kentucky	drought	storm	storm	drought	NOHSDP	MUNIT
louisiana	drought	storm	storm	drought	NOHSDP	MUNIT
maine	drought	climate	storm	fire	NOHSDP	LIMENG
maryland	fire	storm	drought	flood	DISABL	NOVEH
massachusetts	fire	storm	storm	fire	MOBILE	LIMENG
michigan	drought	storm	storm	fire	DISABL	GROUPQ
minnesota	drought	storm	storm	fire	DISABL	POV
mississippi	drought	storm	heat	drought	UNINSUR	GROUPQ
missouri	drought	storm	storm	drought	MOBILE	MINRTY
montana	drought	climate	climate	drought	DISABL	MUNIT
nebraska	drought	storm	heat	fire	DISABL	MUNIT
nevada	fire	climate	drought	storm	MOBILE	LIMENG
new hampshire	fire	storm	storm	fire	DISABL	LIMENG
new jersey	fire	storm	drought	fire	MOBILE	LIMENG
new mexico	fire	heat	heat	fire	DISABL	LIMENG
new york	fire	storm	drought	fire	MOBILE	NOVEH
north carolina	drought	storm	storm	drought	DISABL	GROUPQ
north dakota	drought	storm	storm	drought	NOHSDP	MUNIT
ohio	drought	storm	heat	fire	DISABL	LIMENG
oklahoma	drought	climate	storm	fire	MOBILE	LIMENG
oregon	drought	climate	storm	heat	MOBILE	MUNIT
pennsylvania	fire	storm	storm	fire	MOBILE	MINRTY
rhode island	fire	storm	storm	fire	MOBILE	LIMENG
south carolina	drought	storm	heat	drought	DISABL	GROUPQ
south dakota	drought	climate	drought	heat	DISABL	GROUPQ
tennessee	drought	climate	heat	fire	MINRTY	LIMENG
texas	fire	climate	heat	fire	DISABL	LIMENG
utah	fire	heat	drought	fire	DISABL	LIMENG
vermont	drought	storm	heat	drought	UNINSUR	LIMENG
virginia	drought	storm	storm	drought	DISABL	MUNIT
washington	drought	climate	drought	fire	DISABL	LIMENG
west virginia	drought	climate	heat	drought	NOHSDP	MINRTY
wisconsin	drought	storm	drought	fire	DISABL	GROUPQ
wyoming	fire	flood	fire	storm	DISABL	NOVEH

[a] HV: Hazard Vertical; HH: Hazard Horizontal; IH: Social Indicator Horizontal

Table 3.11: National spatial inequality statistics across climate hazards.

hazard	moranUnivariate	moranBivariate	Gini	nearbyGini	distantGini
storm	0.994	-0.042	0.198	0	0.198
heat	0.993	0.044	0.238	0	0.238
drought	0.947	0.040	0.367	0	0.367
fire	0.868	-0.084	0.408	0	0.408
flood	0.701	-0.095	0.148	0	0.148
climate	0.903	-0.043	0.105	0	0.105

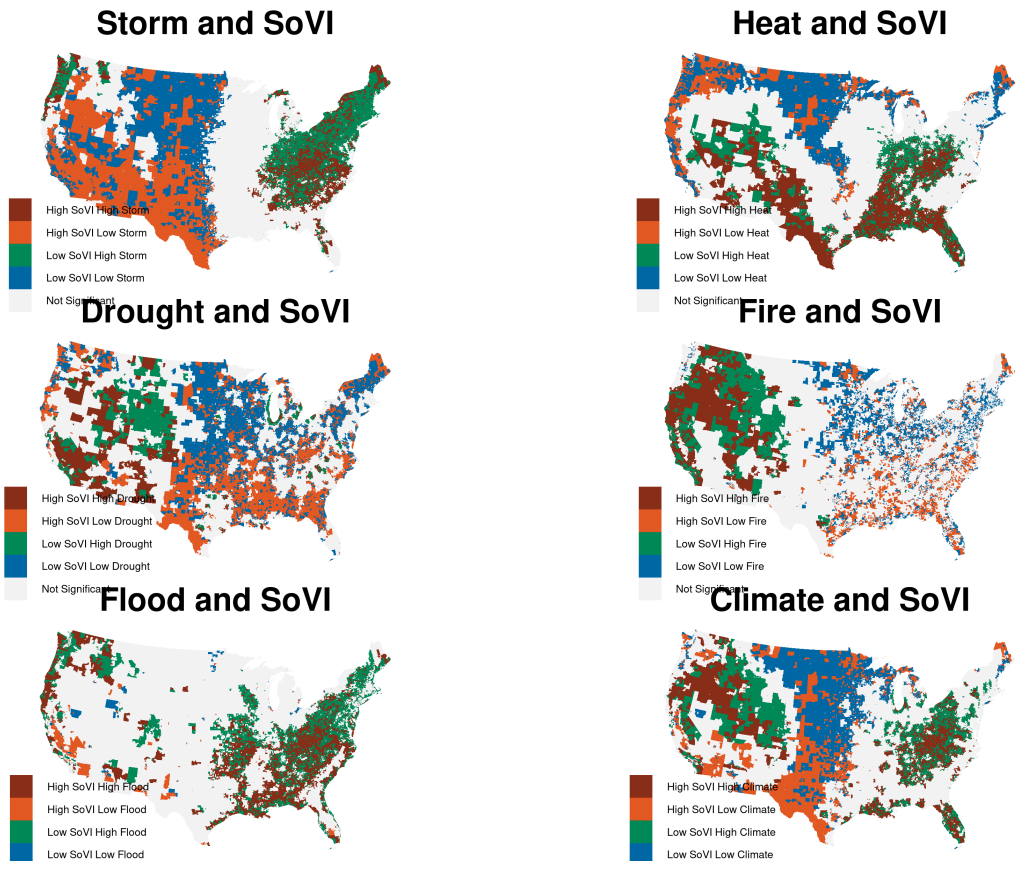

Figure 3.14: Local Indicators of Spatial Association (LISA) show high climate risk and high social vulnerability clusters for each hazard.

Chapter 4

Measuring climate risk perception with Twitter data

Concern over climate risk varies greatly across individuals and places. To measure this variation, studies typically conduct expensive and time consuming qualitative studies and surveys that have limited spatiotemporal and sociodemographic coverage of climate risk trends. This study contributes to a growing body of social and behavioral science research that substitutes survey data with user-generated big data. To that end, we build a dataset for modeling the determinants of climate risk perception using data provided by the microblogging service Twitter. We apply natural language processing to textual data and analyze social networks to construct this dataset. Validation of our measurements is conducted in two phases, first against statistical model results from a published survey measuring the same climate risk perception determinants and next with the spatial distribution of climate risk perceptions measured by an annual survey. Although the instruments and data we gathered require additional refinement, preliminary results obtained as part of this validation study indicate that Twitter may soon serve as an

appropriate supplementary data source for measuring complex phenomena.

Introduction

Concern over climate risk varies greatly across individuals and places. This variability, despite overwhelming scientific consensus on the causes and broad consequences of anthropogenic climate change, generates a great deal of interest in understanding the determinants and spatiotemporal patterning of climate risk perception (CRP). Explaining CRP is of special interest to practitioners since it influences individual policy support for and behavioral intentions towards climate change mitigation and adaptation (Brody et al., 2012; Krosnick et al., 2006; O'Connor et al., 1999; Smith & Leiserowitz, 2014). Qualitative studies and surveys, the standard for measuring CRP, are expensive and time consuming, resulting in limited spatiotemporal and sociodemographic coverage of CRP trends. User generated big data (UGBD), an alternative source for measuring social, behavioral, and psychological phenomena (including risk perception), could help fill these coverage gaps and improve existing estimates. General quality concerns raise doubt about the usefulness of UGBD, particularly since these data do not represent solicited responses and are instead considered 'found'. Researchers have recently begun building a framework for implementing UGBD quality control, which could pave a generalizable path forward to measure social and psychological indicators for modeling complex outcomes with these data. However, even with quality controls, UGBD should undergo measurement-specific validation before being used to describe or infer characteristics about a target population.

We propose addressing the aforementioned issues in several ways. First, to determine the suitability of conducting individual-level CRP studies with UGBD, we measure CRP with Twitter data using a theoretical model. Second, to assess the reliability of our CRP

measurements from UGBD sources, we validate against two sources of peer-reviewed survey data. Third, to present the applicability of these methods in an applied context, we compare statistical models of the relationship between climate hazard estimates and CRP measured from survey and Twitter data. Through these experiments we aim to provide further evidence towards answering the following questions:

Research questions

1. Does Twitter data provide a robust and reliable basis for measuring individual-level predictors of complex phenomena, such as climate risk perception?
2. How closely do climate risk perception measurements from Twitter data match those from survey data?
3. What is the relationship between statistical climate risk and climate risk perception?

Beyond efficiency gains in measuring CRP trends over time, space, and population, Twitter data may also prove useful for studying a variety of CRP related topics, such as: measuring CRP change throughout the hazard/disaster event process, assessing how different types of messaging influence CRP, and exploring the relationship between information reliability and CRP. Validating CRP measurements from Twitter data is an essential first step towards answering any of these questions.

Literature Review

Everyone experiences some degree of risk. This is often represented as statistical risk, such as being twice as likely to die in the event of a traffic accident without a seatbelt.

We typically derive statistical risk from observed, historical data related to risk event frequency and magnitude, careful measurement of the exposed population, income or technological protections[/mediators?] from the event for sub-populations, among other metrics. However, people perceive this risk differently, even when provided with statistical risk estimates, according to subjective valuations (Slovic, 2000; Slovic, Fischhoff, & Lichtenstein, 1980). Therefore, statistical risk and perceived risk typically differ. One of the highest profile topics with the starkest differences between perceived and statistical values is climate risk. Despite high current and projected statistical risk at both the individual and global levels, climate risk perception varies vastly among individuals (Maibach et al., 2011).

Climate risk is unique relative to other risks subjected to perception studies due to the magnitude, complexity, and spatiotemporal scale (Breakwell, 2010). Some research suggests that because of this, it is difficult for individuals to experience climate change directly (Weber, 2010), although recent record-breaking events and subsequent attribution efforts indicate otherwise (Burger, Wentz, & Horton, 2020; Zhai, Zhou, & Chen, 2018). Similarly, from an evolutionary perspective, climate risk differs from the set of short-term and small area risks present during much of human existence (Griskevicius, Cantú, & van Vugt, 2012). However, since agricultural civilization, humans have had to manage risk and adapt to challenges presented by variability in weather and climate (Bocco & Napoletano, 2017; Orlove, 2005; Taraz, 2017).

The dominant way of measuring CRP is by administering a survey to a putatively representative sample from a target population, such as the national UK sample used by van der Linden (2015). Yet, these studies tend to have small, quasi-representative samples, limited geographic extent and/or spatial variation, exist at just at one point in time, and require substantial planning and coordination. Despite the shortcomings of these

surveys, they are undoubtedly the gold standard for CRP measurement (Howe, Mildenberger, Marlon, & Leiserowitz, 2015; Leiserowitz, 2006). Table 4.1 contains a selection of sampling schemes.

General problems with these sampling schemes are small sample sizes, skewed sample demographics, non-probabilistic sampling, and self selection of participants (especially if using something like Mechanical Turk). User generated big data (UGBD), while also potentially selective and unrepresentative, could be an additional source for measuring CRP trends over space-time, inferring significant statistical relationships between explanatory factors and CRP, and further explaining CRP variability. UGBD, specifically from social media platforms, have become increasingly useful for answering questions related to migration patterns (Zagheni, Weber, & Gummadi, 2017), male fertility (Rampazzo, Zagheni, Weber, Testa, & Billari, 2020), public transit ridership sentiments (Collins, Hasan, & Ukkusuri, 2013), as well as assessing the quality of municipal disaster management via social media during floods (Scott & Errett, n.d.). Papers such as Yuan & Liu (2018) and Martín, Cutter, & Li (2020) verified Twitter as a legitimate source for studying hurricanes and the disaster process: rapid damage assessment and evacuation behavior, respectively. Although we found no studies specifically looking at climate risk perception, many studies use data from the microblogging service Twitter to study different types of perception, some of which are related to risk, including:

- internet of things (Bian et al., 2016)
- genetically modified organism risk (Whittingham, Boecker, & Grygorczyk, 2020)
- neighborhood quality (Hess, Iacobucci, & Väiko, 2017)
- users' moods (Bollen, Mao, & Pepe, 2011)
- reputation of other users (Schultz, Utz, & Göritz, 2011)
- breast cancer (Modave et al., 2019)

- HPV vaccine (Keim-Malpass, Mitchell, Sun, & Kennedy, 2017)
- eco-friendliness of luxury fashion (Blasi, Brigato, & Sedita, 2020)
- lead in school drinking water (Ekenga, McElwain, & Sprague, 2018)
- risks/benefits of self-driving cars (Kohl, Mostafa, Böhm, & Krcmar, 2017)
- impacts of weather on COVID (Gupta et al., 2021)
- H1N1 pandemic (Chew & Eysenbach, 2010)
- earthquakes, using a space-time weighted index to better capture the occurrence of local events (D'Auria & Convertito, 2016).

Studies looking at climate change-related perceptions include prevalence of climate change discussions as a function of temperature variability (Kirilenko, Molodtsova, & Stepchenkova, 2015) and real time risk of a tropical cyclone (Bec & Becken, 2019). The first paper found that Twitter users do associate extreme temperature anomalies with climate change while the latter found meaningful relationships between emotional characteristics and risk perception of Cyclone Debbie. Authors in most of these studies tend to use the words 'attitude' and 'perception' interchangeably. Many focus on binary measures of perception, i.e. sentiments (Thelwall, Buckley, & Paltoglou, 2011). Some manually categorize these sentiments, but most use natural language processing, a computational toolbox for analyzing human language. Other studies simply use the word 'perception' as a generic term for topic prevalence (Hamed et al., 2015).

There are obvious issues with UGBD and how studies utilize it. First, there are general quality concerns since UGBD do not represent survey responses and instead are considered 'found data'. The unstructured and unsolicited nature of UGBD leads to reliability issues, specifically regarding accuracy. Even so, compelling reasons to utilize UGBD include abundant observations, spatiotemporal resolution and extent, open access, and limited overhead. Salvatore, Biffignandi, & Bianchi (2020) have outlined a wealth of

statistical and measurement issues with Twitter data and proposed a quality framework, which borrows from the vast literature on survey and UGBD quality control. With sufficient quality frameworks and validation, UGBD has the potential to bolster our ability to conduct scientific research.

Aside from quality issues, many studies employing UGBD tend to oversimplify the theoretical conceptualization, model specification, and statistical measurement of complex phenomena. Specifically, there are fundamental problems with the way most studies utilize Twitter data to study perception. Psychologists, who are the most likely to correctly operationalize perception in statistical models, are not well represented in the disciplinary spread of researchers using Twitter data. Most authors are computer scientists or come from environmental and climate change studies. It's therefore not surprising that Twitter data studies we reviewed neglected to appropriately operationalize perception or risk perception. The risk perception-as-sentiment approach, whereby researchers reduce perception to a binary sentiment (more correctly termed *affect* in the psychology literature) is understandable insofar as simple representations suffice in addressing the stated research goals. However, most studies barely endeavor to distinguish perception from awareness. The limitations of this simplistic specification are thus innumerable. Even when studies make a distinction, the overlap between psychological concepts related to perception can muddle the analysis. A brief definition of some perception-adjacent concepts from the American Psychological Association (*APA Dictionary of Psychology*, n.d.):

- *perception:* the process or result of becoming aware of objects, relationships, and events by means of the senses, which includes such activities as recognizing, observing, and discriminating.
- *attitude:* a relatively enduring and general evaluation of an object, person, group, issue, or concept on a dimension ranging from negative to positive.

- *thought:* ideas, images, mental representations, or other hypothetical elements of thought are experienced or manipulated. In this sense, thinking includes imagining, remembering, problem solving, daydreaming, free association, concept formation, and many other processes.
- *feeling:* a self-contained phenomenal experience. Feelings are subjective, evaluative, and independent of the sensations, thoughts, or images evoking them.
- *emotion:* a complex reaction pattern, involving experiential, behavioral, and physiological elements, by which an individual attempts to deal with a personally significant matter or event. The specific quality of the emotion (e.g., fear, shame) is determined by the specific significance of the event.
- *knowledge:* the state of being familiar with something or aware of its existence, usually resulting from experience or study.
- *opinion:* attitude, belief, or judgment.

The study of risk perception, in contrast to perception, has a well defined framework with clear applicability to any-type risk: how and why does the perception of risk differ from statistical risk? Perception studies concern the neuropsychological factors involved in the process of perception. It should be stated that operationalizing concepts is not a straightforward task (Asadzadeh, Kötter, Salehi, & Birkmann, 2017; Moscati, 2018). To the non-psychologist, there appears to be a tendency for these definitions to blend together as it may be difficult to specify what uniquely distinguishes each concept. It is therefore typical, even for psychologists, to misrepresent a concept when it is operationalized for a model or study, such as the oft noted confusion between affect, attitude, and emotion (Sjöberg, 2006). Non-psychologists similarly tend to equivocate measurements from a Twitter corpus, such as 'topic prevalence' or 'sentiment', with perception. It is therefore important to employ a theoretically-driven, clear, and parsimonious model

specification when studying such complex concepts. Risk perception is no exception.

Building on the varied theories of risk perception and existing theoretical models, van der Linden (2015) proposed a social-psychological model of climate risk perceptions, which divides determinants into three dimensions: *cognitive factors*, *experiential processing*, and *socio-cultural influences*. The model explains over 70% of the variance in risk perception when controlling for a fourth dimension, *socio-demographics*. The model sits firmly within the psychometric paradigm, yet readily incorporates the *cultural theory of risk*, *social amplification of risk* and *social representations theory*. The dimensions included in the model borrow from (Helgeson, Linden, & Chabay, 2012). Figure **??** displays a conceptual framework for this model. For further detail, van der Linden (2017) thoroughly describe each dimension and provide an elaborated fifth dimension, *heuristics and biases*, which was omitted from statistical modeling for the sake of parsimony. A brief description of each dimension follows.

Cognitive factors: climate change knowledge, the main cognitive factor, has a positive association with CRP (Lee, Markowitz, Howe, Ko, & Leiserowitz, 2015). Disagreement still exists about the explained variance attributed to knowledge (Hornsey, Harris, Bain, & Fielding, 2016), when marginal increases in risk perception from greater knowledge begin to significantly decrease (Tobler, Visschers, & Siegrist, 2012), and the relative importance of different types of knowledge (causes, impacts, mitigation, etc.) (Kaiser & Fuhrer, 2003).

Experiential processing: there are two factors in experiential processing, *negative affect* and *personal experience*. Negative affect is a conceptual application of the 'risk-as-feelings' hypothesis (Loewenstein, Weber, Hsee, & Welch, 2001), whereby the strong reaction an individual has to a risk, called a somatic marker (Damasio, 2006), forms the foundation of our 'affect heuristic' (Slovic, Finucane, Peters, & MacGregor, 2004).

A negative affect is therefore a negative association, i.e. dislike, dread, etc., with a risk, which in turn has a positive association with risk perception (Finucane, 2012; Leiserowitz, 2006). Although personal experience with climate change has a hypothetically positive association with risk perception, it does depend on a few facets. Personal experience can be either objective (e.g. measured weather anomaly) or subjective (…"this is the hottest summer I can remember.") (Akerlof, Maibach, Fitzgerald, Cedeno, & Neuman, 2013), how we measure and qualify personal experiences with climate change varies substantially (Capstick & Pidgeon, 2014), and what constitutes an experience that is representative of climate change is unclear (Howe & Leiserowitz, 2013).

Socio-cultural influences: these are broken into two factors, *the social construction of risk* and *culture, values, and worldviews*. Although the social construction of risk is difficult to measure at the individual level and even considered by some as vague meta-theory (Voelklein & Howarth, 2005), it certainly plays a role in how people perceive risk (Joffe, 2003), especially from climate change (N. Smith & Joffe, 2013). The general understanding of how this influences risk perception is through descriptive and prescriptive norms. Hence risk perception is greater when those around us are concerned with climate change risk (descriptive) and they implore us to also be concerned (prescriptive) (Cialdini, Kallgren, & Reno, 1991; van der Linden, 2015). The way culture, values, and worldviews influence risk perception is based on grid-group theory (Douglas & Wildavsky, n.d.), a typological system orienting individuals within some position among egalitarianism, individualism, hierarchism, and fatalism. Different typologies have modified this initial conceptualization and distinct theories derive from it, namely 'cultural cognition' (Kahan, 2012). General concerns address the role that culture plays in risk perception, whether we can measure culture as neatly as researchers try to operationalize it, and if it's even possible to infer culture at the individual level.

Socio-demographics: There isn't much consensus about the role of most of these characteristics. Gender, race, and political ideology are the few exceptions. Particularly, being a white male conservative has a negative association with CRP (McCright & Dunlap, 2013). Conservative political ideologies, specifically in the US, tend to positively associate with distrust in science and media (Leiserowitz, Maibach, Roser-Renouf, Smith, & Dawson, 2013). The 'white male' effect reduces risk perception and is pervasive across many other types of risk (Finucane, Alhakami, Slovic, & Johnson, 2000; McCright & Dunlap, 2011)

Data and Methods

Climate risk perception (CRP) measurements try to gauge how concerned individuals are about present and future risk from a changing climate. We intend to measure CRP with user generated big data (UGBD), conduct two validations of these measurements, and compare how well UGBD and survey measurements match statistical climate risk over space and time. The first validation we conduct tests the accuracy of our UGBD proxy-survey instrument and the next assesses whether we achieve similar enough results against the spatial distribution of climate risk perception measured through an established US national survey.

Instead of through a survey, the standard for measuring CRP, our data come from Twitter's Application Programming Interface (API) (Twitter, 2020). We primarily leverage methods from the natural language processing toolbox to infer CRP from UGBD, but also utilize machine learning and network analysis methods. Many recent papers explain natural language processing, such as sentiment analysis, for disaster and climate-related research (An et al., 2014; Dahal, Kumar, & Li, 2019; Ruz, Henríquez, & Mascareño,

2020).

Twitter allows access to the full archive of tweets since 2008 for academic research. Our query finds posts (tweets) from the past ten years that include keywords such as wildfire, hurricane, climate change, climate risk, etc. These raw responses are then parsed and configured into a data table. As of May 13, 2021, we have collected approximately 23 million tweets. These tweets come with rich contextual information, which we uniquely use for a variety of different tasks. Most of these data come from directing an API call at the full archive endpoint, but some must be obtained by specifying the requested data and user ID at a particular endpoint (e.g. get the 20 most recent tweets liked by a user). Table 4.2 outlines some of the types of information accessed via the API.

To clean the tweet dataset, we remove systematic false positive matches (i.e. unrelated posts such as 'this song is like wildfire') by manually examining a randomly sampled subset of the full data (approximately ~10k tweets, each from a different author). Automated posting from problem users, such as bots, is filtered out by removing tweets from user IDs who are within the top 1 percent of posting frequency. We also remove all posts from organizations using a demographic inference tool developed by Wang et al. (2019), which is an open source multimodal deep learning system trained on over 35 million Twitter profiles to classify age, gender, and organization. After cleaning our tweet sample, we find the latitude and longitude of the home profile for each user ID. Nominatim, the open source geocoder that powers Open Street Maps (*Osm-Search/Nominatim*, 2021), locates the center point of each matching location name. The last step in data processing is to consolidate tweets by user and convert the individual-level text collections to a bag of words corpus (BoW), whereby each collection represents a list of unordered words with all rare and stop words (the, at, my, etc.) removed. After gathering, cleaning, geocoding, and consolidating, the Twitter data is ready for analysis.

The van der Linden (2015) model serves as the theoretical foundation in our approach to measuring climate risk perception. We chose this model since it achieved the highest explained variance of any model we reviewed and integrated different theoretical frameworks for understanding risk perception. The Twitter data measurement tool we develop seeks to replicate each van der Linden (2015) model dimension across the multiple CRP determinants (*cognitive factors*, *experiential processing*, and *socio-cultural influences socio-demographics*). We continue the same model specification so that we can verify the accuracy of our Twitter measurements when compared to the original survey data.

Figure **??** provides a tabular breakdown of the dependent variable (risk perception) and explanatory variables. *Model Term* refers to the determinants of risk perception posited by van der Linden (2015), *Specification* describes the numerical-theoretical relationship of the concepts to their numerical representation and risk perception (all variables have been transformed to positively associate with risk perception), *Survey Instrument* contains the questions used in the original study to measure each risk perception determinant, and *Twitter Proxy* describes our proposed approach for appropriately measuring the determinants using Twitter data, while maintaining a similar enough operationalization to the original survey instrument. All explanatory variables, except for socio-altruistic and egoistic value orientations, have a positive relationship with risk perception, meaning higher values (e.g. better knowledge about climate change) increase risk perception. Although van der Linden (2015) did not find a statistically significant relationship among socio-altruistic and egoistic value orientations and CRP, we still choose measure these terms for experimental purposes.

Our Twitter dataset is a sample of users (i.e. study participants) who have previously posted about some aspect of climate change risk. Much of our measurement relies on

passing the tweet corpus per user through peer-reviewed lexicons, a list of words and their associations (Riloff & Shepherd, 1997). These can be adopted from existing sources, generated for specific purposes, or augmented from existing sources for specific purposes. We measure *risk perception* with emotional analysis using the NRC Word-Emotion Association Lexicon (Mohammad & Turney, 2010) to associate textual data with eight basic emotions (anger, fear, anticipation, trust, surprise, sadness, joy, disgust). From this we take the average of all negative emotion and sentiment scores (anger, fear, sadness, disgust). Proportions are relative to the user. Integer values range from 0 to 10.

Knowledge about climate change comes from three proportions: (a) tweets with climate science-related language, (b) links with reliable sources, and (c) tweets with technical words. The first is the proportion of words matching the NASA Earth Observatory glossary (earthobservatory.nasa.gov/glossary). We manually remove those that are common (e.g. force) or false cognates (e.g. wave) as well as from our original Twitter query (e.g. wildfire, precipitation, etc.). The second is the proportion of credible links (.gov or .org), with designated climate disinformation .org websites omitted (desmogblog.com/climate-disinformation-database). The third is the proportion of rare and technical words using the De-Jargonizer (Baram-Tsabari et al., 2020; Rakedzon, Segev, Chapnik, Yosef, & Baram-Tsabari, 2017). We take the average of these three proportions. Continuous values range from 0 to 1.

Holistic affect is measured with sentiment analysis, which provides a rating for textual data on a continuous scale from negative to positive. Similar to the approach used for measuring risk perception except that we do not measure emotions. Many sentiment analysis approaches exist, ranging from simple and lexicon-based, such as the Valence Aware Dictionary and sEntiment Reasoner (VADER) (Gilbert & Hutto, 2014), to complex and machine learning-based, such as deep convolutional neural networks (Severyn

& Moschitti, 2015). We use the microblogging-specific lexicon AFINN (Nielsen, 2011). Integer values range from -5 to 5.

We measure *personal experience with extreme weather* using disaster event frequency over the past five years from the Spatial Hazard Events and Losses Database for the United States (SHELDUS) (CEMHS, 2020), which provides annual disaster occurrence for multiple natural hazards. These data are county-level, so we consider an event to be experienced by an individual if it happened in a county within 100km of their home location.

Broad value orientations are split into three categories: biospheric, socio-altruistic, and egoistic values. We use a validated personal values lexicon (Wilson, Shen, & Mihalcea, 2018) to assign numerical values based on word associations. Integer values range from 0 to 10 for each value category.

To estimate the influence of *social norms*, we estimate adherence to the biospheric value orientation for user IDs connected to each of our participants. Connectivity is found through a variety of social network indicators (following, likes, replys, retweets, mentions). Each 'connected' user ID will then be assessed for adherence to the biospheric value orientation. We estimate the expected value of social norms using the relative frequencies of interaction between participants and connected user IDs, i.e.:

$$EV_{sn} = \sum_{i=1}^{n} P(X_i^{rf}) * X_i^{bv} \tag{4.1}$$

Where EV_{sn} is the expected value of social norms, $P(X^{rf})$ is the relative frequency of interaction, and X^{bv} is the biospheric value orientation, all for connected user i, and estimated for each participant.

Demographic characteristics are obtained through a variety of open source inference

tools. *Age* comes from a multimodal deep learning system (Wang et al., 2019); *political ideology* from a machine learning model (Preoţiuc-Pietro, Liu, Hopkins, & Ungar, 2017); *education* from a distance supervised regression method (Culotta, Ravi, & Cutler, 2016); and *income* from predictive models with graph embeddings (Aletras & Chamberlain, 2018). We do not measure gender and race using any inference tool since we do not believe it is appropriate to do so given the current state of these methods (Fosch-Villaronga, Poulsen, Søraa, & Custers, 2021; Hao, 2019; Keyes, 2018). The primary issue is that race and gender are subjective characteristics that study participants typically self-assess. However, age, political ideology, education, and income are more or less objective and can be measured by observational procedure, such as through birth certificates, voting records, diplomas, and tax returns, respectively. However, inferring these demographic characteristics still presents ethical and methodological issues.

Once we've compiled metrics for all participants, we map the distribution of each variable onto the distributions obtained by van der Linden (2015). Proxy measurements map onto the survey instruments (all of which are indices) using the mean and standard deviation. We use an inverse transform method to approach similarity in the numerical distributions for substitutable variables across model specifications, which allows greater comparability in the following experiments.

The first analysis compares our risk perception estimate, which we obtained by emotional analysis of fear for climate risk-related tweets, to risk perception predicted with the parameterization from van der Linden (2015) (analysis 1). We then test how well our proxy measurements compare to the original model specification, with the dependent variable as 'fear for climate hazards' (analysis 2). Lastly, we employ a Bayesian model to infer risk perception using parameter estimates from analysis 2 and van der Linden (2015) (analysis 3).

Analysis 1 predicts risk perception with the statistical model built by van der Linden (2015) using new data from our proxy Twitter measurements. We estimate an OLS regression with survey measurements of each construct (climate change knowledge, holistic effect, etc.) from the van der Linden (2015) data. This model serves as a prediction tool to test the data gathered via Twitter. Our goal is to compare risk perception inferred by natural language processing of Twitter data to risk perception estimated in an explanatory statistical model. Analysis 2 fits an ordinary least squares regression to our proxy measurements. This experiment compares the relative importance and direction of predictor variables between the original and Twitter statistical models.

Analysis 3 is a Bayesian model of climate risk perception. The model uses prior knowledge of the effect that each model term has, represented by means and variances of OLS regression coefficients produced from the original and proxy models. We use this model to predict climate risk perception across the conterminous USA for each participant. The predictions from experiment 3 are used to compare to a survey dataset that measures CRP, *Climate Change in the American Mind*, conducted by Yale University's Climate Change Communication Research Program and partners (Leiserowitz et al., 2019). Specifically, the survey question we use for this comparison is, "How much do you think global warming will harm you personally?". Howe et al. (2015) downscaled responses from Leiserowitz et al. (2019) over many survey waves to produce county level estimates, called the Yale Climate Opinion Maps 2020 (YCOM). We calculate the z-scores of both estimates to be able to compare relative risk perceptions. YCOM approximates that the downscaled results are accurate to within ± 8 percentage point ("Yale Climate Opinion Maps 2020," n.d.), which equates to a z-score range of ± 1.27.

Next we demonstrate in an applied context the overall comparability of our Twitter CRP estimates to those of YCOM while also exploring the relationship between climate

risk perception and statistical climate risk. Although a similar relationship, evidence for increased risk perception with higher statistical climate risk is neither clear nor abundant, unlike that for personal experience (Akerlof et al., 2013; Lujala, Lein, & Rød, 2015). We estimate generalized linear models for five climate hazards (extreme precipitation, extreme heat, drought, wildfire, and flooding) as well as a multi-hazard climate risk estimated from the average of all five. The hazard term in each is modeled with regression splines to capture the expected non-linear relationship between a hazard level and the associated risk perception. We control for all the variables presented in van der Linden (2015) across both types of climate risk perception estimates.

Results

Our study seeks validation of individual-level climate risk perception data gathered via Twitter, a microblogging service with tens of millions of monthly users across the United States. Each user provides potentially informative data about themselves, their life histories, and their social context by submitting short posts embedded with web links and images. Engagement with the Twitter community offers further information about patterns of social interaction. Not only do these patterns allow researchers to study social networks within Twitter but also to perform demographic inference due to the predictive nature of social connections. Moreover, users unwittingly divulge other details about themselves, such as clues about income from language use, to inform additional characteristics.

Validating our Twitter-sourced data as an acceptable substitute for survey data was conducted in several steps. We first compared the risk perception metric, which was gathered independently from the other model terms, to a risk perception variable predicted with

the statistical model built by (van der Linden, 2015). Next we contrast the model results for the survey and Twitter data. Coefficient estimates from these statistical models built were then used as priors in a Bayesian model. The predicted risk perception from this model was compared to an established survey dataset to assess how accurately the Twitter data measurements represent the geography of climate risk perception. Lastly we compare both risk perception metrics with statistical climate risk to demonstrate a use case for these large area estimates.

We first map the spatial distribution of users in our Twitter dataset, shown in Figure 4.3. We see that user locations closely align with population. Despite there being lower density west of the Mississippi, there is still sufficient spatial spread to conduct county-level estimates. Figure **??** shows the county-level spatial distributions for our Twitter data proxy measurements of climate risk perception model terms. We later compare these spatial distributions to those measured by the Yale Climate Opinion Maps 2020.

Figure **??** provides intercorrelations for the original variables and our proxy measurements. Values along the diagonal represent Cronbach's alpha for the same variable between the original and proxy data. Cronbach's alpha is a measure of mean scale reliability, i.e. the similarity in numerical distributions for each item comprising an index or representing a feature. The bottom triangle is from the original data and the top triangle is the Twitter data. Relationships are mostly consistent between the two datasets, with a notable difference that personal experience has a much weaker relationship to risk perception for the Twitter data. Cronbach's alpha across all variables suggests sufficient (above 0.6) measurement similarity.

A comparison between risk perception estimated with statistically modeled and natural language processing (NLP) methods is presented at the county level in Figure 4.7. These are reported as relative differences between the two risk perception metrics. The Twit-

ter metric appears higher in most places. Most of the counties with higher values for predicted risk perception occur in the US Midwest. We then calculated the number of counties precisely hit by the Twitter metric. Since around 30 percent of variance remains unexplained from the original model, we find the proportion of counties that have risk perception estimates with less than 30 percent difference to assess the comparability of the two risk perception measurement methods, which is about 67 percent.

Table 4.3 offers a comparison of model results between the statistical model built with survey data by (van der Linden, 2017) and that built from Twitter data. We present coefficient estimates for the original and proxy models. The last four columns describe whether there was a change in the effect direction for predictors between the original and proxy models as well as the change in the relative ranking of explained variance. Coefficients and relative rankings are similar except for a much higher effect in the Twitter model from a biospheric value orientation. Climate change knowledge also has a substantially lower relative effect.

The final validation exercise compares predicted results from a Bayesian model with Twitter data to the YCOM survey data. Figure 4.8 provides the spatial distribution of the Bayesian predicted estimates, Figure 4.9 shows the spatial distribution for the downscaled YCOM data, and Figure 4.10 presents how many counties have Twitter risk perception estimates that fall within the YCOM 95% confidence interval, of which there are approximately 75 percent. There doesn't appear to be any spatial patterning or regionalization for counties above or below the risk perception estimates.

Our last experiment compares statistical climate risk to two metrics of perceived climate risk, illustrated in Figure **??**. We found increasing risk perception for storm hazard when comparing against the Twitter risk perception metric whereas the YCOM metric shows higher risk perception for drought and wildfire. All other hazards for both metrics had

either constant or decreasing risk perception as a function of statistical risk.

Discussion

Survey data serves a fundamental role in empirical scientific research. Since the early 1900s, surveys have been in use and enabled inquiry into many facets of social views, intentions, and behaviors. Methodological improvements generated more refined and sophisticated survey instruments and responses while advancing technology allowed for new modes of data collection, from mail to telephone to online. We designed an experiment to test whether it is possible to reliably construct a proxy survey dataset from found data, in this case using the online microblogging service Twitter. Our research questions were: does Twitter data lend to measuring individual-level predictors of complex phenomena, such as climate risk perception; how closely do climate risk perception measurements from Twitter data match those from survey data; and what is the relationship between statistical climate risk and climate risk perception?

Overall, results suggest that we are within an acceptable range for validating this method of 'survey design'. The intercorrelations shown in Figure **??** among our dependent variables are nearly all positive (except for between holistic affect and biospheric value orientation), the differences in relationship strengths are notable but not without possible explanation, and Cronbach's Alpha show sufficient convergence in numerical distributions (0.6 is usually considered a minimum allowable level). One reason biospheric value orientation holds a negative association with holistic affect is that the latter is generalized, i.e., not specific to climate change as a hazardous problem. It will require more sophisticated natural language processing (NLP) to distinguish between holistic affect *for* climate change as a hazardous problem and *against* climate change as a political issue,

among the many other conceptualizations and reactive affects climate change holds.

We do find some concordance between risk perception estimated from natural language processing and risk perception predicted with the statistical model advancing the climate risk perception model that we used as a theoretical basis for this study (van der Linden, 2015). Figure shows this comparison 4.7, which presents nearly 67% of counties within a permissible range. This proportion could be much higher, The likely culprit, again, is limitations in the NLP methods. We simply used emotion analysis to measure risk perception (fear, anger, etc). This type of analysis neither captures risk as an emotion nor risk specific to climate hazards.

Existing machine learning methods for building domain-specific language models do offer a path forward (e.g. specific to climate risk perception). Typically, a researcher conducts supervised learning by training a model for a specific task, such as estimating the degree of climate risk perception. Supervised learning requires labeled data for training, i.e., data that has been coded to represent the degree of climate risk perception. These training datasets are usually thousands to millions of records long, which clearly presents a massive undertaking since labeling is a non-automated, human annotated task. Alternatively, fine tuning a pre-trained model can be done with unlabeled data for self supervised learning, for example by feeding the model pop science books about climate change impacts. This all goes to say that any refinement of our risk perception measurement is possible but sits beyond the scope of the present study.

Building a statistical model from Twitter data for climate risk perception is feasible. Table 4.3 shows that effect directions and relative rankings are similar for the Twitter model. However, a biospheric value orientation appears to be far more influential in the Twitter model than in the original. Again, this could be due to a difference in what is being measured between the two approaches. The original survey specifically

asks about adherence to particular aspects of the various value orientations (biospheric, socio-altruistic, and egoistic) such as, "How important is respecting the earth to you on a scale of -1 to 9 with -1 being opposed to my values and 9 being of supreme importance." A solution to this discrepancy in measurement validity would be to conduct a similar model building exercise for specific tasks outlined in the risk perception example above.

Despite Twitter-derived survey datasets showing promise, these types of data collection are not a replacement for traditional survey instruments. The Bayesian model specified with priors (probabilistic parameters) from a combination of coefficient estimates from survey and Twitter statistical models illustrates this point. Risk perception predicted from a Bayesian model achieves greater concordance with a national measurement of climate risk perception than a frequentist OLS model, shown in Figures 4.8. Therefore, social listening with Twitter data should be thought of as a supplemental research tool for ascertaining both stated and realized intentions as well as improving spatiotemporal extent and resolution.

Wrapping up our analysis with an experiment teasing apart the origins of risk perception research, to better understand why statistical risk and risk perception differ, we observed the relationship between two risk perception measures and five climate hazards, shown in Figure **??**. Assuming that the YCOM data is a benchmark, we only found increasing risk perception with statistical risk for drought and fire. The Twitter data inversely found increasing risk perception only for storm. This experiment offers more evidence that our Twitter dataset requires further refinement. Ideally we would see similar shapes and ranges in predicted curves across both risk perception measures. In addressing potential reasons for why we observe these relationships, we know fire and drought hazards tend to exhibit coincidence, higher frequency and a greater areal extent (if we include wildfire smoke) than flooding, and impacts primarily in the western USA. Working through how

these factors may influence different relationships for drought and fire than the other hazards, hazards that people experience annually or even multiple times a year reduce the gap between statistical and perceived risk. Risk perception is higher on average in the western USA. Lastly, if risk perception increases for one hazard it would also increase for any coincident hazard.

Decreasing risk perception with greater storm, heat, and flood hazard doesn't point to a convincing reason. Heat and flood are the most spatially even hazards, i.e., the highest probability of experiencing high hazard when drawing a random spatial sample of points. These hazards also tend to be higher in rural areas and the southeastern USA, which are more politically conservative and as such exhibit greater dismissiveness of climate change and the risk it poses. Storm hazard is highest in the pacific northwest and the northeast, regions for which overall climate risk is relatively low thus giving those with the greatest hazard a feeling of limited exposure.

Areas for future research include applying more sophisticated machine learning methods to measuring climate risk perception and its determinants, as explained earlier in the discussion. Testing the sensitivity of these measurements when implementing a Twitter data quality framework could also improve measurement accuracy and precision. Finding additional data sources to validate every indicator would assist in fine tuning our measurement instruments. Lastly, applying the methodological approach proposed here to related topics may even further highlight the advantages of supplementing survey data with Twitter data, such as observing how CRP changes throughout the hazard/disaster event process, assessing how different types of messaging influence CRP, and exploring the relationship between information reliability and CRP.

Conclusion

This study is one of the first validations of climate risk perception and its determinants using data from the microblogging service Twitter. We constructed a proxy survey dataset to conduct this validation by applying natural language processing and network analysis to text and social connections, respectively. Our risk perception measurement suitably compared to predicted risk perception from a theoretically-based statistical model proposed by van der Linden (2015); the determinants of risk perception that we measured aligned in effect size and direction to the aforementioned model; and a final iteration of risk perception, predicted by a Bayesian model including priors from modeling both survey and Twitter data, found sufficient agreement with an established survey. However, our statistical and perceived risk comparisons between climate risk perception measurements from Twitter and the established survey did not represent similar trends across climate hazards. One way to reach greater concordance between the two measures may be through applying UGBD quality control frameworks to fine tune measurement instruments.

Groves (2011) outline three eras of survey data collection. The nascent period (1930-1960) which witnessed the introduction and formalization of survey methods, the institutionalizing period (1961-1990) of widespread adoption by governments and other industries, and the digital period (1991-present) that embraced alternative collection modes, particularly from the internet, in large part due to declining survey participation rates. It is possible that we are entering a fourth era, the find-and-retrieve period (for lack of a better term), whereby researchers construct 'survey' datasets by collecting characteristics provided by individuals via social networks and the internet of things (among other sources). As happened in other periods, newer modes of data collection and analysis will

supplement older, thoroughly validated, and rigorous methods to afford researchers and the public a more accurate representation of reality.

Appendix

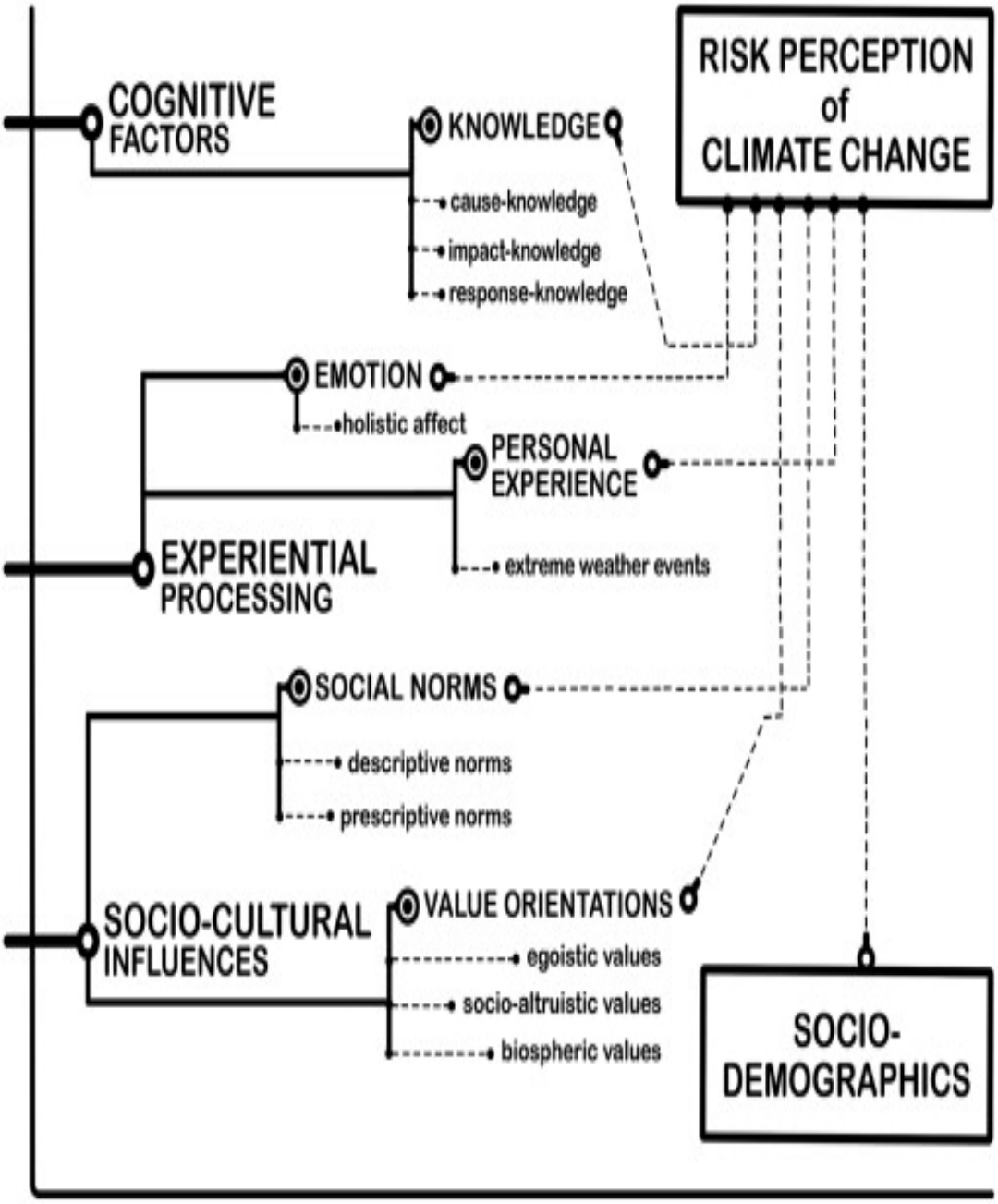

Figure 4.1: Theoretical climate risk rerception model (CRPM) from van der Linden (2015). A social-psychological model of climate risk perceptions which divides determinants into three dimensions: *cognitive factors*, *experiential processing*, and *socio-cultural influences*. The model explains over 70% of the variance in risk perception when controlling for a fourth dimension, *socio-demographics*.

MODEL TERM *Variables included are...*	**SPECIFICATION** *Higher values represent...*	**SURVEY INSTRUMENT** *Metrics from the original model are...*	**TWITTER PROXY** *Metrics for our experimental model are...*
		dependent variable	
risk perception	greater risk perception, which signifies greater concern for climate change.	7 option ordinal scale across three categories: 1. global 2. personal 3. holistic	emotional analysis of 'fear'
		EXPLANATORY VARIABLES	
		socio-cognitive	
knowledge about climate change	Better knowledge about climate change	4 option nominal scale across three categories: 1. causes 2. impacts 3. responses	1. proportion tweets with expert scientific language 2. proportion links with reliable sources 3. proportion technical words
holistic affect	Greater negative affect.	7 option ordinal scale across three affects: 1. pleasant/unpleasant 2. favorable/unfavorable 3. positive/negative	sentiment analysis
personal experience with extreme weather	More experience with extreme weather.	4 option ordinal scale	historical extreme weather events
social norms	More exposure to climate change mitigation intention and behavior	7 option ordinal scale across two categories: 1. descriptive norms 2. prescriptive norms	biospheric value orientation of connected users *(following, likes, replys, retweets, @s)*
broad value orientations	Greater adherance to the value orientation.	11 option ordinal scale across three categories: 1. biospheric 2. socio-altruistic 3. egoistic	Lexical association with each value orientation: *Biospheric Values:* Respecting the Earth (harmony with other species), Protecting the Environment (preserving nature), Preventing Pollution (protecting natural resources), Unity with Nature (fitting into nature). *Socio-Altruistic Values:* Peace (a world free of war and conflict), Equality (equal opportunity for all), Helpful (working for the welfare of others), Social Justice (correcting injustice, care for the weak). *Egoistic Values:* Authority (the right to lead or command), Influential (having an impact on people and events), Social Power (control over others, dominance), Wealth (material possessions, money).
		socio-demographic	
gender	Female	male, female	
age	Older	discrete	
education	More educated	higher, lower	
political party	More progressive	conservative, liberal	
income	Higher income	discrete	
religion	More religious	religious, no religion	

Figure 4.2: Methodological approach to modeling climate risk perception with Twitter data.

Table 4.1: Review of climate risk perception survey sampling methods.

sample size (n)	place	contact mode	method	explained variance (pct)
808	UK	in-person	nationally representative	69.00
500	UK	online	quota	49.00
673	US	mail	nationally representative	47.00
921	Australia	online	quota	72.00
1111	US	online	quota	43.00
765	Alger County, Michigan, USA	mail	locally semi-representative	55.00
1822	Great Britain	interviews	nationally representative	54.00
1001	USA	two waves: (1) mail out and (2) telephone	nationally representative	52.00
1093	USA	telephone	quota	43.00
1093	USA	telephone	quota	42.00
269	New Zealand	mail	nationally representative 1-year panel	43-48
157	Mannheim, Germany	in-person	locally representative	31.00
621	Sweden	mail	nationally representative	24-26
1002	USA	telephone	nationally representative	22-25

Table 4.2: Available data fields from the Twitter Application Programming Interface (API).

variables	description
text	input text from Twitter user or referenced tweet (retweet)
userID	unique identifier of Twitter user
location	text-based location of userID (e.g. Santa Barbara, California)
tweetID	unique identifier of tweet
timeStamp	date and time of tweet posting
language	preferred lanugage of Twitter user
links	url for any content embedded in tweet
retweetID	unique identifier for referenced tweet
replyID	unique identifier for replied tweet
mentionID	unique identifier for any mentioned userID
likes	tweets liked by a userID
followers	userIDs following a userID
following	userIDs that a userID follows
hashtags	metadata tag related to a theme

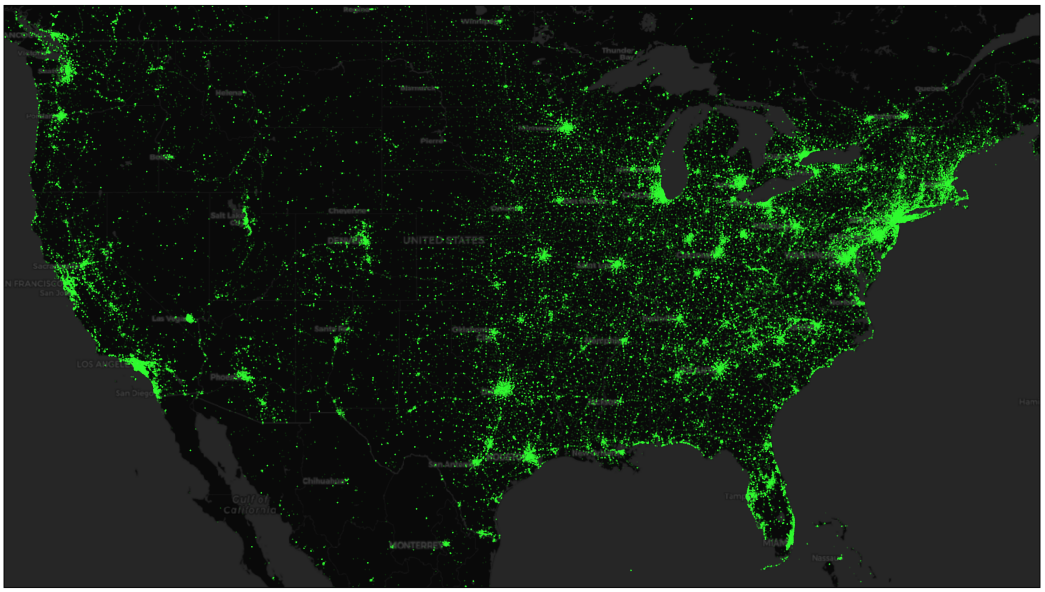

Figure 4.3: Spatial distribution of Tweets across the Conterminous USA.

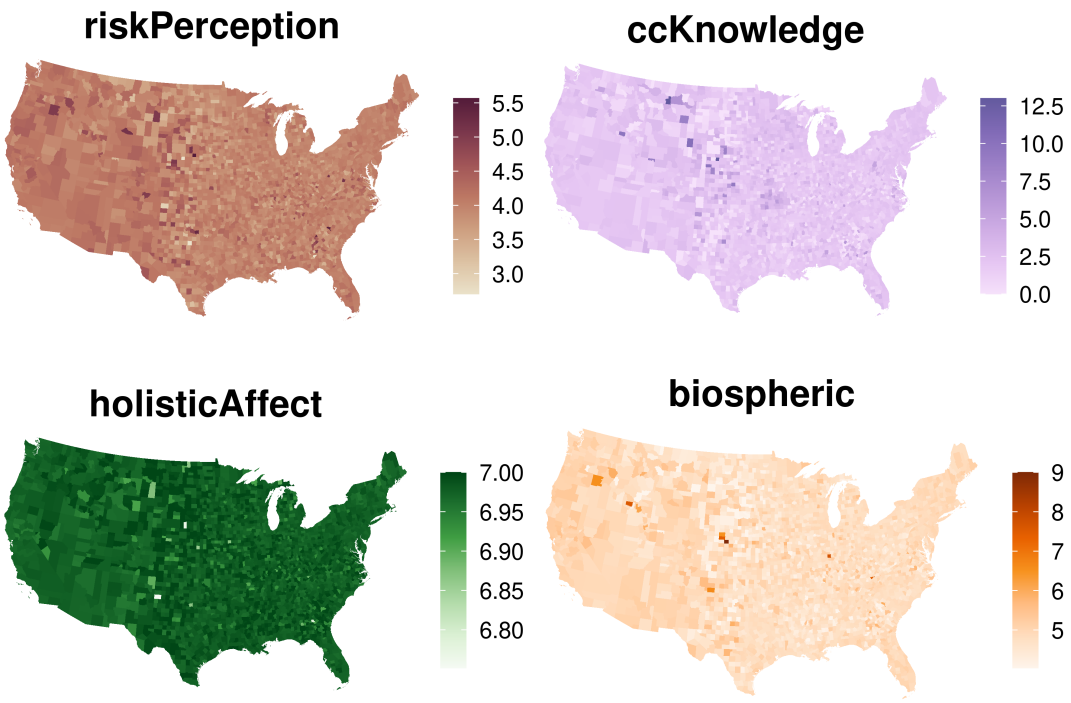

Figure 4.4: County-level spatial distribution of climate risk perception predictors estimated from Twitter data.

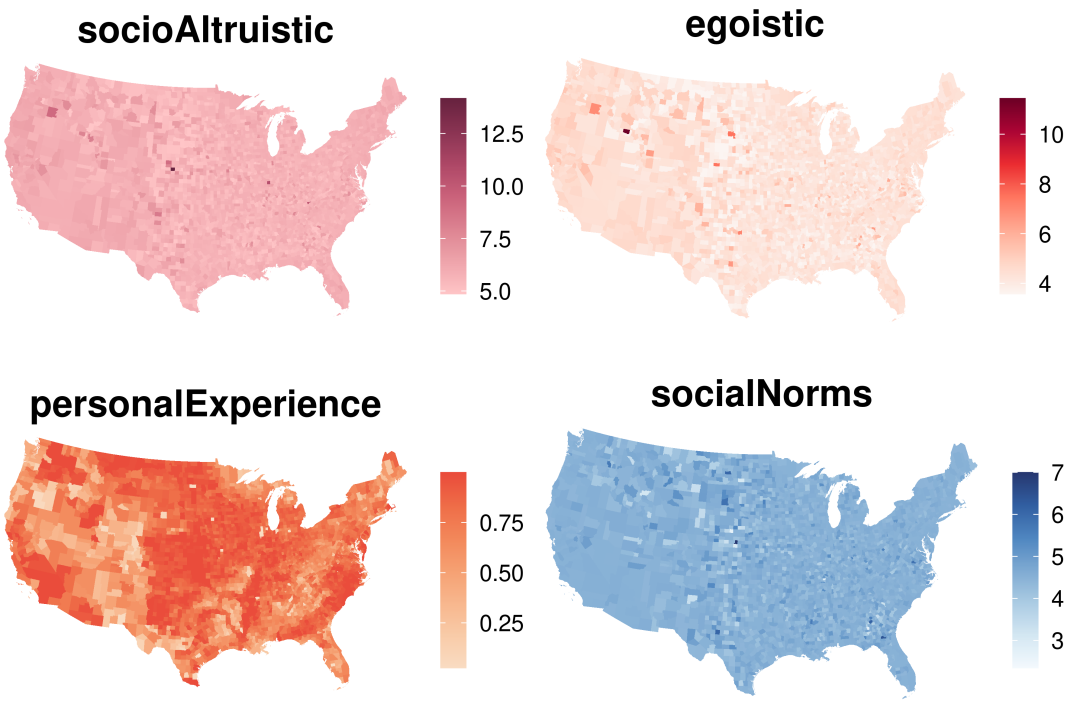

Figure 4.5: County-level spatial distribution of climate risk perception predictors estimated from Twitter data.

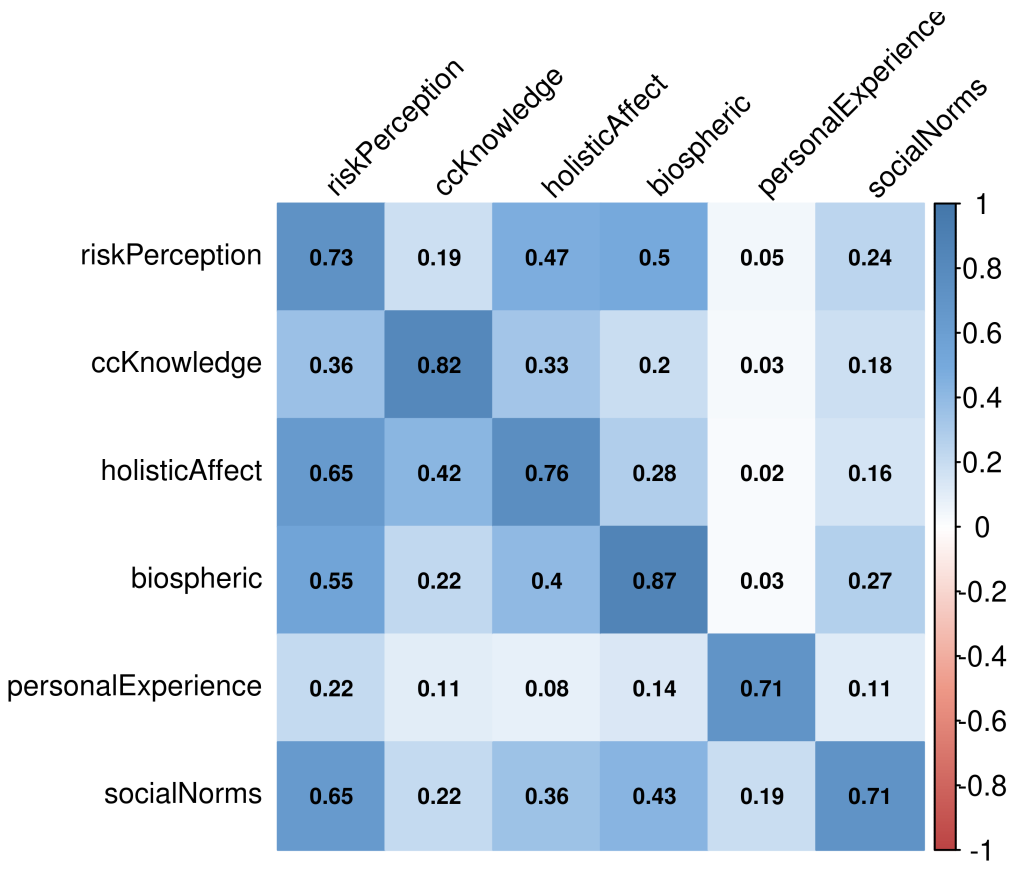

Figure 4.6: Intercorrelations among climate risk perception predictors with Cronbach's Alpha along the diagonal.

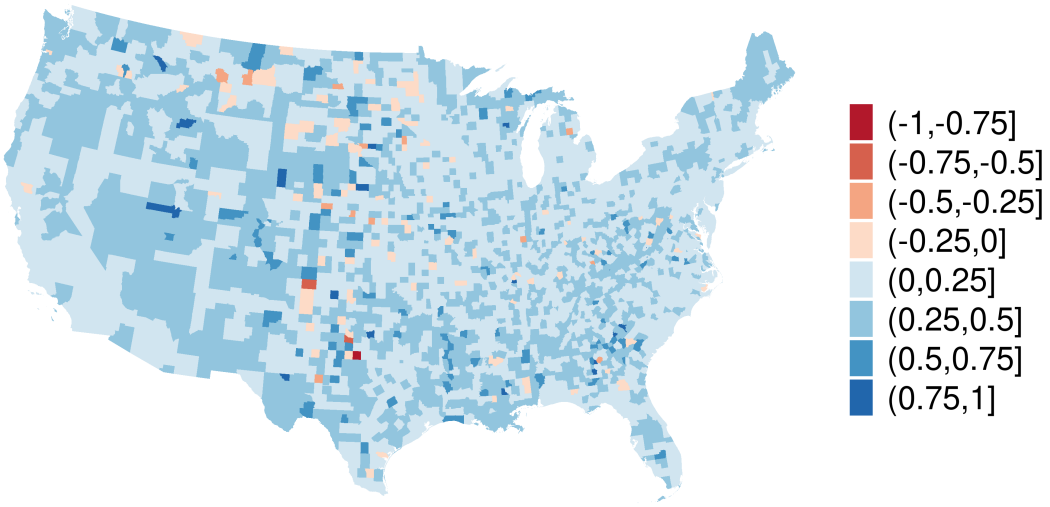

Figure 4.7: Relative difference in risk perception predicted with regression model and natural language processing (NLP) methods presented at the county level and reported as relative differences between the two estimates.

Table 4.3: Original and Proxy Model Coefficients with Effect Directions and Relative Rankings

predictors	originalCoefficient	proxyCoefficient	signChange	origRank	proxyRank	rankChange
holisticAffect	0.37	0.11	no	1	3	-2
personalExperience	0.20	0.17	no	2	2	0
socialNorms	0.20	0.01	no	3	5	-2
ccKnowledge	0.10	0.03	no	4	4	0
biospheric	0.05	0.39	no	5	1	4

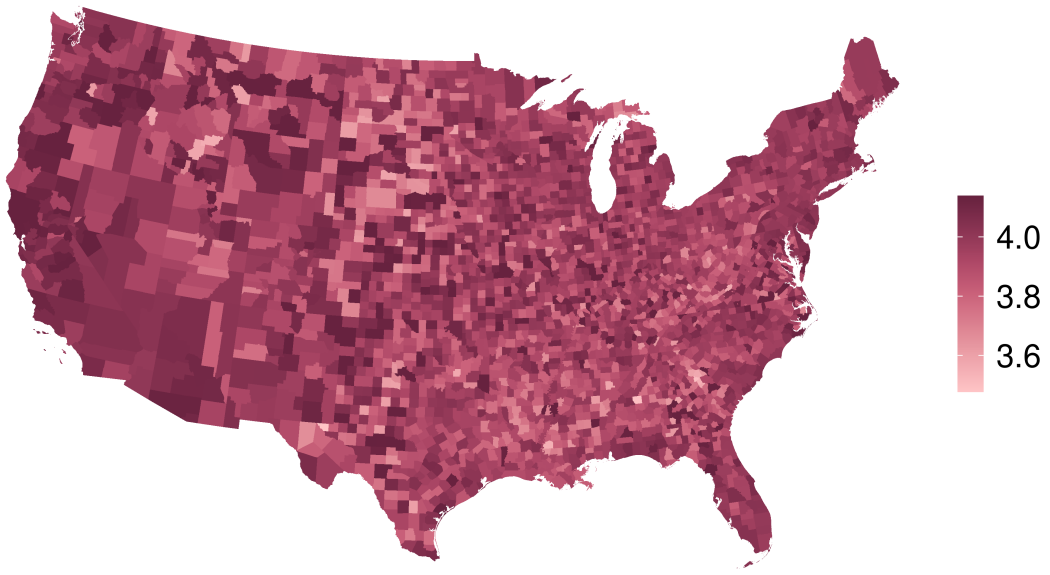

Figure 4.8: Predicted risk perception from Twitter data with a Bayesian model.

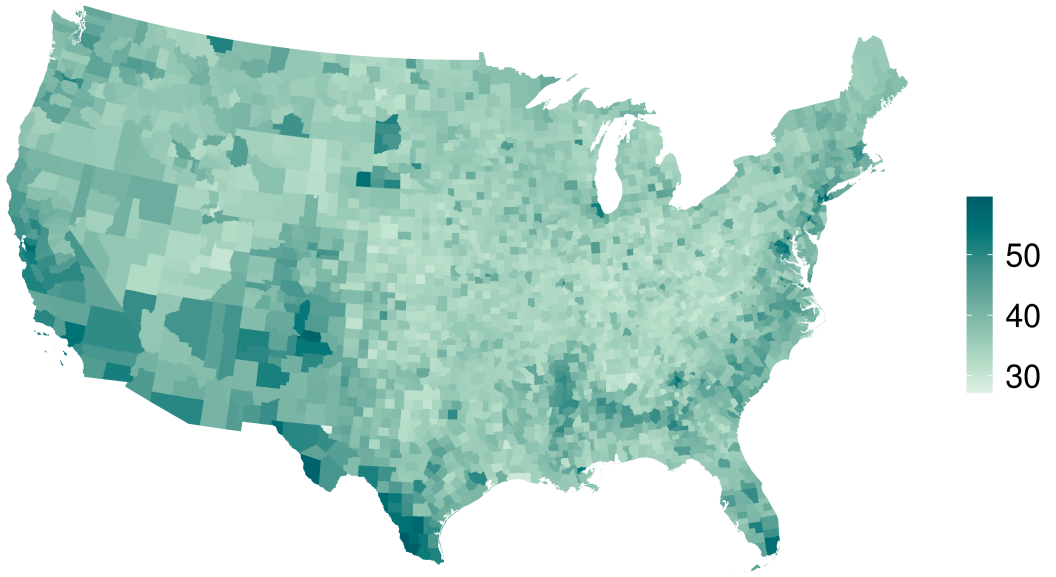

Figure 4.9: County-level percent concerned climate change will harm them personally from Yale Climate Opinion Maps (YCOM).

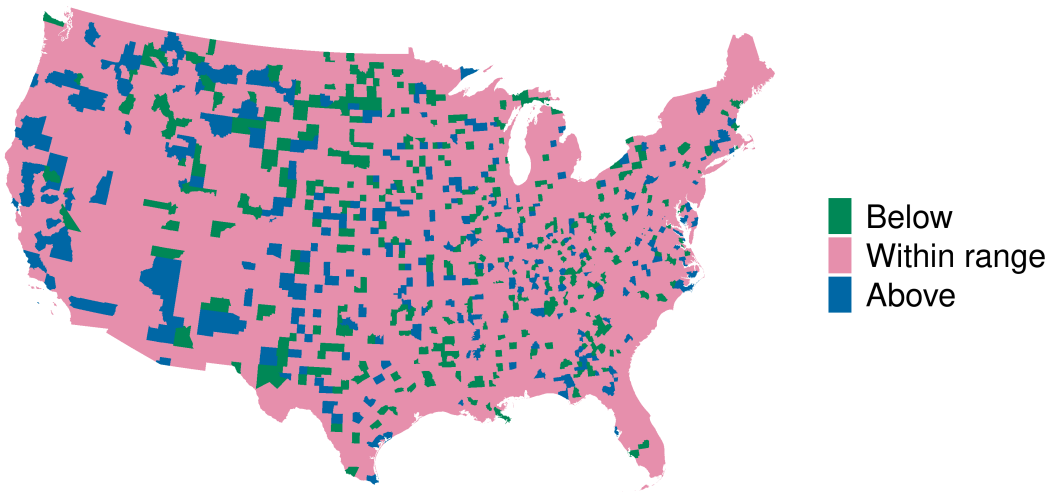

Figure 4.10: County comparison of Twitter and YCOM risk perception. Estimates that fall within the YCOM survey instrument .95 confidence interval.

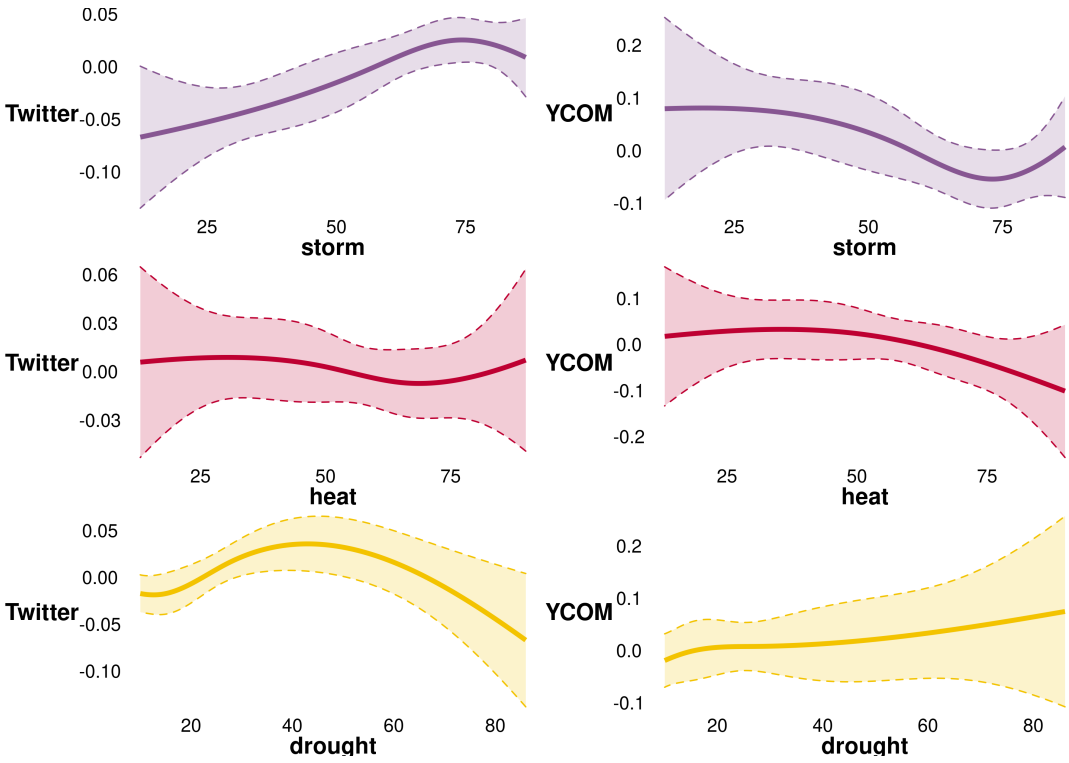

Figure 4.11: The relationship between statistical climate risk and climate risk perception. An upward trend along the x-axis indicates a positive association between statistical and perceived risk.

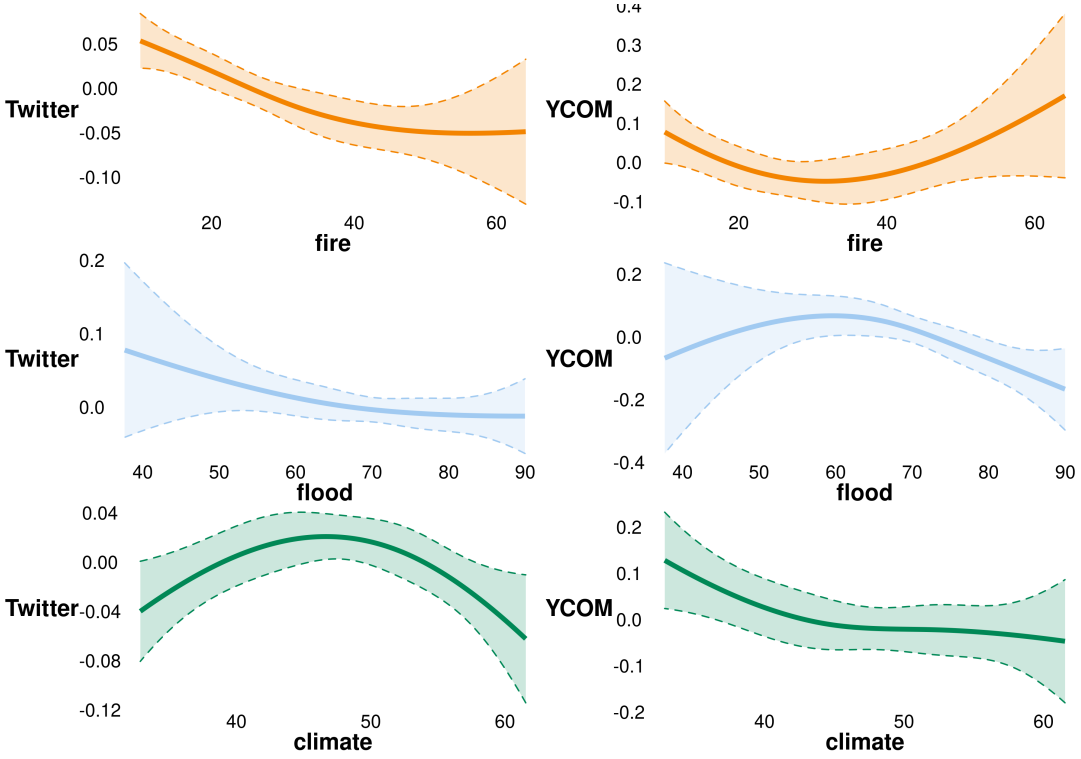

Figure 4.12: The relationship between statistical climate risk and climate risk perception. An upward trend along the x-axis indicates a positive association between statistical and perceived risk.

Chapter 5

Conclusion

Climate risk is an increasingly important area of study due to climate change, the rate of population and economic growth, and widening social inequalities. The fields of risk research on climate hazards have evolved over time from only estimating physical hazard and modeling structural solutions, then accounting for individual and organizational decision making as a determinant of exposure, and eventually considering the multidimensionality of vulnerability to negative consequences resulting from hazard events. These paradigm shifts in selecting factors for climate risk assessment happened alongside developments in modeling the determinants of risk perception as well as the implications for deviations between statistical and perceived risk. The unequal distribution of climate risk among marginalized groups and places has garnered scientific and policy attention to mitigate inequitable outcomes over the next several decades.

This dissertation contributes to answering pressing questions in climate risk research. We began with a climate risk literature review that covered the history of related fields and explained prominent concepts and methods for each parameter of climate risk. Each of the subsequent chapters took an empirical approach to studying distinct aspects of

climate risk across five different climate hazards–extreme precipitation, extreme heat, drought, wildfire, and flooding. The second chapter, 'Modeling Social Vulnerability Determinants of Disaster Loss,' estimated the relative contribution of social indicators to variability in disaster loss. The third chapter, 'Mapping Climate Risk Inequalities,' assessed the social and spatial distribution of climate hazards by comparing multiple types of inequality metrics. The fourth chapter, 'Measuring Climate Risk Perception with Twitter Data,' built a dataset of socio-cognitive characteristics from user-generated social media data. Our goals in conducting these studies were to advance measurement and modeling of climate risk, both the contributing factors and the societal implications of changing physical hazard and risk information. We proceed with a summary of each chapter including future research outlines, follow this by recommending a topical area for research and policy attention, and conclude with thoughts on how to integrate concepts and methods from this dissertation into a generalizable framework for climate risk modeling.

'Modeling Social Vulnerability Determinants of Disaster Loss,' took a statistical modeling approach to validating social indicators that have been identified in the literature and in practice as influential for moderating adverse outcomes from environmental hazards. We first demonstrated that social vulnerability indices, measures for aggregating multiple social indicators into one variable, are not internally consistent as values range drastically when including different input data nor are they theoretically consistent since the relative contribution of each indicator to index values also changes. We then built several statistical models of the relationship between climate hazard, social vulnerability, and disaster loss in order to examine which social indicators are the strongest predictors of loss. Our results suggest that climate risk modeling should account for social vulnerability and that the relative contribution of social indicators varies across hazards.

Context also appears to be important, whereby certain indicators may represent a larger explanatory share of outcome variation, in this case loss, depending on the levels of other indicators and model parameters.

We recommend several ways to attain a better sense of how exactly social indicators relate to disaster loss and the climate risk model. First, include data on hazard mitigation. This could come from a range of sources, including government repositories such as the National Inventory of Dams, FEMA FIRM maps, state and local climate action plans, and private data from the insurance industry. Second, include an overall hazard estimate alongside event specific characteristic measurements. It is not possible to correctly measure event characteristics for every event sampled, but an overall hazard estimate can provide added explanatory support. Third, utilize diverse types and sources of outcomes with higher spatial resolution that is accurately spatially attributed. It will be reasonable to recommend that institutions focus resources towards specific social indicators for disaster loss mitigation when enough studies consistently validate their influence. Localized studies of specific hazards still likely provide the best evidence to support mitigation planning.

'Mapping Climate Risk Inequalities,' leveraged differences among distinct metric formulations and types to examine diverse representations of inequality. Vertical, horizontal, and spatial inequality were the three dimensions that we studied. Vertical inequalities manifest across either space or population, horizontal inequalities are those between population groups, and spatial inequalities assess the similarity of nearby values. Each hazard had varying degrees of vertical inequality when looking among states and at the national level. Horizontal inequalities were present between high and low social vulnerability groups, but it was not necessarily the case that lower social vulnerability groups lived in more hazardous places. Hazards tend to be highly spatially unequal, which is in

accordance with the underlying physical processes producing hazard geographies. This study suggests that–since inequality varies greatly across hazards, places, and metrics–researchers should carefully select inequality metrics specific not only to the research question but also based on the identification of theoretical processes for inequality formation and policy-relevant implications.

There are a few avenues for future research that would add to better understanding of vertical, horizontal, and spatial hazard inequalities. Exploring hazard inequalities at larger scales using higher resolution hazard data to illuminate intra- county and city and inequalities. Examining how inequalities change over time along with population characteristics, both historically and by projecting out to the future, will provide evidence regarding differences among groups for selection into and out of hazardous areas. Investigating the processes underlying spatial inequality formation and opportunity structures is an imminently important endeavor, but one that likely necessitates place-based, qualitative, legal, and other research approaches extending beyond the methodological scope of this type of study. A crucially important research topic will be to understand how society responds to shifting climate hazard from an inequality lens. Extending our analysis beyond social vulnerability indicators to features of disaster mitigation and climate adaptation would tease out processes underway that will either ameliorate or exacerbate existing inequalities.

'Measuring Climate Risk Perception with Twitter Data,' contributed to a growing body of social and behavioral science research that substitutes census and survey data with user-generated big data. To that end, we built a dataset for modeling the determinants of climate risk perception using data provided by the microblogging service Twitter. We primarily applied natural language processing to textual data and analyzed social networks to construct this dataset. Validation of our measurements was conducted in two

phases, first against statistical model results from a published survey measuring the same climate risk perception determinants and next with the spatial distribution of climate risk perceptions measured by an annual survey. Although the instruments and data we gathered require additional refinement, preliminary results obtained as part of this validation study indicate that Twitter may soon serve as an appropriate supplementary data source for measuring complex phenomena.

Improvements in measuring and modeling climate risk perception estimated with Twitter data include applying more sophisticated machine learning methods to measuring climate risk perception and its determinants. Testing the sensitivity of these measurements when implementing a Twitter data quality framework, similar in purpose to those established for survey data, could also improve measurement accuracy and precision. Finding additional data sources to validate every indicator included as part of the modeling would assist in fine tuning our measurement instruments. Lastly, applying the methodological approach proposed here to related topics may further highlight the advantages of supplementing survey data with Twitter data, such as observing how CRP changes throughout the hazard/disaster event process, assessing how different types of messaging influence CRP, and exploring the relationship between information reliability and CRP.

Beyond specific future research directions stemming from these papers, there is a climate risk topic of increasing importance for the next several decades that was laid out in the introduction of this dissertation. We suggested that, as a climate risk management strategy, the risk averse will select out of residing and investing in places with higher hazard based on both statistical and perceived climate risk. Individuals and households will likely sort on climate hazard by social advantage. Housing services firms–mortgage lenders, insurance underwriters, and developers–will disinvest from hazardous areas. This may proceed in a similar way to redlining, where the most vulnerable end up living in

more hazardous places with fewer resources to participate in housing markets and manage climate risk. Disinvestment justified by unmanageable climate risk is not prohibited under current law:

"Redlining on a racial basis has been held by the courts to be an illegal practice. It is unlawful under the Fair Housing Act only when done on a prohibited basis. Redlining an area on the basis of such considerations as the fact that the area lies on a fault line or a flood plain is not prohibited." Federal Reserve Board (Interagency Fair Lending Examination Procedures, n.d.)

It does seem that the precipice is clearly marked. Climate adaptive risk management will be the least equitable in places with housing market disinvestment and out-migration of the socially advantaged. Communities with disproportionately high social vulnerability will face additional barriers to affordable housing. Historic redlining practices and the newer practice of climate lining– a potential term for these tandem processes of out-migration and disinvestment–may compound to increase socioeconomic inequity and environmental injustice. Property-level climate hazard data has already begun to impact housing markets. Housing services firms are disinvesting in areas with high flood hazard exposure, which is also a product of urban stormwater and floodplain infrastructure. Higher risk typically falls in places with lower tax bases, many of which were historically redlined, because they lacked the resources and investment to construct essential hazard management infrastructure (Bloomberg, 2020).

Even before the process just described takes shape, an initial issue with improved climate hazard estimation is additional requirements to purchase insurance or retrofit a home, for example if new flood models place the property in the 100-year floodplain (Pralle, 2019). In other cases where insurance is not mandatory but highly recommended, the less advantaged may not be able to afford it yet a disaster without insurance could be devastating.

Safransky (2020) finds that this contemporary data-driven approach to disinvestment is not unique to climate risk. Urban planners now employ algorithmic decision-making for spatial governance and capital investment. This approach has led to the racialization of space and the spatialization of poverty (Lipsitz (2007); Safransky, 2020), whereby race influences the physical locations and societal spaces in which people live and those spaces reciprocally play a role in opportunity structures and social outcomes.

In any place where disinvestment and depopulation is justified by unmanageable climate risk, marginalized communities will face increasing housing market barriers. Just and equitable climate adaptive risk management should ensure access to affordable housing, quality neighborhoods, and low climate hazard. Understanding where, how, and why climate lining occurs is therefore crucial for implementing effective regulatory measures to prevent disinvestment, especially in the most socially vulnerable neighborhoods. Some research questions stemming from these developments are as follows. What is the spatial relationship between historical housing disenfranchisement (e.g. redlining) and climate hazards? Do historical trends in housing data suggest that neighborhood sorting on climate hazards is already happening? How will households and housing markets respond to advances in the production and provision of climate hazard information? What are the socioeconomic and demographic distributions of people living in areas with climate hazard-driven out-migration and disinvestment? What are the consequences for households in areas deemed to be too hazardous by individuals and organizations but that do not have access to support, such as managed retreat programs?

An approach to developing a research agenda for the study of climate lining and other climate risk topics must be inclusive of the topics studied in this dissertation. Thinking back to the equation presented in the introduction:

$$ClimateRisk_{itj} = H_{itj} \cdot E_{itj} \cdot V_{itj}$$

Where climate risk is a function of hazard H, exposure E, and vulnerability V, all per geographic unit i at time t for outcome j (Kron, 2002). This generalizable modeling approach can be easily applied to any combination of subscripts, such as property loss for households in the year 2050. The papers in this dissertation studied dimensions of climate risk using census tracts and counties as the geographic unit and disaster loss as the outcome. Time varied depending on the modeling experiment. We did not explicitly assess risk for a specific combination of geographic unit, outcome, and time period. Although specifying subscripts for the climate risk equation depends on the research question and application, it is not the case that modeling climate risk for a specific subscript combination represents all determinants of risk. This is to say that household climate risk depends not only on household vulnerability but also the vulnerability of neighborhood, city, state, and country. The same applies for exposure and hazard. Because of this, we recommend that risk assessments select an outcome and geographic unit for a set time range before carefully specifying the data required in a climate risk model.

Climate risk assessments for future time periods need to take into account that risk perception mediates each parameter in the model. Examples include greater risk perception: encouraging climate change mitigation to reduce hazard, decreasing exposure as units would move out of hazardous places, and reducing vulnerability through resiliency and capacity building. Furthermore, climate adaptation and the disaster cycle may exhibit feedback loops that increase existing socioeconomic and hazard inequalities. Widening inequalities, particularly an expansion at the lower end of socioeconomic distributions as well as hazard distributions along socioeconomic lines, would limit the capacity for units in aggregate to reduce exposure and vulnerability, thus increasing climate risk. It is also

important to note that selecting one outcome is not representative of the full risk profile.

Pursuing a comprehensive climate risk assessment at the household level with these considerations in mind therefore requires a multitude of model specifications and input data. Instead of estimating a full risk profile, we recommend that climate risk assessment should instead consider the most consequential outcomes facing a geographic unit. Quantifiable risks at the household level are likely property loss and damage, insurance and utilities costs, and disruptions to daily life. Winnowing down the risks to a specifiable set such as this allows researchers and practitioners to feasibly select relevant outcomes and parameter values that overlap and thus reduce the amount of data and effort required, which is particularly useful for those with limited resources.

Climate risk threatens human well-being and economic systems across the United States. We demonstrated that social vulnerability moderates how well prepared communities are for disaster events. Governments can implement climate adaptation planning to decrease risk from climate hazards but will need to target resources towards social indicators and places that need them most. In spite of even the most accurate resource targeting, communities will determine hazard mitigation according to the way they perceive and respond. This dissertation added to our understanding of the roles that climate hazard, social vulnerability, and sociocognitive factors play in climate risk assessment. We hope our findings and recommendations will support strategies for more equitable, effective, and efficient climate risk assessments.

Appendix A

Climate Hazard Estimation

To assess climate risks we first determine the relevant spatial unit of analysis and integrate many datasets to comparable spatial and temporal scales. Data from historical observations and modeled projections establish baseline and future risks for each climate hazard. We weight future risk estimates with the change in risk over the next several decades. Climate risk projections come from tens of internationally accepted global climate models which have been validated as part of the Coupled Model Intercomparison Project Phase 5 (Taylor et al., 2012). When available, we choose output for Representative Concentration Pathway 8.5 (RCP8.5), a conservative, worst-case scenario for the continued release of CO2 into the atmosphere. Researchers have downscaled these projections to higher resolution across the US by utilizing local information (e.g. weather patterns, vegetation, hydrodynamics, topography, etc.) and leveraging the empirical links between climate at large scales and that at finer scales. We take these downscaled data products to produce high spatiotemporal resolution estimates of how climate risk will change over the 21st century. Figure **??** displays the climate hazards we estimate and the average climate hazard aggregated at the county level. Table **??** provides summary statistics.

Drought (water scarcity)

We estimate drought risk based on the Water Supply Stress Index (WaSSI) hydrologic model, which measures how much available water in a location is used by human activity. WaSSI is specific to each watershed, a land area with the same water outlet. The geographic unit of analysis is USGS hydrologic designation HUC-8, the sub-basin level, analogous to medium-sized river basins. WaSSI takes into account current and projected water supply (surface and ground water), demand due to population size and water use, and features of the watershed, such as soil properties and land cover. The underlying analysis uses downscaled data from CMIP5 climate models under the RCP8.5 scenario as inputs (Averyt et al., 2013; Duan et al., 2019).

Heat and storm (extreme high temperatures and precipitation)

Climate models project extreme heat and precipitation events to increase globally. We measure projected changes to extreme events using Localized Constructed Analogs, global climate model (GCM) output that has been enriched for statistical downscaling to a higher geographic resolution (Pierce, Cayan, & Thrasher, 2014). Downscaled projections better match local conditions at a high $5km2$ resolution. We conduct all statistical estimates, e.g. annual extreme counts, per GCM model and then average across 27 GCMs from the Climate Model Intercomparison Project (CMIP5). Precipitation estimates are based on the annual average counts of extremely wet (or snowy) two-day storms and the annual total amount of precipitation that will fall during those storms. Heat estimates are based on annual average counts of extremely hot days. The 'extreme' threshold is based on the cell-wise 98th percentile of observed values during the historic baseline, from 1981-2005.

Wildfire: spatiotemporality, intensity, and severity

We measure wildfire risk by areal extent and return interval (proportion burned), intensity (flame length exceedance probability), and severity (conditional risk to potential structures). The first two parameters, *areal extent* and *return interval*, are based on the MC2 dynamic global vegetation model, which uses information from an ensemble of 19 CMIP5 climate models on changing temperatures, precipitation, and atmospheric CO2. MC2 simulates the competition among plants for light, nitrogen, and soil water to project vegetation coverage in the future; this projected vegetation coverage is translated into an expected proportion of area likely to burn across the U.S. These data come as annual estimates of proportion burned until 2100 (Abatzoglou, 2013; Abatzoglou & Brown, 2012; Bachelet & Turner, 2015; Barbero, Abatzoglou, Larkin, Kolden, & Stocks, 2015).

The other two parameters derive from US Forest Service data products: *intensity* represents the likelihood that flame length exceeds four feet if a fire were to occur, and *severity* represents the risk posed to a hypothetical structure if a fire occurred (Scott et al., 2020). Neither of these estimates factor in wildfire probability, which we instead capture using the MC2 data. We produce a wildfire risk rating from the weighted geometric average of relative ranked values for these statistics. The weighting is .5 for areal extent and return interval, .25 for intensity, and .25 for severity.

We enhance the MC2 data with observed Western US fire occurrence from the Monitoring Trends in Burn Severity remotely sensed data product (Eidenshink et al., 2007) and localized improvements in quality, resolution, and coverage, such as probabilistic wildfire projections for California's Fourth Climate Change Assessment (Westerling, 2018). Typically, we average across estimates from different datasets that cover the same time and place. However, when spatiotemporal resolutions are misaligned or very coarse, we take the maximum value across datasets to represent the absolute probability of fire occurrence. We apply a mask to reduce the risk estimate in cells representing non-vegetated

land and the presence of human activity, such as agriculture and densely built environments, which lower the risk of wildfire.

5. Flood: high tide, storm surge, pluvial, fluvial

Flood risk is a combination of several types of flooding: storm surge, high tide, fluvial, and pluvial. Coastal flooding, storm surge and high tide, occurs when coastal areas become inundated by sea water. Precipitation-based flooding can occur anywhere and generally represents two distinct types: bodies of water overflowing (fluvial) and surface water floods (pluvial). Flood risk estimates come from the occurrence probability and likely depth of all four types of flooding between 2020 and 2050 for both Representative Concentration Pathway (RCP) 4.5 and 8.5. We estimate each type of flood risk independently and calculate a marginal cumulative sum to produce the flood risk rating. This approach accounts for accumulation of any-type flooding and does not discount for lower or non-existent any-type flooding. For example, if risk is present across three types of flood for a parcel, with a risk of 50 across each type we observe a flood risk rating of 87.5; 90.6 if risk is 25, 50, and 75 across types; and 96 if risk is 0, 80, and 80. Property-level flood risk estimates are calculated as the average value of all cells within the entire property parcel.

Coastal flooding: high tide

High-tide coastal flooding occurs when water inundates land during the highest tides. It is a cyclically occurring phenomenon where coastal waters exceed mean higher high water (MHHW), the average height of the highest tide recorded each day. The land above MHHW is dry most of the time. MHHW has a baseline average from the most recent National Tidal Datum Epoch from 1983-2001 and locally varies by relative sea level, tidal behavior, and geomorphological features and processes, such as elevation and

coastal erosion. Similarly, high tide flooding probability is a function of local relative sea level and elevation. This means that as the planet warms and sea levels rise, high tide flooding is likely to become more frequent and cover a greater spatial extent in coastal communities. However, the increase in frequency depends on local relative sea level rise.

We use several National Oceanic and Atmospheric Administration (NOAA) data and modeling products to estimate high tide flooding: daily observed tidal variability measured at over 100 tide gauges, a $50m^2$ MHHW interpolated surface, $10m^2$ digital elevation models (DEM), and relative sea level rise projections (Kopp et al., 2014; Marcy et al., 2011; Sweet, Dusek, Marcy, Carbin, & Marra, 2019; Sweet et al., 2017; Sweet, Dusek, Obeysekera, & Marra, 2018). We utilize established coastal flooding models to quantify the typical range of high tide heights for a location and the associated inundation. We then use forecasts of relative sea level rise through 2050 to augment these tidal heights and estimate how much land will be effectively inundated in the future.

A simple explanation of the method to estimate high tide flooding is:

1. Interpolate MHHW, relative sea level rise, and daily tidal distributions with inverse distance weighting for each cell of the DEM.
2. Non-parametric probability density estimation to produce theoretical high tide flooding probability density functions (HTF PDF) with the maximum daily tidal distributions.
3. Shift the HTF PDFs by projected relative sea level rise in ten-year time steps.
4. Apply DEM elevation values to HTF PDFs to produce high tide flooding probability estimates. These values represent our high tide flood risk rating, the daily probability of high tide flooding. We multiply the probability by 365 to find the expected annual number of high tide flooding days.
5. Finish with a geospatial cleanup. We remove cells representing hydrographic fea-

tures and those with risk larger than 0 but disconnected from the sea using region grouping.

Coastal flooding: storm surge

A storm surge is a rise in ocean water, higher than any normal tide, generated by a storm. Storm surges happen when extreme storm winds push water toward the shore. The depth of the resulting flood depends on the strength of the storm and its direction, as well the shape of the coastline and local terrain. Similar to high tide flooding, sea level rise will increase the depth of storm surge in coastal communities. We use models from NOAA and the National Hurricane Center (NHC) that estimate the worst-case scenario flood depth at a $10m^2$ resolution along the Atlantic and Gulf coasts for each category of hurricane. To quantify the likelihood of these floods historically and in the future, we analyze hurricane tracks to measure how often category 1-5 storms pass within about 50 miles of a location.

Precipitation-based flooding: fluvial and pluvial

These types of flooding occur in both coastal and inland areas. Fluvial, or riverine, flooding happens when a river or body of water overflows onto surrounding land. Pluvial, or surface, flooding occurs when extreme rainfall creates flash flooding or surface water buildup away from a body of water. These types of flooding comprise our most intensive modeling efforts due to their inherent complexity. The remainder of this document focuses on precipitation-based flooding.

We utilize the open-source cellular automata-based model, Weighted Cellular Automata 2D (WCA2D), to quantify present and future precipitation-based flood risk. WCA2D has dynamic parameterization and modern computing hardware capabilities for fast simulations (Guidolin et al., 2016). WCA2D is part of the CADDIES framework, a toolkit for

efficient, high resolution computational flood modeling (Ghimire et al., 2012; Guidolin et al., 2012). Initially developed for small area urban surface water runoff and sewer network simulations (Austin, Chen, Savić, & Djordjević, 2014), CADDIES has expanded to become a generalizable tool for modeling precipitation-based flood risk.

The CADDIES framework has been validated with UK Environment Agency test cases and the Infoworks model (Guidolin et al., 2016); identified as a suitable tool for identifying flood hazard in urban and rural catchments (Webber, Booth, Gunasekara, Fu, & Butler, 2019); and applied in case studies ranging from the cascading effects of flooding on critical infrastructure (Gibson et al., 2019; Vamvakeridou-Lyroudia et al., 2020) to how green infrastructure mitigates urban flooding (Webber et al., 2020).

We establish current (2020) flood risk using historical meteorological observations and global climate models (GCMs) validated under Coupled Model Intercomparison Project Phase 5 (Taylor et al., 2012). These data feed models of rainfall and runoff that capture flooding behavior across the United States. Flood risk in 2050 is modeled using the same GCM ensemble under the RCP 4.5 and 8.5 scenarios. We estimate expected occurrence probability and likely depth of a flood between 2020 and 2050.

References

Aalst, M. K. V. (2006). The impacts of climate change on the risk of natural disasters. *Disasters*, *30*(1), 5–18. https://doi.org/10.1111/j.1467-9523.2006.00303.x

Aaronson, D., Hartley, D., & Mazumder, B. (2017). *The effects of the 1930s HOLC "redlining" maps* (Working Paper No. 2017-12). Working Paper.

Abatzoglou, J. T. (2013). Development of gridded surface meteorological data for ecological applications and modelling. *International Journal of Climatology*, *33*(1), 121–131. https://doi.org/10.1002/joc.3413

Abatzoglou, J. T., & Brown, T. J. (2012). A comparison of statistical downscaling methods suited for wildfire applications. *International Journal of Climatology*, *32*(5), 772–780. https://doi.org/10.1002/joc.2312

Abatzoglou, J. T., & Williams, A. P. (2016). Impact of anthropogenic climate change on wildfire across western US forests. *Proceedings of the National Academy of Sciences*, *113*(42), 11770–11775. https://doi.org/10.1073/pnas.1607171113

Abraham, R. G., Bergh, S. van den, & Nair, P. (2003). A New Approach to Galaxy Morphology. I. Analysis of the Sloan Digital Sky Survey Early Data Release. *The Astrophysical Journal*, *588*(1), 218. https://doi.org/10.1086/373919

References

Adger, W. N. (2006). Vulnerability. *Global Environmental Change*, *16*(3), 268–281. https://doi.org/10.1016/j.gloenvcha.2006.02.006

Akerlof, K., Maibach, E., Fitzgerald, D., Cedeno, A., & Neuman, A. (2013). Do people "personally experience" global warming, and if so how, and does it matter? *Global Environmental Change*, *23*, 81–91. https://doi.org/10.1016/j.gloenvcha.2012.07.006

Aletras, N., & Chamberlain, B. P. (2018). Predicting Twitter User Socioeconomic Attributes with Network and Language Information. *arXiv:1804.04095 [Cs]*. Retrieved from http://arxiv.org/abs/1804.04095

Allison, P. D. (1978). Measures of Inequality. *American Sociological Review*, *43*(6), 865–880. https://doi.org/10.2307/2094626

Ambler, G., & Benner, A. (2015). Mfp: Multivariable Fractional Polynomials. *R Package Version 1.5.2. Https://CRAN.R-Project.org/Package=mfp*.

An, X., Ganguly, A. R., Fang, Y., Scyphers, S. B., Hunter, A. M., & Dy, J. G. (2014). Tracking climate change opinions from twitter data. *Workshop on Data Science for Social Good*, 1–6.

Anda, J., Golub, A., & Strukova, E. (2009). Economics of climate change under uncertainty: Benefits of flexibility. *Energy Policy*, *37*(4), 1345–1355. https://doi.org/10.1016/j.enpol.2008.11.034

Anderson, M. W. (2007). *Cities Inside Out: Race, Poverty, and Exclusion at the Urban Fringe* (SSRN Scholarly Paper No. ID 1007359). Rochester, NY: Social Science Research Network. https://doi.org/10.2139/ssrn.1007359

Anderson G. Brooke, & Bell Michelle L. (2011). Heat Waves in the United States:

Mortality Risk during Heat Waves and Effect Modification by Heat Wave Characteristics in 43 U.S. Communities. *Environmental Health Perspectives*, *119*(2), 210–218. https://doi.org/10.1289/ehp.1002313

APA Dictionary of Psychology. (n.d.). https://dictionary.apa.org/.

Asadzadeh, A., Kötter, T., Salehi, P., & Birkmann, J. (2017). Operationalizing a concept: The systematic review of composite indicator building for measuring community disaster resilience. *International Journal of Disaster Risk Reduction*, *25*, 147–162. https://doi.org/10.1016/j.ijdrr.2017.09.015

Ash, M., & Fetter, T. R. (2004). Who Lives on the Wrong Side of the Environmental Tracks? Evidence from the EPA's Risk-Screening Environmental Indicators Model*. *Social Science Quarterly*, *85*(2), 441–462. https://doi.org/10.1111/j.0038-4941.2004.08502011.x

Atkinson, A. B. (1970). On the measurement of inequality. *Journal of Economic Theory*, *2*(3), 244–263. https://doi.org/10.1016/0022-0531(70)90039-6

Austin, R. J., Chen, A. S., Savić, D. A., & Djordjević, S. (2014). Quick and accurate Cellular Automata sewer simulator. *Journal of Hydroinformatics*, *16*(6), 1359–1374. https://doi.org/10.2166/hydro.2014.070

Averyt, K., Meldrum, J., Caldwell, P., Sun, G., McNulty, S., Huber-Lee, A., & Madden, N. (2013). Sectoral contributions to surface water stress in the coterminous United States. *Environmental Research Letters*, *8*(3), 035046. https://doi.org/10.1088/1748-9326/8/3/035046

Bachelet, D., & Turner, D. (2015). *Global vegetation dynamics*. Wiley Online Library.

Bakkensen, L. A., Fox-Lent, C., Read, L. K., & Linkov, I. (2017). Validating Resilience

and Vulnerability Indices in the Context of Natural Disasters. *Risk Analysis*, *37*(5), 982–1004. https://doi.org/10.1111/risa.12677

Bakkensen, L. A., & Ma, L. (2020). Sorting over flood risk and implications for policy reform. *Journal of Environmental Economics and Management*, *104*, 102362. https://doi.org/10.1016/j.jeem.2020.102362

Bansal, R., Ochoa, M., & Kiku, D. (2016). *Climate Change and Growth Risks* (Working Paper No. 23009). National Bureau of Economic Research. https://doi.org/10.3386/w23009

Baram-Tsabari, A., Wolfson, O., Yosef, R., Chapnik, N., Brill, A., & Segev, E. (2020). Jargon use in Public Understanding of Science papers over three decades. *Public Understanding of Science*, *29*(6), 644–654. https://doi.org/10.1177/0963662520940501

Barbero, R., Abatzoglou, J. T., Larkin, N. K., Kolden, C. A., & Stocks, B. (2015). Climate change presents increased potential for very large fires in the contiguous United States. *International Journal of Wildland Fire*, *24*(7), 892. https://doi.org/10.1071/WF15083

Bates, P. D., Horritt, M. S., & Fewtrell, T. J. (2010). A simple inertial formulation of the shallow water equations for efficient two-dimensional flood inundation modelling. *Journal of Hydrology*, *387*(1), 33–45. https://doi.org/10.1016/j.jhydrol.2010.03.027

BEA. (2021). *Gross Domestic Product by County*. Bureau of Economic Analysis.

Bec, A., & Becken, S. (2019). Risk perceptions and emotional stability in response to Cyclone Debbie: An analysis of Twitter data. *Journal of Risk Research*, *0*(0), 1–19.

https://doi.org/10.1080/13669877.2019.1673798

Bedford, T., & Cooke, R. (2001). *Probabilistic Risk Analysis: Foundations and Methods*. Cambridge: Cambridge University Press. https://doi.org/10.1017/CBO9780511813597

Bell, M. L., & Ebisu, K. (2012). Environmental Inequality in Exposures to Airborne Particulate Matter Components in the United States. *Environmental Health Perspectives*, *120*(12), 1699–1704. https://doi.org/10.1289/ehp.1205201

Bergstrand, K., Mayer, B., Brumback, B., & Zhang, Y. (2015). Assessing the Relationship Between Social Vulnerability and Community Resilience to Hazards. *Social Indicators Research*, *122*(2), 391–409. https://doi.org/10.1007/s11205-014-0698-3

Bernstein, P. L. (1996). *Against the gods: The remarkable story of risk*. New York: John Wiley & Sons.

Bertrand, M., & Mullainathan, S. (2003). *Are Emily and Greg More Employable than Lakisha and Jamal? A Field Experiment on Labor Market Discrimination* (No. w9873). National Bureau of Economic Research. https://doi.org/10.3386/w9873

Bian, J., Yoshigoe, K., Hicks, A., Yuan, J., He, Z., Xie, M., … Modave, F. (2016). Mining Twitter to Assess the Public Perception of the "Internet of Things". *PLOS ONE*, *11*(7), e0158450. https://doi.org/10.1371/journal.pone.0158450

Birkmann, J., & Wisner, B. (2006). Measuring the unmeasurable: The challenge of vulnerability. *Undefined*.

Blanc, É. (2017). Statistical emulators of maize, rice, soybean and wheat yields from global gridded crop models. *Agricultural and Forest Meteorology*, *236*, 145–161. https://doi.org/10.1016/j.agrformet.2016.12.022

References

Blanc, E., & Sultan, B. (2015). Emulating maize yields from global gridded crop models using statistical estimates. *Agricultural and Forest Meteorology*, *214–215*, 134–147. https://doi.org/10.1016/j.agrformet.2015.08.256

Blasi, S., Brigato, L., & Sedita, S. R. (2020). Eco-friendliness and fashion perceptual attributes of fashion brands: An analysis of consumers' perceptions based on twitter data mining. *Journal of Cleaner Production*, *244*, 118701. https://doi.org/10.1016/j.jclepro.2019.118701

Bloomberg. (2020). *The Truth About Flood Risk Can Worsen American Inequality.*

Bocco, G., & Napoletano, B. M. (2017). The prospects of terrace agriculture as an adaptation to climate change in Latin America. *Geography Compass*, *11*(10), e12330. https://doi.org/10.1111/gec3.12330

Boholm, Å. (2015). *Anthropology and Risk.* London: Routledge. https://doi.org/10.4324/9781315797793

Bollen, J., Mao, H., & Pepe, A. (2011). Modeling Public Mood and Emotion: Twitter Sentiment and Socio-Economic Phenomena. *Proceedings of the International AAAI Conference on Web and Social Media*, *5*(1).

Boyce, J. K., Zwickl, K., & Ash, M. (2016). Measuring environmental inequality. *Ecological Economics*, *124*, 114–123. https://doi.org/10.1016/j.ecolecon.2016.01.014

Bradley, G. L., Babutsidze, Z., Chai, A., & Reser, J. P. (2020). The role of climate change risk perception, response efficacy, and psychological adaptation in pro-environmental behavior: A two nation study. *Journal of Environmental Psychology*, *68*, 101410. https://doi.org/10.1016/j.jenvp.2020.101410

Braun, B., Oßenbrügge, J., & Schulz, C. (2018). Environmental economic geography

and environmental inequality: Challenges and new research prospects. *Zeitschrift Für Wirtschaftsgeographie*, *62*(2), 120–134. https://doi.org/10.1515/zfw-2018-0001

Breakwell, G. M. (2010). Models of risk construction: Some applications to climate change. *WIREs Climate Change*, *1*(6), 857–870. https://doi.org/10.1002/wcc.74

Brewer, N. T., Weinstein, N. D., Cuite, C. L., & Herrington, J. E. (2004). Risk perceptions and their relation to risk behavior. *Annals of Behavioral Medicine*, *27*(2), 125–130. https://doi.org/10.1207/s15324796abm2702_7

Briscoe, L. S., Tony. (2020). *Millions of Homeowners Who Need Flood Insurance Don't Know It to FEMA*. ProPublica.

Brody, S., Grover, H., & Vedlitz, A. (2012). Examining the willingness of Americans to alter behaviour to mitigate climate change. *Climate Policy*, *12*(1), 1–22. https://doi.org/10.1080/14693062.2011.579261

Brown, D. B., & Sim, M. (2008). Satisficing Measures for Analysis of Risky Positions. *Management Science*, *55*(1), 71–84. https://doi.org/10.1287/mnsc.1080.0929

Bryant, B. P., & Westerling, A. L. (2014). Scenarios for future wildfire risk in California: Links between changing demography, land use, climate, and wildfire. *Environmetrics*, *25*(6), 454–471. https://doi.org/10.1002/env.2280

Bullard, R. D. (2001). Environmental Justice in the 21st Century: Race Still Matters. *Phylon (1960-)*, *49*(3/4), 151–171. https://doi.org/10.2307/3132626

Bullard, R. D. (2005). *The quest for environmental justice: Human rights and the politics of pollution*. San Francisco: Sierra Club Books.

Bullard, R. D. (2011). Sacrifice Zones: The Front Lines of Toxic Chemical Exposure in the United States. *Environmental Health Perspectives*, *119*(6), A266.

References

Bulut, H. (2017). Managing Catastrophic Risk in Agriculture through Ex Ante Subsidized Insurance or Ex Post Disaster Aid. *Journal of Agricultural and Resource Economics*, *42*(3), 406–426.

Bureau, U. C. (2019). *CPS Historical Geographic Mobility/Migration Graphs*. The United States Census Bureau.

Bureau, U. C. (2020). *Demographic Turning Points for the United States*. The United States Census Bureau.

Burger, M., Wentz, J., & Horton, R. (2020). The Law and Science of Climate Change Attribution. *Columbia Journal of Environmental Law*, *45*(1), 57–240.

Burton, I. (1993). *The Environment as Hazard*. Guilford Press.

Capstick, S. B., & Pidgeon, N. F. (2014). Public perception of cold weather events as evidence for and against climate change. *Climatic Change*, *122*(4), 695–708. https://doi.org/10.1007/s10584-013-1003-1

Cazelles, B., & Hales, S. (2006). Infectious Diseases, Climate Influences, and Nonstationarity. *PLOS Medicine*, *3*(8), e328. https://doi.org/10.1371/journal.pmed.0030328

CEMHS. (2020). *Spatial Hazard Events and Losses Database for the United States, Version 19.0*. Center for Emergency Management and Homeland Security, Arizona State University.

Center for Disaster Philanthropy. (2019). *2019 Catastrophic River Flooding*.

Center for Public Integrity. (2020). *Climate change is killing Americans. Health departments aren't equipped to respond*.

Chaves, K., Wilson, N., Gray, D., Barton, B., Bonnett, D., & Azam, I. (2018). 2018 National Healthcare Quality and Disparities Report. *Agency for Healthcare Research and Quality*, 222.

Chew, C., & Eysenbach, G. (2010). Pandemics in the age of Twitter: Content analysis of Tweets during the 2009 H1N1 outbreak. *PloS One*, *5*(11), e14118. https://doi.org/10.1371/journal.pone.0014118

Cialdini, R. B., Kallgren, C. A., & Reno, R. R. (1991). A Focus Theory of Normative Conduct: A Theoretical Refinement and Reevaluation of the Role of Norms in Human Behavior. In M. P. Zanna (Ed.), *Advances in Experimental Social Psychology* (Vol. 24, pp. 201–234). Academic Press. https://doi.org/10.1016/S0065-2601(08)60330-5

Clinton, W. J. (1994). Federal actions to address environmental justice in minority populations and low-income populations. *Environment*, *36*(4).

Cole, E. (2011). Credit Card Redlining. *Review of Economics and Statistics*.

Collins, C., Hasan, S., & Ukkusuri, S. (2013). A Novel Transit Rider Satisfaction Metric: Rider Sentiments Measured from Online Social Media Data. *Journal of Public Transportation*, *16*(2). https://doi.org/10.5038/2375-0901.16.2.2

Covello, V. T., & Mumpower, J. (1985). Risk Analysis and Risk Management: An Historical Perspective. *Risk Analysis*, *5*(2), 103–120. https://doi.org/10.1111/j.1539-6924.1985.tb00159.x

Cowell, F. (2011). *Measuring Inequality*. Oxford University Press.

Crain, W. M., & Oakley, L. K. (1995). The Politics of Infrastructure. *The Journal of Law and Economics*, *38*(1), 1–17. https://doi.org/10.1086/467323

References

Cromley, G. A. (2019). Measuring differential access to facilities between population groups using spatial Lorenz curves and related indices. *Transactions in GIS*, *23*(6), 1332–1351. https://doi.org/10.1111/tgis.12577

Culotta, A., Ravi, N. K., & Cutler, J. (2016). Predicting Twitter User Demographics using Distant Supervision from Website Traffic Data. *Journal of Artificial Intelligence Research*, *55*, 389–408. https://doi.org/10.1613/jair.4935

Cutter, S. L. (1996). Vulnerability to environmental hazards. *Progress in Human Geography*, *20*(4), 529–539. https://doi.org/10.1177/030913259602000407

Cutter, S. L., Boruff, B. J., & Shirley, W. L. (2003). Social Vulnerability to Environmental Hazards*. *Social Science Quarterly*, *84*(2), 242–261. https://doi.org/10.1111/1540-6237.8402002

Cutter, S. L., Mitchell, J. T., & Scott, M. S. (2000). Revealing the Vulnerability of People and Places: A Case Study of Georgetown County, South Carolina. *Annals of the Association of American Geographers*, *90*(4), 713–737. https://doi.org/10.1111/0004-5608.00219

Dahal, B., Kumar, S. A. P., & Li, Z. (2019). Topic modeling and sentiment analysis of global climate change tweets. *Social Network Analysis and Mining*, *9*(1), 24. https://doi.org/10.1007/s13278-019-0568-8

Dai, A. (2011). Drought under global warming: A review. *WIREs Climate Change*, *2*(1), 45–65. https://doi.org/10.1002/wcc.81

Damasio, A. R. (2006). *Descartes' Error*. Random House.

Damodaran, A. (2012). *Investment Valuation: Tools and Techniques for Determining the Value of Any Asset* (3rd edition). Hoboken, N.J: Wiley.

Daniel, V. E., Florax, R. J., & Rietveld, P. (2009). Floods and Residential Property Values: A Hedonic Price Analysis for the Netherlands. *Built Environment (1978-)*, *35*(4), 563–576.

D'Auria, L., & Convertito, V. (2016). Real-Time Mapping of Earthquake Perception Areas in the Italian Region from Twitter Streams Analysis. In S. D'Amico (Ed.), *Earthquakes and Their Impact on Society* (pp. 619–630). Cham: Springer International Publishing. https://doi.org/10.1007/978-3-319-21753-6_26

Di Baldassarre, G., Viglione, A., Carr, G., Kuil, L., Salinas, J. L., & Blöschl, G. (2013). Socio-hydrology: Conceptualising human-flood interactions. *Hydrology and Earth System Sciences*, *17*(8), 3295–3303. https://doi.org/10.5194/hess-17-3295-2013

Dietz, S., Bowen, A., Dixon, C., & Gradwell, P. (2016). "Climate value at risk" of global financial assets. *Nature Climate Change*, *6*(7), 676–679. https://doi.org/10.1038/nclimate2972

Diffenbaugh, N. S., & Giorgi, F. (2012). Climate change hotspots in the CMIP5 global climate model ensemble. *Climatic Change*, *114*(3), 813–822. https://doi.org/10.1007/s10584-012-0570-x

DiPrete, T. A., & Eirich, G. M. (2006). Cumulative Advantage as a Mechanism for Inequality: A Review of Theoretical and Empirical Developments. *Annual Review of Sociology*, *32*(1), 271–297. https://doi.org/10.1146/annurev.soc.32.061604.123127

Donner, W., & Rodríguez, H. (2008). Population composition, migration and inequality: The influence of demographic changes on disaster risk and vulnerability. *Social Forces*, *87*(2), 1089–1114. https://doi.org/10.1353/sof.0.0141

Dorfman, R. (1979). A Formula for the Gini Coefficient. *The Review of Economics and Statistics*, *61*(1), 146–149. https://doi.org/10.2307/1924845

Douglas, J. (2007). Physical vulnerability modelling in natural hazard risk assessment. *Natural Hazards and Earth System Sciences*, *7*(2), 283–288. https://doi.org/10.5194/nhess-7-283-2007

Douglas, M. (2004). *Natural Symbols: Explorations in Cosmology*. Routledge.

Douglas, M., & Wildavsky, A. (n.d.). *Risk and Culture*.

Downey, L. (2005). Assessing Environmental Inequality: How the Conclusions We Draw Vary According to the Definitions We Employ. *Sociological Spectrum*, *25*(3), 349–369. https://doi.org/10.1080/027321790518870

Duan, K., Caldwell, P. V., Sun, G., McNulty, S. G., Zhang, Y., Shuster, E., … Bolstad, P. V. (2019). Data on projections of surface water withdrawal, consumption, and availability in the conterminous United States through the 21st century. *Data in Brief*, *23*, 103786. https://doi.org/10.1016/j.dib.2019.103786

Dudula, J., & Randhir, T. O. (2016). Modeling the influence of climate change on watershed systems: Adaptation through targeted practices. *Journal of Hydrology*, *541*, 703–713. https://doi.org/10.1016/j.jhydrol.2016.07.020

Dunlap, R. E., & Brulle, R. J. (2015). *Climate Change and Society: Sociological Perspectives*. Oxford University Press.

Dunning, N. P., Beach, T. P., & Luzzadder-Beach, S. (2012). Kax and kol: Collapse and resilience in lowland Maya civilization. *Proceedings of the National Academy of Sciences*, *109*(10), 3652–3657. https://doi.org/10.1073/pnas.1114838109

Duro, J. (2012). On the automatic application of inequality indexes in the analysis of

the international distribution of environmental indicators. *Ecological Economics*, *76*. https://doi.org/10.1016/j.ecolecon.2011.12.019

Dwarka, K., & Feitelson, E. (2013). The political economy of urban infrastructure. *International Handbook on Mega-Projects*.

Eakin, H., & Luers, A. L. (2006). Assessing the Vulnerability of Social-Environmental Systems. *Annual Review of Environment and Resources*, *31*(1), 365–394. https://doi.org/10.1146/annurev.energy.30.050504.144352

Echavarren, J. M., Balžekienė, A., & Telešienė, A. (2019). Multilevel analysis of climate change risk perception in Europe: Natural hazards, political contexts and mediating individual effects. *Safety Science*, *120*, 813–823. https://doi.org/10.1016/j.ssci.2019.08.024

Eidenshink, J., Schwind, B., Brewer, K., Zhu, Z.-L., Quayle, B., & Howard, S. (2007). A Project for Monitoring Trends in Burn Severity. *Fire Ecology*, *3*(1), 3–21. https://doi.org/10.4996/fireecology.0301003

Ekenga, C. C., McElwain, C.-A., & Sprague, N. (2018). Examining Public Perceptions about Lead in School Drinking Water: A Mixed-Methods Analysis of Twitter Response to an Environmental Health Hazard. *International Journal of Environmental Research and Public Health*, *15*(1), 162. https://doi.org/10.3390/ijerph15010162

Emrich, C. T., & Cutter, S. L. (2011). Social Vulnerability to Climate-Sensitive Hazards in the Southern United States. *Weather, Climate, and Society*, *3*(3), 193–208. https://doi.org/10.1175/2011WCAS1092.1

Fekete, A. (2009). Validation of a Social Vulnerability Index in Context to River-floods in Germany. *Natural Hazards and Earth System Sciences*, *9*. https://doi.org/10.

5194/nhess-9-393-2009

FEMA. (1991). *TR-060 the east bay hills fire.*

Fielding, J., & Burningham, K. (2005). Environmental inequality and flood hazard. *Local Environment*, *10*(4), 379–395. https://doi.org/10.1080/13549830500160875

Finch, C., Emrich, C. T., & Cutter, S. L. (2010). Disaster disparities and differential recovery in New Orleans. *Population and Environment*, *31*(4), 179–202. https://doi.org/10.1007/s11111-009-0099-8

Finucane, M. L. (2012). The Role of Feelings in Perceived Risk. In S. Roeser, R. Hillerbrand, P. Sandin, & M. Peterson (Eds.), *Handbook of Risk Theory: Epistemology, Decision Theory, Ethics, and Social Implications of Risk* (pp. 677–691). Dordrecht: Springer Netherlands. https://doi.org/10.1007/978-94-007-1433-5_26

Finucane, M. L., Alhakami, A., Slovic, P., & Johnson, S. M. (2000). The affect heuristic in judgments of risks and benefits. *Journal of Behavioral Decision Making*, *13*(1), 1–17. https://doi.org/10.1002/(SICI)1099-0771(200001/03)13:1<1::AID-BDM333>3.0.CO;2-S

Flanagan, B. E., Gregory, E. W., Hallisey, E. J., Heitgerd, J. L., & Lewis, B. (2011). *A Social Vulnerability Index for Disaster Management.* 24.

Flanagan, B. E., Hallisey, E. J., Adams, E., & Lavery, A. (2018). Measuring Community Vulnerability to Natural and Anthropogenic Hazards: The Centers for Disease Control and Prevention's Social Vulnerability Index. *Journal of Environmental Health*, *80*(10), 34–36.

Flavelle, C., Lu, D., Penney, V., Popovich, N., & Schwartz, J. (2020). New Data Reveals Hidden Flood Risk Across America. New York: New York Times Company.

Fosch-Villaronga, E., Poulsen, A., Søraa, R. A., & Custers, B. H. M. (2021). A little bird told me your gender: Gender inferences in social media. *Information Processing & Management*, *58*(3), 102541. https://doi.org/10.1016/j.ipm.2021.102541

Frankenberg, E., Laurito, M., & Thomas, D. (2014). The demography of disasters. *Prepared for the International Encyclopedia of the Social and Behavioral Sciences. 2nd Ed.(Area)*, *3*, 12.

Frazier, T., Boyden, E. E., & Wood, E. (2020). Socioeconomic implications of national flood insurance policy reform and flood insurance rate map revisions. *Natural Hazards*, *103*(1), 329–346. https://doi.org/10.1007/s11069-020-03990-1

Frosch, R. M., Pastor, M., Sadd, J., & Shonkoff, S. (2018). The Climate Gap: Inequalities in How Climate Change Hurts Americans and How to Close the Gap. In *Planning for Climate Change*. Routledge.

Funk, C. C., Hoell, A., & Stone, D. (2014). Examining the contribution of the observed global warming trend to the California droughts of 2012/13 and 2013/14 [Journal Article]. *Bulletin of the American Meteorological Society*, *95*(9), 5. https://doi.org/10.1175/1520-0477-95.9.S1.1

Funk, C., & Kennedy, B. (2020). How Americans see climate change and the environment in 7 charts.

Gaither, C. J., Poudyal, N. C., Goodrick, S., Bowker, J. M., Malone, S. L., & Gan, J. (2011). Wildland fire risk and social vulnerability in the Southeastern United States: An exploratory spatial data analysis approach. *Forest Policy and Economics. 13: 24-36.*, *13*, 24–36. https://doi.org/10.1016/j.forpol.2010.07.009

Galster, G., & Sharkey, P. (2017). Spatial Foundations of Inequality: A Conceptual

Model and Empirical Overview. *RSF: The Russell Sage Foundation Journal of the Social Sciences*, *3*(2), 1–33. https://doi.org/10.7758/rsf.2017.3.2.01

Ghimire, B., Chen, A. S., Guidolin, M., Keedwell, E. C., Djordjević, S., & Savić, D. A. (2012). Formulation of a fast 2D urban pluvial flood model using a cellular automata approach. *Journal of Hydroinformatics*, *15*(3), 676–686. https://doi.org/10.2166/hydro.2012.245

Gibson, M. J., Chen, A. S., Khoury, M., Vamvakeridou-Lyroudia, L. S., Stewart, D., Wood, M., … Djordjević, S. (2019). Case study of the cascading effects on critical infrastructure in Torbay coastal/pluvial flooding with climate change and 3D visualisation. *Journal of Hydroinformatics*, *22*(1), 77–92. https://doi.org/10.2166/hydro.2019.032

Giglio, S., Maggiori, M., Rao, K., Stroebel, J., & Weber, A. (2021). Climate Change and Long-Run Discount Rates: Evidence from Real Estate. *The Review of Financial Studies*, *34*(8), 3527–3571. https://doi.org/10.1093/rfs/hhab032

Gilbert, C., & Hutto, E. (2014). Vader: A parsimonious rule-based model for sentiment analysis of social media text. *Eighth International Conference on Weblogs and Social Media (ICWSM-14). Available at (20/04/16) http://comp. Social. Gatech. Edu/Papers/Icwsm14. Vader. Hutto. Pdf*, *81*, 82.

Gluschenko, K. (2018). Measuring regional inequality: To weight or not to weight? *Spatial Economic Analysis*, *13*(1), 36–59. https://doi.org/10.1080/17421772.2017.1343491

Gosling, S. N., & Arnell, N. W. (2016). A global assessment of the impact of climate change on water scarcity. *Climatic Change*, *134*(3), 371–385. https://doi.org/10.1007/s10584-013-0853-x

Griffin, D., & Anchukaitis, K. J. (2014). How unusual is the 20122014 California drought? *Geophysical Research Letters*, *41*(24), 9017–9023. https://doi.org/10.1002/2014GL062433

Griskevicius, V., Cantú, S. M., & van Vugt, M. (2012). The Evolutionary Bases for Sustainable Behavior: Implications for Marketing, Policy, and Social Entrepreneurship. *Journal of Public Policy & Marketing*, *31*(1), 115–128. https://doi.org/10.1509/jppm.11.040

Groves, R. M. (2011). Three Eras of Survey Research. *Public Opinion Quarterly*, *75*(5), 861–871. https://doi.org/10.1093/poq/nfr057

Guidolin, M., Chen, A. S., Ghimire, B., Keedwell, E. C., Djordjević, S., & Savić, D. A. (2016). A weighted cellular automata 2D inundation model for rapid flood analysis. *Environmental Modelling & Software*, *84*, 378–394. https://doi.org/10.1016/j.envsoft.2016.07.008

Guidolin, M., Duncan, A., Ghimire, B., Gibson, M., Keedwell, E., Chen, A. S., … Savic, D. (2012). *CADDIES: A New Framework for Rapid Development of Parallel Cellular Automata Algorithms for Flood Simulation*.

Gupta, M., Bansal, A., Jain, B., Rochelle, J., Oak, A., & Jalali, M. S. (2021). Whether the weather will help us weather the COVID-19 pandemic: Using machine learning to measure twitter users' perceptions. *International Journal of Medical Informatics*, *145*, 104340. https://doi.org/10.1016/j.ijmedinf.2020.104340

Hajat, A., Hsia, C., & O'Neill, M. S. (2015). Socioeconomic Disparities and Air Pollution Exposure: A Global Review. *Current Environmental Health Reports*, *2*(4), 440–450. https://doi.org/10.1007/s40572-015-0069-5

References

Hamed, A. A., Ayer, A. A., Clark, E. M., Irons, E. A., Taylor, G. T., & Zia, A. (2015). Measuring climate change on Twitter using Google's algorithm: Perception and events. *International Journal of Web Information Systems*, *11*(4), 527–544. https://doi.org/10.1108/IJWIS-08-2015-0025

Hammer, R. B., Radeloff, V. C., Fried, J. S., & Stewart, S. I. (2007). Wildlandurban interface housing growth during the 1990s in California, Oregon, and Washington. *International Journal of Wildland Fire*, *16*(3), 255–265.

Hammer, R. B., Stewart, S. I., & Radeloff, V. C. (2009). Demographic Trends, the WildlandUrban Interface, and Wildfire Management. *Society & Natural Resources*, *22*(8), 777–782. https://doi.org/10.1080/08941920802714042

Handcock, M. S., & Morris, M. (1999). *Relative Distribution Methods in the Social Sciences* (1999th edition). New York: Springer.

Hao, K. (2019). Facebook's ad-serving algorithm discriminates by gender and race'. *Retrieved from MIT Technology Review Website: Https://Www. Technologyreview. Com/S/613274/Facebookalgorithm-Discriminates-Ai-Bias*.

Harries, T. (2008). Feeling secure or being secure? Why it can seem better not to protect yourself against a natural hazard. *Health, Risk & Society*, *10*(5), 479–490. https://doi.org/10.1080/13698570802381162

Harvey, D. (2001). Globalization and the "spatial fix". *Geographische Revue*, *2*, 23–30.

Hauer, M. E., Hardy, R. D., Mishra, D. R., & Pippin, J. S. (2019). No landward movement: Examining 80 years of population migration and shoreline change in Louisiana. *Population and Environment*, *40*(4), 369–387. https://doi.org/10.1007/s11111-019-00315-8

Haughton, J., & Khandker, S. R. (2009). *Handbook on Poverty + Inequality*. World Bank Publications.

Helgeson, Linden, S., & Chabay, I. (2012). *A. Wals & P. B. Corcoran (Eds). Learning for sustainability in times of accelerating change*. Wageningen, NL: Wageningen Academic Publishers.

Hertel, D., & Schlink, U. (2019). Decomposition of urban temperatures for targeted climate change adaptation. *Environmental Modelling & Software*, *113*, 20–28. https://doi.org/10.1016/j.envsoft.2018.11.015

Hess, D. B., Iacobucci, E., & Väiko, A. (2017). Network Connections and Neighbourhood Perception: Using Social Media Postings to Capture Attitudes among Twitter Users in Estonia. *Architecture and Urban Planning*, *13*(1), 67–78. https://doi.org/10.1515/aup-2017-0010

Hewitt, K. (1983). Interpretation of Calamity From the Viewpoint of Human Ecology. *Geographical Review*, *74*. https://doi.org/10.2307/214106

Hillier, A. E. (2003). Redlining and the Home Owners' Loan Corporation. *Journal of Urban History*, *29*(4), 394–420. https://doi.org/10.1177/0096144203029004002

Hino, M., Field, C. B., & Mach, K. J. (2017). Managed retreat as a response to natural hazard risk. *Nature Climate Change*, *7*(5), 364–370. https://doi.org/10.1038/nclimate3252

Hirabayashi, Y., Mahendran, R., Koirala, S., Konoshima, L., Yamazaki, D., Watanabe, S., … Kanae, S. (2013a). Global flood risk under climate change. *Nature Climate Change*, *3*(9), 816–821. https://doi.org/10.1038/nclimate1911

Hirabayashi, Y., Mahendran, R., Koirala, S., Konoshima, L., Yamazaki, D., Watanabe,

S., … Kanae, S. (2013a). Global flood risk under climate change. *Nature Climate Change*, *3*(9), 816–821. https://doi.org/10.1038/nclimate1911

Hoover, K., & Hanson, L. A. (2020). *Wildfire Statistics* (p. 3). Congressional Research Service.

Hornsey, M. J., Harris, E. A., Bain, P. G., & Fielding, K. S. (2016). Meta-analyses of the determinants and outcomes of belief in climate change. *Nature Climate Change*, *6*(6), 622–626. https://doi.org/10.1038/nclimate2943

Howe, P. D., & Leiserowitz, A. (2013). Who remembers a hot summer or a cold winter? The asymmetric effect of beliefs about global warming on perceptions of local climate conditions in the U.S. *Global Environmental Change*, *23*(6), 1488–1500. https://doi.org/10.1016/j.gloenvcha.2013.09.014

Howe, P. D., Mildenberger, M., Marlon, J. R., & Leiserowitz, A. (2015). Geographic variation in opinions on climate change at state and local scales in the USA. *Nature Climate Change*, *5*(6), 596–603. https://doi.org/10.1038/nclimate2583

Hsiang, S., Kopp, R., Jina, A., Rising, J., Delgado, M., Mohan, S., … Houser, T. (2017). Estimating economic damage from climate change in the United States. *Science*, *356*(6345), 1362–1369. https://doi.org/10.1126/science.aal4369

Iacus, S. M., King, G., & Porro, G. (2012). Causal Inference without Balance Checking: Coarsened Exact Matching. *Political Analysis*, *20*(1), 1–24. https://doi.org/10.1093/pan/mpr013

Interagency Fair Lending Examination Procedures. (n.d.). Office of the Comptroller of the Currency Federal Deposit Insurance Corporation Federal Reserve Board Office of Thrift Supervision National Credit Union Administration.

Jayaraj, D., & Subramanian, S. (2006). Horizontal and Vertical Inequality: Some Interconnections and Indicators. *Social Indicators Research*, *75*(1), 123–139.

Jeong, D. I., Sushama, L., & Naveed Khaliq, M. (2014). The role of temperature in drought projections over North America. *Climatic Change*, *127*(2), 289–303. https://doi.org/10.1007/s10584-014-1248-3

Joffe, H. (2003). Risk: From perception to social representation. *British Journal of Social Psychology*, *42*(1), 55–73. https://doi.org/10.1348/014466603763276126

Kahan, D. M. (2012). Cultural Cognition as a Conception of the Cultural Theory of Risk. In S. Roeser, R. Hillerbrand, P. Sandin, & M. Peterson (Eds.), *Handbook of Risk Theory: Epistemology, Decision Theory, Ethics, and Social Implications of Risk* (pp. 725–759). Dordrecht: Springer Netherlands. https://doi.org/10.1007/978-94-007-1433-5_28

Kahneman, D. (2003). Maps of Bounded Rationality: Psychology for Behavioral Economics. *The American Economic Review*, *93*(5), 1449–1475.

Kaiser, F. G., & Fuhrer, U. (2003). Ecological Behavior's Dependency on Different Forms of Knowledge. *Applied Psychology*, *52*(4), 598–613. https://doi.org/10.1111/1464-0597.00153

Kamin, K. A., & Rachlinski, J. J. (1995). Ex post $\neq$ ex ante - Determining Liability in Hindsight. *Law and Human Behavior*, *19*(1), 89–104. https://doi.org/10.1007/BF01499075

Kaplan, S., & Garrick, B. J. (1981). On The Quantitative Definition of Risk. *Risk Analysis*, *1*(1), 11–27. https://doi.org/10.1111/j.1539-6924.1981.tb01350.x

Kasperson, R. E., Renn, O., Slovic, P., Brown, H. S., Emel, J., Goble, R., … Ratick, S.

(1988). The Social Amplification of Risk: A Conceptual Framework. *Risk Analysis*, *8*(2), 177–187. https://doi.org/10.1111/j.1539-6924.1988.tb01168.x

Kates, R. W. (1971). Natural Hazard in Human Ecological Perspective: Hypotheses and Models. *Economic Geography*, *47*(3), 438–451. https://doi.org/10.2307/142820

Kates, R. W., & Burton, I. (2008). Gilbert F. White, 19112006 Local Legacies, National Achievements, and Global Visions. *Annals of the Association of American Geographers*, *98*(2), 479–486. https://doi.org/10.1080/00045600801925656

Keellings, D., & Ayala, J. J. H. (2019). Extreme Rainfall Associated With Hurricane Maria Over Puerto Rico and Its Connections to Climate Variability and Change. *Geophysical Research Letters*, *46*(5), 2964–2973. https://doi.org/10.1029/2019GL082077

Keenan, J. M., & Bradt, J. T. (2020). Underwaterwriting: From theory to empiricism in regional mortgage markets in the U.S. *Climatic Change*, *162*(4), 2043–2067. https://doi.org/10.1007/s10584-020-02734-1

Keenan, J. M., Hill, T., & Gumber, A. (2018). Climate gentrification: From theory to empiricism in Miami-Dade County, Florida. *Environmental Research Letters*, *13*(5), 054001. https://doi.org/10.1088/1748-9326/aabb32

Keim-Malpass, J., Mitchell, E. M., Sun, E., & Kennedy, C. (2017). Using Twitter to Understand Public Perceptions Regarding the #HPV Vaccine: Opportunities for Public Health Nurses to Engage in Social Marketing. *Public Health Nursing*, *34*(4), 316–323. https://doi.org/10.1111/phn.12318

Kellenberg, D., & Mobarak, A. M. (2011). The Economics of Natural Disasters. *Annual Review of Resource Economics*, *3*(1), 297–312. https://doi.org/10.1146/

annurev-resource-073009-104211

Keyes, O. (2018). The Misgendering Machines: Trans/HCI Implications of Automatic Gender Recognition. *Proceedings of the ACM on Human-Computer Interaction*, *2*(CSCW), 88:1–88:22. https://doi.org/10.1145/3274357

Khunwishit, S., & McEntire, D. A. (2012). Testing Social Vulnerability Theory: A Quantitative Study of Hurricane Katrina's Perceived Impact on Residents living in FEMA Designated Disaster Areas. *Journal of Homeland Security and Emergency Management*, *9*(1). https://doi.org/10.1515/1547-7355.1950

King, A. D., & Harrington, L. J. (2018). The Inequality of Climate Change From 1.5 to 2C of Global Warming. *Geophysical Research Letters*, *45*(10), 5030–5033. https://doi.org/10.1029/2018GL078430

Kirilenko, A. P., Molodtsova, T., & Stepchenkova, S. O. (2015). People as sensors: Mass media and local temperature influence climate change discussion on Twitter. *Global Environmental Change*, *30*, 92–100. https://doi.org/10.1016/j.gloenvcha.2014.11.003

Kloster, S., Mahowald, N. M., Randerson, J. T., & Lawrence, P. J. (2012). The impacts of climate, land use, and demography on fires during the 21st century simulated by CLM-CN. *Biogeosciences*, *9*(1), 509–525. https://doi.org/10.5194/bg-9-509-2012

Knutson, T. R., McBride, J. L., Chan, J., Emanuel, K., Holland, G., Landsea, C., … Sugi, M. (2010). Tropical cyclones and climate change. *Nature Geoscience*, *3*(3), 157–163. https://doi.org/10.1038/ngeo779

Kohl, C., Mostafa, D., Böhm, M., & Krcmar, H. (2017). Disruption of Individual Mobility Ahead? A Longitudinal Study of Risk and Benefit Perceptions of Self-Driving Cars

on Twitter. *Wirtschaftsinformatik 2017 Proceedings*.

Kopp, R. E., Horton, R. M., Little, C. M., Mitrovica, J. X., Oppenheimer, M., Rasmussen, D. J., … Tebaldi, C. (2014). Probabilistic 21st and 22nd century sea-level projections at a global network of tide-gauge sites. *Earth's Future*, *2*(8), 383–406. https://doi.org/10.1002/2014EF000239

Kron, W. (2002). Keynote lecture: Flood risk= hazard exposure vulnerability. *Flood Defence*, 82–97.

Krosnick, J. A., Holbrook, A. L., Lowe, L., & Visser, P. S. (2006). The Origins and Consequences of democratic citizens' Policy Agendas: A Study of Popular Concern about Global Warming. *Climatic Change*, *77*(1), 7–43. https://doi.org/10.1007/s10584-006-9068-8

Kuil, L., Carr, G., Viglione, A., Prskawetz, A., & Blöschl, G. (2016). Conceptualizing socio-hydrological drought processes: The case of the Maya collapse. *Water Resources Research*, *52*(8), 6222–6242. https://doi.org/10.1002/2015WR018298

Kundzewicz, Z. W., Kanae, S., Seneviratne, S. I., Handmer, J., Nicholls, N., Peduzzi, P., … Sherstyukov, B. (2014). Flood risk and climate change: Global and regional perspectives. *Hydrological Sciences Journal*, *59*(1), 1–28. https://doi.org/10.1080/02626667.2013.857411

Kuznets, S. (1955). Economic Growth and Income Inequality. *The American Economic Review*, *45*(1), 1–28.

Kwan, M.-P. (2021). The stationarity bias in research on the environmental determinants of health. *Health & Place*, *70*, 102609. https://doi.org/10.1016/j.healthplace.2021.102609

Lau, N.-C., & Nath, M. J. (2012). A Model Study of Heat Waves over North America: Meteorological Aspects and Projections for the Twenty-First Century. *Journal of Climate*, *25*(14), 4761–4784. https://doi.org/10.1175/JCLI-D-11-00575.1

Lee, T. M., Markowitz, E. M., Howe, P. D., Ko, C.-Y., & Leiserowitz, A. A. (2015). Predictors of public climate change awareness and risk perception around the world. *Nature Climate Change*, *5*(11), 1014–1020. https://doi.org/10.1038/nclimate2728

Lehnert, E. A., Wilt, G., Flanagan, B., & Hallisey, E. (2020). Spatial exploration of the CDC's Social Vulnerability Index and heat-related health outcomes in Georgia. *International Journal of Disaster Risk Reduction*, *46*, 101517. https://doi.org/10.1016/j.ijdrr.2020.101517

Leiserowitz, A. (2006). Climate Change Risk Perception and Policy Preferences: The Role of Affect, Imagery, and Values. *Climatic Change*, *77*(1), 45–72. https://doi.org/10.1007/s10584-006-9059-9

Leiserowitz, A. A., Maibach, E. W., Roser-Renouf, C., Smith, N., & Dawson, E. (2013). Climategate, Public Opinion, and the Loss of Trust. *American Behavioral Scientist*, *57*(6), 818–837. https://doi.org/10.1177/0002764212458272

Leiserowitz, A., Maibach, E. W., Rosenthal, S., Kotcher, J., Bergquist, P., Ballew, M., … Gustafson, A. (2019). Climate change in the American mind: April 2019. *Yale University and George Mason University. New Haven, CT: Yale Program on Climate Change Communication*.

Leroy, S. A. G. (2006). From natural hazard to environmental catastrophe: Past and present. *Quaternary International*, *158*(1), 4–12. https://doi.org/10.1016/j.quaint.2006.05.012

Levees. (2017).

L'Horty, Y., Bunel, M., & Petit, P. (2019). Testing for redlining in the labour market. *Spatial Economic Analysis*, *14*(2), 153–173. https://doi.org/10.1080/17421772.2019.1559347

Lichter, D. T., Parisi, D., Grice, S. M., & Taquino, M. (2007). Municipal Underbounding: Annexation and Racial Exclusion in Small Southern Towns*. *Rural Sociology*, *72*(1), 47–68. https://doi.org/10.1526/003601107781147437

Lipsitz, G. (2007). The Racialization of Space and the Spatialization of Race: Theorizing the Hidden Architecture of Landscape. *Landscape Journal*, *26*(1), 10–23.

Liu, Y., L. Goodrick, S., & A. Stanturf, J. (2013). Future U.S. Wildfire potential trends projected using a dynamically downscaled climate change scenario. *Forest Ecology and Management*, *294*, 120–135. https://doi.org/10.1016/j.foreco.2012.06.049

Loewenstein, G. F., Weber, E. U., Hsee, C. K., & Welch, N. (2001). Risk as feelings. *Psychological Bulletin*, *127*(2), 267–286. https://doi.org/10.1037/0033-2909.127.2.267

Lowe, D., Ebi, K. L., & Forsberg, B. (2013). Factors Increasing Vulnerability to Health Effects before, during and after Floods. *International Journal of Environmental Research and Public Health*, *10*(12), 7015–7067. https://doi.org/10.3390/ijerph10127015

Luber, G., & McGeehin, M. (2008). Climate Change and Extreme Heat Events. *American Journal of Preventive Medicine*, *35*(5), 429–435. https://doi.org/10.1016/j.amepre.2008.08.021

Lujala, P., Lein, H., & Rød, J. K. (2015). Climate change, natural hazards, and risk

perception: The role of proximity and personal experience. *Local Environment*, *20*(4), 489–509. https://doi.org/10.1080/13549839.2014.887666

Lusk, J. L., & Coble, K. H. (2005). Risk Perceptions, Risk Preference, and Acceptance of Risky Food. *American Journal of Agricultural Economics*, *87*(2), 393–405.

Maibach, E. W., Leiserowitz, A., Roser-Renouf, C., & Mertz, C. K. (2011). Identifying Like-Minded Audiences for Global Warming Public Engagement Campaigns: An Audience Segmentation Analysis and Tool Development. *PLOS ONE*, *6*(3), e17571. https://doi.org/10.1371/journal.pone.0017571

Mallya, G., Zhao, L., Song, X. C., Niyogi, D., & Govindaraju, R. S. (2013). 2012 Midwest Drought in the United States. *Journal of Hydrologic Engineering*, *18*(7), 737–745. https://doi.org/10.1061/(ASCE)HE.1943-5584.0000786

Marcy, D., Brooks, W., Draganov, K., Hadley, B., Haynes, C., Herold, N., … others. (2011). New mapping tool and techniques for visualizing sea level rise and coastal flooding impacts. In *Solutions to coastal disasters 2011* (pp. 474–490).

Marlon, J. R., Bartlein, P. J., Gavin, D. G., Long, C. J., Anderson, R. S., Briles, C. E., … Walsh, M. K. (2012). Long-term perspective on wildfires in the western USA. *Proceedings of the National Academy of Sciences*, *109*(9), E535–E543. https://doi.org/10.1073/pnas.1112839109

Marlon, J. R., Bartlein, P. J., Walsh, M. K., Harrison, S. P., Brown, K. J., Edwards, M. E., … Whitlock, C. (2009). Wildfire responses to abrupt climate change in North America. *Proceedings of the National Academy of Sciences*, *106*(8), 2519–2524. https://doi.org/10.1073/pnas.0808212106

Marsooli, R., Lin, N., Emanuel, K., & Feng, K. (2019). Climate change ex-

acerbates hurricane flood hazards along US Atlantic and Gulf Coasts in spatially varying patterns. *Nature Communications*, *10*(1), 3785. https://doi.org/10.1038/s41467-019-11755-z

Martín, Y., Cutter, S. L., & Li, Z. (2020). Bridging Twitter and Survey Data for Evacuation Assessment of Hurricane Matthew and Hurricane Irma. *Natural Hazards Review*, *21*(2). https://doi.org/10.1061/(ASCE)NH.1527-6996.0000354

McCarthy, M., Brennan, M., Boer, M. D., & Ritson, C. (2008). Media risk communication what was said by whom and how was it interpreted. *Journal of Risk Research*, *11*(3), 375–394. https://doi.org/10.1080/13669870701566599

McCright, A., & Dunlap, R. (2013). Bringing Ideology In: The Conservative White Male Effect on Worry about Environmental Problems in the USA. *Journal of Risk Research*, *16*. https://doi.org/10.1080/13669877.2012.726242

McCright, A. M., & Dunlap, R. E. (2011). The Politicization of Climate Change and Polarization in the American Public's Views of Global Warming, 20012010. *The Sociological Quarterly*, *52*(2), 155–194. https://doi.org/10.1111/j.1533-8525.2011.01198.x

Mendelsohn, R., Emanuel, K., Chonabayashi, S., & Bakkensen, L. (2012). The impact of climate change on global tropical cyclone damage. *Nature Climate Change*, *2*(3), 205–209. https://doi.org/10.1038/nclimate1357

Millimet, D. L., & Slottje, D. (2002). An environmental Paglin-Gini. *Applied Economics Letters*, *9*(4), 271–274. https://doi.org/10.1080/13504850110062031

Mitchell, G., & Dorling, D. (2003). An Environmental Justice Analysis of British Air Quality. *Environment and Planning A: Economy and Space*, *35*(5), 909–929. https:

//doi.org/10.1068/a35240

Mitchell, G., & Walker, G. (2007). Methodological Issues in the Assessment of Environmental Equity and Environmental Justice. In *Sustainable Urban Development Volume 2*. Routledge.

Mitchell, J. K., Devine, N., & Jagger, K. (1989). A Contextual Model of Natural Hazard. *Geographical Review*, *79*(4), 391–409. https://doi.org/10.2307/215114

Modave, F., Zhao, Y., Krieger, J., He, Z., Guo, Y., Huo, J., … Bian, J. (2019). Understanding Perceptions and Attitudes in Breast Cancer Discussions on Twitter. *Studies in Health Technology and Informatics*, *264*, 1293–1297. https://doi.org/10.3233/SHTI190435

Mohammad, S., & Turney, P. (2010). Emotions evoked by common words and phrases: Using mechanical turk to create an emotion lexicon. *Proceedings of the NAACL HLT 2010 Workshop on Computational Approaches to Analysis and Generation of Emotion in Text*, 26–34.

Moran, P. a. P. (1948). The Interpretation of Statistical Maps. *Journal of the Royal Statistical Society: Series B (Methodological)*, *10*(2), 243–251. https://doi.org/10.1111/j.2517-6161.1948.tb00012.x

Moritz, M. A., Parisien, M.-A., Batllori, E., Krawchuk, M. A., Dorn, J. V., Ganz, D. J., & Hayhoe, K. (2012). Climate change and disruptions to global fire activity. *Ecosphere*, *3*(6), art49. https://doi.org/10.1890/ES11-00345.1

Morris, M., Bernhardt, A. D., & Handcock, M. S. (1994). Economic Inequality: New Methods for New Trends. *American Sociological Review*, *59*(2), 205–219. https://doi.org/10.2307/2096227

Morris, M., & Western, B. (1999). Inequality in Earnings at the Close of the Twentieth Century. *Annual Review of Sociology*, *25*(1), 623–657. https://doi.org/10.1146/annurev.soc.25.1.623

Moscati, I. (2018). Measuring Utility: From the Marginal Revolution to Behavioral Economics. In *Measuring Utility*. Oxford University Press.

Moscovici, S. (1984). The phenomenon of social representations. *Social Representations.*, 3–69.

Mostegl, N. M., Pröbstl-Haider, U., Jandl, R., & Haider, W. (2019). Targeting climate change adaptation strategies to small-scale private forest owners. *Forest Policy and Economics*, *99*, 83–99. https://doi.org/10.1016/j.forpol.2017.10.001

Motel, S. (2014). Most Americans Believe in Climate Change, But Give It Low Priority.

NASA. (2012). *Historic Heat in North America Turns Winter to Summer* [Text.Article].

Nelson, K. S., Abkowitz, M. D., & Camp, J. V. (2015). A method for creating high resolution maps of social vulnerability in the context of environmental hazards. *Applied Geography*, *63*, 89–100. https://doi.org/10.1016/j.apgeog.2015.06.011

Neumann, B., Vafeidis, A. T., Zimmermann, J., & Nicholls, R. J. (2015). Future Coastal Population Growth and Exposure to Sea-Level Rise and Coastal Flooding - A Global Assessment. *PLOS ONE*, *10*(3), e0118571. https://doi.org/10.1371/journal.pone.0118571

Nielsen, F. Å. (2011). A new ANEW: Evaluation of a word list for sentiment analysis in microblogs. *arXiv:1103.2903 [Cs]*. Retrieved from http://arxiv.org/abs/1103.2903

NOAA. (2019). *Hurricane Michael upgraded to a Category 5 at time of U.S. Landfall |*

National Oceanic and Atmospheric Administration.

NOAA. (2020). *Hurricane Costs*.

Nordhaus, W. D. (2007). A Review of the *Stern Review on the Economics of Climate Change*. *Journal of Economic Literature*, *45*(3), 686–702. https://doi.org/10.1257/jel.45.3.686

Nordhaus, W. D. (2013). The Climate Casino: Risk, Uncertainty, and Economics for a Warming World. In *The Climate Casino*. Yale University Press. https://doi.org/10.12987/9780300203813

O'Connor, R. E., Bord, R. J., & Fisher, A. (1999). Risk Perceptions, General Environmental Beliefs, and Willingness to Address Climate Change. *Risk Analysis*, *19*(3), 461–471. https://doi.org/10.1023/A:1007004813446

O'Neill, J., & O'Neill, M. (2012). *Social Justice and the Future of Flood Insurance*. https://philarchive.org.

O'Neill, P. (2018). Capital Projects And Infrastructure In Urban And Economic Development. In *The Routledge Companion to the Geography of International Business*. Routledge.

Orlove, B. (2005). Human adaptation to climate change: A review of three historical cases and some general perspectives. *Environmental Science & Policy*, *8*(6), 589–600. https://doi.org/10.1016/j.envsci.2005.06.009

Osm-search/Nominatim. (2021). osm-search.

Overpeck, J. T. (2013). The challenge of hot drought. *Nature*, *503*(7476), 350–351. https://doi.org/10.1038/503350a

Papalexiou, S. M., & Montanari, A. (2019). Global and Regional Increase of Precipitation Extremes Under Global Warming. *Water Resources Research*, *55*(6), 4901–4914. https://doi.org/10.1029/2018WR024067

Peduzzi, P., Dao, H., Herold, C., & Mouton, F. (2009). Assessing global exposure and vulnerability towards natural hazards: The Disaster Risk Index. *Natural Hazards and Earth System Sciences*, *9*(4), 1149–1159. https://doi.org/10.5194/nhess-9-1149-2009

PELLOW, D. N. (2000). Environmental Inequality Formation: Toward a Theory of Environmental Injustice. *American Behavioral Scientist*, *43*(4), 581–601. https://doi.org/10.1177/0002764200043004004

Peterson, T. C., Stott, P. A., & Herring, S. (2012). Explaining Extreme Events of 2011 from a Climate Perspective. *Bulletin of the American Meteorological Society*, *93*(7), 1041–1067. https://doi.org/10.1175/BAMS-D-12-00021.1

Piantadosi, S., Byar, D. P., & Green, S. B. (1988). The Ecological Fallacy. *American Journal of Epidemiology*, *127*(5), 893–904. https://doi.org/10.1093/oxfordjournals.aje.a114892

Pierce, D. W., Cayan, D. R., & Thrasher, B. L. (2014). Statistical downscaling using localized constructed analogs (LOCA). *Journal of Hydrometeorology*, *15*(6), 2558–2585.

Piketty, T., & Saez, E. (2003). Income Inequality in the United States, 19131998*. *The Quarterly Journal of Economics*, *118*(1), 1–41. https://doi.org/10.1162/00335530360535135

Pizer, W. A. (1999). The optimal choice of climate change policy in the presence of

uncertainty. *Resource and Energy Economics*, *21*(3), 255–287. https://doi.org/10.1016/S0928-7655(99)00005-6

Plattner, T., Plapp, T., & Hebel, B. (2006). Integrating public risk perception into formal natural hazard risk assessment. *Natural Hazards and Earth System Sciences*, *6*(3), 471–483. https://doi.org/10.5194/nhess-6-471-2006

Preoţiuc-Pietro, D., Liu, Y., Hopkins, D., & Ungar, L. (2017). Beyond Binary Labels: Political Ideology Prediction of Twitter Users. *Proceedings of the 55th Annual Meeting of the Association for Computational Linguistics (Volume 1: Long Papers)*, 729–740. Vancouver, Canada: Association for Computational Linguistics. https://doi.org/10.18653/v1/P17-1068

Quillian, L., Lee, J. J., & Honoré, B. (2020). Racial Discrimination in the U.S. Housing and Mortgage Lending Markets: A Quantitative Review of Trends, 19762016. *Race and Social Problems*, *12*(1), 13–28. https://doi.org/10.1007/s12552-019-09276-x

Quinn, N., Bates, P. D., Neal, J., Smith, A., Wing, O., Sampson, C., … Heffernan, J. (2019). The Spatial Dependence of Flood Hazard and Risk in the United States. *Water Resources Research*, *55*(3), 1890–1911. https://doi.org/10.1029/2018WR024205

Radeloff, V. C., Helmers, D. P., Kramer, H. A., Mockrin, M. H., Alexandre, P. M., Bar-Massada, A., … Stewart, S. I. (2018). Rapid growth of the US wildland-urban interface raises wildfire risk. *Proceedings of the National Academy of Sciences*. https://doi.org/10.1073/pnas.1718850115

Rakedzon, T., Segev, E., Chapnik, N., Yosef, R., & Baram-Tsabari, A. (2017). Automatic jargon identifier for scientists engaging with the public and science communication educators. *PLOS ONE*, *12*(8), e0181742. https://doi.org/10.1371/journal.pone.

0181742

Rampazzo, F., Zagheni, E., Weber, I., Testa, M. R., & Billari, F. (2020). *Mater Certa Est, Pater Numquam: What Can Facebook Advertising Data Tell Us about Male Fertility Rates?* 4.

Reardon, S. F., & O'Sullivan, D. (2004). 3. Measures of Spatial Segregation. *Sociological Methodology*, *34*(1), 121–162. https://doi.org/10.1111/j.0081-1750.2004.00150.x

Rey, S. J., & Janikas, M. V. (2005). Regional convergence, inequality, and space. *Journal of Economic Geography*, *5*(2), 155–176. https://doi.org/10.1093/jnlecg/lbh044

Riloff, E., & Shepherd, J. (1997). A Corpus-Based Approach for Building Semantic Lexicons. *arXiv:Cmp-Lg/9706013*. Retrieved from http://arxiv.org/abs/cmp-lg/9706013

Rufat, S., Tate, E., Burton, C. G., & Maroof, A. S. (2015). Social vulnerability to floods: Review of case studies and implications for measurement. *International Journal of Disaster Risk Reduction*, *14*, 470–486. https://doi.org/10.1016/j.ijdrr.2015.09.013

Rufat, S., Tate, E., Emrich, C. T., & Antolini, F. (2019). How Valid Are Social Vulnerability Models? *Annals of the American Association of Geographers*, *109*(4), 1131–1153. https://doi.org/10.1080/24694452.2018.1535887

Ruz, G. A., Henríquez, P. A., & Mascareño, A. (2020). Sentiment analysis of Twitter data during critical events through Bayesian networks classifiers. *Future Generation Computer Systems*, *106*, 92–104. https://doi.org/10.1016/j.future.2020.01.005

Salvatore, C., Biffignandi, S., & Bianchi, A. (2020). Social Media and Twitter Data Quality for New Social Indicators. *Social Indicators Research*. https://doi.org/10.1007/s11205-020-02296-w

Samset, B. H., Fuglestvedt, J. S., & Lund, M. T. (2020). Delayed emergence of a global temperature response after emission mitigation. *Nature Communications*, *11*(1), 3261. https://doi.org/10.1038/s41467-020-17001-1

Scheffer, M., Bavel, B. van, Leemput, I. A. van de, & Nes, E. H. van. (2017). Inequality in nature and society. *Proceedings of the National Academy of Sciences*, *114*(50), 13154–13157. https://doi.org/10.1073/pnas.1706412114

Schmidtlein, M. C., Deutsch, R. C., Piegorsch, W. W., & Cutter, S. L. (2008). A sensitivity analysis of the social vulnerability index. *Risk Analysis: An Official Publication of the Society for Risk Analysis*, *28*(4), 1099–1114. https://doi.org/10.1111/j.1539-6924.2008.01072.x

Schoennagel, T., Balch, J. K., Brenkert-Smith, H., Dennison, P. E., Harvey, B. J., Krawchuk, M. A., … Whitlock, C. (2017). Adapt to more wildfire in western North American forests as climate changes. *Proceedings of the National Academy of Sciences*, *114*(18), 4582–4590. https://doi.org/10.1073/pnas.1617464114

Schultz, F., Utz, S., & Göritz, A. (2011). Is the medium the message? Perceptions of and reactions to crisis communication via twitter, blogs and traditional media. *Public Relations Review*, *37*(1), 20–27. https://doi.org/10.1016/j.pubrev.2010.12.001

Schumacher, I., & Strobl, E. (2011). Economic development and losses due to natural disasters: The role of hazard exposure. *Ecological Economics*, *72*, 97–105. https://doi.org/10.1016/j.ecolecon.2011.09.002

References

Scott, J. H., Gilbertson-Day, J. W., Moran, C., Dillon, G. K., Short, K. C., & Vogler, K. C. (2020). *Wildfire Risk to Communities: Spatial datasets of landscape-wide wildfire risk components for the United States*. Forest Service Research Data Archive. https://doi.org/10.2737/RDS-2020-0016

Scott, K. K., & Errett, N. A. (n.d.). Content, Accessibility, and Dissemination of Disaster Information via Social Media During the 2016 Louisiana Floods. *Journal of Public Health Management and Practice*, *24*(4), 370–379. https://doi.org/10.1097/PHH.0000000000000708

Seager, R., Hoerling, M., Schubert, S., Wang, H., Lyon, B., Kumar, A., … Henderson, N. (2015). Causes of the 201114 California Drought. *Journal of Climate*, *28*(18), 6997–7024. https://doi.org/10.1175/JCLI-D-14-00860.1

Sen, A. (2000). *Development as Freedom* (Reprint edition). New York: Anchor.

Severyn, A., & Moschitti, A. (2015). Twitter Sentiment Analysis with Deep Convolutional Neural Networks. *Proceedings of the 38th International ACM SIGIR Conference on Research and Development in Information Retrieval*, 959–962. New York, NY, USA: Association for Computing Machinery. https://doi.org/10.1145/2766462.2767830

Sherbinin, A. de, Castro, M., Gemenne, F., Cernea, M. M., Adamo, S., Fearnside, P. M., … Shi, G. (2011). Preparing for Resettlement Associated with Climate Change. *Science*, *334*(6055), 456–457. https://doi.org/10.1126/science.1208821

Shogren, J. F., & Crocker, T. D. (1991). Risk, self-protection, and ex ante economic value. *Journal of Environmental Economics and Management*, *20*(1), 1–15. https://doi.org/10.1016/0095-0696(91)90019-F

Siders, A. R. (2019). Managed Retreat in the United States. *One Earth*, *1*(2), 216–225. https://doi.org/10.1016/j.oneear.2019.09.008

Sitthiyot, T., & Holasut, K. (2020). A simple method for measuring inequality. *Palgrave Communications*, *6*(1), 1–9. https://doi.org/10.1057/s41599-020-0484-6

Sjöberg, L. (2006). Will the Real Meaning of Affect Please Stand Up? *Journal of Risk Research*, *9*(2), 101–108. https://doi.org/10.1080/13669870500446068

Slovic, P. (1987). Perception of risk. *Science*, *236*(4799), 280–285. https://doi.org/10.1126/science.3563507

Slovic, P. (Ed.). (2000). *The perception of risk* (pp. xxxvii, 473). London, England: Earthscan Publications.

Slovic, P., Finucane, M. L., Peters, E., & MacGregor, D. G. (2004). Risk as Analysis and Risk as Feelings: Some Thoughts about Affect, Reason, Risk, and Rationality. *Risk Analysis*, *24*(2), 311–322. https://doi.org/10.1111/j.0272-4332.2004.00433.x

Slovic, P., Fischhoff, B., & Lichtenstein, S. (1980). Facts and Fears: Understanding Perceived Risk. In R. C. Schwing & W. A. Albers (Eds.), *Societal Risk Assessment: How Safe is Safe Enough?* (pp. 181–216). Boston, MA: Springer US. https://doi.org/10.1007/978-1-4899-0445-4_9

Slovic, P., Fischhoff, B., & Lichtenstein, S. (1982). Why Study Risk Perception? *Risk Analysis*, *2*(2), 83–93. https://doi.org/10.1111/j.1539-6924.1982.tb01369.x

Smith, A. (2020). *U.S. Billion-dollar Weather and Climate Disasters, 1980 - present (NCEI Accession 0209268)*. NOAA. https://doi.org/10.25921/STKW-7W73

Smith, K. (2013). *Environmental Hazards: Assessing Risk and Reducing Disaster*. Routledge.

Smith, N., & Joffe, H. (2013). How the public engages in climate change: A social representations approach. *Public Understanding of Science*, *22*(1), 16–32. https://doi.org/10.1177/0963662512440913

Smith, N., & Leiserowitz, A. (2014). The Role of Emotion in Global Warming Policy Support and Opposition. *Risk Analysis*, *34*(5), 937–948. https://doi.org/10.1111/risa.12140

Smith, S. K., & McCarty, C. (1996). Demographic effects of natural disasters: A case study of hurricane andrew*. *Demography*, *33*(2), 265–275. https://doi.org/10.2307/2061876

Smith, T. T., Zaitchik, B. F., & Gohlke, J. M. (2013). Heat waves in the United States: Definitions, patterns and trends. *Climatic Change*, *118*(3), 811–825. https://doi.org/10.1007/s10584-012-0659-2

Spielman, S. E., Tuccillo, J., Folch, D. C., Schweikert, A., Davies, R., Wood, N., & Tate, E. (2020). Evaluating social vulnerability indicators: Criteria and their application to the Social Vulnerability Index. *Natural Hazards*, *100*(1), 417–436. https://doi.org/10.1007/s11069-019-03820-z

Squires, G. D. (2003). Racial Profiling, Insurance Style: Insurance Redlining and the Uneven Development of Metropolitan Areas. *Journal of Urban Affairs*, *25*(4), 391–410. https://doi.org/10.1111/1467-9906.t01-1-00168

Squires, G. D., Velez, W., & Taeuber, K. E. (1991). Insurance Redlining, Agency Location, and the Process of Urban Disinvestment. *Urban Affairs Quarterly*, *26*(4), 567–588. https://doi.org/10.1177/004208169102600407

Steel, Z. L., Safford, H. D., & Viers, J. H. (2015). The fire frequency-severity relationship

and the legacy of fire suppression in California forests. *Ecosphere*, *6*(1), art8. https://doi.org/10.1890/ES14-00224.1

Swain, S., & Hayhoe, K. (2015). CMIP5 projected changes in spring and summer drought and wet conditions over North America. *Climate Dynamics*, *44*(9), 2737–2750. https://doi.org/10.1007/s00382-014-2255-9

Sweet, W., Dusek, G., Marcy, D. C., Carbin, G., & Marra, J. (2019). *2018 state of US high tide flooding with a 2019 outlook*.

Sweet, W. V., Kopp, R. E., Weaver, C. P., Obeysekera, J., Horton, R. M., Thieler, E. R., & Zervas, C. (2017). *Global and regional sea level rise scenarios for the United States*.

Sweet, W. W. V., Dusek, G., Obeysekera, J., & Marra, J. J. (2018). *Patterns and projections of high tide flooding along the US coastline using a common impact threshold*.

Taraz, V. (2017). Adaptation to climate change: Historical evidence from the Indian monsoon. *Environment and Development Economics*, *22*(5), 517–545. https://doi.org/10.1017/S1355770X17000195

Tate, E. (2012). Social vulnerability indices: A comparative assessment using uncertainty and sensitivity analysis. *Natural Hazards*, *63*(2), 325–347. https://doi.org/10.1007/s11069-012-0152-2

Taylor, K. E., Stouffer, R. J., & Meehl, G. A. (2012). An Overview of CMIP5 and the Experiment Design. *Bulletin of the American Meteorological Society*, *93*(4), 485–498. https://doi.org/10.1175/BAMS-D-11-00094.1

Tellman, B., Schank, C., Schwarz, B., Howe, P. D., & de Sherbinin, A. (2020). Using Disaster Outcomes to Validate Components of Social Vulnerability to Floods: Flood Deaths and Property Damage across the USA. *Sustainability*, *12*(15), 6006. https:

//doi.org/10.3390/su12156006

Thelwall, M., Buckley, K., & Paltoglou, G. (2011). Sentiment in Twitter events. *Journal of the American Society for Information Science and Technology*, *62*(2), 406–418. https://doi.org/10.1002/asi.21462

Tobler, C., Visschers, V., & Siegrist, M. (2012). Consumers' knowledge about climate change. *Climatic Change*, *114*(2), 189–209.

Tohver, I. M., Hamlet, A. F., & Lee, S.-Y. (2014). Impacts of 21st-Century Climate Change on Hydrologic Extremes in the Pacific Northwest Region of North America. *JAWRA Journal of the American Water Resources Association*, *50*(6), 1461–1476. https://doi.org/10.1111/jawr.12199

Trenberth, K. E. (2011). Changes in precipitation with climate change. *Climate Research*, *47*(1-2), 123–138. https://doi.org/10.3354/cr00953

Trenberth, K. E., Cheng, L., Jacobs, P., Zhang, Y., & Fasullo, J. (2018). Hurricane Harvey Links to Ocean Heat Content and Climate Change Adaptation. *Earth's Future*, *6*(5), 730–744. https://doi.org/10.1029/2018EF000825

Troesken, W. (2002). The Limits of Jim Crow: Race and the Provision of Water and Sewerage Services in American Cities, 1880-1925. *The Journal of Economic History*, *62*(3), 734–772.

Tuholske, C., Caylor, K., Funk, C., Verdin, A., Sweeney, S., Grace, K., … Evans, T. (2021). Global urban population exposure to extreme heat. *Proceedings of the National Academy of Sciences*, *118*(41). https://doi.org/10.1073/pnas.2024792118

Turner, B. L., Kasperson, R. E., Matson, P. A., McCarthy, J. J., Corell, R. W., Christensen, L., … Schiller, A. (2003). A framework for vulnerability analysis in sustain-

ability science. *Proceedings of the National Academy of Sciences*, *100*(14), 8074–8079. https://doi.org/10.1073/pnas.1231335100

Twitter. (2020). *Advancing Academic Research with Twitter Data*.

Union of Concerned Scientists. (2018). *Underwater: Rising seas, chronic floods, and the implications for US coastal real estate (2018) | union of concerned scientists*.

USGCRP. (2017). *Climate Science Special Report*. https://science2017.globalchange.gov/; U.S. Global Change Research Program, Washington, DC.

Vamvakeridou-Lyroudia, L. S., Chen, A. S., Khoury, M., Gibson, M. J., Kostaridis, A., Stewart, D., … Savic, D. A. (2020). Assessing and visualising hazard impacts to enhance the resilience of Critical Infrastructures to urban flooding. *Science of the Total Environment*, *707*, 136078. https://doi.org/10.1016/j.scitotenv.2019.136078

van der Linden, S. (2015). The social-psychological determinants of climate change risk perceptions: Towards a comprehensive model. *Journal of Environmental Psychology*, *41*, 112–124. https://doi.org/10.1016/j.jenvp.2014.11.012

van der Linden, S. (2017). *Determinants and Measurement of Climate Change Risk Perception, Worry, and Concern* (SSRN Scholarly Paper No. ID 2953631). Rochester, NY: Social Science Research Network. https://doi.org/10.2139/ssrn.2953631

van der Wiel, K., Kapnick, S. B., van Oldenborgh, G. J., Whan, K., Philip, S., Vecchi, G. A., … Cullen, H. (2017). Rapid attribution of the August 2016 flood-inducing extreme precipitation in south Louisiana to climate change. *Hydrology and Earth System Sciences*, *21*(2), 897–921. https://doi.org/10.5194/hess-21-897-2017

Van Heerden, I. L. (2007). The Failure of the New Orleans Levee System Following Hurricane Katrina and the Pathway Forward. *Public Administration Review*, *67*(s1),

24–35. https://doi.org/10.1111/j.1540-6210.2007.00810.x

Voelklein, C., & Howarth, C. (2005). A Review of Controversies about Social Representations Theory: A British Debate. *Culture & Psychology*, *11*(4), 431–454. https://doi.org/10.1177/1354067X05058586

Vogel, M. M., Zscheischler, J., Wartenburger, R., Dee, D., & Seneviratne, S. I. (2019). Concurrent 2018 Hot Extremes Across Northern Hemisphere Due to Human-Induced Climate Change. *Earth's Future*, *7*(7), 692–703. https://doi.org/10.1029/2019EF001189

Walker, G. (2011). *Environmental Justice: Concepts, Evidence and Politics* (1st edition). London ; New York: Routledge.

Walker, G., Mitchell, G., Fairburn, J., & Smith, G. (2005). Industrial pollution and social deprivation: Evidence and complexity in evaluating and responding to environmental inequality. *Local Environment*, *10*(4), 361–377. https://doi.org/10.1080/13549830500160842

Walsh, K. J. E., McBride, J. L., Klotzbach, P. J., Balachandran, S., Camargo, S. J., Holland, G., … Sugi, M. (2016). Tropical cyclones and climate change. *WIREs Climate Change*, *7*(1), 65–89. https://doi.org/10.1002/wcc.371

Wanders, N., & Wada, Y. (2015). Human and climate impacts on the 21st century hydrological drought. *Journal of Hydrology*, *526*, 208–220. https://doi.org/10.1016/j.jhydrol.2014.10.047

Wang, Z., Hale, S., Adelani, D. I., Grabowicz, P., Hartman, T., Flöck, F., & Jurgens, D. (2019). Demographic Inference and Representative Population Estimates from Multilingual Social Media Data. *The World Wide Web Conference*, 2056–2067. New

York, NY, USA: Association for Computing Machinery. https://doi.org/10.1145/3308558.3313684

Watts, M. (2008). On the poverty of theory: Natural hazards research in context. In *Environment*. Routledge.

Webber, J. L., Booth, G., Gunasekara, R., Fu, G., & Butler, D. (2019). Validating a rapid assessment framework for screening surface water flood risk. *Water and Environment Journal*, *33*(3), 427–442. https://doi.org/10.1111/wej.12415

Webber, J. L., Fletcher, T. D., Cunningham, L., Fu, G., Butler, D., & Burns, M. J. (2020). Is green infrastructure a viable strategy for managing urban surface water flooding? *Urban Water Journal*, *17*(7), 598–608. https://doi.org/10.1080/1573062X.2019.1700286

Weber, E. U. (2010). What shapes perceptions of climate change? *WIREs Climate Change*, *1*(3), 332–342. https://doi.org/10.1002/wcc.41

Weinberg, A. S. (1998). The Environmental Justice Debate: A Commentary on Methodological Issues and Practical Concerns. *Sociological Forum*, *13*(1), 25–32. https://doi.org/10.1023/A:1022151813591

Westerling, A. L. (2018). *California's Fourth Climate Change Assessment*. 57.

Westerling, A. L., & Bryant, B. P. (2008). Climate change and wildfire in California. *Climatic Change*, *87*(1), 231–249. https://doi.org/10.1007/s10584-007-9363-z

Westerling, A. L., Hidalgo, H. G., Cayan, D. R., & Swetnam, T. W. (2006). Warming and earlier spring increase western U.S. Forest wildfire activity. *Science*, *313*(5789), 940–943. https://doi.org/10.1126/science.1128834

Wheeler, T., & Braun, J. von. (2013). Climate Change Impacts on Global Food Security.

Science, *341*(6145), 508–513. https://doi.org/10.1126/science.1239402

White, G. F. (1945). *Human Adjustment to Floods: A Geographical Approach to the Flood Problem in the United States*. University of Chicago.

White, G. F. (1974). *Natural hazards, local, national, global*. New York: Oxford University Press.

Whittingham, N., Boecker, A., & Grygorczyk, A. (2020). Personality traits, basic individual values and GMO risk perception of twitter users. *Journal of Risk Research*, *23*(4), 522–540. https://doi.org/10.1080/13669877.2019.1591491

Wilby, R. L., & Keenan, R. (2012). Adapting to flood risk under climate change. *Progress in Physical Geography: Earth and Environment*, *36*(3), 348–378. https://doi.org/10.1177/0309133312438908

Williams, A. P., Abatzoglou, J. T., Gershunov, A., Guzman-Morales, J., Bishop, D. A., Balch, J. K., & Lettenmaier, D. P. (2019). Observed Impacts of Anthropogenic Climate Change on Wildfire in California. *Earth's Future*, *7*(8), 892–910. https://doi.org/10.1029/2019EF001210

Wilson, S. R., Shen, Y., & Mihalcea, R. (2018). Building and Validating Hierarchical Lexicons with a Case Study on Personal Values. In S. Staab, O. Koltsova, & D. I. Ignatov (Eds.), *Social Informatics* (pp. 455–470). Cham: Springer International Publishing. https://doi.org/10.1007/978-3-030-01129-1_28

Wing, O. E. J., Bates, P. D., Sampson, C. C., Smith, A. M., Johnson, K. A., & Erickson, T. A. (2017). Validation of a 30 m resolution flood hazard model of the conterminous United States. *Water Resources Research*, *53*(9), 7968–7986. https://doi.org/10.1002/2017WR020917

Wing, O. E. J., Bates, P. D., Smith, A. M., Sampson, C. C., Johnson, K. A., Fargione, J., & Morefield, P. (2018). Estimates of present and future flood risk in the conterminous United States. *Environmental Research Letters*, *13*(3), 034023. https://doi.org/10.1088/1748-9326/aaac65

Wing, O. E. J., Pinter, N., Bates, P. D., & Kousky, C. (2020). New insights into US flood vulnerability revealed from flood insurance big data. *Nature Communications*, *11*(1), 1444. https://doi.org/10.1038/s41467-020-15264-2

Wisner, B. (2016). Vulnerability as concept, model, metric, and tool. In *Oxford research encyclopedia of natural hazard science*.

Wisner, B., Blaikie, P. M., Blaikie, P., Cannon, T., & Davis, I. (2004). *At risk: Natural hazards, people's vulnerability and disasters*. Psychology Press.

Woodhouse, C. A., Meko, D. M., MacDonald, G. M., Stahle, D. W., & Cook, E. R. (2010). A 1,200-year perspective of 21st century drought in southwestern North America. *Proceedings of the National Academy of Sciences*, *107*(50), 21283–21288. https://doi.org/10.1073/pnas.0911197107

Woods, L. L. (2012). The Federal Home Loan Bank Board, Redlining, and the National Proliferation of Racial Lending Discrimination, 19211950. *Journal of Urban History*, *38*(6), 1036–1059. https://doi.org/10.1177/0096144211435126

Xie, B., Brewer, M. B., Hayes, B. K., McDonald, R. I., & Newell, B. R. (2019). Predicting climate change risk perception and willingness to act. *Journal of Environmental Psychology*, *65*, 101331. https://doi.org/10.1016/j.jenvp.2019.101331

Yale Climate Opinion Maps 2020. (n.d.).

Yarmuth, J. A. (2021). *H.R.5376 - 117th Congress (2021-2022): Build Back Better Act*

[Legislation]. https://www.congress.gov/bill/117th-congress/house-bill/5376.

Yoon, D. K. (2012). Assessment of social vulnerability to natural disasters: A comparative study. *Natural Hazards*, *63*(2), 823–843. https://doi.org/10.1007/s11069-012-0189-2

Yuan, F., & Liu, R. (2018). Feasibility study of using crowdsourcing to identify critical affected areas for rapid damage assessment: Hurricane Matthew case study. *International Journal of Disaster Risk Reduction*, *28*, 758–767. https://doi.org/10.1016/j.ijdrr.2018.02.003

Zagheni, E., Weber, I., & Gummadi, K. (2017). Leveraging Facebook's Advertising Platform to Monitor Stocks of Migrants. *Population and Development Review*, *43*(4), 721–734. https://doi.org/10.1111/padr.12102

Zahran, S., Brody, S. D., Peacock, W. G., Vedlitz, A., & Grover, H. (2008). Social vulnerability and the natural and built environment: A model of flood casualties in Texas. *Disasters*, *32*(4), 537–560. https://doi.org/10.1111/j.1467-7717.2008.01054.x

Zhai, P., Zhou, B., & Chen, Y. (2018). A Review of Climate Change Attribution Studies. *Journal of Meteorological Research*, *32*(5), 671–692. https://doi.org/10.1007/s13351-018-8041-6

Zhang, Z. (2016). Multivariable fractional polynomial method for regression model. *Annals of Translational Medicine*, *4*(9), 174. https://doi.org/10.21037/atm.2016.05.01